High-throughput sequencing based early warning and outbreak investigation

I n a u g u r a l d i s s e r t a t i o n

zur

Erlangung des akademischen Grades eines

Doktors der Naturwissenschaften (Dr. rer. nat.)

der

Mathematisch-Naturwissenschaftlichen Fakultät

der

Universität Greifswald

vorgelegt von

Pauline Dianne Santos

Greifswald, 31. Mai 2021

Dekan: Prof. Dr. Gerald Kerth

1. Gutachter :   Prof. Dr. Dr. h.c. Thomas C. Mettenleiter

2. Gutachter: Prof. Dr. Stefanie C. Becker

Tag der Promotion: 28.10.2021

"Nothing in life is to be feared, it is only to be understood. Now is the time to understand more, so that we may fear less."

- Marie Skłodowska Curie

Table of Contents

1. Introduction

1.1 Viral infectious disease outbreaks and response

Viral infectious diseases have always been a significant threat to global human and animal populations, causing unexpected illnesses and deaths that instigated detrimental impacts on the economy and society and interfered with everyday life activities [1,2]. Currently, the world is experiencing the devastating effects of the coronavirus disease 2019 (COVID-19) pandemic caused by a novel coronavirus. Within a year, COVID-19 has claimed more than 3 million human lives and prompted the largest global economic crisis in history [3,4]. The world has also encountered several emerging infectious disease outbreaks caused by hitherto unknown viruses over the past three decades: Hendra virus, Nipah virus, severe acute respiratory syndrome coronavirus (SARS-CoV), and Middle East respiratory syndrome coronavirus (MERS-CoV) [5–8]. Simultaneously, numerous known viruses are posing constant threats to the well-being of humans and animals, with several known viruses reported to re-emerge into local areas (*e.g.,* Ebola virus, Dengue virus, and Chikungunya virus) [9–11] or introduced into new geographic locations with naïve populations (*e.g.,* West Nile virus, Zika virus, and African swine fever virus) [12–15].

Prior to their emergence, these viruses are naturally occurring within their animal reservoirs. Disturbances in their natural host populations' ecology can change viral transmission dynamics, which escalate the probability of "spillover" infections to non-reservoir animal hosts [16]. A zoonotic spillover event can occur directly from animal reservoirs to human hosts or indirectly through intermediary hosts or arthropod vectors [17]. An emerging virus can cause an individual or a few sporadic cases and may proceed to a localized outbreak. An outbreak can develop into an epidemic (or epizooty when non-human animal hosts are affected) if public health interventions are delayed and insufficient, or progress into a pandemic in worst-case scenarios [18]. Due to the considerable number of pathogens and limited resources for research and development, the World Health Organization specified nine priority diseases posing the greatest public health risk due to their epidemic potential or insufficient countermeasures [19]. At present, these priority diseases include (1) COVID-19, (2) Crimean-Congo haemorrhagic fever, (3) Ebola virus disease and Marburg virus disease, (4) Lassa fever, (5) SARS and MERS-CoV, (6) Nipah and henipaviral diseases, (7) Rift Valley fever, (8) Zika, and (9) "Disease X." While known viruses caused the eight priority diseases, an unknown pathogen with pandemic potential can cause the "Disease X." Another novel virus will probably bring upon the next pandemic.

The World Health Organization warned that the world is still ill-prepared for these

emerging threats based on our responses to the 2009 H1N1 pandemic and the 2014-16 West African Ebola epidemic [20–22]. Experts have appealed for a centralized pandemic preparedness and response agency and closer collaborations among multiple stakeholders such as government, academics, industry, public health networks, and civil society [23–25]. Although the ongoing COVID-19 pandemic confirmed that the world was underprepared for a pandemic, the world has witnessed the fastest scientific response to a major infectious disease epidemic due to significant advances in fundamental science and collaborations among international research groups [reviewed in Publication I].

Diagnostics and surveillance are fundamental components of outbreak response and preparedness. However, serological testing and nucleic acid-based testing (*e.g.,* polymerase chain reaction; PCR) are often pathogen-specific and inefficient for screening novel or highly diverse etiological agents [reviewed in 26, 27]. Therefore, genomic approaches are especially suitable for broad pathogen identification and characterization since nearly all infectious agents have genetic materials. Consensus PCR, microarrays, and high-throughput sequencing (HTS) are genomic approaches that can detect a broad range of known pathogens and discover novel pathogens in clinical samples [reviewed in 26]. However, only the generic HTS approach can investigate any sample without prior sequence knowledge, leading to the accelerated rate of virus discovery [reviewed in 27,28].

1.2 Second-generation high-throughput sequencing technologies

Illumina (Illumina Inc.) and Ion Torrent systems (Thermo Fischer Scientific) are the most dominant second-generation HTS technologies in the market [reviewed in 29]. These sequencers remain the state-of-the-art technologies for population genomics, phylogenomics, and metagenomics for some years since these second-generation technologies have lower error rates and higher throughput than third-generation sequencing platforms [reviewed in 30]. In this study, the term high-throughput sequencing (HTS) will refer only to the second-generation HTS unless mentioned otherwise.

Different HTS approaches follow a conventional workflow consisting of sample pre-processing, library preparation, sequencing, and bioinformatic analysis (Figure 1) [reviewed in 31]. Sample pre-processing includes nucleic acid extraction from sample materials; the extracted RNA materials are reverse transcribed into complementary DNA (cDNA). The cDNA or extracted DNA are subjected to second-strand synthesis. For generic library preparation, double-stranded DNA/cDNA are fragmented, end-repaired, phosphorylated, tailed with A-overhang (for adapters with sticky-ends), and ligated with adapters at their 5' and 3' ends [32]. These platform-specific adapters contain sequences that enable hybridization, polymerase binding, and amplification. Each adapter consists of unique sequences for sample identification.

Size-selected library molecules are spatially separated and hybridized to oligonucleotides attached on a solid phase. Ligated adapters enable the clonal amplification of bound library molecules to enhance signal detection during the sequencing run. Ion Torrent and Illumina sequencing platforms employ the "sequencing-by-synthesis (SBS)" technology. The stepwise addition of nucleotides to the elongating strand is followed by the release of signals, detected by a sensor [33,34].

Bioinformatic analyses and computational tools are required in raw data processing, assembly of contiguous sequences (contigs), and research-specific data analyses. Signals detected in a sequencing run (raw data) are converted into legible sequence reads (base calling) [33,35]and base quality scores (Phred scores) [36]. A single sequencing run can produce millions to billions of sequence reads. Contigs are assembled by tiling overlapping short sequence reads (*de novo* assembly) or mapping sequence reads to a known reference genome. Taxonomic classification of contigs and individual sequence reads (singletons) can be inferred using homology search against a nucleotide or protein sequence database [reviewed in 37].

Strategies employed in Ion Torrent and Illumina sequencing platforms are different in terms of commercially available sequencing adapters, clonal amplification, sequencing run, and signal detection. Hence, the following sections will discuss these platforms in more detail.

A. Sample pre-processing and library preparation

RNA extraction   cDNA synthesis

Second strand synthesis   (c)DNA fragmentation   End repair and Adapter ligation   Size selection

DNA extraction

B. Clonal amplification, Sequencing and Bioinformatic analyses

dNTPs   signal

CS TS   CS TS   sensor

@Seq_ID
ACGCGTC **G**
+
(+%15Cm **~**

sequence read

...**ACGCGTCGTGTTTG**...

solid phase

Physical separation and hybridization to a solid phase   Clonal amplification   Sequencing-by-synthesis   Signal release and detection   Base calling   Assembly
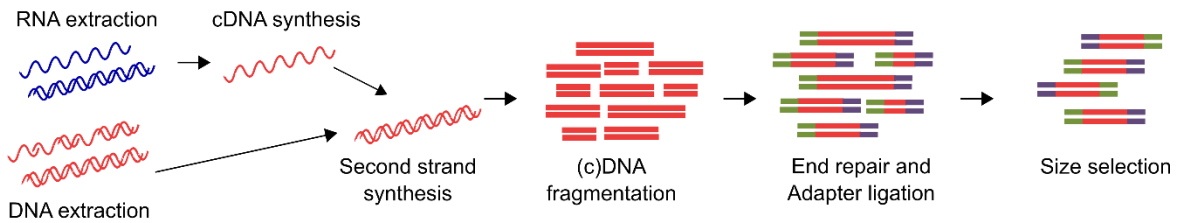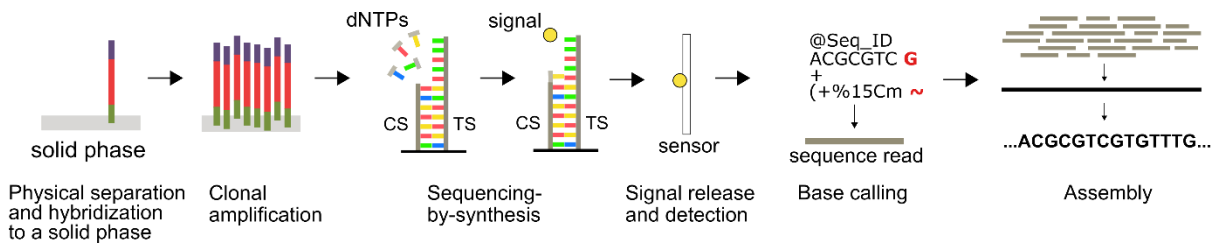
Figure 1. Schematic diagram of a second-generation high-throughput sequencing workflow for generic shotgun library preparation. Green and violet boxes indicate adapters and red boxes indicate nucleic acid from samples. Abbreviation: dNTPs - deoxynucleoside triphosphates, TS-template strand, CS-complementary strand. Figure 1 was based on Srivastav & Suneja [38] and atdbio Ltd. [39].

1.2.1 Ion Torrent sequencing

In a typical Ion Torrent library preparation, fragmented DNA templates were end-repaired and phosphorylated at their 5' ends. These steps are followed by blunt-end ligation of two different linear adapters (A and P1) to both ends of DNA fragments (Figure 2A). Both A and P1 must be incorporated in this step to perform the necessary functionalities during a

sequencing run [40]. A water-in-oil emulsion compartmentalizes the amplification of each single library molecule (so-called emulsion PCR). Ideally, each droplet consists of one library molecule, ion sphere particle (ISP), and necessary reagents for amplification (Figure 2B). The emulsion PCR consists of two primers complementary to sequence library adapters: one is present in the solution while the other is bound to the ISP. This setup selects library molecules ligated with A and P1 adapters, ensuring a uniform orientation of bound library molecules to the ISP [41,42]. The ISP-bound library molecule is amplified to generate millions of identical copies (clones). Subsequently, magnetic bead-based separation enriches template-positive ISPs [34].

A sequencing run is performed in a complementary metal-oxide-semiconductor (CMOS) chip, which contains an array of microwells coupled with ion-sensitive field-effect transistors (ISFET) sensors (Figure 2C). Each template-positive ISPs incubated with sequencing primers and DNA polymerase are loaded into a microwell. The sequencing chip is sequentially flooded with one type of deoxynucleoside triphosphates (dNTPs; N = A, T, C, G) per flow. In each microwell, the polymerase incorporates complementary nucleotides to elongating strands that simultaneously release hydrogen ions. The ISFET sensor detects the shift in pH in a microwell caused by the release of protons. The DNA polymerase can incorporate more than one nucleotide per-flow when the template strand consists of a series of similar nucleotides (homopolymers). The released signals are nearly proportional to the number of incorporated nucleotides per flow (Figure 2D). A washing step after each nucleotide flow ensures the removal of unbound nucleotides in microwells [34].

The Ion Torrent sequencing technology employs natural, unmodified dNTP molecules and high-fidelity DNA-polymerase that lowers substitution errors. This technology is independent of optical sensors allowing faster sequencing runs [43]. Moreover, this technology's sequencing adapters consist of a "key sequence" (TCAG), which facilitates the raw flow-value normalization. It can also sequence library molecules that are several hundred bases long. However, this technology faces a challenge in quantitating the length of homopolymer regions consisting of 5 – 10 bases, which arises from the inaccurate measurement of the magnitude of the released signals leading to insertion and deletion errors [44,45].

1.2.2 Illumina sequencing

The typical library preparation for Illumina sequencing entails the sticky-end ligation of Y-adapters to DNA fragments, which are end-repaired, phosphorylated at their 5' ends, and added A-tail at their 3' ends (Figure 2A). The Y-adapter consists of a short complementary region that binds top and bottom oligonucleotides, a T-overhang that ensures efficient adapter binding, and unique sequences that serve as annealing sites for clonal amplification and sequencing. After Y-adapter ligation, each strand becomes a functional sequencing library

molecule [reviewed in 32,46]. Library molecules are denatured and washed to an acrylamide-coated glass flow cell containing an array of oligonucleotides, which serve as annealing and attachment sites for library molecules (Figure 2B). Each immobilized library molecule is clonally amplified ("bridge amplification") to form a cluster consisting of up to 1000 clones of the template molecule [47]. After cluster generation, reverse strands are cleaved and washed off from the flow cell. The 3' ends of forward strands are then blocked, which facilitates its unidirectional sequencing.

Primers anneal to adapter primer binding sites of each library molecule. Four types of fluorescent-labeled dNTPs are flushed on the flow cell in each cycle. The polymerase incorporates one complementary nucleotide at each elongating strand, and unbound nucleotides are washed off (Figure 2C). Bound fluorophores are excited by a light source to emit characteristic fluorescent signals, which are captured by an optical system [33]. Tris(2-carboxyethyl) phosphine treatment cleaves the fluorophores and the blocking group at the 3'-hydroxyl group allowing the next round of nucleotide incorporation [47]. These steps are repeated until the sequencing run is finished. Stacked images with identified clusters are analyzed to generate sequences of library molecules (Figure 2D).

The bridge amplification enables paired-end sequencing, which involves the denaturation of synthesized products from the first SBS round and bridge amplification to reconstitute the reverse strands of the libraries. Compared to the Ion Torrent sequencing technology, Illumina has lower insertion and deletion error rates due to the termination step after every nucleotide addition [48]. However, this technology utilizes modified nucleotides and engineered polymerases, resulting in higher substitution error rates [48]. Moreover, index hopping happens during bridge amplification due to missing physical barriers between clusters [49].

1.3. High-throughput sequencing approaches for viral genome sequencing

Three HTS approaches are typically employed to sequence virus genomes: (1) generic HTS, (2) target-enrichment HTS, and (3) PCR amplicon-HTS [reviewed in 50] (Figure 3). Each approach has its complexities and costs. Generally, a suitable HTS approach can be selected based on research objectives and virus concentration in sample materials.

(1) The generic (or non-targeted) HTS approach sequences total DNA or RNA extracted from clinical or environmental samples, including genetic materials from the host, bacteria, viruses, fungi, parasites, other pathogens, and commensals (Figure 3) [51]. This approach is often employed in combination with metagenomics, which studies an entire biological community in a given sample using genomes or transcriptomes [52]. Metagenomics utilizes a computational workflow to classify sequence reads based on a reference sequence database [reviewed in 53]. Nooij and colleagues [54] reviewed different metagenomic workflows and their potential

suitability for various purposes: time-constrained diagnostics, discovery, biodiversity analysis,
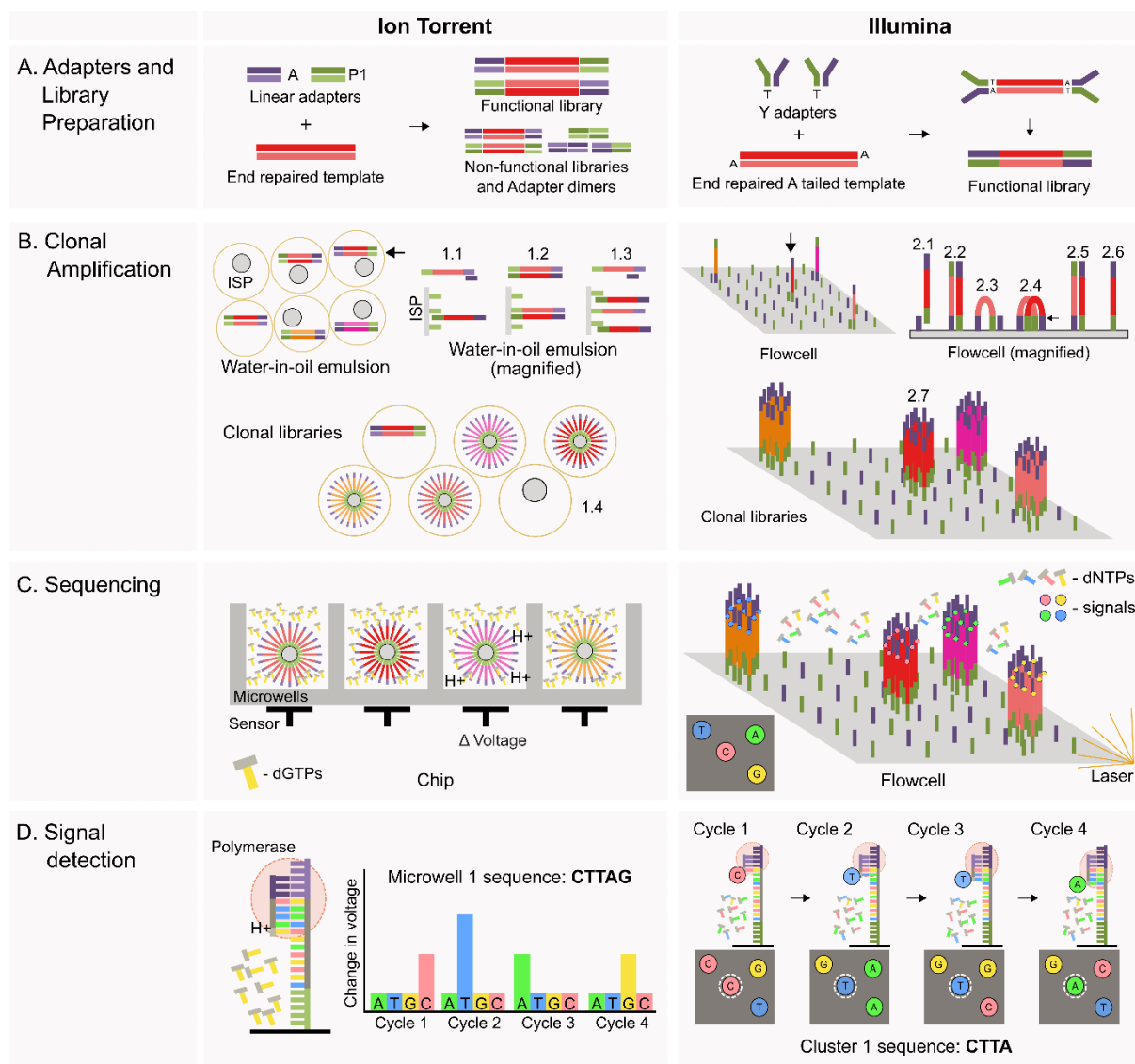

Figure 2. Significant differences of Ion Torrent and Illumina sequencing technologies. (A) Adapters and library preparation steps for both sequencing technologies. Figure 2A is based on Figure 1 in. (B) Differences in clonal amplification in two sequencing technologies. Ion Torrent technology: After the water-in-oil emulsion step, (1.1) each library molecule is denatured, and one of the strands hybridizes with the oligonucleotide attached to the ISP. (1.2) Polymerase covalently attaches the template strand on the ISP and copies the unhybridized strand, and (1.3) the resulting strands serve as templates for the next round of amplification. (1.4) The ISP is covered with cloned template strands after several amplification cycles. Illumina sequencing technology: (2.1) single-stranded libraries anneal to oligonucleotides bound on the flow cell. (2.2) The polymerase synthesizes the complementary strand, which covalently linked the strand to a bound oligonucleotide, and (2.3) the template strand is washed away after a denaturation step. (2.3-2.4) Isothermal bridge amplification enables (2.7) cluster generation. (2.5) The library molecule in each cluster is linearized by cleavage, and (2.6) another cleavage step removes one of the strands that facilitates the unidirectional sequencing-by-synthesis of the remaining strand. (C) Steps for sequencing-by-synthesis and (D) signal detection for both sequencing technologies were shown. Figure 2 was based on studies and figures of Forth and Höper [55] (Figure 2A), Shendure et al. [56] and Bentley et al. [47] (Figure 2B), Rothberg et al. [34] and Illumina Inc. [33] (Figure 2C and 2D).

surveillance, and outbreak source tracing.

The metagenomic HTS is a universal and hypothesis-free approach for detecting pathogens in clinical samples. It is also better suited to discover novel and highly divergent viruses and identify co-infecting pathogens, which cannot be recognized by pathogen-specific diagnostic assays [reviewed in 53,57]. Thus, the metagenomic HTS approach is more efficient in identifying pathogens than using a large panel of species-specific molecular assays or poorly designed diagnostic assays [reviewed in 57]. The metagenomic HTS identified hitherto unknown viruses in different outbreaks: Lujo virus, MERS-CoV, Schmallenberg orthobunyavirus, atypical porcine pestivirus, and SARS-CoV-2 [8,58–61]. However, several issues hinder its adoption for routine diagnostics, which will be discussed in section 1.4.2.

The generic HTS approach can also obtain viral whole-genome sequences in samples with adequate virus-to-host nucleic acid (NA) ratio. Otherwise, two targeted HTS approaches can be utilized for improved viral whole-genome sequencing [reviewed in 50] (Figure 3).

(2) The target-enrichment HTS approach utilizes biotinylated DNA or RNA probes (baits) complementary to specified viral sequences. In this enrichment step, probes hybridize with target library molecules. Probe-library molecule hybrids are bound to a solid phase (*e.g.,* streptavidin-labeled magnetic beads), and untargeted library molecules are washed away [62] (Figure 3). This approach enables the assembly and characterization of clinically relevant viral genomes of varying sizes, ranging from hepatitis C virus (9.6 kilobases) to human cytomegalovirus (236 kilo-base pairs) [62–64]. Binding affinity can also tolerate several mismatches between bait and target, allowing variant detection [65]. The specificity of this approach improves as the number of reference sequences for probe design increases. However, this approach is time-consuming, expensive, requires high technical expertise, and unsuitable for detecting novel viruses with low homology to reference sequences [reviewed in 50].

(3) In the PCR amplicon-HTS approach, primers bind to target sequences and these regions are amplified. Typical primer design employs a tiling amplicon scheme to cover a viral whole-genome sequence [66]. These amplicons are prepared for HTS (Figure 3). Compared to the other two HTS approaches, the PCR amplicon-HTS approach is cheaper and demonstrates, in most cases, higher sensitivity and specificity in enriching viral sequences. This approach was employed to investigate several epidemics caused by the Ebola virus, Zika virus, Usutu virus, and SARS-CoV-2 [66–69]. However, few mismatches between primers and template genome can prevent primer binding and amplification. A priori sequence knowledge is also necessary for the primer design. Thus, this HTS approach is unsuitable for targeting sequences from novel and highly diverse viruses [reviewed in 50]. Moreover, the DNA polymerase can incorporate wrong nucleotides during synthesis, and these errors can accumulate when a high number of PCR cycles is used [66].
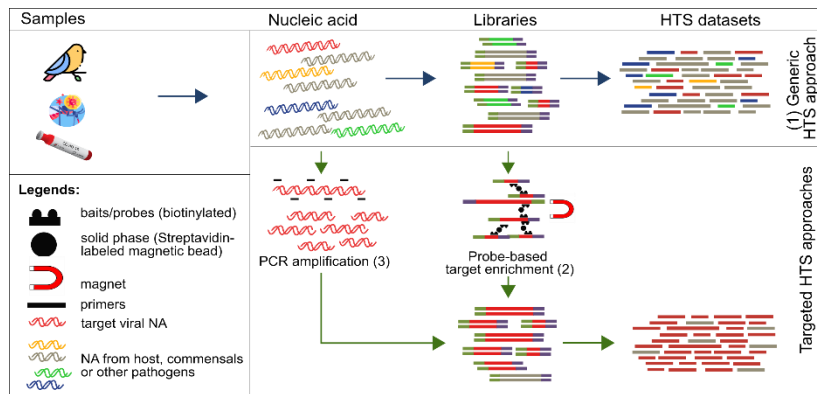
Figure 3. Different high throughput sequencing (HTS) approaches for viral genome sequencing: (1) Generic HTS approach enables the sequencing of all nucleic acid (NA) in a given sample, (2) Target enrichment HTS approach includes enriching target sequences using a panel of probes. (3) PCR amplicon HTS approach includes the amplification of target sequences with specific primers. This figure was based on the review of Houldcroft et al. [50]. Images acquired from Pixabay under Pixabay license (https://pixabay.com/service/terms/#license).

1.4. Utilizing HTS approaches in improving preparedness and response to outbreaks

High-throughput sequencing technologies are reshaping the surveillance of emerging infectious diseases, which enable the rapid identification of causative agents in diseases and genome-based outbreak investigations [61,70]. Furthermore, HTS technologies can be utilized to actively screen for novel pathogens with epidemic potential, allowing evidence-based preparedness and control for future outbreaks [71].

1.4.1 Sequence-based virus outbreak investigation

Traditional epidemiological approaches depend on case/incidence reports, including epidemiological metadata (*e.g.,* sample collection date and location) and interview-based contact tracing to estimate key epidemic parameters, reconstruct transmission chains, and devise an informed epidemic control policy [72–74]. For several decades, virus genomics has also been employed to investigate infectious disease outbreaks [reviewed in 75], and this is termed genomic epidemiology [reviewed in 18].

Viral genomes (particularly RNA virus genomes) accumulate genetic variations through high mutation and replication rates on a similar timescale as their epidemiological spread [76,77]. Hence, viral genome sequences collected over short epidemic periods can reveal the epidemiological dynamics and emergence of an infectious disease outbreak. Thus, genomic epidemiology empowers traditional outbreak investigation and infectious disease surveillance [74].

Phylogenetic inference is typically utilized to resolve evolutionary relationships between viruses based on the temporal resolution found in their sequences [78,79]. The 'traditional' approach (multiple tree search on bootstrapped data) and the Bayesian approach are two statistical inference methodologies for reconstructing phylogenies [reviewed in 80]. The

maximum likelihood (ML), a 'traditional' approach, calculates all possible mutational pathways compatible with the aligned sequences [81]. This method provides consistent and robust statistical inference; however, it requires long computational times [reviewed in 80]. As an alternative, the faster Bayesian approach for phylogenetic analyses has been introduced [82]. The Bayesian approach integrates the prior probability of a phylogeny with tree likelihood to yield trees with posterior probability distribution [82,83]. This method enables the implementation of complex models of sequence evolution and integration of relevant data for phylogenetic inferences [reviewed in 80]. Epidemiological data and mathematical models can be included in the reconstruction of a phylogenetic tree. For instance, the "phylodynamic approach" integrates phylogenetic inferences, population genetics, epidemiological data, and mathematical modeling to reconstruct the evolutionary history and transmission dynamics of a pathogen [79,84]. Additionally, the "phylogeographic approach" incorporates phylogenetic inferences with discrete traits (*e.g.,* geographic location, hosts) to determine the effect of each trait in infectious disease outbreak emergence and dynamics [85,86].

Viral genome sequencing and phylogenetic analysis can be utilized for precise taxonomic identification and classification of known and also novel viruses. They are also instrumental for understanding emerging viruses' spillover dynamics and identifying their natural host reservoirs [78]. Moreover, recent advances in HTS approaches and phylogenetic analyses enabled the resolution of some basic questions regarding infectious disease outbreaks [reviewed in 18], to name a few: (1) large-scale sequencing and phylogenetic analyses revealed that the 2009 H1N1 influenza A pandemic originated in swine populations from Mexico [87,88]; (2) genomic epidemiology provided evidence that the intermediate hosts of MERS-CoV are dromedary camels [89]; (3) sequencing and phylogeographic analyses exhibited the spread and evolution of WNV in the Americas for 20 years [90].

1.4.2 Sequenced-based virus discovery and characterization as tools for outbreak preparedness?

Early detection and rapid genetic characterization of emerging infectious diseases might enable the containment of an outbreak at a local level, reducing its devastating effects on human and animal populations [91]. The global early warning and response system focused more on recognizing the early onset outbreaks [92]. However, Carroll and colleagues [93] emphasized the necessity for an early warning system (EWS) that detects novel viral spillover before it emerges to a local outbreak. In both cases, metagenomic HTS (metagenomic analysis of generic HTS datasets) has proven to be a powerful tool for virus discovery, hypothesis-free pathogen identification, and virus genome characterization.

For early outbreak recognition, metagenomic HTS rapidly identified the etiological

agent (SARS-CoV-2) in a cluster of patients with atypical pneumonia in China that progressed into the current COVID-19 pandemic [61], which is remarkably faster compared to the identification of causative agents of previous global epidemics (Table 1). Moreover, the early availability of novel SARS-CoV-2 whole-genome sequences enabled the rapid development of diagnostic assays [94,95], virus reconstruction using reverse genetic systems [96], and swift vaccine development [97], which all are essential tools in pandemic response and mitigation [reviewed in detail in Publication I].

Table 1. Timelines of recent global epidemics.

Disease	Virus	First report/ Index case	Pathogen identification (Date)	Genome available (Date)	References
SARS	SARS-CoV	Nov 2002	Mar 2003	Apr 2003	[98–101]
2009 H1N1 pandemic	H1N1	25 Mar 2009	15 Apr 2009	24 Apr 2009	[20,102, 103]
MERS	MERS-CoV	13 Jun 2012	24 Sep 2012	27 Sep 2012	[8,104]
COVID-19	SARS-CoV-2	31 Dec 2019	9 Jan 2020	20 Jan 2020	[61]

For surveillance of virome diversity, numerous novel viral sequences in humans [99,100], domestic animals [105,106], wildlife [107–111], blood-sucking vectors [reviewed in 112], other arthropods [113,114], and specific environments [115,116] were discovered and characterized using metagenomic HTS approaches. However, most of these newly discovered viruses have unknown pathogenicity. Thus, Canuti and van der Hoek [117] recommend that sequence-based pathogen discovery should be accompanied by virus characterization to understand the role of newly discovered viruses in a disease. Virus characterization includes but is not limited to *in silico* analyses of viral genomes, epidemiological investigation, virus isolation, and disease association testing. Association between virus and disease can be established when the Henle-Loeffler-Koch's postulates are fulfilled [118]. One of the postulates requires that the pathogen must be isolated from a diseased organism; however, numerous viruses cannot be propagated *in vivo* [119]. To overcome this problem, Mokili and colleagues [27] proposed a modified metagenomic Henle-Loeffler-Koch's postulates that require differential metagenomic traits between healthy and diseased individuals. Mokili and colleagues' modified postulates only involve inoculating healthy individuals with a diseased subject instead of a pathogen grown in pure culture [27].

However, the analytic sensitivity of metagenomic HTS is influenced by several variables that depend on test design (*e.g.,* completeness of reference database), pathogen (*e.g.,* genome size), and specimen type (*e.g.,* pathogen-to-host ratio) [120]. Furthermore, this approach is challenged by specificity issues (misclassification or cross-contamination), inconsistency of bioinformatics pipelines, and costs [reviewed in 121]. These challenges hinder the adoption of metagenomic HTS for routine diagnostics [120] and active surveillance of novel pathogens in wildlife reservoirs [reviewed in 122].

2. Objectives

Due to increasing threats of viral infectious diseases in humans and animals, a training network that focuses on outbreak preparedness and response was established. In line with this program, this thesis aimed to establish a unified pipeline for routine outbreak investigation and early warning system, which could enhance the outbreak preparedness and response through the early detection of pathogens with outbreak potential.

This thesis focused on the following objectives:

(1) to develop an early warning system for the detection of novel and unexpected pathogens using generic and unbiased HTS datasets derived from routine outbreak investigations

(2) to investigate causative agents of infectious disease outbreaks and suspected pathogens with outbreak potential, which were identified either by the routine surveillance or the early warning system, with regards to genetic characterization, molecular-based screening, and/or *in vitro* isolation

3. Publications

(I) Preparedness needs research: How fundamental science and international collaboration accelerated the response to COVID-19

Cormac M. Kinsella, Pauline Dianne Santos, Ignacio Postigo-Hidalgo, Alba Folgueiras-Gonzalez, Tim Casper Passchier, Kevin P. Szillat, Joyce Odeke Akello, Beatriz Alvarez Rodrıguez, and Joan Martı-Carreras

PLOS PATHOGENS

Preparedness needs research: How fundamental science and international collaboration accelerated the response to COVID-19

Cormac M. Kinsella[1]*, Pauline Dianne Santos[2], Ignacio Postigo-Hidalgo[3], Alba Folgueiras-González[4], Tim Casper Passchier[5], Kevin P. Szillat[2], Joyce Odeke Akello[6,7,8], Beatriz Álvarez-Rodríguez[5], Joan Martí-Carreras[9]

1 Laboratory of Experimental Virology, Department of Medical Microbiology and Infection Prevention, Amsterdam UMC, University of Amsterdam, Amsterdam, the Netherlands, 2 Institute of Diagnostic Virology, Friedrich-Loeffler-Institut, Greifswald-Insel Riems, Germany, 3 Charité –Universitätsmedizin Berlin, Corporate Member of Freie Universität Berlin, Humboldt-Universität zu Berlin, and Berlin Institute of Health, Institute of Virology, Berlin, Germany, 4 Department of Discovery and Technology, MSD Animal Health, Boxmeer, the Netherlands, 5 School of Molecular and Cellular Biology, Faculty of Biological Sciences, University of Leeds, Leeds, United Kingdom, 6 Institute for Infectious Diseases, University of Bern, Bern, Switzerland, 7 Biology Division, Spiez Laboratory, Swiss Federal Office for Civil Protection, Spiez, Switzerland, 8 Graduate School for Cellular and Biomedical Sciences, University of Bern, Bern, Switzerland, 9 Laboratory of Clinical and Epidemiological Virology, Department of Microbiology, Immunology and Transplantation, Rega Institute for Medical Research, KU Leuven, Leuven, Belgium

☯ These authors contributed equally to this work.
* c.m.kinsella@amsterdamumc.nl

Abstract

The first cluster of patients suffering from coronavirus disease 2019 (COVID-19) was identified on December 21, 2019, and as of July 29, 2020, severe acute respiratory syndrome coronavirus 2 (SARS-CoV-2) infections have been linked with 664,333 deaths and number at least 16,932,996 worldwide. Unprecedented in global societal impact, the COVID-19 pandemic has tested local, national, and international preparedness for viral outbreaks to the limits. Just as it will be vital to identify missed opportunities and improve contingency planning for future outbreaks, we must also highlight key successes and build on them. Concomitant to the emergence of a novel viral disease, there is a 'research and development gap' that poses a threat to the overall pace and quality of outbreak response during its most crucial early phase. Here, we outline key components of an adequate research response to novel viral outbreaks using the example of SARS-CoV-2. We highlight the exceptional recent progress made in fundamental science, resulting in the fastest scientific response to a major infectious disease outbreak or pandemic. We underline the vital role of the international research community, from the implementation of diagnostics and contact tracing procedures to the collective search for vaccines and antiviral therapies, sustained by unique information sharing efforts.

Introduction

Since 1950, the global population has tripled to 7.8 billion, with expansion in meat consumption and living area thought to increase human exposure to microbes infecting wildlife, with occasional 'spillover' to people [1]. Approximately 60% of human infectious diseases are zoonotic [2] (transmitted from animals). Zoonoses capable of human-to-human transmission can emerge as catastrophic diseases; acquired immunodeficiency syndrome (AIDS) alone has killed an estimated 32 million [3], whilst coronavirus disease 2019 (COVID-19) has caused the largest global economic crisis since the Great Depression [4].

Speed of response is critical with respect to mitigation of infectious outbreaks, since in a susceptible population, the number of infections may increase exponentially. The aim of outbreak preparedness is therefore to ensure that contingency planning is in place beforehand to avoid delays associated with an ad hoc response, thus enabling intervention whilst case numbers are low. For well-established diseases such as measles in humans, this preparation includes systems for (1) **detection** by routine surveillance, (2) **confirmation** by designated specialist laboratories, and (3) **response**, which will be uniquely tailored to the situation [5]. Contrastingly, spillover of a novel pathogen entails additional complications caused by gaps in fundamental knowledge and validated technical resources. Since this 'research and development gap' impinges on the effectiveness and rate of response, it is an important factor that must be considered in the context of preparedness [6].

The novel pathogen research and development landscape

An outbreak caused by a novel pathogen requires a rapid research effort across the experimental and clinical spectrum. As an outbreak response progresses, research and development continue to play an integral role at each stage (summarised in Fig 1). Here, we describe the various aspects of this research and development landscape using COVID-19 as an example, with emphasis on recent factors that have accelerated the response to the outbreak.

The detection of COVID-19 and the discovery of SARS-CoV-2

When unusually high incidence of a clinical syndrome is observed in a group of patients (a cluster), there may be suspicion of a shared infection, which could constitute an outbreak. Initial investigation must therefore identify what pathogen is present in order to confirm an outbreak and kick-start a response. The first cluster of patients with COVID-19 was identified on December 21, 2019, after which investigations were carried out by the Chinese Center for Disease Control and Prevention and the National Institute of Viral Disease Control and Prevention [7,8]. A diagnostic panel covering 22 human pathogens was run on these patients, with universally negative results [8]. This immediately raised suspicion of a novel pathogen, requiring discovery methods.

Virus discovery methods include polymerase chain reaction (PCR) assays targeting conserved genome regions specific to all members of a taxonomic family (potentially even unknown ones), attempted virus isolation in cell culture, microscopy to study the virion morphology, and metagenomic analysis of human samples for the identification of the pathogen. These analyses were carried out on samples from the initial COVID-19 cluster and published in a remarkably short 34 days [8] (Fig 2). Virus was grown in primary human airway epithelial cell cultures, which provide optimal substrates for coronavirus replication [9,10], and transmission electron microscopy images were generated, showing the spherical virion and surface spikes characteristic of coronaviruses [8]. The first severe acute respiratory syndrome coronavirus 2 (SARS-CoV-2) genomes were published online on January 10, 2020 (Fig 2), 20 days after cluster detection (GISAID accessions EPI_ISL_402119 and EPI_ISL_402121), and phylogenetic analyses showed the virus was a relative of both severe acute respiratory syndrome
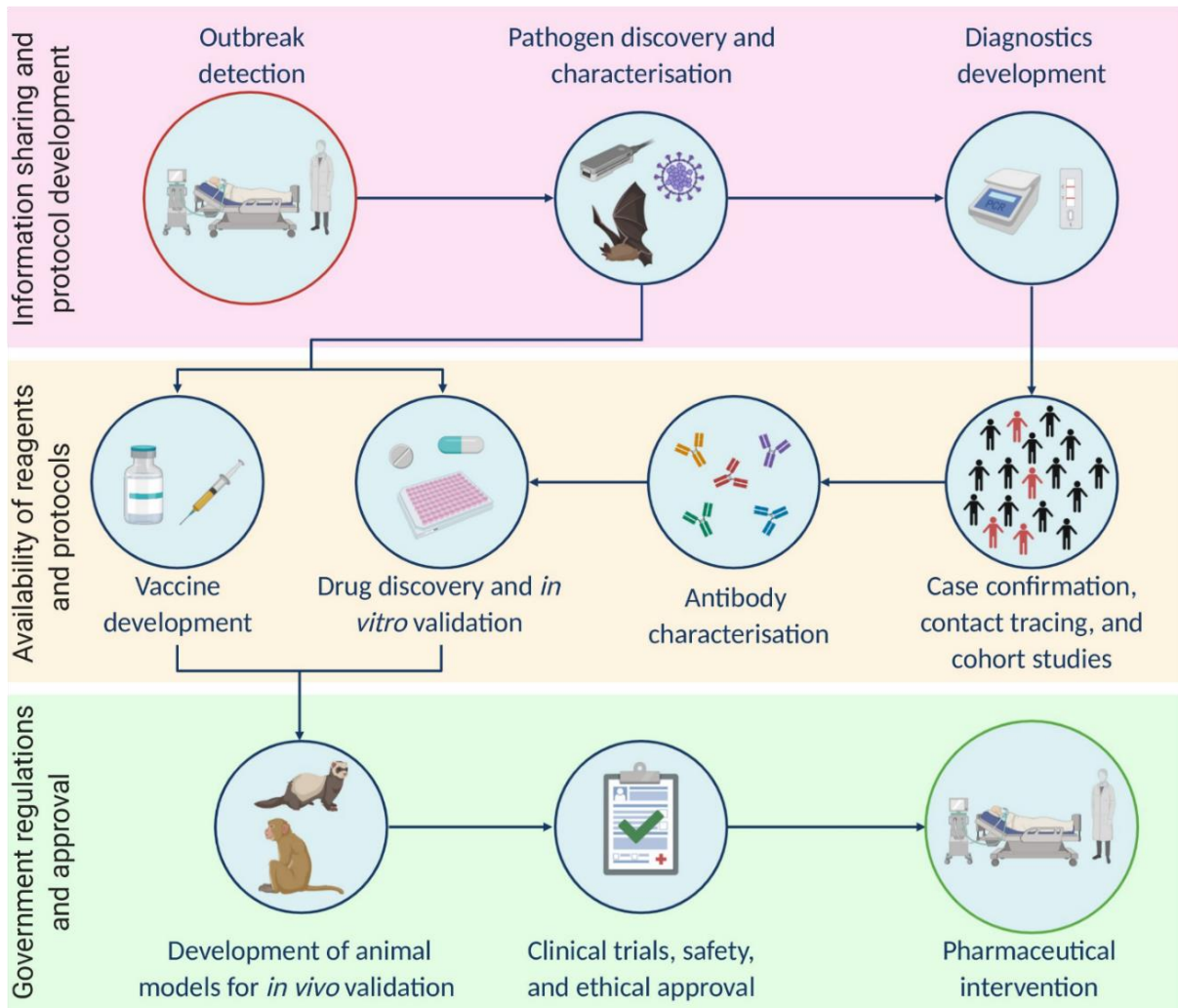
Fig 1. Key components of the research response to viral outbreaks are shown as a simplified workflow. Factors complicating the delivery of each step are annotated on the left.

coronavirus (SARS-CoV-1) [7] (i.e., the etiological agent of the 2002–2004 SARS outbreak) and a strain sampled from a bat [11], confirming a novel zoonotic virus outbreak and kick-starting research efforts worldwide.

Testing, tracing, and isolating

When facing a novel pathogen, an immediate research priority is the development of diagnostic assays to detect infected individuals. Testing in the clinic ensures that COVID-19 patients are separated from SARS-CoV-2 negative individuals and confirms viral shedding has ceased before discharge. Testing in the community uncovers viral transmission dynamics to support
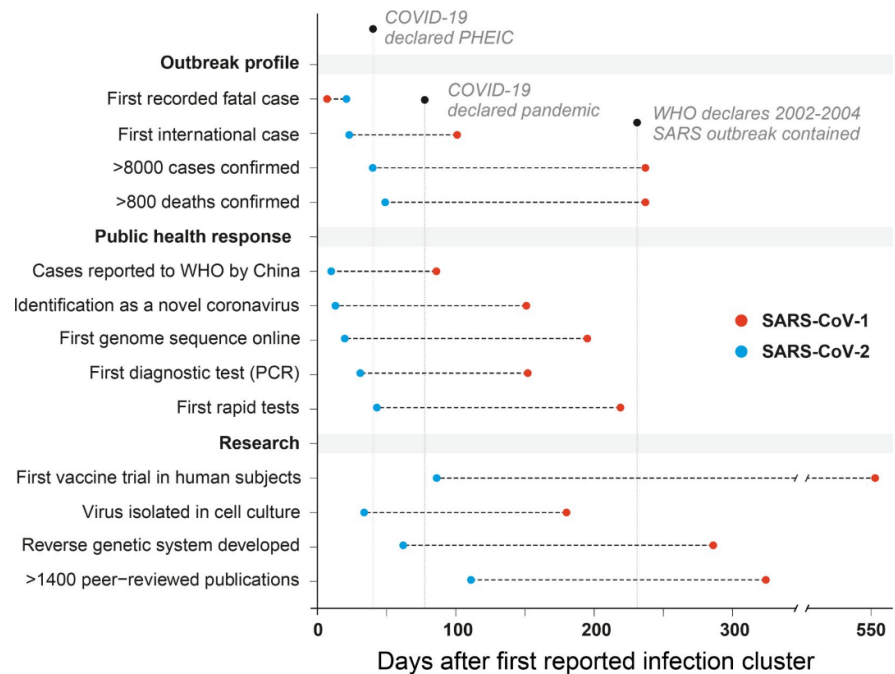
Fig 2. The changing dynamics of research response: contrasting the SARS-CoV-1 and SARS-CoV-2 outbreaks. COVID-19, coronavirus disease 2019; PCR, polymerase chain reaction; PHEIC, Public Health Emergency of International Concern; SARS-CoV-1, severe acute respiratory syndrome coronavirus; SARS-CoV-2, severe acute respiratory syndrome coronavirus 2; WHO, World Health Organization.

control policies, such as prevalence in vulnerable demographics [12], case fatality [13], or the viral basic reproduction number [14] (i.e., R_0, the average number of further infections arising from 1 case in a naïve population). The first specific PCR assay for SARS-CoV-2 RNA was designed, validated, and published [15] within 13 days of the first genome being made available online (Fig 2). Loop-mediated isothermal amplification (LAMP) assays, which can rapidly and sensitively detect viral RNA or cDNA with minimal equipment, were also validated on patient samples only 2 months after the outbreak emerged [16–18].

Tracing viral spread by identifying infected individuals and their potential contacts enables interventions such as selective quarantine, a method that has long been deployed as a firebreak to epidemic spread. Contact tracing is being applied during the current pandemic; however, with the surge in COVID-19 cases, it has become increasingly challenging to conduct [19]. Technological solutions in the form of privacy-protecting open-source contact tracing apps have emerged rapidly, such as the TraceTogether app of Singapore, released in March 2020. This uses Bluetooth to log other app users that come in close proximity, storing their phone numbers in encrypted form for 14 days, data which are only accessible by the Health Ministry after approach by a contact tracer. With Apple and Google engaged in a similar effort [20], in the future, such software solutions may be integrated with standard phone operating systems and become status quo tools during epidemics.

In addition to diagnostic testing and contact tracing, genomic epidemiology can today be used to describe the evolution of a virus in time and space, uncovering transmission patterns

[21]. Importantly, this is now a real-time tool rather than a retrospective one. Whereas the first SARS-CoV-1 genome was published over 6 months into the 2002–2004 outbreak [22] (Fig 2), nearly 5 months into the SARS-CoV-2 pandemic, over 27,000 complete genomes could be downloaded from the GISAID sequence repository (www.gisaid.org). Technological advances in high-throughput sequencing have made this possible, first via short-read technologies such as Solexa (now Illumina), first available in 2006, and second by the 2014 commercial implementation of nanopore sequencing by Oxford Nanopore Technologies. These platforms are commonly used to investigate SARS-CoV-2 transmission clusters, for example, by the COVID-19 Genomics UK (COG-UK) consortium [23], which has sequenced thousands of virus genomes during the pandemic. Due to a relatively low entry price, nanopore technology has been decisive in improving accessibility to sequencing, reinforced by initiatives including the ARTIC Network [24], who quickly developed and published primer schemes and protocols for amplicon sequencing of whole SARS-CoV-2 genomes. Analysis of this wealth of data has also been made more accessible by online tools; for example, the Nextstrain platform [25] is being used to integrate genomic, geographical, and temporal data to visualise patterns of SARS-CoV-2 spread, whilst CoV-GLUE, an online resource created using the Genes Linked by Underlying Evolution (GLUE) [26] software environment, focuses on identifying and tracking new variants.

Utilising the genome: Fundamental research and development

A viral genome sequence is a launchpad for a range of parallel research goals aiming to deliver technical resources and fundamental knowledge about a new pathogen. The genome provides the sequences of protein-coding genes, which are used to safely produce pure stocks of individual viral proteins. The gene sequence is first amplified from a clinical sample or viral culture using PCR or is synthetically constructed. The DNA is delivered to cells, which produce (express) the protein encoded by the gene. Viral proteins are used in the generation of traditional antibody-based diagnostic assays, such as enzyme-linked immunosorbent assays (ELISAs), which are designed to detect viral proteins in patient samples or patient antibodies against the virus [27]. Although PCR is considered the gold standard for laboratory diagnosis of an active SARS-CoV-2 infection [28], serological assays can detect historical infections and play a key role in determining population attack rates and potentially protective immunity levels [29,30]. Lateral flow assays (LFAs) are used as rapid tests for prior viral exposure and were first reported 2 months after cluster identification [31–33].

Whilst the amino acid sequence of a protein can be accurately predicted from the nucleotide sequence of its encoding gene, the protein conformational structure that determines its function cannot, and must be solved using structural biology techniques. Hardware and data processing performance revolutions in recent years have dramatically accelerated the generation of high-resolution structures; only 2 months after the first SARS-CoV-2 genome was released, a 3.5 Å resolution cryogenic electron microscopy (cryo-EM) structure of the spike protein was published [34], revealing differences to SARS-CoV-1 that preclude the binding of some anti-SARS-CoV-1 antibodies. This was followed in short order by structures including the cellular receptor ACE2 [35] bound to the spike protein [36], the SARS-CoV-2 nucleocapsid RNA-binding domain [37], and the SARS-CoV-2 main protease [38]. This structural information is useful for in silico modelling of protein–protein interactions and high-throughput computational screening of chemical compounds with potential antiviral properties. Another remarkable approach to find drug targets exploited expression of SARS-CoV-2 proteins in human cells, followed by separation of the viral proteins (and bound host proteins) from the host background. Identification of bound host proteins by mass spectrometry revealed a number of druggable candidates that may represent therapeutic targets [39].

In vivo studies such as those in livestock, frugivorous bats, and companion animals are necessary to establish their potential role in forming viral reservoirs and to provide data that are informative on the possible pathways of SARS-CoV-2 transmission from its wild reservoir to humans [40,41]. Furthermore, nonhuman primate models will be key to expediting preclinical evaluation of vaccines and other therapeutics for use in humans [42,43]. Establishment of viral cultures is vital for numerous downstream applications, including generating these in vivo infection models for therapeutic testing [44], antiviral screening [45], and fundamental virus characterisation [46]. Traditionally, a clinical sample containing replication competent virus would be required; however, access to samples for researchers in countries without active cases is often logistically difficult in the early phases of an outbreak. Today, only a genome sequence is required—synthetic DNA technology allows the reconstruction of viral genomes in artificial vectors—from which viable infectious RNA can be produced and replicating virus rescued. The first such SARS-CoV-2 culture was achieved only 1 week after delivery of synthetic DNA constructs spanning the genome [47] and reported 42 days after the first genome became available. This technology offers a powerful platform to carry out reverse genetic approaches using genetic engineering to study genotype-to-phenotype relationships and the function of viral components, and also enables validation of diagnostic tests in the absence of clinical specimens [15].

Delivering pharmaceutical interventions to the clinic

The future trajectory of the SARS-CoV-2 pandemic is uncertain; however, elimination of the virus may depend on the availability of antiviral treatments and vaccines. Delivery of novel pharmaceutical interventions from conception to clinic is a prolonged process with numerous practical and regulatory hurdles to cross, necessitating short-term stopgaps. Repurposing of drugs already approved for human usage is an attractive option: their production is already optimised and upscaled, and they have known safety and bioavailability data, allowing human clinical trials to proceed rapidly after testing of in vitro efficacy. However, the repurposing of approved drugs can have major consequences in outbreak situations, causing acute shortages and rendering them unavailable to patients using them for the licensed indication [48]. Furthermore, medications can have potentially serious side effects, and emergency use approval may entail an uncertain risk/benefit profile, as seen with the example of hydroxychloroquine, which recently had its emergency use authorisation (EUA) revoked by the United States Food and Drug Administration (FDA) [49].

Clinical trials of therapeutic drugs involving hundreds of COVID-19 patients were ongoing by early February [50]. During March and April, numerous compounds were identified that either have direct action on SARS-CoV-2 in vitro [45,51–53] or may have indirect action via host proteins [39,54], paving the way for in vivo efficacy trials (Fig 1). Furthermore, on the basis of 2 clinical trials, the FDA granted an EUA of remdesivir for COVID-19 treatment on May 1, 2020 [55]. This was the first direct antiviral approval, just over 4 months into the outbreak.

Delivery of neutralising antibodies (nAbs) to patients early in disease is another treatment option. Serum from convalescent COVID-19 patients contains anti-SARS-CoV-2 antibodies, and donated serum can be infused to acutely ill patients [56,57]. Other options include products containing purified polyclonal antibodies from the pooled sera of COVID-19 survivors [58], through to the identification and characterisation of monoclonal nAbs, since these have the potential to be produced in large quantities and delivered as immunotherapy. By February, a SARS-CoV-1 nAb (CR3022) was reported to bind the receptor-binding domain of SARS-CoV-2 spike protein [59]; however, it was later shown not to cross-neutralise the virus [60]. In

early April, an antibody (S309) from a SARS-CoV-1 survivor was found to neutralise SARS-CoV-2 [61], followed in May by a humanised antibody (47D11) capable of blocking infection with both SARS-CoV-1 and SARS-CoV-2 in vitro [62]. Also in May, a team demonstrated in vivo protection against high-dose SARS-CoV-2 challenge in Syrian hamsters after injection of a human monoclonal nAb [63], whilst another reported identification of 19 SARS-CoV-2 nAbs [64]. This was accomplished by isolating individual B cells reacting to native-like SARS-CoV-2 spike protein, followed by expression of the encoded antibodies and virus neutralisation assays. Importantly, highly potent nAbs were found that targeted different regions of the spike protein, implying suitability as a cocktail therapy with reduced risk of viral escape.

Vaccines are used to safely increase immunity levels against pathogens in populations in order to protect individuals and reduce pathways to viral spread. For SARS-CoV-2, a remarkably fast and broad vaccine development response was initiated, with the first candidate reaching human trials only 86 days after cluster identification [65], over 6 times faster than the first SARS-CoV-1 human vaccine trial [66] (Fig 2). At the time of writing, 35 candidates had reached human trials, with 122 more in preclinical development [67]. A range of vaccine platforms (different core approaches to elicit antibody-based immunity and their associated manufacturing pipelines) are being trialled [68]. Amongst them are next-generation techniques like mRNA vaccination [65], which requires relatively little development time after viral genome sequencing. If successfully tested and deployed, these novel concepts may establish themselves more firmly within the vaccine ecosystem and potentially accelerate vaccine development beyond the SARS-CoV-2 pandemic. However, the implementation of novel pharmaceutical interventions will ultimately be subject to the normal technical challenges involved with upscaling production to meet massive demand and will be dependent on the availability of appropriate production lines [68]. Many of the novel vaccine approaches currently being trialled have never been manufactured at this scale, suggesting unforeseen scalability issues may place future roadblocks.

Information, property, and knowledge sharing

Against the backdrop of technological advancements that have boosted outbreak research capacity in recent years, key paradigm shifts in information sharing have also occurred, dramatically increasing how quickly and widely new results and data are received by other researchers and the public. In a rapidly evolving situation, maximum data utility is achieved by prompt release. The pace of viral genome publication during crises was highlighted as a problem during the 2014–2016 Ebola outbreak [69], yet arguably a sea change has occurred since. Furthermore, databases have emerged that compile COVID-19 publications and data resources [70] or provide daily updates on outbreak data worldwide [71–74], accessible to all. For researchers, the open access *bioRxiv* and *medRxiv* preprint servers (launched in 2013 and 2019, respectively) have become invaluable resources for the rapid dissemination of results, hosting a combined 7,060 articles by July 29, 2020. The cost of this speed is the absence of peer review, which can sometimes result in the publication of data falling below a necessary quality standard. Encouragingly, this openness has not been limited to academic spheres; many major technology companies including Intel, Microsoft, and Amazon have temporarily granted open access to their patent libraries for SARS-CoV-2-related research as part of the 'Open COVID Pledge' [75] to encourage innovation via sharing of intellectual property. Some pharmaceutical companies have also made similar moves, from AbbVie (North Chicago, USA) agreeing not to enforce patent rights on a drug in COVID-19 trials [76] to Roche (Basel, Switzerland) sharing the composition of a buffer in their diagnostic kit with the Dutch government [77]. Numerous community-driven efforts have also sprouted, from 3D printing and donation of personal

protective equipment [78] to the repurposing of company production lines to manufacture and donate essential materials such as hand sanitiser [79].

Timely and high-quality scientific research relies on knowledge sharing between teams with varying expertise and facilities, making connectivity a keystone component of research preparedness for outbreaks. Whilst the World Health Organization (WHO) plays a crucial role in coordinating global research efforts in response to the COVID-19 pandemic, pre-existing networks and formal consortia of trusted partners can immediately coordinate to form focus groups and share resources [15]; several of these have been formed in response to major epidemics of recent years (Table 1). Some of these, such as Platform for European

Table 1. A selection of the many networks and consortia conducting research into SARS-CoV-2 and COVID-19.

Networks	Focus	Website
ACTIV	Accelerating COVID-19 Therapeutic Interventions and Vaccines	https://www.nih.gov/research-training/medical-research-initiatives/activ
ARTIC Network	Real-time molecular epidemiology for outbreak response	https://artic.network/
CEPI	Coalition for Epidemic Preparedness Innovations	https://cepi.net/
COMPARE	COllaborative Management Platform for detection and Analyses of (Re-)emerging and foodborne outbreaks in Europe	https://www.compare-europe.eu/
COPCOV	Chloroquine/ hydroxychloroquine prevention of Coronavirus Disease (COVID-19) in the healthcare setting; a randomised, placebo-controlled prophylaxis	https://www.tropmedres.ac/covid-19/copcov
COV-IRT	COVID-19 International Research Team	https://covirt19.org/
COVID-19 CRC	COVID-19 Clinical Research Coalition	https://covid19crc.org/
ECRAID	European Clinical Research Alliance on Infectious Diseases	https://www.ecraid.eu/
eMERGE	Electronic Medical Records and Genomics	https://emerge-network.org/
GLOPID-R	Global Research Collaboration for Infectious Disease Preparedness	https://www.glopid-r.org/
HONOURs	Host switching pathogens, infectious outbreaks, and zoonosis	https://www.honours.eu/
IDCRC	Infectious Diseases Clinical Research Consortium	https://med.emory.edu/departments/medicine/divisions/infectious-diseases/idcrc/index.htm
INITIATE	Innate-Immunometablism as Antiviral Target	https://initiate-itn.eu/
ISARIC	International Severe Acute Respiratory and emerging Infection Consortium	https://isaric.tghn.org/
PANDORA	Pan-African Network For Rapid Research, Response and Preparedness for Infectious Diseases Epidemics	https://pandora.tghn.org/
PREPARE	Platform for European Preparedness Against (Re-)emerging Epidemics	https://www.prepare-europe.eu/
RECOVER	Understand the COVID-19 pandemic through clinical research in order to transform patient care and public health responses	https://www.recover-europe.eu/
Solidarity	International clinical trial to help find an effective treatment for COVID-19, launched by WHO and partners	https://www.who.int/emergencies/diseases/novel-coronavirus-2019/global-research-on-novel-coronavirus-2019-ncov/solidarity-clinical-trial-for-covid-19-treatments
VIRUS-X	Viral metagenomics for innovation value	http://virus-x.eu/
ZAPI	Zoonotic Anticipation and Preparedness Initiative	https://www.imi.europa.eu/projects-results/project-factsheets/zapi

ACTIV, Accelerating COVID-19 Therapeutic Interventions and Vaccines; CEPI, Coalition for Epidemic Preparedness Innovations; COMPARE, COllaborative Management Platform for detection and Analyses of (Re-)emerging and foodborne outbreaks in Europe; COPCOV, Chloroquine/ hydroxychloroquine prevention of Coronavirus Disease (COVID-19) in the healthcare setting; COVID-19, coronavirus disease 2019; COVID-19 CRC, COVID-19 Clinical Research Coalition; COV-IRT, COVID-19 International Research Team; ECRAID, European Clinical Research Alliance on Infectious Diseases; eMERGE, Electronic Medical Records and Genomics; GLOPID-R, Global Research Collaboration for Infectious Disease Preparedness; IDCRC, Infectious Diseases Clinical Research Consortium; INITIATE, Innate-Immunometablism as Antiviral Target; ISARIC, International Severe Acute Respiratory and emerging Infection Consortium; PANDORA, Pan-African Network For Rapid Research, Response and Preparedness for Infectious Diseases Epidemics; PREPARE, Platform for European Preparedness Against (Re-)emerging Epidemics; RECOVER, Rapid European COVID-19 Emergency Response research; SARS-CoV-2, severe acute respiratory syndrome coronavirus 2; WHO, World Health Organization; ZAPI, Zoonotic Anticipation and Preparedness Initiative.

https://doi.org/10.1371/journal.ppat.1008902.t001

Preparedness Against (Re-)emerging Epidemics (PREPARE) [80] and HONOURs [81], specifically train research preparedness concepts to the next generation of scientists. An advantage of larger networks is the ability to coordinate multi-armed studies with unified procedures and centralised administration, in order to maximise sample size and achieve consensus faster. For this purpose, WHO launched the Solidarity clinical trial for testing COVID-19 treatments [82], which involves over 100 countries and intends to complete 80% faster than a typical randomised clinical trial. Representative national ethics committees supported by WHO, funding agencies, and relevant collaborative research consortia provided statements guiding the conduct of COVID-19 research, which helps to standardise and expedite ethical research [83]. Another important contribution of international collaborations, such as the COVID-19 Clinical Research Coalition (CRC) (Table 1), is the acceleration of COVID-19 research in low-to-middle-income countries (LMIC) where research resources, laboratory facilities, and manufacturing infrastructures are commonly limited relative to high-income countries [84].

Outlook

The SARS-CoV-2 pandemic has been an unprecedented test of novel pathogen outbreak preparedness, revealing strengths and weaknesses in all domains. As we have highlighted here, research capacity to respond to novel outbreaks is at an all-time high. The massive threat that viral outbreaks pose to lives and economies underscores the need to build on this success by promoting fundamental research capacity and networks of collaboration.

Acknowledgments

We thank all investigators and early stage researchers associated with the HONOURs programme for their enthusiasm and feedback, particularly Dr Lia van der Hoek as coordinator. We also thank Dr Robert Gifford, Dr Christian Beuret, Alexis Hoste, and Dr Mathieu Claireaux for specific feedback on the manuscript. Fig 1 was created with BioRender.com.

References

1. Plowright RK, Parrish CR, McCallum H, Hudson PJ, Ko AI, Graham AL, et al. Pathways to zoonotic spillover. Nat Rev Microbiol. 2017; 15:502–510. https://doi.org/10.1038/nrmicro.2017.45 PMID: 28555073

2. Taylor LH, Latham SM, Woolhouse MEJ. Risk factors for human disease emergence. Philos Trans R Soc B Biol Sci. 2001; 356:983–989.

3. Joint United Nations Programme on HIV/AIDS. Global HIV & AIDS statistics—2019 fact sheet. 2019. Available from: https://www.unaids.org/en/resources/fact-sheet.

4. International Monetary Fund. World Economic Outlook, April 2020: The Great Lockdown. In: World Economic Outlook Reports. 2020. Available from: https://www.imf.org/en/Publications/WEO/Issues/2020/04/14/weo-april-2020.

5. World Health Organization. Guidelines for epidemic preparedness and response to measles outbreaks. Geneva; 1999.

6. World Health Organization. R&D Blueprint. 2016. Available from: https://www.who.int/teams/blueprint.

7. Tan W, Zhao X, Ma X, Wang W, Niu P, Xu W, et al. Notes from the field: a novel coronavirus genome identified in a cluster of pneumonia cases—Wuhan, China 2019−2020. China CDC Wkly. 2020; 2:61–62.

8. Zhu N, Zhang D, Wang W, Li X, Yang B, Song J, et al. A novel coronavirus from patients with pneumonia in China, 2019. N Engl J Med. 2020; 382:727–733. https://doi.org/10.1056/NEJMoa2001017 PMID: 31978945

9. Pyrc K, Sims AC, Dijkman R, Jebbink M, Long C, Deming D, et al. Culturing the unculturable: human coronavirus HKU1 infects, replicates, and produces progeny virions in human ciliated airway epithelial cell cultures. J Virol. 2010; 84:11255–11263. https://doi.org/10.1128/JVI.00947-10 PMID: 20719951

10. Jonsdottir HR, Dijkman R. Coronaviruses and the human airway: a universal system for virus-host interaction studies Coronaviruses: emerging and re-emerging pathogens in humans and animals Susanna

Lau Emerging viruses. Virol J. 2016; 13:1–9. https://doi.org/10.1186/s12985-015-0456-4 PMID: 26728778

11. Zhou P, Yang X, Lou WXG, Hu B, Zhang L, Zhang W, et al. A pneumonia outbreak associated with a new coronavirus of probable bat origin. Nature. 2020; 579:270–273. https://doi.org/10.1038/s41586-020-2012-7 PMID: 32015507

12. Baggett TP, Keyes H, Sporn N, Gaeta JM. Prevalence of SARS-CoV-2 infection in residents of a large homeless shelter in Boston. J Am Med Assoc. 2020.

13. Verity R, Okell LC, Dorigatti I, Winskill P, Whittaker C, Imai N, et al. Estimates of the severity of corona-virus disease 2019: a model-based analysis. Lancet Infect Dis. 2020.

14. Li Q, Guan X, Wu P, Wang X, Zhou L, Tong Y, et al. Early transmission dynamics in Wuhan, China, of novel coronavirus–infected pneumonia. N Engl J Med. 2020; 382:1199–1207. https://doi.org/10.1056/NEJMoa2001316 PMID: 31995857

15. Corman VM, Landt O, Kaiser M, Molenkamp R, Meijer A, Chu DK, et al. Detection of 2019 novel corona-virus (2019-nCoV) by real-time RT-PCR. Eur Secur. 2020; 25:2000045.

16. Yu L, Wu S, Hao X, Dong X, Mao L, Pelechano V, et al. Rapid detection of COVID-19 coronavirus using a reverse transcriptional loop-mediated isothermal amplification (RT-LAMP) diagnostic platform. Clin Chem. 2020; 66:975–977. https://doi.org/10.1093/clinchem/hvaa102 PMID: 32315390

17. Zhang Y, Odiwuor N, Xiong J, Sun L, Nyaruaba RO, Wei H, et al. Rapid molecular detection of SARS-CoV-2 (COVID-19) virus RNA using colorimetric LAMP. medRxiv. 2020.

18. Ben-Assa N, Naddaf R, Gefen T, Capucha T, Hajjo H, Mandelbaum N, et al. SARS-CoV-2 on-the-spot virus detection directly from patients. medRxiv. 2020.

19. Ferretti L, Wymant C, Kendall M, Zhao L, Nurtay A, Abeler-Dörner L, et al. Quantifying SARS-CoV-2 transmission suggests epidemic control with digital contact tracing. Science. 2020; 368:eabb6936. https://doi.org/10.1126/science.abb6936 PMID: 32234805

20. Google Company Announcements. 2020. Available from: https://www.blog.google/inside-google/company-announcements/apple-and-google-partner-covid-19-contact-tracing-technology/.

21. Dellicour S, Durkin K, Hong SL, Vanmechelen B, Martí-Carreras J, Gill MS, et al. A phylodynamic work-flow to rapidly gain insights into the dispersal history and dynamics of SARS-CoV-2 lineages. bioRxiv. 2020.

22. Marra MA, Jones SJM, Astell CR, Holt RA, Brooks-Wilson A, Butterfield YSN, et al. The genome sequence of the SARS-associated coronavirus. Science. 2003; 300:1399–1404. https://doi.org/10.1126/science.1085953 PMID: 12730501

23. COVID-19 Genomics UK Consortium. Available from: https://www.cogconsortium.uk/.

24. ARTICnetwork. Available from: https://artic.network/.

25. Hadfield J, Megill C, Bell SM, Huddleston J, Potter B, Callender C, et al. Nextstrain: real-time tracking of pathogen evolution. Bioinformatics 2018; 34:4121–4123. https://doi.org/10.1093/bioinformatics/bty407 PMID: 29790939

26. Singer JB, Thomson EC, McLauchlan J, Hughes J, Gifford RJ. GLUE: a flexible software system for virus sequence data. BMC Bioinformatics 2018; 19:532. Available from: https://bmcbioinformatics.biomedcentral.com/articles/10.1186/s12859-018-2459-9. https://doi.org/10.1186/s12859-018-2459-9 PMID: 30563445

27. Stadlbauer D, Amanat F, Chromikova V, Jiang K, Strohmeier S, Arunkumar GA, et al. SARS-CoV-2 seroconversion in humans: a detailed protocol for a serological assay, antigen production, and test setup. Curr Protoc Microbiol. 2020; 57:e100. https://doi.org/10.1002/cpmc.100 PMID: 32302069

28. World Health Organization. Interim guidance: Laboratory testing for 2019 novel coronavirus (2019-nCoV) in suspected human cases. 2020. Available from: https://www.who.int/publications-detail/laboratory-testing-for-2019-novel-coronavirus-in-suspected-human-cases-20200117.

29. Spellberg B, Haddix M, Lee R, Butler-Wu S, Holtom P, Yee H, et al. Community prevalence of SARS-CoV-2 among patients with influenzalike illnesses presenting to a Los Angeles Medical Center in March 2020. J Am Med Assoc. 2020.

30. Bendavid E, Mulaney B, Sood N, Shah S, Ling E, Bromley-Dulfano R, et al. COVID-19 antibody sero-prevalence in Santa Clara County, California. medRxiv. 2020.

31. Li Z, Yi Y, Luo X, Xiong N, Liu Y, Li S, et al. Development and clinical application of a rapid IgM-IgG com-bined antibody test for SARS-CoV-2 infection diagnosis. J Med Virol. 2020:1–7.

32. Broughton JP, Deng X, Yu G, Fasching CL, Singh J, Streithorst J, et al. Rapid detection of 2019 novel coronavirus SARS-CoV-2 using a CRISPR-based DETECTR lateral flow assay. medRxiv. 2020.

33. Lassaunière R, Frische A, Harboe ZB, Nielsen AC, Fomsgaard A, Krogfelt KA, et al. Evaluation of nine commercial SARS-CoV-2 immunoassays. medRxiv. 2020.

34. Wrapp D, Wang N, Corbett KS, Goldsmith JA, Hsieh CL, Abiona O, et al. Cryo-EM structure of the 2019-nCoV spike in the prefusion conformation. Science. 2020; 367:1260–1263. https://doi.org/10.1126/science.abb2507 PMID: 32075877

35. Hoffmann M, Kleine-Weber H, Schroeder S, Krüger N, Herrler T, Erichsen S, et al. SARS-CoV-2 cell entry depends on ACE2 and TMPRSS2 and is blocked by a clinically proven protease inhibitor. Cell. 2020; 181:271–280.e8. https://doi.org/10.1016/j.cell.2020.02.052 PMID: 32142651

36. Yan R, Zhang Y, Li Y, Xia L, Guo Y, Zhou Q. Structural basis for the recognition of SARS-CoV-2 by full-length human ACE2. Science. 2020; 367:1444–1448. https://doi.org/10.1126/science.abb2762 PMID: 32132184

37. Kang S, Yang M, Hong Z, Zhang L, Huang Z, Chen X, et al. Crystal structure of SARS-CoV-2 nucleo-capsid protein RNA binding domain reveals potential unique drug targeting sites. Acta Pharm Sin B. 2020; 10:1228–1238. https://doi.org/10.1016/j.apsb.2020.04.009 PMID: 32363136

38. Zhang L, Lin D, Sun X, Curth U, Drosten C, Sauerhering L, et al. Crystal structure of SARS-CoV-2 main protease provides a basis for design of improved α-ketoamide inhibitors. Science. 2020; 368:409–412. https://doi.org/10.1126/science.abb3405 PMID: 32198291

39. Gordon DE, Jang GM, Bouhaddou M, Xu J, Obernier K, White KM, et al. A SARS-CoV-2 protein interaction map reveals targets for drug repurposing. Nature. 2020; 583:459–468. https://doi.org/10.1038/s41586-020-2286-9 PMID: 32353859

40. Shi J, Wen Z, Zhong G, Yang H, Wang C, Huang B, et al. Susceptibility of ferrets, cats, dogs, and other domesticated animals to SARS-coronavirus 2. Science. 2020; 368:1016–1020. https://doi.org/10.1126/science.abb7015 PMID: 32269068

41. Schlottau K, Rissmann M, Graaf A, Schön J, Sehl J, Wylezich C, et al. SARS-CoV-2 in fruit bats, ferrets, pigs, and chickens: an experimental transmission study. Lancet Microbe. 2020.

42. Gao Q, Bao L, Mao H, Wang L, Xu K, Yang M, et al. Development of an inactivated vaccine candidate for SARS-CoV-2. Science. 2020; 369:eabc1932.

43. Yu J, Tostanoski LH, Peter L, Mercado NB, McMahan K, Mahrokhian SH, et al. DNA vaccine protection against SARS-CoV-2 in rhesus macaques. Science. 2020:eabc6284.

44. Boudewijns R, Thibaut HJ, Kaptein SJF, Li R, Vergote V, Seldeslachts L, et al. STAT2 signaling as double-edged sword restricting viral dissemination but driving severe pneumonia in SARS-CoV-2 infected hamsters. bioRxiv. 2020.

45. Weston S, Haupt R, Logue J, Matthews K, Frieman M. FDA approved drugs with broad anti-coronaviral activity inhibit SARS-CoV-2 in vitro. bioRxiv. 2020.

46. Yu P, Qi F, Xu Y, Li F, Liu P, Liu J, et al. Age-related rhesus macaque models of COVID-19. Animal Model Exp Med. 2020; 3:93–97. https://doi.org/10.1002/ame2.12108 PMID: 32318665

47. Thao TTN, Labroussaa F, Ebert N, V'kovski P, Stalder H, Portmann J, et al. Rapid reconstruction of SARS-CoV-2 using a synthetic genomics platform. Nature. 2020; 582:561–565. https://doi.org/10.1038/s41586-020-2294-9 PMID: 32365353

48. Jakhar D, Kaur I. Potential of chloroquine and hydroxychloroquine to treat COVID-19 causes fears of shortages among people with systemic lupus erythematosus. Nat Med. 2020; 26:632.

49. U.S. Food & Drug Administration. FDA statements on hydroxychloroquine and chloroquine. Available from: https://www.fda.gov/drugs/drug-safety-and-availability/fda-cautions-against-use-hydroxychloroquine-or-chloroquine-covid-19-outside-hospital-setting-or.

50. Li G, De Clercq E. Therapeutic options for the 2019 novel coronavirus (2019-nCoV). Nat Rev Drug Discov. 2020; 19:149–150. https://doi.org/10.1038/d41573-020-00016-0 PMID: 32127666

51. Riva L, Yuan S, Yin X, Martin-Sancho L, Matsunaga N, Burgstaller S, et al. A large-scale drug repositioning survey for SARS-CoV-2 antivirals. bioRxiv. 2020.

52. Ellinger B, Bojkova D, Zaliani A, Cinatl J, Claussen C, Westhaus S, et al. Identification of inhibitors of SARS-CoV-2 in-vitro cellular toxicity in human (Caco-2) cells using a large scale drug repurposing collection. Res Sq. 2020.

53. Touret F, Gilles M, Barral K, Nougairède A, Decroly E, de Lamballerie X, et al. In vitro screening of a FDA approved chemical library reveals potential inhibitors of SARS-CoV-2 replication. bioRxiv. 2020.

54. Zhou Y, Hou Y, Shen J, Huang Y, Martin W, Cheng F. Network-based drug repurposing for novel coronavirus 2019-nCoV/SARS-CoV-2. Cell Discov. 2020; 6:1–18. https://doi.org/10.1038/s41421-019-0132-8 PMID: 31934347

55. Hinton DM. Remdesivir EUA Letter of Authorization. Available from: https://www.fda.gov/media/137564/download.

56. Duan K, Liu B, Li C, Zhang H, Yu T, Qu J, et al. Effectiveness of convalescent plasma therapy in severe COVID-19 patients. Proc Natl Acad Sci U S A. 2020; 117:9490–9496. https://doi.org/10.1073/pnas.2004168117 PMID: 32253318

57. Casadevall A, Pirofski LA. The convalescent sera option for containing COVID-19. J Clin Invest. 2020; 130:1545–1548. https://doi.org/10.1172/JCI138003 PMID: 32167489

58. Takeda News Releases. Takeda Initiates Development of a Plasma-Derived Therapy for COVID-19. 2020. Available from: https://www.takeda.com/newsroom/newsreleases/2020/takeda-initiates-development-of-a-plasma-derived-therapy-for-covid-19/.

59. Tian X, Li C, Huang A, Xia S, Lu S, Shi Z, et al. Potent binding of 2019 novel coronavirus spike protein by a SARS coronavirus-specific human monoclonal antibody. Emerg Microbes Infect. 2020; 9:382–385. https://doi.org/10.1080/22221751.2020.1729069 PMID: 32065055

60. Yuan M, Wu NC, Zhu X, Lee C-CD, So RTY, Lv H, et al. A highly conserved cryptic epitope in the receptor-binding domains of SARS-CoV-2 and SARS-CoV. Science. 2020; 368:630–633. https://doi.org/10.1126/science.abb7269 PMID: 32245784

61. Pinto D, Park Y-J, Beltramello M, Walls AC, Tortorici MA, Bianchi S, et al. Structural and functional analysis of a potent sarbecovirus neutralizing antibody. bioRxiv. 2020.

62. Wang C, Li W, Drabek D, Okba NMA, van Haperen R, Osterhaus ADME, et al. A human monoclonal antibody blocking SARS-CoV-2 infection. Nat Commun. 2020; 11:2251. https://doi.org/10.1038/s41467-020-16256-y PMID: 32366817

63. Rogers TF, Zhao F, Huang D, Beutler N, Burns A, He W, et al. Isolation of potent SARS-CoV-2 neutralizing antibodies and protection from disease in a small animal model. Science. 2020:eabc7520.

64. Brouwer PJM, Caniels TG, van der Straten K, Snitselaar JL, Aldon Y, Bangaru S, et al. Potent neutralizing antibodies from COVID-19 patients define multiple targets of vulnerability. Science. 2020:eabc5902.

65. Safety and Immunogenicity Study of 2019-nCoV Vaccine (mRNA-1273) for Prophylaxis of SARS-CoV-2 Infection (COVID-19). Available from: https://clinicaltrials.gov/ct2/show/NCT04283461.

66. Orellana C, Phase I. SARS vaccine trial in China. Lancet Infect Dis. 2004; 4:388. https://doi.org/10.1016/s1473-3099(04)01071-0 PMID: 15252932

67. BioRender. COVID-19 Vaccine Tracker. Available from: https://biorender.com/covid-vaccine-tracker.

68. Lurie N, Saville M, Hatchett R, Halton J. Developing Covid-19 vaccines at pandemic speed. N Engl J Med. 2020.

69. Yozwiak NL, Schaffner SF, Sabeti PC. Data sharing: make outbreak research open access. Nature 2015; 518:477–479. Available from: https://www.nature.com/news/data-sharing-make-outbreak-research-open-access-1.16966. https://doi.org/10.1038/518477a PMID: 25719649

70. Centers for Disease Control and Prevention. COVID-19 Databases and Journals. Available from: https://www.cdc.gov/library/researchguides/2019novelcoronavirus/databasesjournals.html.

71. Worldometer: Coronavirus. Available from: https://www.worldometers.info/coronavirus/.

72. nCoV2019.live. Available from: https://ncov2019.live/.

73. HealthMap COVID-19. Available from: https://www.healthmap.org/covid-19/.

74. Center for Systems Science and Engineering at Johns Hopkins University. COVID-19 Dashboard. Available from: https://coronavirus.jhu.edu/map.html.

75. Open COVID Pledge. Available from: https://opencovidpledge.org/about.

76. Financial Times. AbbVie drops patent rights for Kaletra antiviral treatment. Available from: https://www.ft.com/content/5a7a9658-6d1f-11ea-89df-41bea055720b.

77. Netherlands Authority for Consumers and Markets. ACM has confidence in commitments made by Roche to help solve problems with test materials. Available from: https://www.acm.nl/en/publications/acm-has-confidence-commitments-made-roche-help-solve-problems-test-materials.

78. Operation Shields Up! Available from: https://www.opshieldsup.org/about.

79. Brewdog Hand Sanitiser. Available from: https://www.brewdog.com/uk/hand-sanitiser.

80. Platform for European Preparedness Against (Re-)emerging Epidemics. Available from: https://www.prepare-europe.eu/.

81. van der Hoek L, Verschoor E, Beer M, Höper D, Wernike K, Van Ranst M, et al. Host switching pathogens, infectious outbreaks and zoonosis: a Marie Skłodowska-Curie innovative training network (HONOURs). Virus Res. 2018; 257:120–124. https://doi.org/10.1016/j.virusres.2018.09.002 PMID: 30316331

82. World Health Organization. "Solidarity" clinical trial for COVID-19 treatments. Available from: https://www.who.int/emergencies/diseases/novel-coronavirus-2019/global-research-on-novel-coronavirus-2019-ncov/solidarity-clinical-trial-for-covid-19-treatments.

83. World Health Organization. Global health ethics: resources on ethics and COVID-19. 2020. Available from: https://www.who.int/ethics/topics/outbreaks-emergencies/covid-19/en/.

84. COVID-19 Clinical Research Coalition. Global coalition to accelerate COVID-19 clinical research in resource-limited settings. The Lancet. 2020; 395:1322–1325.

(II) West Nile Virus Epidemic in Germany Triggered by Epizootic Emergence, 2019

Ute Ziegler, <u>Pauline Dianne Santos</u>, Martin H. Groschup, Carolin Hattendorf, Martin Eiden, Dirk Höper, Philip Eisermann, Markus Keller, Friederike Michel, Robert Klopfleisch, Kerstin Müller, Doreen Werner, Helge Kampen, Martin Beer, Christina Frank, Raskit Lachmann, Birke Andrea Tews, Claudia Wylezich, Monika Rinder, Lars Lachmann, Thomas Grünewald, Claudia A. Szentiks, Michael Sieg, Jonas Schmidt-Chanasit, Daniel Cadar and Renke Lühken

viruses

Article

West Nile Virus Epidemic in Germany Triggered by Epizootic Emergence, 2019

Ute Ziegler [1,2,†], Pauline Dianne Santos [3,†], Martin H. Groschup [1,2], Carolin Hattendorf [4],
Martin Eiden [1], Dirk Höper [3], Philip Eisermann [4], Markus Keller [1], Friederike Michel [1],
Robert Klopfleisch [5], Kerstin Müller [6], Doreen Werner [7], Helge Kampen [8], Martin Beer [3],
Christina Frank [9], Raskit Lachmann [9], Birke Andrea Tews [8], Claudia Wylezich [3],
Monika Rinder [10], Lars Lachmann [11], Thomas Grünewald [12], Claudia A. Szentiks [13],
Michael Sieg [14], Jonas Schmidt-Chanasit [4,15], Daniel Cadar [4,†] and Renke Lühken [4,15,†,*]

[1] Friedrich-Loeffler-Institut, Federal Research Institute for Animal Health, Institute of Novel and Emerging Infectious Diseases, 17493 Greifswald-Insel Riems, Germany; ute.ziegler@fli.de (U.Z.); martin.groschup@fli.de (M.H.G.); martin.eiden@fli.de (M.E.); markus.keller@fli.de (M.K.); friederike.michel@gmx.net (F.M.)

[2] German Centre for Infection Research, partner site Hamburg-Luebeck-Borstel-Riems, 20359 Hamburg, Germany

[3] Friedrich-Loeffler-Institut, Federal Research Institute for Animal Health, Institute of Diagnostic Virology, 17493 Greifswald-Insel Riems, Germany; pauline.santos@fli.de (P.D.S.); dirk.hoeper@fli.de (D.H.); martin.beer@fli.de (M.B.); claudia.wylezich@fli.de (C.W.)

[4] Bernhard Nocht Institute for Tropical Medicine, WHO Collaborating Centre for Arbovirus and Hemorrhagic Fever Reference and Research, 20359 Hamburg, Germany; carolin.hattendorf@bnitm.de (C.H.); philip.eisermann@gmail.com (P.E.); schmidt-chanasit@bnitm.de (J.S.-C.); danielcadar@gmail.com (D.C.)

[5] Freie Universitat Berlin, Institute of Veterinary Pathology, 14163 Berlin, Germany; robert.klopfleisch@fu-berlin.de

[6] Freie Universität Berlin, Department of Veterinary Medicine, Small Animal Clinic, 14163 Berlin, Germany; kerstin.Mueller@fu-berlin.de

[7] Leibniz-Centre for Agricultural Landscape Research, 15374 Müncheberg, Germany; doreen.werner@zalf.de

[8] Friedrich-Loeffler-Institut, Federal Research Institute for Animal Health, Institute of Infectiology, 17493 Greifswald-Insel Riems, Germany; helge.kampen@fli.de (H.K.); birke.tews@fli.de (B.A.T.)

[9] Robert Koch Institute, Department of Infectious Disease Epidemiology, 13353 Berlin, Germany; frankc@rki.de (C.F.); lachmannr@rki.de (R.L.)

[10] Ludwig Maximilians University Munich, Centre for Clinical Veterinary Medicine, Clinic for Birds, Small Mammals, Reptiles and Ornamental Fish, 85764 Oberschleißheim, Germany; monika.rinder@vogelklinik.vetmed.uni-muenchen.de

[11] Nature and Biodiversity Conservation Union, 10117 Berlin, Germany; lars.lachmann@nabu.de

[12] Klinikum Chemnitz, Infectious Diseases and Tropical Medicine Clinic, 09116 Chemnitz, Germany; t.gruenewald@skc.de

[13] Leibniz-Institute for Zoo- and Wildlife Research (IZW), 10315 Berlin, Germany; szentiks@izw-berlin.de

[14] Leipzig University, Faculty of Veterinary Medicine, Institute of Virology, 04103 Leipzig, Germany; michael.sieg@vetmed.uni-leipzig.de

[15] Universität Hamburg, Faculty of Mathematics, Informatics and Natural Sciences, 20148 Hamburg, Germany

* Correspondence: renkeluhken@gmail.com

† These authors contributed equally to this work.

Abstract: One year after the first autochthonous transmission of West Nile virus (WNV) to birds and horses in Germany, an epizootic emergence of WNV was again observed in 2019. The number of infected birds and horses was considerably higher compared to 2018 (12 birds, two horses), resulting in the observation of the first WNV epidemy in Germany: 76 cases in birds, 36 in horses and five confirmed mosquito-borne, autochthonous human cases. We demonstrated that Germany

experienced several WNV introduction events and that strains of a distinct group (Eastern German WNV clade), which was introduced to Germany as a single introduction event, dominated mosquito, birds, horse and human-related virus variants in 2018 and 2019. Virus strains in this clade are characterized by a specific-Lys2114Arg mutation, which might lead to an increase in viral fitness. Extraordinary high temperatures in 2018/2019 allowed a low extrinsic incubation period (EIP), which drove the epizootic emergence and, in the end, most likely triggered the 2019 epidemic. Spatiotemporal EIP values correlated with the geographical WNV incidence. This study highlights the risk of a further spread in Germany in the next years with additional human WNV infections. Thus, surveillance of birds is essential to provide an early epidemic warning and thus, initiate targeted control measures.

Keywords: West Nile virus; Germany; epizooty; epidemic; human; bird; horses; mosquitoes; transmission risk; zoonoses

1. Introduction

West Nile virus (WNV, family *Flaviviridae*, genus *Flavivirus)* is maintained in a transmission cycle between birds as amplification hosts and mosquito vectors [1]. Spillover events have significant public health and veterinary relevance [2]. A total of 25% of the infected people develop West Nile fever (WNF) and become symptomatic (e.g., headache or muscle pain) [3]. Severe disease progressions manifesting as WNV neuroinvasive disease (WNND) are rare (<1%) [4]. These include syndromes of meningitis, encephalitis, and acute flaccid paralysis/poliomyelitis. Case-fatality rate of WNND is approximately 10% [5]. Age is the most important risk factor for WNND and a fatal disease outcome [2]. Thus, WNV circulation poses considerable risk for transfusion and organ transplantation safety [6].

WNV is distributed in wide areas of Europe. The main focus of WNV circulation is in south-eastern Europe and Italy [7]. However, low WNV activity is also observed in the neighboring countries of Germany (France, Austria, and Czech Republic). Therefore, over the last decade, different monitoring programs were implemented in Germany to screen for WNV RNA and antibodies in birds, horses, mosquitoes and chicken eggs [8–12]. In 2018, an epizootic emergence of WNV was observed in Germany for the first time [13]. All WNV-positive birds and horses were infected with the same WNV lineage 2 strain of the central European subclade II. WNV activity was detected in eastern Germany over a distance of almost 900 km (Munich to Rostock). At the same time, a large WNV outbreak was observed in south-eastern and southern Europe [7]. However, phylogenetic analysis in combination with the wide distribution in Germany indicates that WNV may have been introduced from the Czech Republic to Germany already before 2018 [13]. The emergence of WNV in Germany and the focus in the central part of eastern Germany was correlated with outstandingly high summer temperatures. As demonstrated for other European countries, WNV is probably predominantly transmitted by different native *Culex* species. *Culex pipiens* biotype *pipiens*, *Culex pipiens* biotype *molestus* and *Culex torrentium* from Germany were experimentally proven to be susceptible to WNV infection [14].

In this study, we report a WNV epidemic in Germany, 2019, triggered by an epizootic emergence among birds with spillover to horses and humans. Human and animal cases were located in the same area, showing a high WNV activity also in 2018. In both years, the region was characterized by suitable temperature conditions allowing a short extrinsic incubation period (EIP). Phylogenetic and phylogeographic analysis showed that Germany experienced several WNV introduction events. Several virus variants circulate in the affected German regions with Austria and Czech Republic as possible origins. The majority of the WNV strains involved in the German outbreak clustered together into a distinct and dominating group (Eastern German WNV clade) comprising of mosquito, bird, horse and human-related virus variants.

2. Materials and Methods

2.1. WNV Screening of Birds, Horses and Mosquitoes

Since the first outbreak of Usutu virus (USUV) in Germany (2011/12), a nationwide bird surveillance network (living and dead birds) was set up to monitor for zoonotic arboviruses with a focus on WNV and USUV. In this context, a variety of dead birds and organ samples were submitted to the Bernhard Nocht Institute for Tropical Medicine and the national reference laboratory for WNV at the Friedrich-Loeffler-Institut (FLI) by the regional veterinary laboratories of the federal states of Germany, by the German Mosquito Control Association (KABS), the Nature and Biodiversity Conservation Union (NABU), citizens and independent bird clinics and zoological gardens. WNV infection in birds and horses is a notifiable disease in Germany if a recent infection is detected by a WNV-specific RT-qPCR result and/or a positive result of horses by IgM-ELISA, i.e., the detection of a fresh WNV infection. A previous vaccination of horses must be excluded. A positive IgG or neutralizing antibody detection is not notifiable in Germany.

Requests for the submission of dead birds were made via press releases of involved institutes and subsequent dissemination of the information by different kinds of media, including newspaper articles, television and radio. Total RNA from homogenized tissue samples (brain, liver, lung, or heart) was extracted and analyzed for the presence of flavivirus RNA by using a modified pan-flavivirus reverse transcription PCR [15] or WNV-specific reverse transcription quantitative PCR (RT-qPCR) [16]. Furthermore, all samples were also tested using the USUV-specific RT-qPCR described by Jöst et al. [17] (data not shown).

Organ samples from affected horses were also tested by the RT-qPCR as stated above. In the case of diseased horses, often with neurological symptoms typical for WNV disease, the serum samples were screened by IgM-and/or IgG-ELISA (IDVet, Grabels, France) and positive samples were confirmed by differentiating virus neutralization tests to exclude cross-reacting flaviviruses (USUV, tick-borne encephalitis virus (TBE)) [12].

Following the first confirmed avian WNV case in the Tierpark Berlin (Wildlife Park) in 2019, mosquitoes were collected in that park by EVS (Heavy Duty Encephalitis Vector Survey) traps (BioQuip Products, Rancho Dominguez, CA, USA) equipped with dry ice as an attractant. Traps were continuously operated from mid-September to early October and emptied daily. Captured mosquitoes were morphologically identified to species or complex using the determination key by Becker et al. [18] and pooled with up to ten specimens per pool. Pools were homogenized and subjected to RNA extraction and WNV RT-qPCR as described above [16]. Positive samples were inoculated on C6/36 cells (L 1299, Collection of Cell Lines in Veterinary Medicine (CCLV), Friedrich-Loeffler-Institut, Greifswald – Insel Riems, Germany). Six days after inoculation, the supernatant of infected cultures was tested again with WNV RT-qPCR and the two samples with the lowest Ct-value were used for NGS analysis [19].

2.2. Risk of WNV Transmission

The extrinsic incubation period (EIP) gives the time between ingestion of a pathogen via blood meals and the vectors' ability to retransmit the pathogen. In contrast to other indices for transmission risk (e.g., field-measured infection rates of vectors), this approach is a theoretical risk assessment using information on the temperature-dependent EIP from the literature. However, EIP values give an approximation of virus transmission risk through the mosquito vector under local temperature conditions. Therefore, daily EIP values (EIP_d) of WNV were calculated with the formula $-0.132 + 0.0092 \times$ temperature [13,20]. The day-to-day mean E-OBS temperature dataset v20.0e (July 2018 to August 2019) was downloaded from http://www.ecad.eu [21]. Data analysis and visualization was conducted with the program R [22] using the packages lubridate [23] and raster [24]. For the risk assessment, EIP_d values for the subsequent days were summed up until the virus development was completed (=EIP). For each grid cell and year, EIP values were averaged for the period from 15th July to 14th August (=EIP_{ave}).

2.3. Data Sets and Genome Characterization of WNV

A total of 39 WNV genomes from birds, humans, mosquitoes and horses were newly acquired as part of this study (Table 1, Figure 1, Supplementary Table S1). The extracted viral RNA of WNV positive specimens was subjected to a next-generation sequencing (NGS) workflow [25], or to random RT-PCR amplification followed by library preparation by using the QIAseq FX DNA Library Kit (Qiagen, Hilden, Germany). They were normalized, sampled and sequenced using 150-cycle NextSeq550 Reagent Kits v2.5 (Illumina, San Diego, CA) on a NextSeq550 platform (Illumina, San Diego, CA) or the Ion Torrent S5 chemistry (ThermoFisher Scientific, Waltham, MA, USA) on an Ion Torrent S5 XL platform (ThermoFisher Scientific, Waltham, MA, USA). All whole genome sequences of WNV with known sampling time (year) and geographical origin (country) from Europe were retrieved from GenBank (n = 98) and combined with those sequenced in this study. Two data sets have been created: one containing all genomes from Europe incl. Germany, and a second one comprising the "Eastern German clade only." Sequences were aligned using the MAFFT algorithm and then visually inspected in Geneious v2020.0.2 (https://www.geneious.com, Biomatters, Auckland, New Zealand). All sequences were confirmed as non-recombinant by the various methods for recombination detection implemented in RDP4 [26]. The obtained full-length recovered genome sequences of the WNV were submitted to GenBank or the European Nucleotide Archive (accession no. MN794935-MN794939, LR743421-LR743437, and LR743442-LR743458).

2.4. Evolutionary Dynamics and Phylogeography of German WNV

Genomes obtained for the German WNV strains were compared with all European complete or near complete genomes sequences publicly available. For molecular clock phylogenetics, maximum clade credibility (MCC) trees were inferred using the Bayesian Markov chain Monte Carlo (MCMC) approach available in BEAST v1.10 [27]. Analyses were performed under the best fit nucleotide substitution model identified as GTR +Γ for the complete genome data set including "all European" genomes and TN93+Γ for the data set for "Germany only" using jModelTest 2 [28]. To search among maximum likelihood (ML) trees, we employed both nearest neighbor interchange (NNI) and subtree pruning and regrafting (SPR) branch swapping. To assess the robustness of each node, a bootstrap resampling process was performed (1000 replicates) again using the NNI branch-swapping method available in PhyML [29] (data not shown). We have employed the TempEst tool for an interactive regression approach to explore the association between genetic divergence through time and sampling dates [30]. In order to assess the spatiotemporal dynamics of WNV, the time to most recent common ancestor (tMRCA), evolutionary rate and the effective population dynamics of WNV was employed with a relaxed uncorrelated log normal and a strict molecular clock under a flexible demographic model (the coalescent Gaussian Markov Random field (GMRF) Bayesian Skyride) as the best demographic scenario detected. In all cases, each of the MCMC chain lengths was run for 5 × 10^7 generations (with 10% burn-in) with subsampling every 10^4 iterations to achieve convergence as assessed using Tracer v1.5 [31]. The MCC trees were visualized using FigTree v1.4.1 (http://tree.bio.ed.ac.uk/software/figtree/). To test the hypothesis that WNV was periodically introduced to Germany, a phylogeographic analysis was conducted using a discrete model attributing state characters represented by the detection locality of each strain and the Bayesian stochastic search variable (BSSV) algorithm implemented in BEAST v1.10 [27]. An MCC tree was summarized using TreeAnnotator v1.10. and visualized in FigTree v1.4.3. SpreadD3 v. 0.9.7.1 (https://rega.kuleuven.be/cev/ecv/software/SpreaD3_tutorial) was used to run BSSV analysis and generate Bayes factor (BF) and posterior probability (PP) to test for statistically significant epidemiological links between discrete sampling locations. The potential transmission networks within and between countries for NS5 WNV were inferred in PopART package v1.7.2 using median joining tree method with an epsilon of zero [32].

3. Results

3.1. Spatial Analysis of West Nile Virus Circulation

A total of 88 birds and 38 horses tested positive for WNV in 2018 (diagnosed between 28.8. and 9.10) and 2019 (diagnosed between 8.7. and 21.11) in Germany. In addition, five probably mosquito-borne human WNV cases were diagnosed with no history of travel to WNV-endemic countries within the last month. Except a single specimen (Hamburg, 2019), all WNV-positive animals originated from the eastern part of Germany with a distinct focus for the federal states Saxony-Anhalt, Saxony, Berlin and Brandenburg (Table 1, Figure 1). In addition, the targeted screening in the Tierpark Berlin revealed seven WNV positive *Culex pipiens* complex mosquito pools in 2019.

Low WNV activity was detected for the federal states Bavaria and Mecklenburg-Western Pomerania in 2018, which was not observed in 2019. WNV cases were found in Hamburg and Thuringia in 2019 for the first time. The number of positive birds and horses rose considerably in 2019 (76 birds and 36 horses) compared to 2018 (12 birds and two horses).

Table 1. West Nile virus (WNV)-positive birds, horses and mosquito-borne, autochthonous humans for the federal states of Germany in 2018/2019. Numbers in brackets indicate the number of samples with WNV sequences acquired in this study.

Federal State	Birds (2018)	Horses (2018)	Birds (2019)	Horses (2019)	Humans (2019)	Sum
Bavaria (BY)	2 (2)	0	0	0	0	**2 (2)**
Berlin (BE)	3 (1)	0	33 (6)	0	1 (1)	**37 (8)**
Brandenburg (BB)	0	1	6 (3)	7	0	**14 (3)**
Hamburg (HH)	0	0	1 (1)	0	0	**1 (1)**
Mecklenburg-Western Pomerania (MV)	1	0	0	0	0	**1**
Saxony (SN)	1 (1)	0	21 (8)	9 (1)	3	**34 (10)**
Saxony-Anhalt (ST)	5 (2)	1	15 (10)	19	1 (1)	**41 (13)**
Thuringia (TH)	0	0	0	1	0	**1**
Sum	**12 (6)**	**2**	**76 (28)**	**36 (1)**	**5 (2)**	**131 (37)**

In addition to the 37 WNV sequences, two more genome sequences were obtained from WNV-positive mosquito pools collected in Berlin.

Especially in 2019, a large number of different bird species was affected (Table 2). A total of 52 birds (59.1% of all WNV-positive birds in 2018/2019) were held in captivity. From the total of 88 infected birds only four goshawks in private aviaries survived the infection. Of the 38 infected horses, 29 animals showed typical clinical symptoms, of which five horses died or were euthanized. Most of the other sick horses recovered in a very short time. Another nine horses were asymptomatic and were detected in the framework of additional investigations of holdings in relation to the clinical outbreaks. All 38 infected horses were positive in the IgM-ELISA and were therefore notified.

Table 2. Detection of WNV infections in different bird species in 2018 and 2019.

Bird Species	Scientific Name	Housing	Number of WNV-Infected Birds	Affected Federal States *
Eurasian Blackbird	*Turdus merula*	wild	3	ST, MV
Andean Flamingo	*Phoenicoparrus andinus*	captive	1	BE
Great Grey Owl	*Strix nebulosa*	captive	6	SN, ST, BY
Unspecified buzzard	*Buteo* sp.	wild	1	ST
Blue Tit	*Parus caeruleus*	wild	3	SN, ST
Chilean Flamingo	*Phoenicopterus chilensis*	captive	6	BE, SN
Eurasian Jay	*Garrulus glandarius*	wild	1	BB
Coconut Lorikeet	*Trichoglossus haematodus*	captive	1	ST
Scarlet-chested Parrot	*Neophema splendida*	captive	1	SN
Eurasian Golden Plover	*Pluvialis apricaria*	wild	1	SN
Northern Goshawk	*Accipiter gentilis*	wild/ captive	19	BB, BE, SN, ST
House Sparrow	*Passer domesticus*	wild	4	SN, ST
Dunnock	*Prunella modularis*	wild	1	HH
Humboldt-Penguin	*Spheniscus humboldti*	captive	1	BB
Inka-Tern	*Larosterna inca*	captive	1	BE
Black-tailed Gull	*Larus crassirostris*	captive	8	BE
Kagu	*Rhynochetos jubatus*	captive	1	BE
Domestic Canary	*Serinus canaria forma domestica*	captive	2	SN
Great Tit	*Parus major*	wild	3	SN
American Flamingo	*Phoenicopterus ruber*	captive	3	BE
Hooded Crow	*Corvus corone cornix*	wild	1	BE
Unspecified pelican	*Pelecanus* sp.	captive	1	ST
Javan Pond Heron	*Ardeola speciosa*	captive	1	BE
Common Wood Pigeon	*Columba palumbus*	wild	1	BE
Snowy Owl	*Bubo scandiacus*	captive	8	BE, ST
Chinese Merganser	*Mergus squamatus*	captive	1	BE
Swift Parrot	*Lathamus discolor*	captive	1	SN
Little Owl	*Athene noctua*	wild	2	BB
European Goldfinch	*Carduelis carduelis*	captive	1	SN
Eurasian Eagle-Owl	*Bubo bubo*	wild	1	SN
Tawny Owl	*Strix aluco*	wild	1	ST
White Eared Pheasant	*Crossoptilon crossoptilon*	captive	2	BE

* abbreviations as in Table 1.

The area with highest activity of WNV circulation was similar in 2018 and 2019, i.e., central-eastern Germany with most WNV-positive samples (mosquitoes, birds and horses) (Figure 1). In addition, all mosquito-borne, autochthonous human WNV cases were observed in this region. This matches the risk analysis based on the temperature conditions during summer, which indicates short EIP_{ave} (<15 days) for this area. The region along the Upper Rhine Valley (south-western Germany) was also characterized by low EIP_{ave} values, but no WNV circulation was detected in either year. Re-emergence of WNV was not observed for the most northern (Rostock) and southern (Poing) foci of WNV from 2018. This correlates with higher EIP_{ave} values for 2019 (>25 d; Poing: 28.4, Rostock: 26.2)

compared to 2018 (<25 d; Poing: 21.6, Rostock: 19.6) for these areas, i.e., lower risk of WNV transmission.
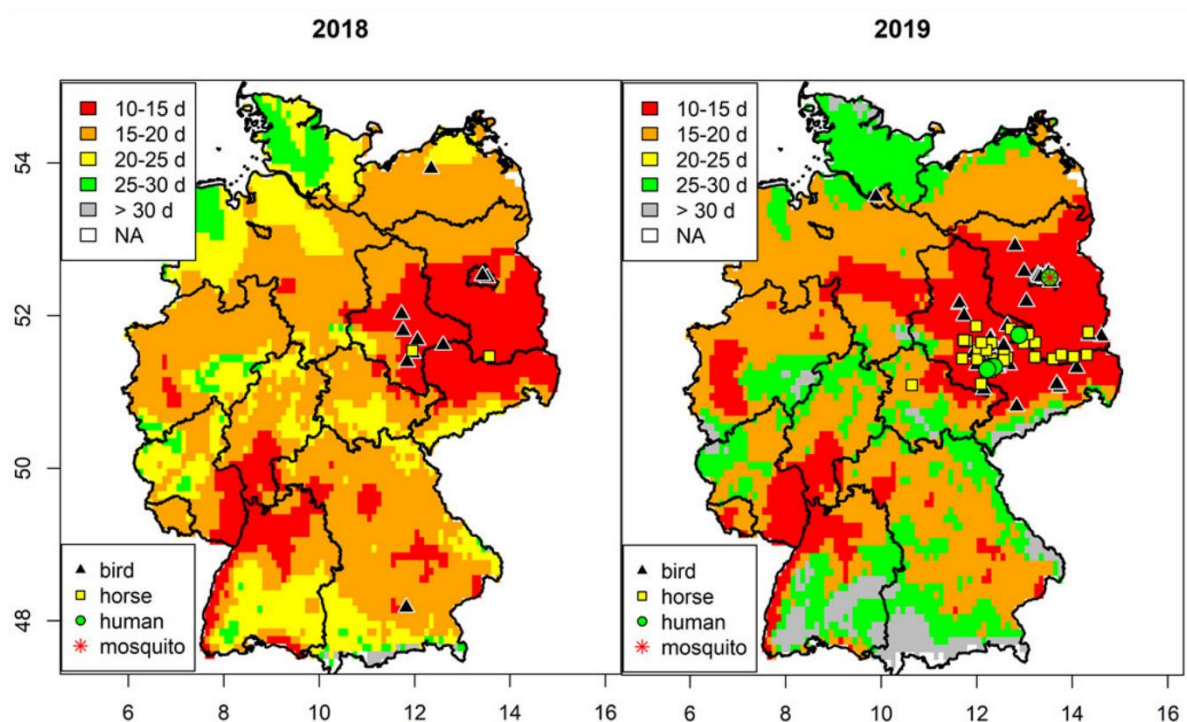
Figure 1. Spatial risk of West Nile virus (WNV) transmission in Germany. Average extrinsic incubation period between 15th July to 14th August 2018/2019 and distribution of WNV-positive birds, horses, humans and mosquitoes.

3.2. Autochthonous Human WNV Cases

In September 2018, a 31-year-old male veterinarian developed flu-like symptoms after necropsy of a WNV-positive owl (https://promedmail.org/promed-post/?id=20181006.6074497). The laboratory confirmation was based on detection of an IgM response against WNV and a cross-reactive IgG response against WNV, which might be also the result of past vaccinations against TBE and yellow fever virus. The first mosquito-borne, autochthonous infection for Germany was confirmed in Leipzig, Federal State of Saxony on 20 September 2019. The 69-year-old male patient presented with WNND, received supportive treatment at the Infectious Diseases (ID) intensive care unit (ICU) between September 3rd and September 20th and was released with restitutio ad integrum. The laboratory confirmation was based on detection of WNV RNA in an early CSF, serum and urine sample and the detection of WNV IgM and IgG in serum samples. A second autochthonous case in Leipzig, an 81-year old male, was admitted to the ICU with presumptive diagnosis of pneumonia, then transferred to the ID-ICU and was found to have WNND confirmed by WNV IgM and IgG in serum samples as well as WNV RNA in CSF samples as early as from 19 September. He also recovered after 12 days of supportive care including mechanical ventilation without neurological sequelae. Both patients reported no history of travel to WNV-endemic countries and routes of non-vector borne transmission were excluded. While one patient had direct contact with the corpse of a Blue Tit (*Parus caeruleus*) five days before onset of fever, the other one reported no obvious contact with animals. Both patients had experienced multiple mosquito bites in the weeks before onset of illness. The third WNV infection was diagnosed on 24 September in a 46-year-old female patient from Berlin, Federal State of Berlin, who presented with West Nile Fever (WNF). The patient did not receive any treatment and recovered within two weeks. The laboratory confirmation was based on detection of WNV RNA in an early serum sample and seroconversion of WNV IgM and IgG in later serum samples. The fourth WNV infection was diagnosed retrospectively based on IgM and IgG detection in a serum sample on 16 October in a 44-year-old female patient from the district Wittenberg

Federal State of Saxony-Anhalt. The patient was initially admitted to a local hospital with WNND-like symptoms on 10 September. After receiving supportive care, she was discharged on 17 September with restitutio ad integrum. The serological diagnosis was confirmed on 23 October by the detection of WNV RNA in a serum sample from the acute phase of infection. The fifth WNV infection was diagnosed on 23 October in a 24-year-old female patient from the district Leipzig, Federal State of Saxony, who presented with WNF (onset of symptoms 6th of October) and did not receive any treatment and recovered within one week. The laboratory confirmation was based on detection of WNV-specific IgM and IgG in a serum sample. As of 20 December, no further cases have been reported.

3.3. Genetic Characterization of German WNV

The genetic variations across the viral genome were low and homogenous (0.1%–0.7%) indicating that the analyzed WNV has maintained genetically stable since its first detection in 2018. The identity matrices for the genome and for individual genes were greater than 99.2%. The greatest variation was observed in the nonstructural genes coding for the NS1, NS2A, NS3 and NS5.

3.4. Phylogeny, Phylogeography and Spatiotemporal Dynamics of WNV

In order to investigate the evolutionary relationship and origin of WNV in Germany, a Bayesian MCMC sampling method and ML method were implemented. Similar topologies inferred by ML (not shown) and Bayesian MCC phylogenies of the European WNV lineage 2 data set revealed that all European strains fell into two distinct highly supported groups designated as Southeastern European clade (SEEC) and Central and Eastern European clade (CEC). All WNV strains from Germany fell into the CEC (Figure 2). The detailed analysis of the CEC showed that the German strains clustered in six distinct subclades (Figure 2) of which four consisted of singleton strains (WNV strains ED-I-155_19/ LR743422, ED-I-177_19/ LR743431, ED-I-201_19/ LR743448 and ED-I-205_19/ LR743454) associated with Austrian relatives (Figure 2). However, the majority of the WNV strains from Germany clustered into a well defined monophyletic group designated as Eastern German clade (EGC). The EGC is also notable for a star-like structure in which several subclades connect viruses sampled from multiple locations and time points (Figures 2a,3). These and other findings revealed that the genetic diversity of WNV in Europe is shaped primarily by in situ evolution rather than by extensive migration. No specific phylogenetic clustering and differences between the WNV strains from birds, horses, mosquitoes and humans in Germany were observed. The genetic variations of WNV combined with sample collection dates and locations can help to identify the possible source and the evolutionary history of the newly emerging viral variants. In order to assess viral migration and explore the origin of the WNV outbreaks in Germany, a discrete-trait phylogeography analysis was used to reconstruct the WNV movements between European countries and within Germany. Both data sets (European and German strains only, EGC) exhibited strong temporal signals ($R^2 = 0.31$ for the "European" data set and 0.19 for the "German strains only," $P < 0.001$). The coefficient of rate variation supports the use of a strict clock model for European data set and a relaxed clock for the data set "German strains only" (data not shown). The Bayesian MCC tree showed that although the WNV diversity in the "German strains only" group appears to have emerged in the last four years, the phylogeny of CEC which includes EGC suggests relative long-term circulation and evolution in Central Europe (Figure 2).

Publications
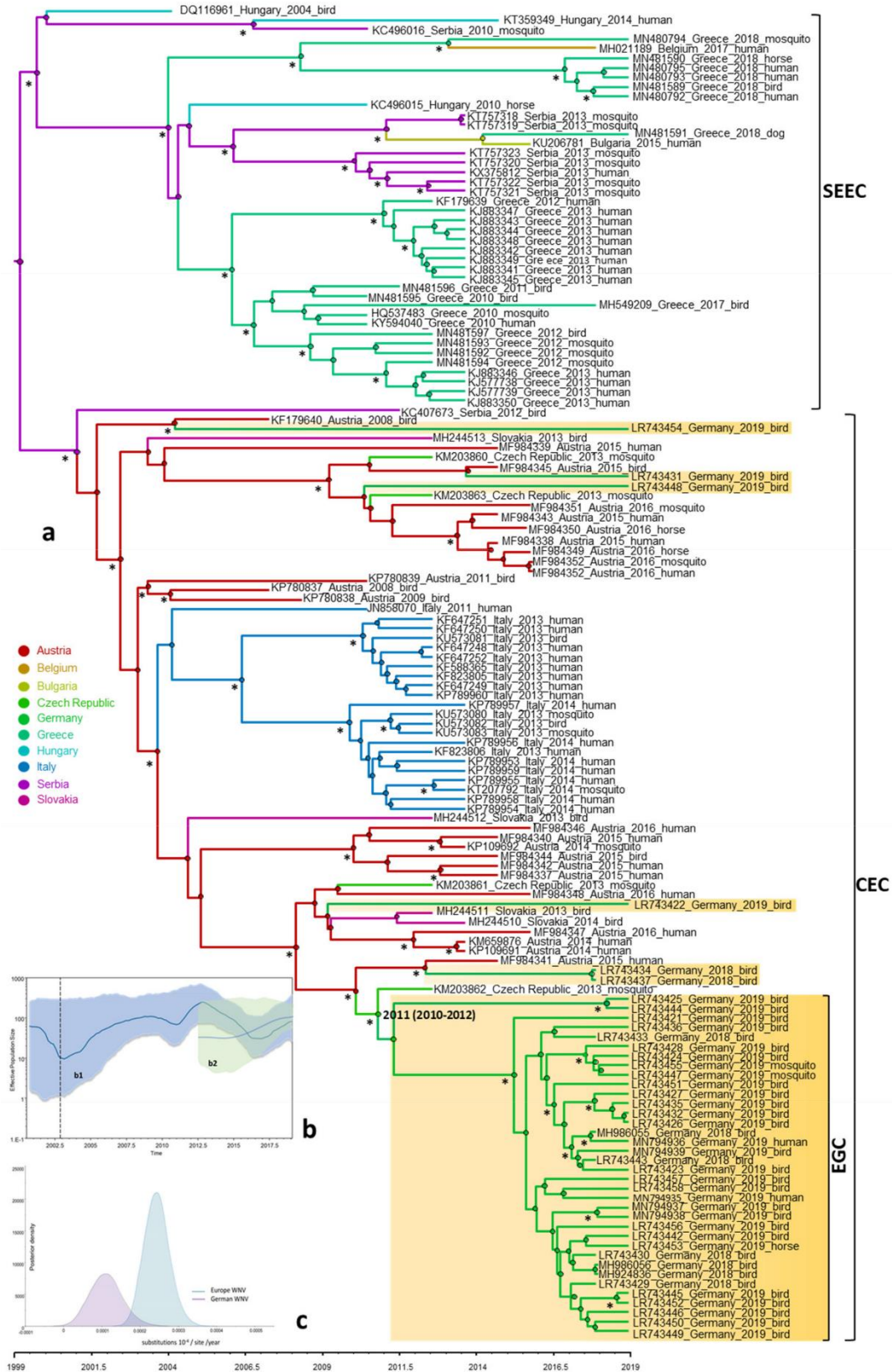
Figure 2. Bayesian maximum clade credibility (MCC) tree; (**a**) representing the time scale phylogeny; (**b**) effective population size; and (**c**) evolutionary rate of the European and German WNV lineage 2. The colored branches of MCC trees represent the most probable geographic location of their descendant nodes (see color codes); (**a**) the main clades are indicated to the right of the tree (SEEC, South Eastern European clade; CEC, Central and Eastern European clade), including the newly proposed German clade (EGC, Eastern German clade). Time is reported in the axis below the tree and

represents the year before the last sampling time (2019). The German WNV strains sequenced in this study are highlighted. The estimated tMRCA of German WNV strains of EGC clade is shown with 95% posterior time intervals in parentheses. Bayesian posterior probabilities (≥90%) and 1000 parallel maximum likelihood bootstrap replicates (≥70%) are indicated at the nodes (asterisks); (**b**) temporal variation in the effective population size of the European WNV lineage 2; (**b1**) and EGC; (**b2**) estimated using the coalescent Gaussian Markov Random field (GMRF) Bayesian Skyride model of polyprotein sequences. The Bayesian Skyride plot represents temporal variation in the virus effective population size (Ne) through time. The blue line represents the median Ne estimate and the shaded area corresponds to the 95% high-probability density (HDP) intervals; (**c**) evolutionary rate estimates with 95% credible intervals for the distribution of evolutionary rates observed for the whole European WNV lineage 2 and for WNV from the 2018–2019 German epidemic.

In further detail, the phylogeographic analysis suggests at least six distinct introductions of WNV into Germany from neighboring countries. It is predicted that all viral clade evolution events occurred during the last 16 years (Figure 2a). It should be noted that unlike its designation may suggest, the EGC can have developed in the wider southeastern and central European hemisphere and may have been translocated only later to Eastern Germany. Sequencing a larger number of more current WNV strains from e.g., Austria, the Czech Republic, and Poland would help to answer the circumstances of when and what in regard to the development of the East German Clade variants. Overall, the number of recent whole genome sequences is limited and should be markedly increased using NGS-based approaches.

Based on the albeit only limited Central European strain data, the tMRCA of the EGC group indicates a very recent emergence which was most likely introduced into Germany as a single introduction event. The progenitor of this Eastern European clade dates back to 2011, most probably circulating in Czech Republic (95% HPD 2010–2012; posterior probability, pp = 0.88) (Figure 2a). The EGC shares a common ancestor with basal WNV from Germany providing strong support for in situ evolution of WNV in Germany (Figures 3,4). Except for the members of the EGC, all other WNV strains found most recently in Germany seem to be descendants of ancestors from Austria (95% HPD for 2000 to 2015; pp = 0.83–0.97). The spatial diffusion pattern of WNV within Germany and between Germany and neighboring countries has been reconstructed using a Bayes Factor (BF) test under Bayesian Stochastic Search Variable Selection analysis (BSSVS). The strongest epidemiological links based on the BF estimates have been detected between Austria–Germany and Czech Republic–Germany, while the links within Germany have been detected between Halle–Berlin, Berlin–Halle, Berlin–Hamburg, Berlin–Dresden and Halle with neighboring localities (Figures 5,6). Similar star-like relationships of the WNV as for EGC have been also observed for Italian and Greek strains within both, SEEC and CEC (Figures 2a,3). These results further provide indication for the in situ evolution of the European lineages.

3.5. Population Dynamics, Protein Changes and Analysis of Selection Pressure

The mean rate of evolution estimated for the polyptrotein of the EGC was 1.26×10^{-4} (95% HPD, 1.15×10^{-5}–2.84×10^{-4}) subs site^{-1} year^{-1} two times lower than for the European data set, 2.51×10^{-4} (95% HPD, 2.13×10^{-4}–2.88×10^{-4}) subs site^{-1} year^{-1} (Figure 2c). EGC population dynamics showed a slightly increased growth phase from the beginning of emergence when the virus effective population size (Ne) remained constant until 2015. From that year, a constant increasing tendency for the Ne values was observed, which is in line with the strong population expansion started in 2015–2016 (Figure 2a,b). The monophyletic LysArg mutation located in the C terminus of the NS3 gene appeared only in Eastern German clade strains, while the paraphyletic Lys$_{3056}$Arg mutation from the NS5 gene was found to be common for EGC strains and some WNV from Austria (MF984341), Czech Republic (KM203862) and Germany (LR743437 and LR743434). There are several non-synonymous mutations in the nonstructural genes, which exhibit geographical structures specific of the members of the CEC (Figure 7). The overall d$_N$/d$_S$ ratios in the polyprotein of EGC, CEC and SEEC were 0.118, 0.136 and 0.154, respectively, indicating that most sites are subject to strong purifying or negative selection.

There was no evidence for positive or episodic diversifying selection in the WNV strains from Germany.
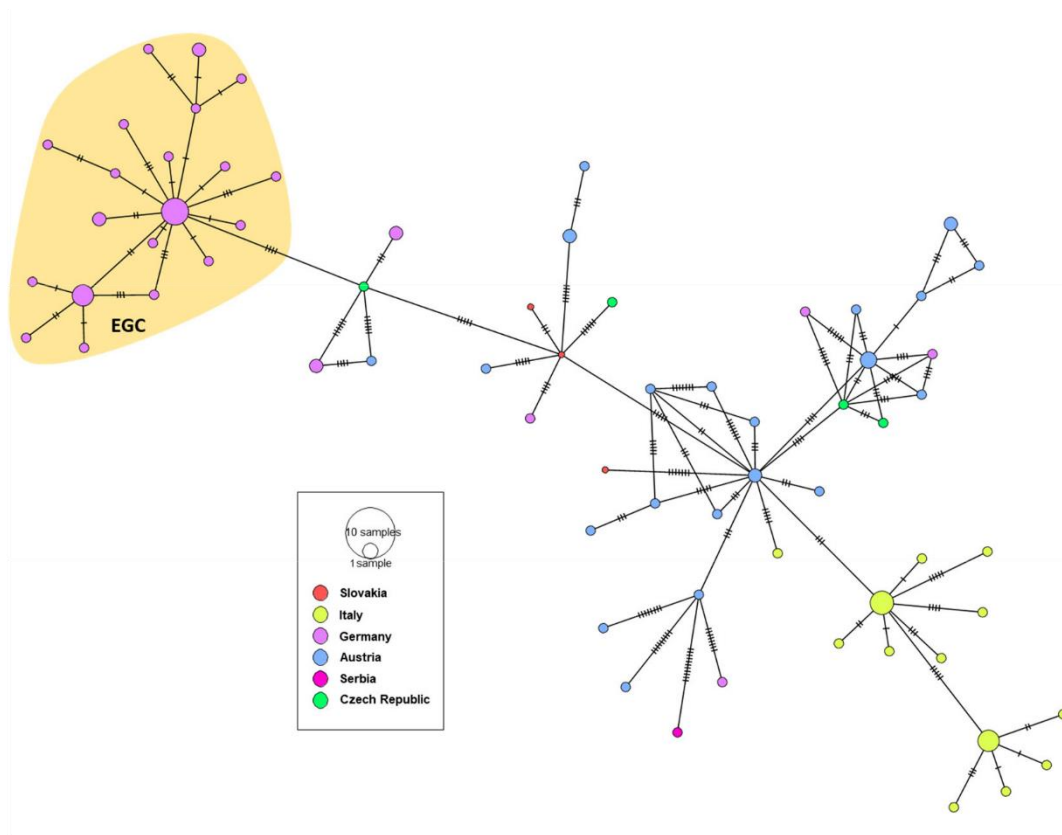
Figure 3. A median-joining haplotype network constructed from complete WNV NS5 gene alignment of the Central European WNV clade (CEC). Each colored vertex represents a sampled viral haplotype, with different colors indicating the different country of origin. The size of each vertex is relative to the number of sampled viral strains and the dashes on branches show the number of mutations between nodes. The Eastern German clade (EGC) is highlighted.
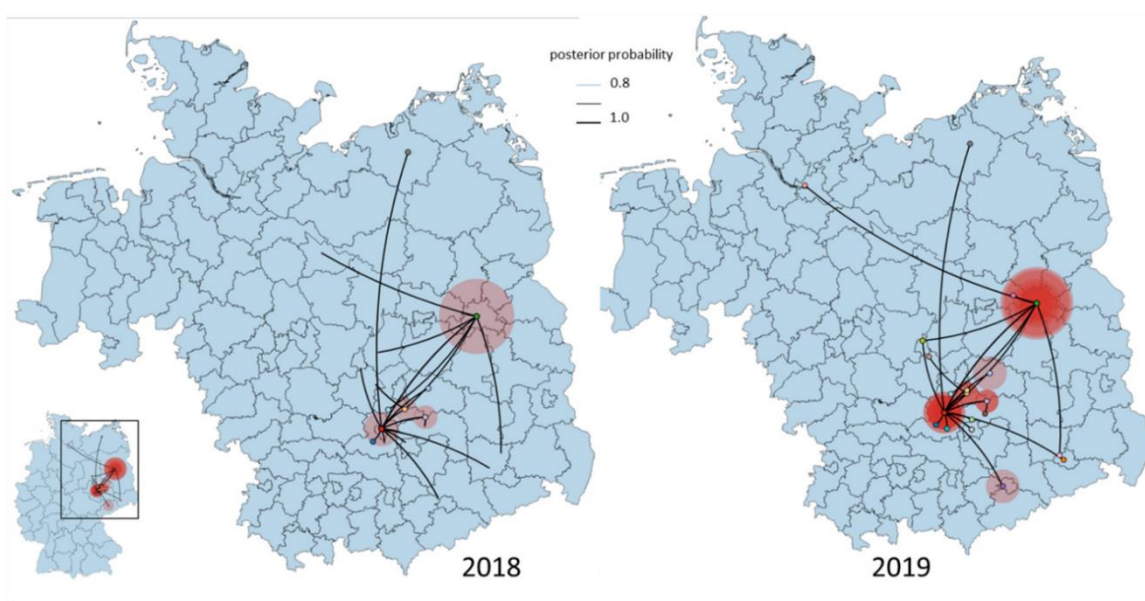
Figure 4. Temporally framed snapshots of the dispersal patterns (2018–2019) among regions in Germany for the Eastern German WNV clade. Lines between locations represent branches in the Bayesian maximum clade credibility (MCC) tree along which the relevant location transition occurs.

Circle diameters are proportional to the square root of the number of MCC branches maintaining a particular location state at each time point.
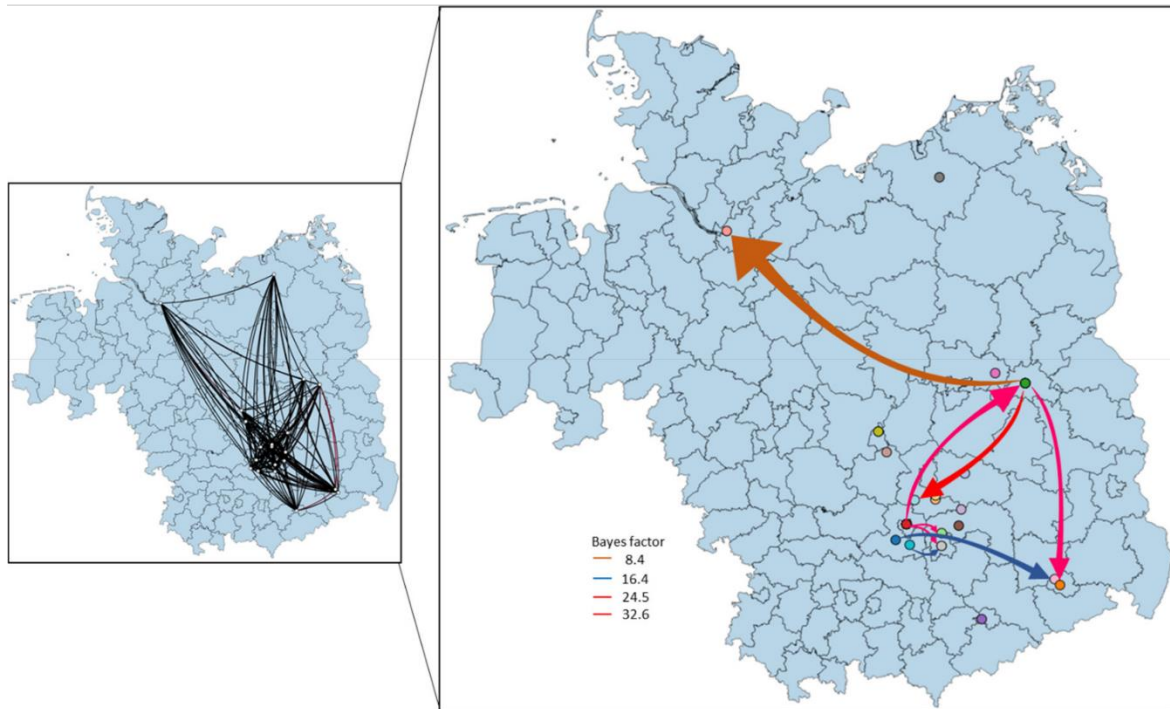
Figure 5. Calculated migration pattern of WNV between German locations based on Bayes factor test for significant non-zero rates. The arrows indicate the origin and the direction of migration between locations, while the colors indicate the strength of the connections.
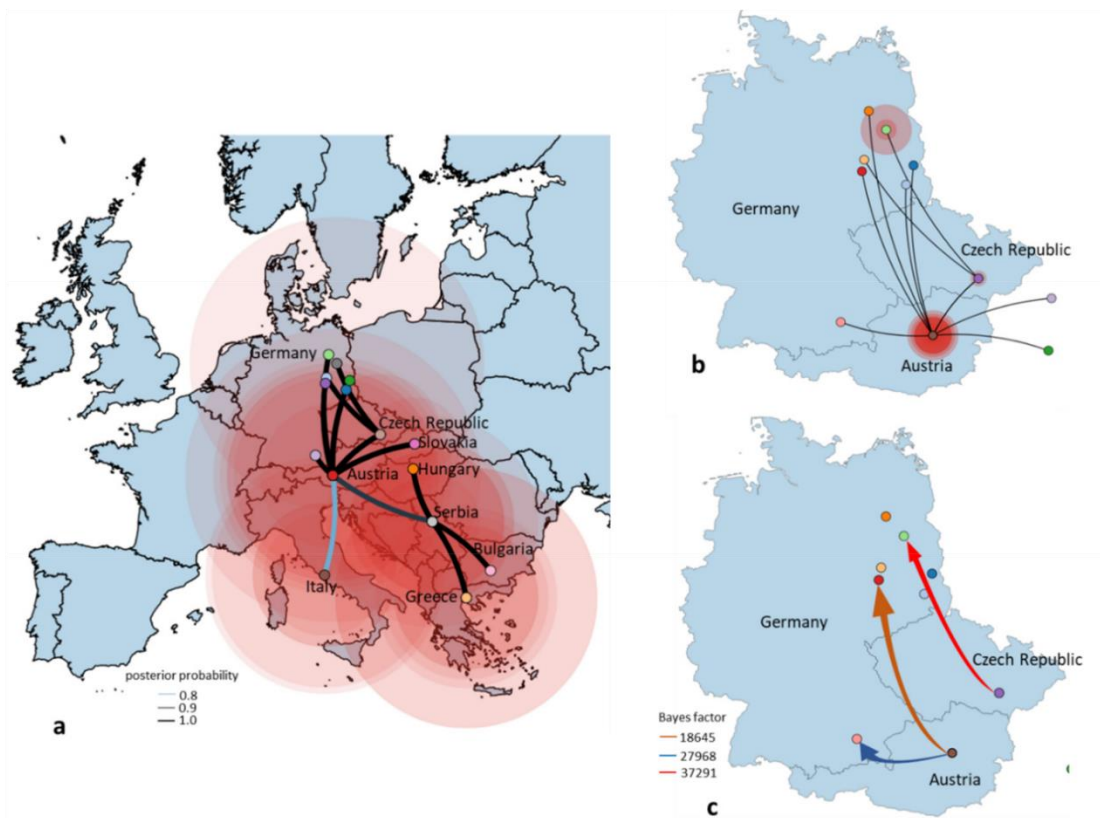
Figure 6. Spatial dynamics of the European clade of WNV lineage 2 including the origin of the German WNV reconstructed from the Bayesian maximum clade credibility (MCC) tree, a flexible demographic

prior with location states and a Bayesian Stochastic Search Variable Selection (BSSVS); (**a**) the directed lines between locations connect the sources and target countries. Circles represent discrete geographical locations of viral strains and represent branches in the MCC tree along with where the relevant location transition occurs. All introductions for Germany are shown. Circle diameters of locations are proportional to square root of the number of MCC branches maintaining a particular location state at each time-point. Discrete locations are geographic coordinates for each European country; (**b**) the directed lines between the source of viral strains (Czech Republic and Austria) and target locations in Germany. Location circle diameters are proportional to square root of the number of MCC branches maintaining a particular location state at each time-point; (**c**) migration pattern of WNV between Czech Republic–Germany and Austria–Germany based on Bayes factor (BF) test for significant non-zero rates. Viral migration patterns are indicated between the different regions of Germany and neighboring countries and are proportional to the strength of the transmission rate. The color of the connections indicates the origin and the direction of migration and are proportional with the strength of connections. Only well supported paths between locations are shown.
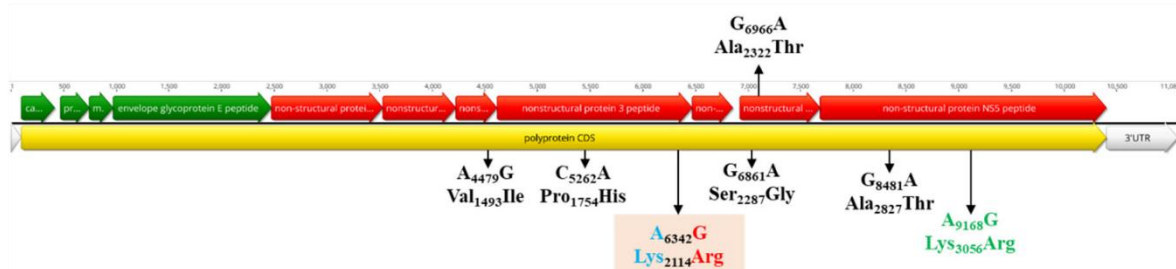
Figure 7. Schematic representation of the WNV genome and the positions of amino acid mutations. The position of the unique amino acid mutation of the Eastern German clade (colored in red/blue) in the NS3 gene is highlighted. The specific non-synonymous amino acid mutations for the CEC are shown in black, while the mutation in the NS5 specific for the subclade including the Eastern German group, one Austrian, one Czech and two German strains is presented in green.

4. Discussion

Globalization and climate change enhance or can lead the migration of exotic pathogens and their hosts to new environments promoting the contacts with naïve and vulnerable hosts. Thus, understanding the local ecological factors and evolutionary processes which navigate the emergence, establishment and spread of newly introduced viral diseases is critical for developing and implementing surveillance strategies for disease control. The present study aimed to elucidate the possible origins, spatiotemporal spread pattern tendencies and eco-epidemiological factors that facilitate WNV becoming an established pathogen in Germany causing neuroinvasive disease in multiple vertebrate species, including humans.

One year after the first observed autochthonous WNV transmission to birds and horses in Germany [9,13], an epizootic emergence of WNV was again observed in 2019. The number of infected birds and horses was considerably higher (76 birds and 36 horses) compared to 2018 (12 birds and two horses). In contrast to the USA, WNV-associated mass mortality in birds had not been observed in Europe before [33]. Previous hypotheses for this difference have been refuted by several research studies, e.g., demonstrating that European birds are susceptible to WNV infections and *Culex* mosquitoes in Europe are competent to transmit WNV. An alternative explanation might by that the bird mortality is so low that it is not detected with current European surveillance programs. A comprehensive USUV/WNV monitoring system is in place, but we also only see the tip of the iceberg of WNV infected birds in Germany. In addition, a huge number of positive specimens were obtained from captive animals (e.g., birds kept in zoos), which have a higher probability of detection compared to wild animals. Furthermore, from these birds, a considerable proportion were birds of prey, which must be considered to have a higher susceptibility to WNV infection [34]. This in combination with

a widespread enzootic circulation of WNV and large number of equine cases—36 in 2019 in contrast to 2 in 2018—indicates an increased risk of WNV spillover into the human population.

This is reflected in the detection of five laboratory confirmed, mosquito-borne, autochthonous human WNV cases in 2019. It has to be kept in mind that less than 25% of infected humans develop noticeable symptoms [3]. Even fewer patients (<1%) have a risk of developing WNND [4]. The number of observed WNND cases (three of the five confirmed human WNV) gives rise to the speculation that hundreds of undetected human WNV infections in Germany occurred during the epidemic in 2019.

WNV transmission and spread is significantly influenced by climatic conditions, e.g., shaping phenology and abundance of the vector. Temperature is one of the most important factors directly affecting the EIP in different mosquito vector species [14]. High daily average temperatures (> 20 °C) over several days are required to allow for WNV transmission, which is correlated to the main distribution of WNV in south-eastern Europe. This also matches the spatial pattern of WNV in Germany. The summers in 2018 and 2019 were both characterized by extraordinarily high temperatures allowing low EIP values. The area in central-eastern Germany as the main focus of WNV circulation in both years was characterized by shorter EIP compared to previous years and most other areas in Germany [13]. Furthermore, these areas in Germany are directly neighboring countries reporting several years of WNV circulation (e.g., Czech Republic), leading to a high risk of short distance introductions e.g., by infected birds. The analysis also indicated that the areas along the Upper Rhine Valley in south-west Germany had a high suitability for WNV circulation, but no WNV activity was observed in all previous surveillance programs [8–11]. Most likely, no WNV introduction and circulation occurred yet, which underpins the thesis of the entries over short distances. Future studies are needed to understand if the virus did not yet spread to this area or if there are other factors reducing the risk of virus circulation (e.g., distribution of suitable vector or host species). The phylogenetic analyses indicated that Germany experienced at least six distinct WNV introduction events, with Austria and Czech Republic as possible origin for the progenitors of the German WNV epizootic strain variants. The majority of these strains clustered together into a distinct subclade (EGC).

The ongoing circulation and dominance of the EGC detected in 2019 indicates successful overwintering of WNV in Germany, e.g., through WNV persistence in hibernating mosquitoes throughout the winter season [35]. The virus variants of the EGC at multiple sites detected in the epidemic in 2019 are descendants of a common ancestor in the wider central European environment which dates back to the time span 2010–2012. Where and when the subsequent virus evolution to the current variants took place and how descendants were eventually transferred to Germany remains elusive. However, such a translocation and subsequent virus amplification may have been fostered by the extremely favorable climatic conditions for mosquitos in Germany in spring/summer 2018, and the short distance transmission with infected birds from neighboring countries.

There has been a comprehensive USUV/WNV monitoring system in place in Germany for over a decade which involves ornithologists, zoological gardens and bird clinics supplying thousands of zoo and wild bird samples for WNV antibody and genome analysis. Moreover, there has been an exhaustive mosquito surveillance in place in Germany since 2009. By both surveillance approaches a variety of viruses were found, such as Sindbis virus, Batai virus and USUV, but not WNV [9–11,13,36,37]. At the same time, different long-distance, partial and short-distance migratory birds showed neutralizing antibodies against WNV before 2018 [9,11]. Although any such monitoring scheme has its predictive limitations due to sampling size constraints, all the negative WNV monitoring results from birds, horses and mosquitos before 2018 and the proximity to a larger region with active WNV circulation supports a recent introduction of multiple WNV descendants e.g., from Czech Republic to Germany. However, sequencing a larger number of more current WNV strains from e.g., Austria or the Czech Republic would help to answer the circumstances of when and what in regard to the development of the East German Clade variants. Overall, the number of recent whole genome sequences is limited and should be markedly increased using NGS-based approaches.

Most of the singleton WNV variants in Germany do not contain the monophyletic Lys2114Arg mutation located in the C terminus of the NS3 gene, even if these strains circulate in the central-eastern part of the country with very high WNV activity and rapid expansion of the EGC. Although these singletons have circulated and evolved under the same ecological conditions as members of EGC, it seems that these variants were not able to perpetuate and establish a stable enzootic cycle leading to a similar epizootic/epidemic scenario as for the EGC group. In case of the EGC, the adaptation to naïve vector and host populations leads to the emergence of local virus variants. The most likely scenario for EGC might be enzootic maintenance similar to that observed for WNV in the United States [38,39]. This hypothesis is supported by the observation that EGC form a star-like structure (population expansion after a single viral introduction) in which the variant viral strains accumulate changes during the rapid adaptation to the local ecological conditions (adaptation of the virus to the host populations and its enzootic maintenance), as observed for Usutu virus [40].

We found evidence that the phylogenetic structure of EGC and virus genetic population growth is shaped by the geographic location and average extrinsic incubation period, which likely facilitated rapid short-distance virus dispersal in 2018/2019. This demonstrates that local ecological factors (e.g., average temperature profile during the vector season) could predict the local and regional dispersal patterns of WNV in our data sets.

The purifying and negative selections observed for WNV in Germany were expected given the transmission and infection modes of arboviruses, leading to the accumulation of synonymous mutations [41]. Mutation observed at amino acid position Lys2114Arg has been found to be involved in the formation of EGC, while Val1493Ile (NS2b), Pro1754His (NS3), Ser2287Gly and Ala2322Thr (NS4b), Ala2827Thr and Lys3056Arg (NS5) are specific for the CEC (convergent evolution). Similar patterns of parallel or convergent evolution have been observed for WNV. This suggests that a limited number of residue changes are permitted due to functional constraints [42]. Viral adaptation in vector and vertebrate hosts by local overwintering or reintroduction of the virus and local ecological conditions (e.g., high average EIP) could be considered key determinants in the spatial dispersal and establishment of WNV. It is interesting to note that the Lys2114Arg mutation is specific for the newly described EGC. The impact of this mutation is unclear; a similar change in the WNV NS3 helicase (Thr1754Pro) generated a highly virulent phenotype to American crows [43]. In vitro and in vivo experiments with strains from the EGC might show the role of fitness and pathogenicity in the future.

5. Conclusions

This study provides a first comprehensive summary and phylogeographic analysis on the WNV epidemic in Germany in 2018 and 2019 and highlights the risk of human WNV infections causing considerable risks for transfusion and organ transplantation safety. Therefore, intensive surveillance of mosquitoes, birds, horses and humans should remain a public health priority, e.g., to monitor the occurrence and subsequent spread of WNV or to develop targeted control mechanisms. Our study also highlights the need for international cooperation in the area of WNV surveillance and monitoring, especially across national borders and as a "one-health" approach for an improved risk analysis. This should also include the generation of higher numbers of whole-genome sequences, allowing for a more precise molecular epidemiology and strain characterization.

Author Contributions: formal analysis, U.Z., P.D.S., M.H.G., D.H., J.S.C., D.C., R.L. (Renke Lühken); investigation, U.Z., P.D.S., M.H.G., C.H., M.E., D.H., P.E., M.K., F.M., R.K., K.M., D.W., H.K., C.F., R.L. (Raskit Lachmann), B.A.T., C.W., M.R., L.L., T.G., C.A.S., M.S., J.S.C., D.C., R.L. (Renke Lühken); writing—original draft preparation, U.Z., P.D.S., M.H.G., D.H., M.B., J.S.C., D.C., R.L. (Renke Lühken). All authors have read and agreed to the published version of the manuscript.

References

1. Kramer, L.D.; Styer, L.M.; Ebel, G.D. A global perspective on the epidemiology of West Nile virus. *Annu. Rev. Entomol.* **2008**, *53*, 61–81.
2. Yeung, M.W.; Shing, E.; Nelder, M.; Sander, B. Epidemiologic and clinical parameters of West Nile virus infections in humans: A scoping review. *BMC Infect. Dis.* **2017**, *17*, 609.
3. Zou, S.; Foster, G.A.; Dodd, R.Y.; Petersen, L.R.; Stramer, S.L. West Nile fever characteristics among viremic persons identified through blood donor screening. *J. Infect. Dis.* **2010**, *202*, 1354–1361.
4. Mostashari, F.; Bunning, M.L.; Kitsutani, P.T.; Singer, D.A.; Nash, D.; Cooper, M.J.; Katz, N.; Liljebjelke, K.A.; Biggerstaff, B.J.; Fine, A.D.; et al. Epidemic West Nile encephalitis, New York, 1999: Results of a household-based seroepidemiological survey. *The Lancet* **2001**, *358*, 261–264.
5. Centers for Disease Control and Prevention. West Nile Virus Disease Cases and Deaths Reported to CDC by Year and Clinical Presentation, 1999–2018. 2019. Available online: https://www.cdc.gov/westnile/statsmaps/cumMapsData.html (accessed on 01 April 2020).
6. Petersen, L.R. Epidemiology of West Nile virus in the United States: Implications for arbovirology and public health. *J. Med. Entomol.* **2019**, *56*, 1456–1462.
7. European Centre for Disease Prevention and Control. Historical Data by Year—West Nile Fever Seasonal Surveillance. 2019. Available online: https://www.ecdc.europa.eu/en/west-nile-fever/surveillance-and-disease-data/historical (accessed on 01 April 2020).
8. Börstler, J.; Engel, D.; Petersen, M.; Poggensee, C.; Jansen, S.; Schmidt-Chanasit, J.; Lühken, R. Surveillance of maternal antibodies against West Nile virus in chicken eggs in South-West Germany. *Trop. Med. Int. Health* **2016**, *21*, 687–690.
9. Michel, F.; Sieg, M.; Fischer, D.; Keller, M.; Eiden, M.; Reuschel, M.; Schmidt, V.; Schwehn, R.; Rinder, M.; Urbaniak, S.; et al. Evidence for West Nile virus and Usutu virus infections in wild and resident birds in Germany, 2017 and 2018. *Viruses* **2019**, *11*, 674.
10. Scheuch, D.; Schäfer, M.; Eiden, M.; Heym, E.; Ziegler, U.; Walther, D.; Schmidt-Chanasit, J.; Keller, M.; Groschup, M.; Kampen, H. Detection of Usutu, Sindbis, and Batai Viruses in mosquitoes (Diptera: Culicidae) collected in Germany, 2011–2016. *Viruses* **2018**, *10*, 389.
11. Michel, F.; Fischer, D.; Eiden, M.; Fast, C.; Reuschel, M.; Müller, K.; Rinder, M.; Urbaniak, S.; Brandes, F.; Schwehn, R.; et al. West Nile virus and Usutu virus monitoring of wild birds in Germany. *Int. J. Environ. Res. Public. Health* **2018**, *15*, 171.

12. Ziegler, U.; Angenvoort, J.; Klaus, C.; Nagel-Kohl, U.; Sauerwald, C.; Thalheim, S.; Horner, S.; Braun, B.; Kenklies, S.; Tyczka, J.; et al. Use of competition ELISA for monitoring of West Nile virus infections in horses in Germany. *Int. J. Environ. Res. Public. Health* **2013**, *10*, 3112–3120.

13. Ziegler, U.; Lühken, R.; Keller, M.; Cadar, D.; van der Grinten, E.; Michel, F.; Albrecht, K.; Eiden, M.; Rinder, M.; Lachmann, L.; et al. West Nile virus epizootic in Germany, 2018. *Antiviral Res.* **2019**, *162*, 39–43.

14. Jansen, S.; Heitmann, A.; Lühken, R.; Leggewie, M.; Helms, M.; Badusche, M.; Rossini, G.; Schmidt-Chanasit, J.; Tannich, E. *Culex torrentium*: A potent vector for the transmission of West Nile virus in Central Europe. *Viruses* **2019**, *11*, 492.

15. Becker, N.; Jöst, H.; Ziegler, U.; Eiden, M.; Höper, D.; Emmerich, P.; Fichet-Calvet, E.; Ehichioya, D.U.; Czajka, C.; Gabriel, M.; et al. Epizootic emergence of Usutu virus in wild and captive birds in Germany. *PLoS ONE* **2012**, *7*, e32604.

16. Eiden, M.; Vina-Rodriguez, A.; Hoffmann, B.; Ziegler, U.; Groschup, M.H. Two new real-time quantitative reverse transcription polymerase chain reaction assays with unique target sites for the specific and sensitive detection of lineages 1 and 2 *West Nile Virus* Strains. *J. Vet. Diagn. Invest.* **2010**, *22*, 748–753.

17. Jöst, H.; Bialonski, A.; Maus, D.; Sambri, V.; Eiden, M.; Groschup, M.H.; Günther, S.; Becker, N.; Schmidt-Chanasit, J. Isolation of Usutu virus in Germany. *Am. J. Trop. Med. Hyg.* **2011**, *85*, 551–553.

18. Becker, N.; Petric, D.; Zgomba, M.; Boase, C.; Madon, M.; Dahl, C.; Kaiser, A. *Mosquitoes and Their Control*, 2nd ed.; Springer: Berlin/Heidelberg, Germany, 2010.

19. Kampen, H.; Holicki, C.M.; Ziegler, U.; Groschup, M.; Tews, B.A.; Werner, D. West Nile virus mosquito vectors (Diptera: Culicidae) in Germany. *Viruses* (in review).

20. Reisen, W.K.; Niu, T.; Gaff, H.D.; Barker, C.M.; Le Menach, A.; Hartley, D.M. Effects of temperature on emergence and seasonality of West Nile virus in California. *Am. J. Trop. Med. Hyg.* **2012**, *86*, 884–894.

21. Cornes, R.C.; van der Schrier, G.; van den Besselaar, E.J.M.; Jones, P.D. An ensemble version of the E-OBS temperature and precipitation data sets. *J. Geophys. Res. Atmospheres* **2018**, *123*, 9391–9409.

22. R Core Team *R: A Language and Environment for Statistical Computing*; R Foundation for Statistical Computing: Vienna, Austria, 2019.

23. Grolemund, G.; Wickham, H. Dates and times made easy with lubridate. *J. Stat. Softw.* **2011**, *40*, 1–25.

24. Hijmans, R.J. *raster: Geographic Data Analysis and Modeling*, R Package Version 2.9-5; 2019. Available online: https://CRAN.R-project.org/package=raster (accessed on 01 April 2020).

25. Wylezich, C.; Papa, A.; Beer, M.; Höper, D. A Versatile sample processing workflow for metagenomic pathogen detection. *Sci. Rep.* **2018**, *8*, 13108.

26. Martin, D.; Rybicki, E. RDP: Detection of recombination amongst aligned sequences. *Bioinformatics* **2000**, *16*, 562–563.

27. Suchard, M.A.; Lemey, P.; Baele, G.; Ayres, D.L.; Drummond, A.J.; Rambaut, A. Bayesian phylogenetic and phylodynamic data integration using BEAST 1.10. *Virus Evol.* **2018**, *4*, vey016.

28. Darriba, D.; Taboada, G.L.; Doallo, R.; Posada, D. jModelTest 2: More models, new heuristics and parallel computing. *Nat. Methods* **2012**, *9*, 772–772.

29. Guindon, S.; Dufayard, J.-F.; Lefort, V.; Anisimova, M.; Hordijk, W.; Gascuel, O. New algorithms and methods to estimate maximum-likelihood phylogenies: Assessing the performance of PhyML 3.0. *Syst. Biol.* **2010**, *59*, 307–321.

30. Rambaut, A.; Lam, T.T.; Max Carvalho, L.; Pybus, O.G. Exploring the temporal structure of heterochronous sequences using TempEst (formerly Path-O-Gen). *Virus Evol.* **2016**, *2*, vew007.

31. Drummond, A.J.; Rambaut, A. BEAST: Bayesian evolutionary analysis by sampling trees. *BMC Evol. Biol.* **2007**, *7*, 214.

32. Leigh, J.W.; Bryant, D. POPART: Full-feature software for haplotype network construction. *Methods Ecol. Evol.* **2015**, *6*, 1110–1116.

33. Koraka, P.; Barzon, L.; Martina, B.E. West Nile Virus Infections in (European) Birds. *J Neuroinfect Dis* **2016**, *7*, 3.

34. Bakonyi, T.; Ferenczi, E.; Erdélyi, K.; Kutasi, O.; Csörgő, T.; Seidel, B.; Weissenböck, H.; Brugger, K.; Bán, E.; Nowotny, N. Explosive spread of a neuroinvasive lineage 2 West Nile virus in Central Europe, 2008/2009. *Vet. Microbiol.* **2013**, *165*, 61–70.

35. Rudolf, I.; Betášová, L.; Blažejová, H.; Venclíková, K.; Straková, P.; Šebesta, O.; Mendel, J.; Bakonyi, T.; Schaffner, F.; Nowotny, N.; et al. West Nile virus in overwintering mosquitoes, central Europe. *Parasit. Vectors* **2017**, *10*, 452.

36. Heym, E.C.; Kampen, H.; Krone, O.; Schäfer, M.; Werner, D. Molecular detection of vector-borne pathogens from mosquitoes collected in two zoological gardens in Germany. *Parasitol. Res.* **2019**, *118*, 2097–2105.

37. Ziegler, U.; Fischer, D.; Eiden, M.; Reuschel, M.; Rinder, M.; Müller, K.; Schwehn, R.; Schmidt, V.; Groschup, M.H.; Keller, M. Sindbis virus—A wild bird associated zoonotic arbovirus circulates in Germany. *Vet. Microbiol.* **2019**, *239*, 108453.

38. Añez, G.; Grinev, A.; Chancey, C.; Ball, C.; Akolkar, N.; Land, K.J.; Winkelman, V.; Stramer, S.L.; Kramer, L.D.; Rios, M. Evolutionary dynamics of West Nile virus in the United States, 1999–2011: Phylogeny, selection pressure and evolutionary time-scale analysis. *PLoS Negl. Trop. Dis.* **2013**, *7*, e2245.

39. Di Giallonardo, F.; Geoghegan, J.L.; Docherty, D.E.; McLean, R.G.; Zody, M.C.; Qu, J.; Yang, X.; Birren, B.W.; Malboeuf, C.M.; Newman, R.M.; et al. Fluid spatial dynamics of West Nile virus in the United States: Rapid spread in a permissive host environment. *J. Virol.* **2016**, *90*, 862–872.

40. Engel, D.; Jöst, H.; Wink, M.; Börstler, J.; Bosch, S.; Garigliany, M.-M.; Jöst, A.; Czajka, C.; Lühken, R.; Ziegler, U.; et al. Reconstruction of the evolutionary history and dispersal of Usutu virus, a neglected emerging arbovirus in Europe and Africa. *mBio* **2016**, *7*, e01938-15.

41. Holmes, E.C. Patterns of intra- and interhost nonsynonymous variation reveal strong purifying selection in dengue virus. *J. Virol.* **2003**, *77*, 11296–11298.

42. Armstrong, P.M.; Vossbrinck, C.R.; Andreadis, T.G.; Anderson, J.F.; Pesko, K.N.; Newman, R.M.; Lennon, N.J.; Birren, B.W.; Ebel, G.D.; Henn, M.R. Molecular evolution of West Nile virus in a northern temperate region: Connecticut, USA 1999–2008. *Virology* **2011**, *417*, 203–210.

43. Brault, A.C.; Huang, C.Y.-H.; Langevin, S.A.; Kinney, R.M.; Bowen, R.A.; Ramey, W.N.; Panella, N.A.; Holmes, E.C.; Powers, A.M.; Miller, B.R. A single positively selected West Nile viral mutation confers increased virogenesis in American crows. *Nat. Genet.* **2007**, *39*, 1162–1166.

Table S1. Epidemiological data of West Nile virus with full genome sequences (except for 1 human sample), their corresponding accession numbers and sequencing protocol performed.

Accession Number	Virus identifier	Library number	Host common name	Host scientific name	City	Region	Sequencing Protocol
LR743437	ED-I-90_18	lib02896	Great Grey Owl	*Strix nebulosa*	Poing	Bavaria	Direct NGS
LR743434	ED-I-114_18	lib02898	Great Grey Owl	*Strix nebulosa*	Poing	Bavaria	Direct NGS
LR743433	ED-I-82_18	lib02914	Goshawk	*Accipiter gentilis*	Klein Weissandt	Saxony-Anhalt	Direct NGS
LR743429	ED-I-142_18	lib02916	Tawny Owl	*Strix aluco*	Bad Lauchstaedt	Saxony-Anhalt	Direct NGS
LR743436	ED-I-89_18	lib02959	Goshawk	*Accipiter gentilis*	Bad Düben	Saxony	Direct NGS
LR743443	ED-I-107-18	lib03041	Snowy Owl	*Bubo scandiacus*	Berlin Friedrichsfelde	Berlin	Direct NGS
LR743425	ED-I-62_19	lib03378	Snowy Owl	*Bubo scandiacus*	Lutherstadt Wittenberg	Saxony Anhalt	Direct NGS
LR743444	ED-I-83_19	lib03379	Great Grey Owl	*Strix nebulosa*	Lutherstadt Wittenberg	Saxony Anhalt	Direct NGS
LR743424	ED-I-85_19	lib03380	Snowy Owl	*Bubo scandiacus*	Berlin Friedrichsfelde	Berlin	Direct NGS
LR743442	ED-I-87_19	lib03381	Blue Tit	*Parus caeruleus*	Halle (Saale)	Saxony-Anhalt	Direct NGS
LR743428	ED-I-118_19	lib03382	Snowy Owl	*Bubo scandiacus*	Berlin Friedrichsfelde	Berlin	Direct NGS
LR743426	ED-I-157_19	lib03415	Snowy Owl	*Bubo scandiacus*	Berlin	Berlin	Direct NGS
LR743432	ED-I-158_19	lib03416	Andean Flamingo	*Phoenicoparrus andinus*	Berlin	Berlin	Direct NGS
LR743427	ED-I-148_19	lib03417	Goshawk	*Accipiter gentilis*	Berlin	Berlin	Direct NGS
LR743423	ED-I-156_19	lib03418	Goshawk	*Accipiter gentilis*	Berlin Friedrichsfelde	Berlin	Direct NGS
LR743435	ED-I-153_19	lib03419	Goshawk	*Accipiter gentilis*	Brieselang	Brandenburg	Direct NGS
LR743422	ED-I-155_19	lib03420	Goshawk	*Accipiter gentilis*	Neuruppin	Brandenburg	Direct NGS
LR743430	ED-I-89_19	lib03421	Blue Tit	*Parus caeruleus*	Radebeul	Saxony	Direct NGS
LR743421	ED-I-139_19	lib03422	Great Tit	*Parus major*	Dresden	Saxony	Direct NGS
LR743431	ED-I-177_19	lib03423	Eurasian Golden Plover	*Pluvialis apricaria*	Kamenz/Biehla	Saxony	Direct NGS
LR743449	ED-I-163_19	lib03424	Goshawk	*Accipiter gentilis*	Sandersdorf	Saxony-Anhalt	Direct NGS
LR743458	ED-I-164_19	lib03425	Snowy Owl	*Bubo scandiacus*	Magdeburg	Saxony-Anhalt	Direct NGS
LR743451	ED-I-165_19	lib03426	Snowy Owl	*Bubo scandiacus*	Magdeburg	Saxony-Anhalt	Direct NGS
LR743446	ED-I-109_19	lib03427	Coconut Lorikeet	*Trichoglossus haematodus*	Halle (Saale)	Saxony-Anhalt	Direct NGS
LR743456	ED-I-134_19	lib03428	House Sparrow	*Passer domesticus*	Rackwitz	Saxony	Direct NGS
LR743445	ED-I-172_19	lib03430	Great Grey Owl	*Strix nebulosa*	Chemnitz	Saxony	Direct NGS
LR743452	ED-I-173_19	lib03431	Great Grey Owl	*Strix nebulosa*	Chemnitz	Saxony	Direct NGS
LR743450	ED-I-202_19	lib03432	Chilean Flamingo	*Phoenicopterus chilensis*	Leipzig	Saxony	Direct NGS
LR743454	ED-I-205_19	lib03433	Great Tit	*Parus major*	Bad Düben	Saxony	Direct NGS
LR743448	ED-I-201_19	lib03449	Humboldt-Penguin	*Spheniscus humboldti*	Cottbus	Brandenburg	Direct NGS
LR743457	ED-I-208_19	lib03450	Goshawk	*Accipiter gentilis*	Merseburg	Saxony-Anhalt	Direct NGS
LR743453	ED-I-94_19	lib03451	Horse	*Equus ferus caballus*	Krostitz	Saxony	Direct NGS with MyBaits treatment
LR743455	C6_T167_20	lib03481	Mosquito	*Culex pipiens*	Berlin Friedrichsfelde	Berlin	Direct NGS
LR743447	C6_T167_57	lib03482	Mosquito	*Culex pipiens*	Berlin Friedrichsfelde	Berlin	Direct NGS
MN794935	BNI-10/19	BNI42493	Human	*Homo sapiens*	Leipzig	Saxony	Direct NGS
MN794936	BNI-Berlin748	BNI45435	Human	*Homo sapiens*	Berlin	Berlin	Direct NGS
MN794937	BNI-2635	BNI41487	Blackbird	*Turdus merula*	Schönebeck	Saxony-Anhalt	Direct NGS
MN794938	BNI-2615	BNI41323	House sparrow	*Passer domesticus*	Jeßwitz	Saxony-Anhalt	Direct NGS
MN794939	BNI-2432	BNI40119	Dunnock	*Prunella modularis*	Hamburg	Hamburg	Direct NGS

45

(III) Co-Infections: Simultaneous Detections of West Nile Virus and Usutu Virus in Birds from Germany

Pauline Dianne Santos, Friederike Michel, Claudia Wylezich, Dirk Höper, Markus Keller, Cora M. Holicki, Claudia A. Szentiks, Martin Eiden, Aemero Muluneh, Antonie Neubauer-Juric, Sabine Thalheim, Anja Globig, Martin Beer, Martin H. Groschup and Ute Ziegler

ORIGINAL ARTICLE

Transboundary and Emerging Diseases   **WILEY**

Co-infections: Simultaneous detections of West Nile virus and Usutu virus in birds from Germany

Pauline Dianne Santos[1] [iD] | Friederike Michel[2] | Claudia Wylezich[1] | Dirk Höper[1] [iD] | Markus Keller[2] | Cora M. Holicki[2] | Claudia A. Szentiks[3] | Martin Eiden[2] [iD] | Aemero Muluneh[4] | Antonie Neubauer-Juric[5] | Sabine Thalheim[6] | Anja Globig[7] | Martin Beer[1] [iD] | Martin H. Groschup[2,8] [iD] | Ute Ziegler[2,8] [iD]

[1]Institute of Diagnostic Virology, Friedrich-Loeffler-Institut, Federal Research Institute for Animal Health, Greifswald-Insel Riems, Germany

[2]Institute of Novel and Emerging Infectious Diseases, Friedrich-Loeffler-Institut, Federal Research Institute for Animal Health, Greifswald-Insel Riems, Germany

[3]Leibniz Institute for Zoo and Wildlife Research (IZW), Berlin, Germany

[4]Saxon State Laboratory of Health and Veterinary Affairs, Dresden, Germany

[5]Bavarian Health and Food Safety Authority, Oberschleissheim, Germany

[6]Berlin-Brandenburg State Laboratory, Frankfurt (Oder), Germany

[7]Institute of International Animal Health/One Health, Friedrich-Loeffler-Institut, Federal Research Institute for Animal Health, Greifswald-Insel Riems, Germany

[8]German Centre for Infection Research, partner site Hamburg-Luebeck-Borstel-Riems, Hamburg, Germany

Correspondence
Ute Ziegler, Institute of Novel and Emerging Infectious Diseases, Friedrich-Loeffler-Institut, Federal Research Institute for Animal Health, Greifswald-Insel Riems 17493, Germany.
Email: ute.ziegler@fli.de

Abstract

The emergence of West Nile virus (WNV) and Usutu virus (USUV) in Europe resulted in significant outbreaks leading to avifauna mortality and human infections. Both viruses have overlapping geographical, host and vector ranges, and are often co-circulating in Europe. In Germany, a nationwide bird surveillance network was established to monitor these zoonotic arthropod-borne viruses in migratory and resident birds. In this framework, co-infections with WNV and USUV were detected in six dead birds collected in 2018 and 2019. Genomic sequencing and phylogenetic analyses classified the detected WNV strains as lineage 2 and the USUV strains as lineages Africa 2 ($n = 2$), Africa 3 ($n = 3$) and Europe 2 ($n = 1$). Preliminary attempts to co-propagate both viruses in vitro failed. However, we successfully cultivated WNV from two animals. Further evidence for WNV-USUV co-infection was obtained by sampling live birds in four zoological gardens with confirmed WNV cases. Three snowy owls had high neutralizing antibody titres against both WNV and USUV, of which two were also positive for USUV-RNA. In conclusion, further reports of co-infections in animals as well as in humans are expected in the future, particularly in areas where both viruses are present in the vector population.

KEYWORDS
arboviruses, birds, co-infection, Germany, Usutu virus, West Nile virus

1 | INTRODUCTION

Mosquito-borne viruses represent a growing threat to Europe and its avifauna (Hubálek et al., 2014). In this context, West Nile virus (WNV) and Usutu virus (USUV) have to be considered as two of the more than seventy relevant members of the family *Flaviviridae* (Calisher & Gould, 2003). These two flaviviruses were historically regarded as viruses of purely African significance, with no evidence of associated bird or human mortality. It was only when these viruses entered Europe and America (for WNV-only) that waves of infection became visible in both birds and mammals (e.g. humans and horses) (Zeller & Schuffenecker, 2004). Although USUV infections in humans are commonly asymptomatic, recent outbreaks in Europe had reported neuroinvasive cases with encephalitis and meningoencephalitis, in patients from Italy and Croatia as summarized by Clé et al., (2019).

USUV and WNV are classified as arthropod-borne viruses (arboviruses) that are primarily transmitted by ornithophilic mosquitoes to birds and mammals. Both viruses are preserved in the environment through a vertebrate host–mosquito life cycle, where different bird species act as amplifying hosts, *Culex* mosquitoes as primary vectors and mammals, such as humans and horses, as dead-end hosts. Viral transmission occurs when an infected mosquito takes a blood meal from a non-immune susceptible host. During this process, the virus present in the salivary glands of the mosquito is transferred to the avian host where it is replicated to high titre and appears in the bloodstream as a viraemia, thereby enabling further mosquito transmission cycles of the virus to other hosts (Chancey et al., 2015; Clé et al., 2019).

WNV and USUV mono-infections were reported in a wide range of avian species including owls, birds of prey, passerines, storks, flamingos and others (as summarized in Nikolay, 2015). Typically, infection in most bird species remains inapparent. However, bird species that are highly susceptible for WNV, such as owls, birds of prey and several passerines (e.g. jays, crows and sparrows), can develop a neurological disease which can be fatal (Komar, 2003; Pérez-Ramírez et al., 2014; Troupin & Colpitts, 2016). The same holds true for USUV, with owls and passerines like blackbirds being more susceptible to disease (Becker et al., 2012; Chvala et al., 2004).

The circulation of WNV and USUV is generally influenced by environmental factors that affect the population dynamics of mosquito vectors, the extrinsic incubation periods (the time needed for a mosquito to become infectious after ingestion of a virus) and the population densities of amplifying hosts (Durand et al., 2010; Rubel et al., 2008). Since both WNV and USUV have very similar prerequisites in these regards, it is no surprise that these two viruses co-circulate in Europe in at least 10 countries and that both viruses have been found to infect 34 common bird species belonging to 11 different orders (Nikolay, 2015). Hence, WNV and USUV transmission cycles overlap substantially in many countries (Nikolay, 2015).

The unusually hot climatic conditions all over Europe in the summer 2018, with an extremely long period of high temperatures, may have provided favourable conditions for the incursion and establishment of WNV and/or USUV into new areas and countries (Camp & Nowotny, 2020). In this context, a large WNV outbreak was observed in southeastern and southern Europe, with a total of 2,083 autochthonous human WNV cases in the European Union (EU) member states and EU neighbouring countries (European Centre for Disease Prevention and Control [ECDC], 2018). In 2018, WNV was detected for the first time in birds and horses in Germany (Ziegler et al., 2019).

While WNV was only recently introduced into Germany, USUV had circulated here for more than ten years. In 2010, USUV was first detected in mosquitoes in southwest Germany (Jöst et al., 2011). One year later, dead common blackbirds (*Turdus merula*) were found frequently around the cities of Mannheim and Heidelberg (Baden-Württemberg) followed by a mass mortality among wild birds in southwest Germany (Becker et al., 2012). In the following years, USUV outbreaks stayed geographically restricted to the Upper Rhine Valley in southwest Germany, apart from a few sporadic cases in Berlin and Bonn (Cadar et al., 2015; Ziegler et al., 2015, 2016). In 2016, however, USUV case numbers increased dramatically not only in southwestern Germany, but also in the federal states of North Rhine-Westphalia (NRW), Saxony and Saxony-Anhalt (Cadar et al., 2017; Sieg et al., 2017). Since its occurrence in Germany, USUV had been responsible for the mortality of thousands of common blackbirds and many captive and free-living owls in the past (Lühken et al., 2017). Currently, there are five USUV lineages circulating in the country, namely Africa 2, Africa 3, Europe 2, Europe 3 and Europe 5 (Michel et al., 2019).

The initial 2018 WNV outbreak located in the eastern regions of Germany was accompanied by a massive and ongoing USUV epizootic in all federal states of Germany (Michel et al., 2019; Naturschutzbund Deutschland e.V. [NABU], 2018) and elsewhere in Europe, such as Austria, Belgium, Croatia and the Netherlands (Benzarti et al., 2020; Oude Munnink et al., 2020; Vilibic-Cavlek et al., 2019; Weidinger et al., 2020). In 2019, an even larger WNV epizootic occurred in Germany with 76 confirmed cases in wild and zoo birds, 36 confirmed cases in horses and five clinical cases in humans (Ziegler et al., 2020). This was also accompanied by numerous USUV outbreaks in wild birds in many different areas in Germany. With regard to the fact that WNV and USUV often occur in the same geographical regions and use an almost identical transmission cycle between mosquitoes and birds (Nikolay, 2015), it is surprising that co-infections with both viruses have so far only been described once in a human. In that case, both WNV- and USUV-RNA were detected in a blood donor from Austria (Aberle et al., 2018).

Surveillance of emerging arboviruses, such as WNV and USUV, is well suited in zoological gardens since these collection sites contain large diversity of captive species including mammals and birds, and are located within or near urban areas. Captive animals from zoological gardens can serve as important sentinels for newly introduced pathogens in an area. Collection animals within zoological gardens are also routinely monitored by veterinarians and technical staff with expertise in wildlife health; thus, gathering samples and detailed medical records can be readily available (Constant

et al., 2020; Cox-Witton et al., 2014). For example, WNV introduction in the western hemisphere and Germany was first recognized in Bronx Zoo/Wildlife Conservation Park, New York City, and Zoo Halle (Saale), Saxony-Anhalt, respectively (Ludwig et al., 2002; Ziegler et al., 2019).

Our study describes for the first time a co-infection with WNV and USUV in six dead birds in Germany. These co-infected birds were detected in the context of the WNV epizootic in 2018 and 2019 and followed by an extensive molecular and serological investigation of apparently healthy birds held in zoological gardens with confirmed cases of WNV infection.

2 | MATERIALS AND METHODS

2.1 | Organ and blood samples from birds

Varying tissue materials from deceased wild and captive birds were submitted to the National WNV reference Laboratory at the Friedrich Loeffler Institute (FLI), Island of Riems, Greifswald, Germany, by the regional veterinary laboratories from different federal states of Germany or directly by the Leibniz Institute for Zoo and Wildlife Research (IZW), Berlin, to confirm WNV or USUV infections. Upon veterinary requests, a total of 67 blood samples were taken from birds held in four zoological gardens with confirmed avian WNV-positive cases (areas A–D). In area A from Berlin ('Tierpark Berlin'), it was possible to collect blood samples in two consecutive years (2018 and 2019) from two adult snowy owls, which are the parent birds of cases #1 and #2. After the first evidence of WNV infection in birds from areas B to D, we collected blood samples from 31 zoo birds held at area B ('Zoo Halle/Saale' in Saxony-Anhalt) and 19 zoo birds held at area C ('Wildpark Poing' in Bavaria) in 2018, and from 15 zoo birds held at area D ('Tierpark Cottbus' in southern Brandenburg) in 2019.

2.2 | Molecular virus characterization

Viral RNA was extracted from the tissue material from the submitted bird samples and from the frozen (−70°C) coagulated blood of the bird samples (cruor) using RNeasy Kit (Qiagen) according to the manufacturer's instructions. Extracted RNA was analysed with reverse transcription quantitative real-time PCR (RT-qPCR) assays specific for WNV lineages 1 and 2 as described by Eiden et al. (2010) and USUV-specific RT-qPCR described by Jöst et al. (2011). Based on the guidelines of the National WNV Reference Laboratory, quantification cycle (C_q) values <37 were regarded as positive, from 37 to 40 as possible, and >40 as negative. In all RT-qPCR assays, positive controls with 10^3 and 10^4 WNV or USUV genome copies per reaction were included.

Full-genome sequencing was performed with WNV- and USUV-positive bird samples. The organ material from these birds was homogenized in 1 ml TRIzol™ LS Reagent (Invitrogen™) using the TissueLyser II (QIAGEN) with 5 mm steal beads for 2 min at 30 Hz.

After the phase separation step, RNA was extracted from the aqueous phase using the RNAdvance Tissue kit (Beckman Coulter) and the KingFisher Flex System (Thermo Fisher Scientific). The resulting RNA extracts were also tested with the RT-qPCR assays mentioned above.

Selected WNV-positive RNA was subjected to cDNA synthesis and library preparation as described in Wylezich et al. (2018). We performed targeted enrichment of virus sequences in sequencing libraries from four bird samples (Table 1) using custom myBaits® target capture kit with VirBaits panel (Arbor Biosciences) based on the panel design and protocol described in Wylezich et al. (2020). The USUV full-genome sequencing was implemented as described in Quick et al. (2017) with some modifications. Briefly, USUV-positive RNA was reverse-transcribed using the SuperScript™ IV First-Strand cDNA Synthesis System (Invitrogen™), followed by the USUV-specific multiplex PCR developed by Oude Munnink et al. (2019). This multiplex PCR was performed in two separate reactions using AccuPrime™ *Taq* DNA Polymerase, High Fidelity (Invitrogen™). Amplicons were purified with 1.8 × volumes of Agencourt AMPure XP beads (Beckman Coulter) and quantified using NanoDrop™ spectrophotometer (Thermo Fisher Scientific). These two purified reactions per sample were pooled and adjusted to 500 ng. Fragmentation and library preparation steps were prepared as described in Wylezich et al. (2018). Quantified libraries (GeneRead DNA Library L Core Kit; QIAGEN) were sequenced using an Ion Torrent S5 XL instrument with Ion 530 or Ion 540 chips and the respective reagents (Thermo Fisher Scientific) in 400 bp mode or 200 bp mode, respectively.

After the analysis of USUV sequences, additional library preparation and sequencing were performed to increase the coverage of specific genome positions. Amplification and preparation steps were similar to procedures mentioned above except for primer pairs included in each multiplex PCR mix (library preparation #2 in Table S1). In order to close the gaps within three USUV genome sequences, selected cDNA was amplified using necessary primer pairs for single-plex PCRs (Table S1) and sequenced with a BigDye Terminator v1.1 Cycle Sequencing kit (Applied Biosystems™, Thermo Fisher Scientific) on a 3500 Genetic Analyzer instrument (Applied Biosystems™, Thermo Fisher Scientific).

2.3 | Genome characterization of WNV and USUV, and phylogenetic analyses

Sequencing adapters and primers were trimmed using Newbler assembler of the Genome Sequencer Software Suite v. 3.0 (Roche), and sequencing reads were quality controlled using FastQC. Initial reference-based mapping alignment against Usutu virus strain V491 (accession no. KY426758) or West Nile virus isolate ED-I-33/18-UM (accession no. MH924836.1) was performed using the Roche/454 software suite v 3.0. The consensus sequences were compared using Blastn, and second reference-based mapping alignment was performed using the most closely related *Flavivirus* strain of the consensus. West Nile virus and Usutu virus sequences acquired in this study

TABLE 1 Sample information of deceased birds with WNV and USUV co-infection. These include scientific name, common name and taxonomical order of birds, the geographical location and housing type, sample (FLI sample code) and virus (nucleotide accession numbers) identifiers, organ samples analysed using RT-qPCR (C_q values) and high-throughput sequencing (library numbers and virus lineages/clade). West Nile virus (except cases #2, #6) and Usutu virus sequences were submitted to European Nucleotide Archive under the project accession PRJEB41417

Case number[a]	Scientific name (Common name) Order	Housing/Area	Federal State, City	Identifiers	Organ sample	C_q values WNV	USUV[b]	USUV[c]	Library numbers WNV	USUV	Lineages WNV	USUV
1	*Bubo scandiacus* (Snowy Owl) Strigiformes	Captive Area A	Berlin	Sample: ED-I-79/18 WNV: LR989893 USUV: LR989886	Brain	neg.	28.76	n.p.	lib03038[d,e]	lib04071 lib04107	Lineage 2 EGC	Africa 2
					Spleen	34.81	37.63	n.p,	lib03039[d,e]	n.p		
2	*Bubo scandiacus* (Snowy Owl) Strigiformes	Captive Area A	Berlin	Sample: ED-I-107/18 WNV: LR743443 USUV: LR989887	Brain	18.21	32.28	n.p.	lib03041	n.p	Lineage 2 EGC	Africa 2
					Kidney	29.5	36.12	n.p.	n.p.	lib04073 lib04109		
								n.p.				
					Liver	29.74	neg.	n.p.	n.p.	n.p.		
					Heart	31.33	neg.	n.p.	n.p.	n.p.		
					Lungs	30.6	neg.	n.p.	n.p.	n.p.		
					Spleen	30.55	neg.	n.p.	n.p.	n.p.		
3	*Mergus squamatus* (Chinese Merganser) Anseriformes	Captive Area A	Berlin	Sample: ED-I-115/19 WNV: LR989891 USUV: LR989889	Brain	32.62	neg.	neg.	n.p.	n.p.	Lineage 2 EGC	Africa 3
					Spleen	31.51	neg.	neg.	lib03988[e]	n.p.		
					Kidney	neg.	37.01	31.32	n.p.	n.p.		
					Liver	neg.	33.53	29.04	n.p.	lib04074 lib04110		
4	*Larus crassirostris* (Black-tailed Gull) Charadriiformes	Captive Area A	Berlin	Sample: ED-I-116/19 WNV: LR989885 USUV: LR989892	Brain	26.28	neg.	neg.	lib03989[e]	n.p.	Lineage 2 EGC	Africa 3
					Liver	32.78	36.27	29.09	n.p.	lib04075 lib04111		
5	*Larus crassirostris* (Black-tailed Gull) Charadriiformes	Captive Area A	Berlin	Sample: ED-I-119/19 WNV: LR989888 USUV: LR989894	Brain	26.72	neg.	neg.	n.p.	n.p.	Lineage 2 EGC	Africa 3
					Heart	28.04	37.83	33.26	n.p.	lib04076 lib04112		
					Liver	27.81	neg.	neg.	n.p.	n.p.		
					Kidney	22.25	38.93	34.58	lib03990[c]	n.p.		
6	*Parus major* (Great Tit) Passeriformes	Wild n.a.	Saxony Dresden	Sample: ED-I-139/19 WNV: LR743421 USUV: LR989890	Liver and Heart	12.89	32	n.p.	lib03422[d]	lib04072 lib04108	Lineage 2 EGC	Europe 2

Note: Possible USUV-positive samples based on C_q value range 37–40 were indicated in italics.

Abbreviation: n.a, not applicable since the sample was a wild bird; n.p, not processed; neg, negative.

[a]Marked in Figure 1 with red dots.

[b]USUV RT-qPCR results based on protocol from Jöst et al. (2011).

[c]USUV RT-qPCR results based on protocol from Cavrini et al. (2011).

[d]USUV sequence reads detected in the library.

[e]Sequencing libraries subjected with targeted enrichment of virus sequence (Wylezich et al., 2020).

FIGURE 1 Geographical distribution of WNV-positive birds (WNV-RNA positive) and horses (WNV-RNA and/or IgM-antibody positive) in Germany in 2018 and 2019 (depicted at the district level). Red dots mark the locations of the six cases of WNV-USUV co-infection in birds, case #1–#5 were situated in the wildlife park 'Tierpark Berlin', and case #6 was situated in the city of Dresden, Saxony. The encircled letters represent the locations of zoological gardens for environmental investigations: Ⓐ wildlife park 'Tierpark Berlin', Ⓑ 'Zoo Halle/Saale' in Saxony-Anhalt, Ⓒ wild park 'Wildpark Poing' in Bavaria and Ⓓ wildlife park 'Tierpark Cottbus' in southern Brandenburg

WNV positive (in 2018)
WNV positive (in 2018 and 2019)
WNV positive (first time in 2019)
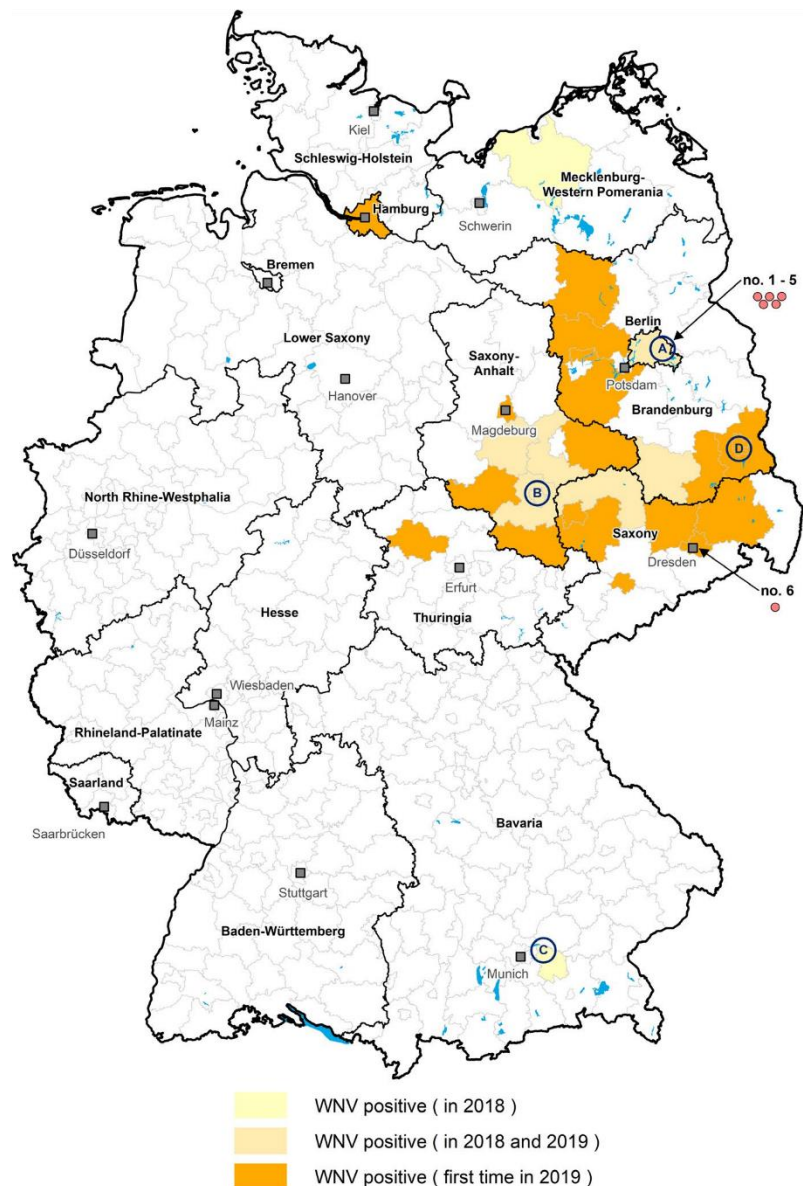
were submitted to European Nucleotide Archive under the BioProject accession number PRJEB41417 (Table 1). All whole-genome sequences of European WNV lineage 2 and USUV were retrieved from GenBank on 01 September 2020 (Tables S2 and S3, respectively). The retrieved USUV and WNV sequences together with the newly obtained sequences were aligned separately per species using MUSCLE (Edgar, 2004). These alignments were visually inspected with Geneious Prime® 2019.2.3 Software (Biomatters), and genomes with >10% 'N' sequences or gaps were not included in the phylogenetic analyses. Best fit nucleotide substitution model identified as GTR+I+G4 for both WNV and USUV complete genome sequence data sets was calculated using jModelTest 2 (Darriba et al., 2012). Maximum likelihood inference under the best-predicted model and ultrafast bootstrap options (Hoang et al., 2018; Minh et al., 2013) with 100,000 replicates

was implemented in IQ-TREE 1.6.8 (Nguyen et al., 2015). Phylogenetic trees were viewed using FigTree version 1.4.4 software (http://tree.bio.ed.ac.uk/software/figtree/). Partial USUV envelope sequences were also assessed using phylogenetic analyses mentioned above. These USUV sequences were retrieved in GenBank on 09 September 2020 (accession nos. indicated in Figures S1 and S2).

2.4 | Serological investigation

We analysed all serum samples collected from birds held in four zoological gardens described in Section 2.1 using two specific virus neutralization tests (VNTs), as described by Seidowski et al. (2010) with minor modifications. Briefly, we used a German USUV strain

FIGURE 2 Phylogenetic analysis of European West Nile virus lineage 2 complete genomes. WNV sequences related to WNV-USUV co-infected birds are highlighted in red and with red dots, while other German WNV sequences are highlighted in green. Taxon information includes the nucleotide accession number, collection year and country of origin of the viruses. Scale bar indicates the number of nucleotide substitutions per site. Bootstrap values ≥80% are indicated in front of the node. The maximum likelihood tree was constructed using the best-selected nucleotide substitution model (GTR+I+G4). The 46 WNV strains from South Eastern European Clade (SEEC) highlighted by the blue box, and 11 Austrian WNV strains and 22 Italian WNV strains (1 imported to Germany) that belong to Central and Eastern European Clade (CEC), which were highlighted by the red-shaded box, were collapsed in triangles. WNV strains in the yellow box belong to the 'Eastern German Clade (EGC)'. WNV sequences from cases #4 to #5 were submitted to European Nucleotide Archive under the project accession PRJEB41417. WNV genomes from cases #2 (accession no. LR743443) and #6 (accession no. LR743421) were deposited in an earlier project (BioProject: PRJEB35552). The rest of the WNV sequences retrieved from GenBank are described in Table S2

(accession no. HE599647; lineage Europe 3) and a WNV strain from Austria (accession no. HM015884; WNV lineage 2, kindly provided by S. Revilla-Fernandez, AGES Mödlingen, Austria) to detect antibodies against USUV and WNV, respectively. The neutralizing antibody titre (ND_{50}) was demonstrated as the reciprocal of the serum dilution that inhibited >50% of cytopathogenic effect, and calculated based on the Behrens–Karber method (Mayr et al., 1977). Serum samples with ND_{50} values above 10 were considered as positive; otherwise, samples were regarded as negative. Birds were only regarded positive for WNV if they had a negative ($ND_{50} < 10$) or significantly lower (fourfold lower) USUV titre. The same criteria were also implemented for interpreting USUV VNT results. If a bird had similar antibody titres against both viruses, it is difficult to discriminate between WNV- and USUV-specific neutralizing antibodies due to cross-reactivities, and the result must therefore often be interpreted as inconclusive. However, in cases where the neutralizing titres are very high against both viruses and a high infection pressure of both viruses in a very dense spatial area with many susceptible birds at the same time is obvious, the results can be interpreted with higher certainty as the consequence of infections with both viruses in those birds.

3 | RESULTS

Since the first report of USUV circulation within bird populations in Germany, a nationwide bird surveillance network was established to systematically monitor zoonotic arboviruses, such as WNV and USUV, in migratory and resident birds using molecular and serological diagnostics tools (Michel et al., 2019). Among 88 WNV-infected birds reported in the 2018–2019 surveillance programme in Germany, our study detected six deceased birds (cases #1–#6) positive with both WNV and USUV genomes (Ziegler et al., 2019, 2020). Figure 1 depicts the sample collection sites of deceased birds with co-infection (cases #1–#6) and areas A to D in relation to the geographical distribution of the reported WNV-infected cases in Germany from 2018 to 2019.

3.1 | Results of RT-PCR screening, sequencing and virus phylogeny

Five of the deceased co-infected birds (cases #1–#5) were collected in 'Tierpark Berlin' in 2018 and 2019, while the sixth co-infected bird (case #6) was detected in Dresden in 2019 (Figure 1, Table 1). These

birds with co-infection belong to the taxonomic orders Strigiformes, Charadriiformes, Anseriformes and Passeriformes (Table 1). The presence of both WNV- and USUV-RNA within individual organs was observed in four birds (Table 1). On the other hand, co-infection at the organ level was not confirmed in case #6 since the liver and heart tissue samples were pooled, and was not observed in case #3. For USUV screening, organ samples with C_q values in the range of 37–40, which were defined as 'possible' USUV-positive, were confirmed either with another USUV-specific RT-qPCR assay or by sequencing (Table 1). In all co-infected organ samples, the RNA loads were higher for WNV than for USUV. Organs that were only USUV-positive were, for example, the brain from a snowy owl (*Bubo scandiacus*, case #1) and both the kidney and the liver from a Chinese merganser (*Mergus squamatus*, case #3), while a few organ samples from cases #2-#5 were WNV-positive only (Table 1).

WNV and USUV genomic sequencing were implemented on selected organ samples of six co-infected birds to confirm the results of the RT-qPCR and determine their respective virus lineages (Table 1). Two complete (cases #4, #5) and two partial (cases #1, #3) WNV genomes were assembled from this study, while two WNV full genomes (cases #2, #6) were sequenced from our previous study (Ziegler et al., 2020) (Table 1). Maximum likelihood phylogeny showed that the four WNV full genomes clustered with the WNV lineage 2 Eastern German clade (EGC) strains as described in Ziegler et al., (2020) (Figure 2). The WNV partial sequences from cases #1 and #3 had 99.9% (4,932 nt) and 99.5% (5,135 nt) pairwise nucleotide (nt) identities, respectively, with the WNV genome from case #2 (accession no. LR743443).

Usutu virus genome sequences were assembled from six co-infected birds despite the low concentration of USUV-RNA (C_q value range: 28.76–37.83). However, the USUV genome from case #4 had 78 nt and 16 nt gaps within the envelope gene (BioProject accession: PRJEB41417). Phylogenetic analysis revealed that these USUV sequences belong to three different lineages: Africa 2 (cases #1–#2), Africa 3 (cases #3–#5) and Europe 2 (cases #6) (Figure 3). Phylogenetic trees were also constructed using selected partial nucleotide sequences of the USUV envelope gene (726 nucleotides and 1,066 nucleotides) to include the 2017–2018 German USUV sequences in the analysis (Figures S1 and S2, respectively; Michel et al., 2019). The USUV lineage Africa 2 from cases #1 and #2 clustered with Africa 2 strains collected from Saxony (Leipzig) and Berlin. The German USUV lineage Africa 3 that circulated in 2017 and 2018 was widespread and could be detected in samples from Saxony (Doberschütz and Leipzig), North Rhine-Westphalia (Brüggen),

WILEY | 7
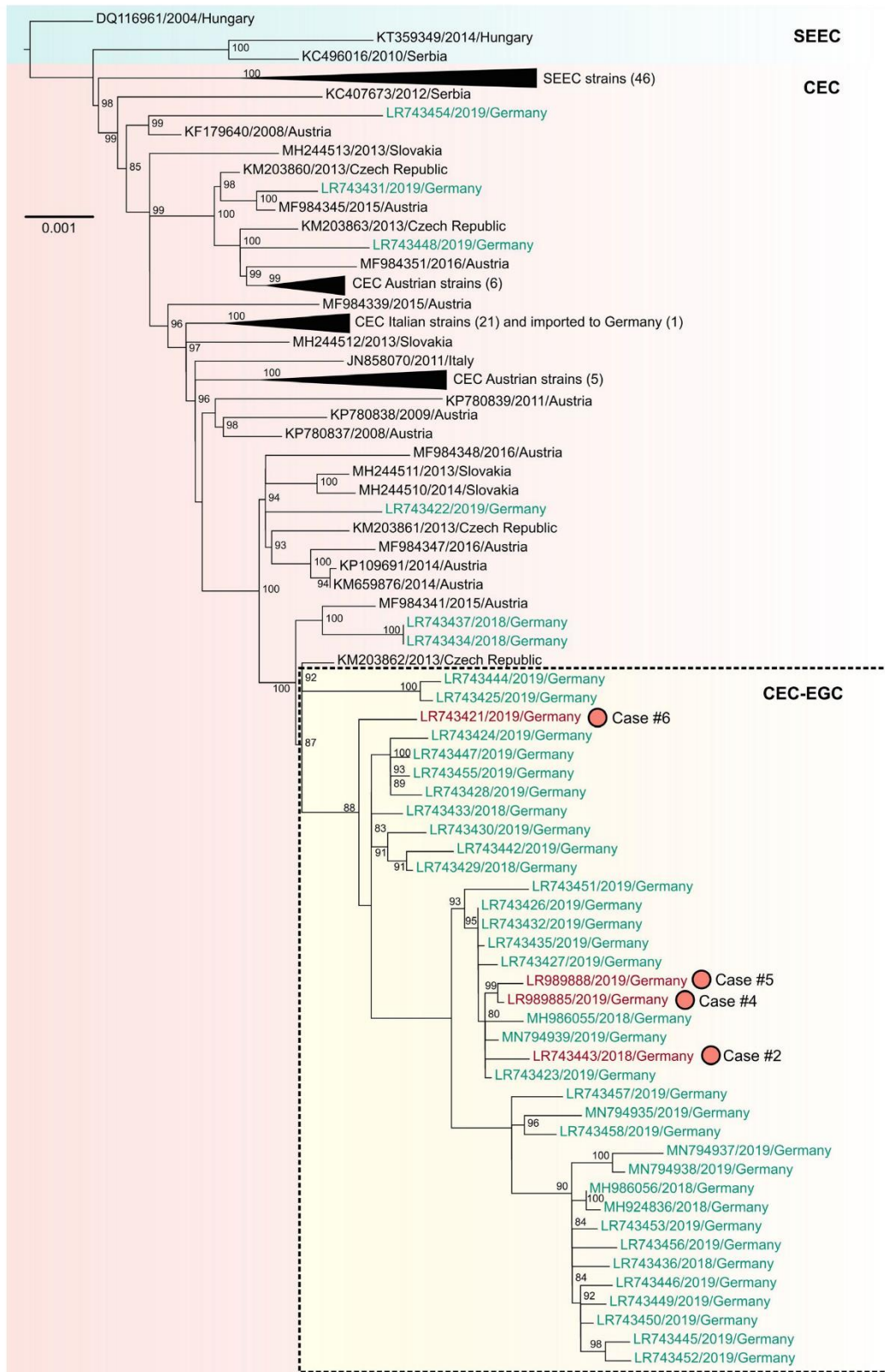
FIGURE 3 Phylogenetic analysis of Usutu virus complete genomes. USUV sequences related to WNV-USUV co-infected birds are highlighted in red and with red dots, while other German USUV sequences are highlighted in green. Taxon information includes the nucleotide accession number, collection year and countries of origin of the samples. The scale bar indicates the number of nucleotide substitutions per site. Numbers before the nodes denote bootstrap values ≥80%. The maximum likelihood tree was constructed using the best-selected nucleotide substitution model (GTR+I+G4). The branch of Europe 5, second cluster of Africa 2, clusters Africa 3.1, Africa 3.2 and several Africa 3.3 strains from the Netherlands, several Italian USUV strains from lineage Europe 2, lineages Europe 1, Europe 4, and Europe 3 were collapsed into triangles, and the numbers in parentheses indicate the number of collapsed USUV strains. USUV sequences from cases #1 to #6 were submitted to European Nucleotide Archive under the project accession: PRJEB41417. Usutu virus sequences retrieved from GenBank are described in Table S3

Saxony-Anhalt (Halle-Saale), Lower Saxony (Wingst, Theene, Nordhorn, Osnabrück), Schleswig-Holstein (Pinneberg, Lübeck, Brickeln) and Mecklenburg-Western Pomerania (Grevesmühlen, Prohn, Rügen). The USUV Europe 2 strain from Saxony (Dresden) clustered with another USUV Europe 2 collected in Saxony (Leipzig) in 2018.

3.2 | Flavivirus monitoring in live captive birds from different zoological gardens

The investigation of WNV-USUV co-infection was continued in captured live birds from four zoological gardens (areas A to D) with confirmed WNV cases using molecular and serological diagnostic assays. Molecular screening revealed that the whole blood samples from 67 birds from zoological gardens located in Berlin (area A, Table 2), Saxony-Anhalt, Brandenburg and Bavaria (areas B to C, Table 3) were WNV-RNA-negative. Likewise, whole blood samples from birds located in areas B to D were all negative of USUV-RNA (Table 3). In contrast, USUV-RNA was detected in two snowy owls from Berlin sampled in 2019 (Table 2). Using the standard USUV-specific RT-qPCR, both owls were weakly positive with C_q values for USUV-RNA of 36.25 and 35.41, and were therefore confirmed by another USUV-specific RT-qPCR assay (Cavrini et al., 2011), with C_q values for USUV-RNA of 36.20 and 37.97 (Table 2). WNV- and USUV-RNA were not detected in these parent owls during the investigation performed in 2018.

Serum samples were collected in different bird species from areas A to D, which included sentinel birds (chickens, geese and pigeons), and avian species that are highly susceptible to WNV and USUV (owls and raptors). Specific VNTs detected neutralizing antibodies against WNV-only, USUV-only, and both WNV and USUV within the serum panel. High titres of neutralizing antibodies against WNV and USUV were simultaneously detected in two parent snowy owls from area A. Serum samples collected from the male parent owl in 2018 and the female parent owl in 2019 have high titres of neutralizing antibodies against both WNV and USUV (Table 2). These parent owls were confined in the same aviary with their two offspring (cases #1, #2) in 2018, which had confirmed WNV and USUV double infection (Table 1). Interestingly, serology of the male parent owl in 2019 had the pattern of a WNV mono-infection.

Another snowy owl located at area B ('Zoo Halle/Saale', Table 3) also showed high neutralizing antibody titres against both flaviviruses. Moreover, five birds harbouring neutralizing antibodies

against either WNV or USUV were detected in area B. A European kestrel (*Falco tinnunculus*) was positive for WNV-specific neutralizing antibodies (ND_{50} value 1:40), while USUV-specific neutralizing antibodies were detected in a snowy owl (ND_{50} value 1:960), a Eurasian eagle owl (*Bubo bubo*, ND_{50} value 1:40) and two Indian runners (*Anas platyrhynchos domesticus*, ND_{50} values 1:480 and 1:1,920). In area D ('Tierpark Cottbus'), one owl had WNV-specific neutralizing antibodies (ND_{50} value 1:1,920) and seven birds had USUV-specific neutralizing antibodies (Table 3). Among these samples, the taxonomic classification of one bird was not possible. Two Eurasian eagle owls from area C ('Wildpark Poing') had USUV-specific neutralizing antibodies, and serological evidence of WNV was not detected at all. Therefore, the evidence of WNV-USUV co-circulation could be especially detected in the birds from areas B and D (Table 3).

4 | DISCUSSION

Although co-circulation of WNV and USUV in the same region has previously been described, co-infection with both viruses in birds has not been reported before. So far, only a single case of WNV and USUV co-infection was reported in humans (Aberle et al., 2018). This is somewhat surprising since co-circulation of both viruses was reported from 14 European countries (Austria, Croatia, the Czech Republic, France, Germany, Greece, Hungary, Italy, the Netherlands, Poland, the Republic of Serbia, Slovakia, Spain and the United Kingdom) (Bahuon et al., 2016; Bażanów et al., 2018; Čabanová et al., 2019; Eiden et al., 2018; Folly et al., 2020; Lim et al., 2018; Nikolay, 2015; Rijks et al., 2016; Sikkema et al., 2020). The co-circulation of WNV and USUV was confirmed in at least 34 common bird species (Nikolay, 2015) and mammals including horses and humans (Zannoli & Sambri., 2019). The mosquito species *Culex pipiens* is the most common vector for WNV and USUV in Europe (Zannoli & Sambri., 2019), yet these flaviviruses have also been detected in other circulating mosquito species in Europe, including *Anopheles maculipennis* s.l., *Ochlerotatus caspius*, *Cx. perixiguus* and *Cx. modestus* (Hönig et al., 2019; Nikolay, 2015; Rudolf et al., 2014). Thus, there is a good chance for WNV-USUV co-infections in areas with reported WNV-USUV co-circulation.

The first confirmed case of a WNV-USUV double infection was described from an asymptomatic blood donor residing in Austria (Aberle et al., 2018). The corresponding blood sample collected in August 2018 was tested positive for both WNV and USUV using RT-qPCR and VNT, and genomic analyses classified these

WILEY | 9
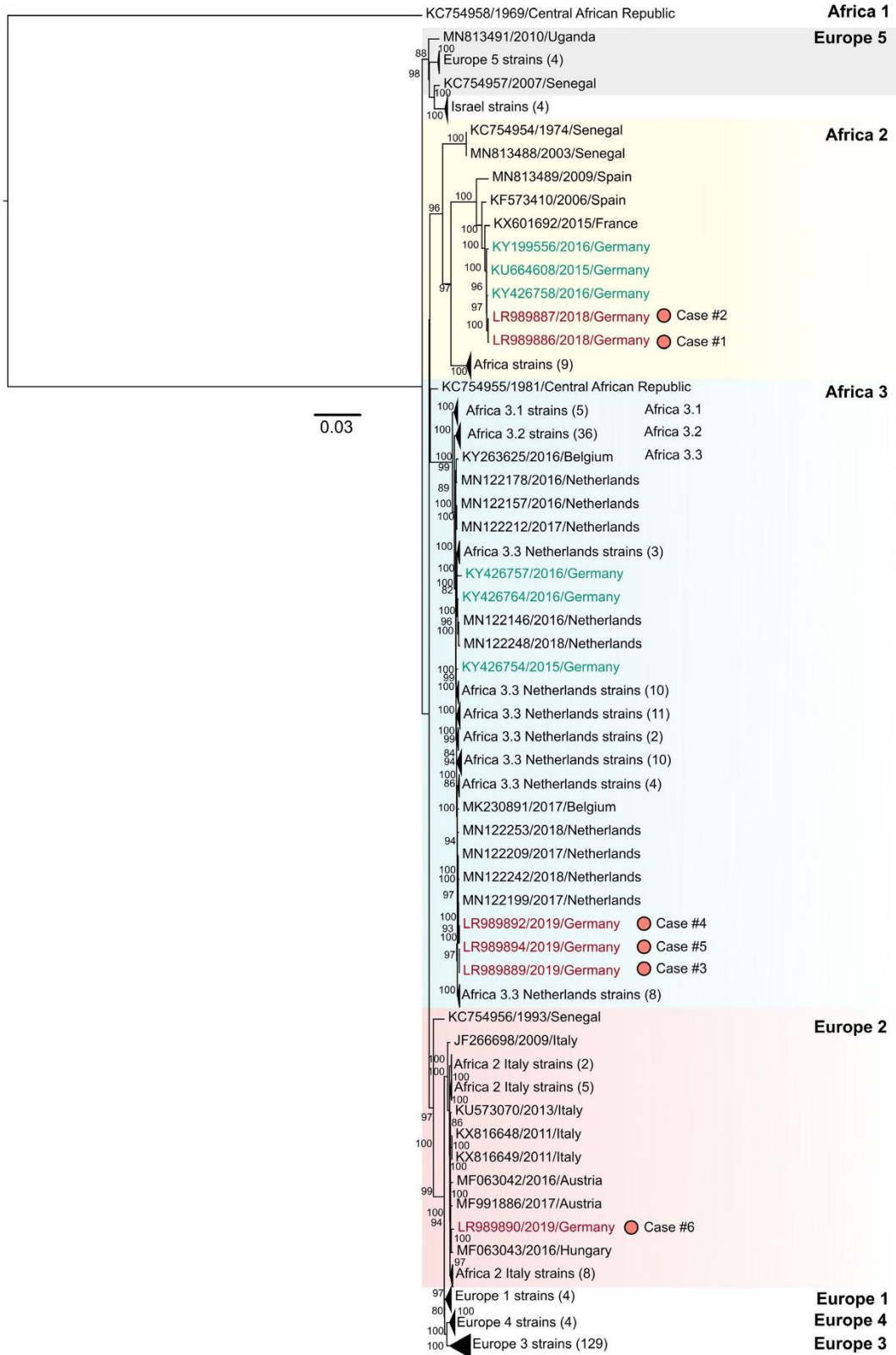
TABLE 2 Detection of WNV- and USUV-RNA using reverse transcription quantitative real-time PCR (RT-qPCR) and specific antibodies by virus neutralization tests (VNTs) in the area A ('Tierpark Berlin', Berlin). Positive serology results are highlighted in red and bold, and cross-reacting antibody titres are also displayed in black

Year of investigation and sex	Common name	Scientific name	WNV RT-qPCR	USUV RT-qPCR[a]	USUV RT-qPCR[b]	WNV ND$_{50}$	USUV ND$_{50}$
2018/Male	Snowy Owl	*Bubo scandiacus*	neg.	neg.	neg.	**480**	**160**
2018/Female	Snowy Owl	*Bubo scandiacus*	neg.	neg.	neg.	20	**320**
2019/Male	Snowy Owl	*Bubo scandiacus*	neg.	36.25	36.20	**≥3,840**	480
2019/Female	Snowy Owl	*Bubo scandiacus*	neg.	35.41	*37.97*	**960**	**480**

Note: Possible USUV-positive samples based on C_q value range 37–40 were indicated in italics.

Abbreviations: ND$_{50}$, neutralization dose 50%; neg, negative.

[a]USUV RT-qPCR results based on protocol from Jöst et al. (2011).

[b]USUV RT-qPCR results based on protocol from Cavrini et al. (2011).

flaviviruses under WNV lineage 2 and USUV lineage Europe 2 (Aberle et al., 2018). In an earlier study, Tamba et al. (2011) described the detection of both WNV- and USUV-RNA in eight *Culex pipiens* pools and three individual birds, two European magpies (*Pica pica*) and one gull (*Larus* sp.), that were collected in 2009 for the WNV surveillance programme at the Po River Delta in Emilia-Romagna, Italy. However, their investigation only focused on the co-circulation of these flaviviruses in the area and an in-depth analysis for WNV and USUV co-infections was not performed. Furthermore, an older study by Buckley et al. (2003) noted that the sera from six birds collected between 2001 and 2002 in the United Kingdom (UK) had neutralizing antibodies against WNV and USUV, which were determined by plaque reduction neutralization tests (PRNT$_{50}$ and PRNT$_{90}$). This serological finding was surprising because neither WNV nor USUV was detected in the UK since 2003. Moreover, the first confirmed avian USUV cases in the UK were only detected in August 2020 (Folly et al., 2020). Nevertheless, WNV has not yet been detected in the UK.

Here, we present a comprehensive surveillance of WNV-USUV co-infections in deceased and live birds from 2018 to 2019, as well as WNV and USUV co-circulation in live birds. The surveillance system reported six deceased birds that tested positive for both WNV- and USUV-RNA (6.8% of WNV-infected birds), and were confirmed by virus genome sequencing. These six deceased birds were classified under avian taxonomic orders with previous evidence of WNV and USUV mono-infections (as reviewed in Clé et al., 2019; Gamino & Höfle, 2013; Nikolay, 2015). We observed that the high WNV and/or USUV infection pressures in an area, which is densely populated with highly susceptible avian species, can lead to the infection of less susceptible avian species such as ducks and gulls. Our earlier study also detected WNV infection in six gulls from area A (Ziegler et al., 2020).

We detected WNV- and USUV-RNA simultaneously in various organ samples from the birds. This finding was expected since both WNV and USUV are known to have a wide tissue tropism in various bird species (Clé et al., 2019; Gamino & Höfle, 2013), but reports of co-infections in the same organs are new. The presence of both WNV- and USUV-RNA was confirmed for six organ samples from

four deceased birds (cases #1, #2, #4, #5; Table 1), which had higher WNV- than USUV-RNA loads. Based on the assumption that a higher RNA load indicates more efficient replication of the virus in the respective tissue, WNV replicated more efficiently in these organ samples compared to USUV. Most likely, WNV played the primary role in the mortality of these birds. Though, the initial WNV and USUV viral loads during transmission to these birds are unknown. It is also undetermined whether these birds acquired these viruses simultaneously or sequentially, but the WNV and USUV infection definitely overlapped. Thus, different factors must be considered to understand the dynamics of flavivirus co-infection in vertebrates.

Our preliminary attempts to co-propagate both flaviviruses in vitro starting from co-infected tissue materials failed. Even with the most promising available material (brain tissue from case #2), we had only evidence of WNV but not USUV replication in Vero B4 cells (Table S4). Possibly, this lack of USUV replication was due to low viral load in the inoculum. These results fit with findings reported by Wang and colleagues, who demonstrated that USUV (lineage Africa 3, accession no. MH891847.1) is outcompeted by WNV (lineage 2, accession no. HQ537483.1) within in vitro co-infection experiments using mammalian (Vero E6 cells), avian (DF-1) and mosquito (C6/36 and Cx.t) cell lines, as well as in co-infection experiments in *Culex pipiens* mosquitoes (Wang et al., 2020). It is possible that the WNV suppressed the productive replication of USUV within cells, which is a process known as superinfection exclusion (Salaman, 1933; Zou et al., 2009). The superinfection exclusion is considered as a protection strategy of the 'primary virus' from the competing related 'secondary virus' within the same host (Wang et al., 2020). This strategy has been observed in different flaviviruses, such as dengue virus, Japanese encephalitis virus, Nhumirim virus and *Culex* flavivirus, in mosquito cells (Goenaga et al., 2020; Kanthong et al., 2010; Kenney et al., 2014; Pepin et al., 2008), and other members of the family Flaviviridae, such as Hepatitis C virus and bovine viral diarrhoea virus in vertebrate cell lines (Lee et al., 2005; Tscherne et al., 2007).

Our study detected USUV belonging to lineages Africa 2, Africa 3 and Europe 2. USUV sequences from two snowy owls (cases #1, #2) collected in 'Tierpark Berlin' in 2018 were identified as lineage

TABLE 3 Detection of WNV- and/or USUV-RNA in samples from areas B, C and D using reverse transcription quantitative real-time PCR (RT-qPCR) and by virus neutralization tests (VNTs) using specific antibodies. Positive serology results are highlighted in red and bold, and cross-reacting antibody titres are also displayed in black

Area	Year	Location/Federal State	Order	Common name	Scientific name	No. of samples tested	WNV RT-qPCR	USUV RT-qPCR	WNV ND$_{50}$	USUV ND$_{50}$
B	2018	'Zoo Halle/Saale' Saxony-Anhalt	Strigiformes	Snowy Owl	Bubo scandiacus	1	neg.	neg.	60	960
				Snowy Owl	Bubo scandiacus	1	neg.	neg.	1,920	3,840
				Northern Long-eared Owl	Asio otus	1	neg.	neg.	<10	<10
				Eurasian Eagle Owl	Bubo bubo[a]	1	neg.	neg.	15	40
				Eurasian Tawny Owl	Strix aluco	1	neg.	neg.	n.t.	n.t.
			Falconiformes	European Kestrel	Falco tinnunculus	1	neg.	neg.	<10	<10
				European Kestrel	Falco tinnunculus	1	neg.	neg.	40	<10
			Passeriformes	Carrion Crow	Corvus corone[a]	1	neg.	neg.	<10	<10
			Anseriformes	Cackling Goose	Branta hutchinsii	1	neg.	neg.	<10	<10
				Canada Goose	Branta canadensis	1	neg.	neg.	<10	<10
				Barnacle Goose	Branta leucopsis	1	neg.	neg.	<10	<10
			Anatidae	Indian Runners	Anas platyrhynchos dom.	16	16xneg.	16xneg.	14 (<10), 2 (40)	14 (<10), 1 (480), 1 (1,920)
			Rheiformes	Darwin's Rhea	Rhea pennata	4	4xneg.	4xneg.	4 (<10)	4 (<10)
C	2018	'Wildpark Poing' Bavaria	Strigiformes	Great Grey Owl	Strix nebulosa	2	2xneg.	2xneg.	2 (<10)	2 (<10)
				Eurasian Eagle Owl	Bubo bubo	1	neg.	neg.	<10	80
				Eurasian Eagle Owl	Bubo bubo	1	neg.	neg.	<10	<10
				Eurasian Eagle Owl	Bubo bubo	1	neg.	neg.	<10	10
			Anseriformes	Graylag Goose	Anser anser	1	neg.	neg.	<10	<10
				Toulouse Goose	Anser anser domesticus	3	3xneg.	3xneg.	3 (< 10)	3 (<10)
				Whooper Swan	Cygnus cygnus	1	neg.	neg.	<10	<10
			Columbiforms	Fantail Pigeons	Columba livia forma dom.	3	3xneg.	3xneg.	3 (< 10)	1 (<10), 2 (n.t.)
			Galliformes	Chicken	Gallus gallus domesticus	6	6xneg.	6xneg.	6 (< 10)	6 (<10)

(Continues)

TABLE 3 (Continued)

Area	Year	Location/Federal State	Order	Common name	Scientific name	No. of samples tested	WNV RT-qPCR	USUV RT-qPCR	WNV ND$_{50}$	USUV ND$_{50}$
D	2019	'Tierpark Cottbus' Brandenburg	Strigiformes	Owl sp.	Unknown	1	neg.	neg.	1,920	120
			Unknown	Unknown bird species	Unknown	1	neg.	neg.	20	240
			Ciconiiformes	White Stork	Ciconia ciconia	1	neg.	neg.	10	320
			Pelecaniformes	Eurasian Spoonbill	Platalea leucorodia	2	2xneg.	2xneg.	1 (< 10), 1 (n.t.)	1 (15), 1 (n.t.)
			Anseriformes	Red-breasted Goose	Branta ruficollis	3	3xneg.	3xneg.	1 (<10), 2 (15, 60)	1 (<10), 1 (120), 1 (480)
				Lesser White-fronted Goose	Anser erythropus	3	3xneg.	3xneg.	3 (<10)	3 (<10)
				Brant Goose	Branta bernicla	2	2xneg.	2xneg.	2 (<10)	2 (<10)
				Ashy-headed Goose	Chloephaga poliocephala	1	neg.	neg.	40	160
				Emperor Goose	Anser canagicus	1	neg.	neg.	<10	30

Abbreviations: dom, domesticus; n.t, not tested due to small sample volume; ND$_{50}$, neutralization dose 50%; neg, negative; <10 = negative.

[a] wild bird.

Africa 2, while USUV from three other captive birds (cases #3-#5) from the same zoological garden in 2019 were identified as Africa 3. Until 2018, USUV lineages Africa 2 and Europe 3 had been reported in Berlin. Hence, the detection of USUV lineage Africa 3 in 2019 indicates the presence of a new circulating USUV lineage in the city, and the expanding geographical distribution of this USUV lineage. Africa 3 was first detected in NRW in 2014 followed by reports from Saxony in 2016 and spread further to Saxony-Anhalt, Lower Saxony, Schleswig-Holstein and Mecklenburg-Western Pomerania in 2018 (Cadar et al., 2015; Michel et al., 2019; Sieg et al., 2017). These three USUV lineage Africa 3 genomes that were acquired from this study specifically branched with cluster Africa 3.3 sequences as described in Oude Munnink et al. (2020), which also included three other German Africa 3.3 strains collected in NRW from 2015 to 2016. The specific clusters of USUV lineage Africa 3 strains were not fully delineated by phylogenies constructed using partial USUV envelope sequences (Figures S1 and S2; Oude Munnink et al., 2020). We also reported the second case of USUV lineage Europe 2 in Germany, following its first detection in Leipzig, Saxony in 2018 (Michel et al., 2019). The incidence of this new lineage in Dresden, Saxony was not surprising due to the short distance between Leipzig and Dresden (ca. 100 km).

Conversely, all of the sequenced German WNV strains from 2018 to 2019 were classified as WNV lineage 2 Central and Eastern European Clade (CEC), and the majority of these strains clustered together to form the Eastern German Clade (EGC) as described in our previous study (Ziegler et al., 2020). Four complete and two partial WNV genomes acquired from birds with co-infections were classified as WNV lineage 2 EGC. This finding was not surprising since cases #1 to #5 were confined in Berlin, which was one of the hotspots for cases infected with WNV lineage 2 EGC in 2018–2019 (Ziegler et al., 2020). In 2020, Berlin remained a WNV hotspot in Germany with again numerous bird cases and occasional reports in both horses and humans (Friedrich-Loeffler-Institut [FLI], 2020).

Specific neutralizing antibodies against USUV had been verified in the German avifauna since 2012 (Michel et al., 2018; Ziegler et al., 2015), while the occurrence of neutralizing antibodies against WNV in German resident birds was not reported before 2018. The detection of WNV-specific antibodies in live birds corresponds to the first WNV-RNA detection in dead birds (Michel et al., 2019). USUV- and WNV-RNA could be detected in blood samples of live birds since 2014 and 2019, respectively. These studies highlight the opportunity that a systematic surveillance of zoological birds can provide, especially as these birds are considered resident birds and follow-up studies can easily be performed. Thus, we collected blood samples in captive birds from four zoological gardens with confirmed WNV cases in 2018 and 2019 to investigate the WNV-USUV co-infections found in six dead birds. Cases #1 to #5 were captive birds located in area A, while case #6 was a wild bird collected in Dresden (outside the defined areas A to –D, see Figure 1). The closest zoological gardens with confirmed WNV cases were in areas B and D. The WNV detected in area C did not belong to the EGC; hence, further investigation was warranted.

We reported also the presence of similarly high titres of neutralizing antibodies against WNV and USUV in three snowy owls located in areas A and B, while USUV-RNA was only detected in two snowy owls from area A. The detection of both WNV- and USUV-specific antibodies exclusively in snowy owls is debatable since the sample set was rather small. Mono-infection of WNV or USUV can cause fatal diseases in different bird species. As an example, the first confirmed case of WNV infection in Germany was reported in area B. This infection resulted in the death of a great grey owl (*Strix nebulosa*, FLI sample code: ED-I-33/18, accession no. MH924836 (Ziegler et al., 2019)). Its partner owl also succumbed to acute viral infection caused by USUV (U. Ziegler and M. Keller, unpublished data).

The observed high titres of neutralizing antibodies against both WNV and USUV could be a rare event due to sequential or simultaneous infections as a consequence of a high infection pressure for both flaviviruses. However, as described in previous surveillance studies (Michel et al., 2018, 2019), some level of serological cross-reactions cannot be ruled out since multiple flaviviruses including WNV and USUV share antigenic characteristics with their structural outer proteins (e.g. envelope protein) (Blázquez et al., 2015). However, the identification of three resident birds with similar and very high titres of neutralizing antibodies against both flaviviruses in zoological gardens with confirmed WNV-USUV co-circulation is more indicative of simultaneous or sequential infections rather than cross-reactions. These data are in line with the observation that two juvenile snowy owls from area A had double infection with WNV and USUV, which was detected by highly specific molecular diagnostics (see Table 1). Therefore, infection with WNV and USUV in the same bird is a possibility that occurs but has so far only been detected in isolated cases either by high titre serological evidence or by specific molecular diagnostics.

USUV circulation in Berlin, Saxony-Anhalt and Saxony was reported at least a year before the introduction of WNV in those regions (Michel et al., 2018, 2019; Sieg et al., 2017). Hence, there was the possibility that the surviving snowy owls acquired a protective USUV infection prior to the WNV infection. This could explain why the parent snowy owls (Table 2) survived the 2018 and 2019 WNV seasons; whereas their offspring died a few months later in 2018 (cases #1, #2, Table 1) and 2019 (accession nos. LR743424 and LR743428) (Ziegler et al., 2020). This hypothesis is also supported by the study of Blázquez et al. (2015), who reported that USUV pre-infected mice challenged with WNV infection were protected against WNV disease and death but not against infection since WNV-RNA was still detected in 50% of WNV-challenged mice 7 days post-infection. Hence, USUV is a potential low pathogenic flaviviral vaccine candidate against WNV since it elicits cross-protective immunity against the heterologous neurovirulent WNV (Blázquez et al., 2015).

It was hypothesized previously that an increased risk of a higher virulence and mortality rate of a secondary infection by a closely related virus could be, *for example*, explained by the so-called 'antibody-dependent enhancement' (ADE) (Porterfield, 1986). This, however, was not detected in the studies of Percivalle et al. (2020) and Sinigaglia et al. (2019). Results reported by Sinigaglia et al. (2019)

implied that prior USUV infections followed by WNV infections did not lead to ADE in humans, likewise in the cases described by Percivalle et al. (2020). There was no clear evidence that a secondary WNV or USUV infection in humans, which were previously infected with either WNV or USUV, caused more severe disease or even death (Percivalle et al. 2020). Hence, we cannot rule out the possibility that a prior WNV infection generated cross-protective immunity against USUV infection in these snowy owls.

Based on these studies, simultaneous infections as well as sequential infections with WNV and USUV can modulate the risks that these viruses pose to the public health. Co-infections can possibly modify the outcome of virus infections in birds and humans compared to mono-infections. So far, only one case of WNV and USUV co-infection in humans had been reported, which had an asymptomatic infection (Aberle et al., 2018). To date, we are still lacking evidence that WNV and USUV co-infections can lead to more severe clinical symptoms. Interestingly, Wang et al. (2020) tested the effect of USUV and WNV co-infections and sequential infections on the vector competence of *Culex* mosquitoes. A pre-infection with USUV 'protected' mosquitoes against WNV. By contrast, a simultaneous infection leads to the selective transmission of WNV. There had been no evidence of WNV and USUV recombination after a simultaneous infection of these viruses in different cells lines and mosquitoes (Wang et al., 2020). Moreover, the observed superinfection exclusion in WNV and USUV co-infected cells and mosquitoes lowers the probability of WNV and USUV recombination.

5 | CONCLUSIONS

WNV and USUV are important arboviruses in the world in the context of public and animal health. Mono-infection as well as co-circulation of WNV and USUV had been previously described in mosquitoes, birds, horses and humans in several countries. We present here the first extensive surveillance of WNV-USUV co-infections in deceased and live birds from 2018 to 2019. The co-infections in five birds from zoological gardens and in one wild bird were detected by RT-qPCR and characterized by genomic sequencing. Flavivirus double infections in three birds from zoological gardens were verified using virus neutralization tests.

Taken together, the use of two virus-specific PCR systems has proven to be successful in the surveillance of wild and captive avian species for WNV and USUV. This study showed that the WNV and USUV RT-qPCR assays used in the surveillance network are highly specific in distinguishing these two flaviviruses. Our study also emphasized the importance of zoological birds, which are resident birds, as a tool for developing an early warning system to detect an introduction and circulation of zoonotic pathogens, especially within cities and urban settings. In the future, further co-infections can be expected in animals as well as humans, in areas with WNV and USUV co-circulation. Therefore, the consequences of co-infections for public health must also be taken into consideration. Possible cross-protections as well as antibody-dependent enhancement in cases of

mono- and double infections in animals with already existing anti-bodies from a prior flavivirus mono-infection must be followed up by both in vitro and in vivo investigations. Follow-up studies in birds from the different zoological gardens from different German federal states are currently being conducted to investigate the extent and course of antibody formation in susceptible bird species. Moreover, full-genome sequencing of recent USUV-positive birds and mosqui-toes is highly recommended to determine the geographical range and the dynamics of the multiple USUV lineages in Germany, and classify the sequences to the level of clusters and sub-clusters.

ETHICAL APPROVAL

Blood samples for this study were taken based on the official vet-erinarian order to screen birds held in areas where WNV had been detected. The collection of the samples was carried out by the re-spective zoo veterinarians. Their handling is, therefore, not subject to further approval.

CONFLICTS OF INTEREST

The authors declare no conflict of interest.

DATA AVAILABILITY STATEMENT

The data that support the findings of this study are available in the main manuscript and in the supplementary material of this article.

ORCID

Pauline Dianne Santos https://orcid.org/0000-0003-4324-5967
Dirk Höper https://orcid.org/0000-0001-8408-2274
Martin Eiden https://orcid.org/0000-0002-1197-8288
Martin Beer https://orcid.org/0000-0002-0598-5254
Martin H. Groschup https://orcid.org/0000-0003-0215-185X
Ute Ziegler https://orcid.org/0000-0001-5295-7339

REFERENCES

Aberle, S. W., Kolodziejek, J., Jungbauer, C., Stiasny, K., Aberle, J. H., Zoufaly, A., Hourfar, M. K., Weidner, L., & Nowotny, N. (2018). Increase in human West Nile and Usutu virus infections, Austria, 2018. *Eurosurveillance Weekly*, *23*(43), 1800545. https://doi.org/10.2807/1560-7917.Es.2018.23.43.1800545

Bahuon, C., Marcillaud-pitel, C., Bournez, L., Leblond, A., Beck, C., Hars, J., Leparc-goffart, I., L'ambert, G., Paty, M.-C., Cavalerie, L., Daix, C., Tritz, P., Durand, B., Zientara, S., & Lecollinet, S. (2016). West Nile virus epizootics in the Camargue (France) in 2015 and rein-forcement of surveillance and control networks. *Revue Scientifique et Technique de l'OIE*, *35*(3), 811–824. https://doi.org/10.20506/rst.35.3.2571

Bażanów, B., Jansen van Vuren, P., Szymański, P., Stygar, D., Frącka, A., Twardoń, J., Kozdrowski, R., & Pawęska, J. (2018). A survey on West Nile and Usutu Viruses in horses and birds in Poland. *Viruses*, *10*(2), 87. https://doi.org/10.3390/v10020087

Becker, N., Jöst, H., Ziegler, U., Eiden, M., Höper, D., Emmerich, P., Fichet-Calvet, E., Ehichioya, D. U., Czajka, C., Gabriel, M., Hoffmann, B., Beer, M., Tenner-Racz, K., Racz, P., Günther, S., Wink, M., Bosch, S., Konrad, A., Pfeffer, M., … Schmidt-Chanasit, J. (2012). Epizootic emergence of Usutu virus in wild and captive birds in Germany. *PLoS One*, *7*(2), e32604. https://doi.org/10.1371/journal.pone.0032604

Benzarti, E., Sarlet, M., Franssen, M., Cadar, D., Schmidt-Chanasit, J., Rivas, J. F., Linden, A., Desmecht, D., & Garigliany, M. (2020). Usutu virus epizootic in Belgium in 2017 and 2018: Evidence of virus endem-ization and ongoing introduction events. *Vector Borne and Zoonotic Disease*, *20*(1), 43–50. https://doi.org/10.1089/vbz.2019.2469

Blázquez, A.-B., Escribano-Romero, E., Martín-Acebes, M. A., Petrovic, T., & Saiz, J.-C. (2015). Limited susceptibility of mice to Usutu virus (USUV) infection and induction of flavivirus cross-protective im-munity. *Virology*, *482*, 67–71. https://doi.org/10.1016/j.virol.2015.03.020

Buckley, A., Dawson, A., Moss, S. R., Hinsley, S. A., Bellamy, P. E., & Gould, E. A. (2003). Serological evidence of West Nile virus, Usutu virus and Sindbis virus infection of birds in the UK. *Journal of General Virology*, *84*(Pt 10), 2807–2817. https://doi.org/10.1099/vir.0.19341-0

Čabanová, V., Šikutová, S., Straková, P., Šebesta, O., Vichová, B., Zubríková, D., Miterpáková, M., Mendel, J., Hurníková, Z., Hubálek, Z., & Rudolf, I. (2019). Co-circulation of West Nile and Usutu Flaviviruses in mosquitoes in Slovakia, 2018. *Viruses*, *11*(7), 639. https://doi.org/10.3390/v11070639

Cadar, D., Bosch, S., Jöst, H., Börstler, J., Garigliany, M. M., Becker, N., & Schmidt-Chanasit, J. (2015). Putative lineage of novel African Usutu virus, Central Europe. *Emerging Infectious Diseases*, *21*(9), 1647–1650. https://doi.org/10.3201/eid2109.142026

Cadar, D., Lühken, R., van der Jeugd, H., Garigliany, M., Ziegler, U., Keller, M., Lahoreau, J., Lachmann, L., Becker, N., Kik, M., Oude Munnink, B. B., Bosch, S., Tannich, E., Linden, A., Schmidt, V., Koopmans, M. P., Rijks, J., Desmecht, D., Groschup, M. H., … Schmidt-Chanasit, J. (2017). Widespread activity of multiple lineages of Usutu virus, Western Europe, 2016. *Euro Surveillance*, *22*(4), 30452. https://doi.org/10.2807/1560-7917.ES.2017.22.4.30452

Calisher, C. H., & Gould, E. A. (2003). Taxonomy of the virus fam-ily Flaviviridae. *Advances in Virus Research*, *59*, 1–19. https://doi.org/10.1016/s0065-3527(03)59001-7

Camp, J. V., & Nowotny, N. (2020). The knowns and unknowns of West Nile virus in Europe: What did we learn from the 2018 outbreak? *Expert Review of Anti-Infective Therapy*, *18*(2), 145–154. https://doi.org/10.1080/14787210.2020.1713751

Cavrini, F., Della Pepa, M. E., Gaibani, P., Pierro, A. M., Rossini, G., Landini, M. P., & Sambri, V. (2011). A rapid and specific real-time RT-PCR assay to identify Usutu virus in human plasma, serum, and ce-rebrospinal fluid. *Journal of Clinical Virology*, *50*(3), 221–223. https://doi.org/10.1016/j.jcv.2010.11.008

Chancey, C., Grinev, A., Volkova, E., & Rios, M. (2015). The global ecology and epidemiology of West Nile virus. *BioMed Research International*, *2015*, 376230. https://doi.org/10.1155/2015/376230

Chvala, S., Kolodziejek, J., Nowotny, N., & Weissenböck, H. (2004). Pathology and viral distribution in fatal Usutu virus infections of birds from the 2001 and 2002 outbreaks in Austria. *Journal of Comparative Pathology, 131*(2–3), 176–185. https://doi.org/10.1016/j.jcpa.2004.03.004

Clé, M., Beck, C., Salinas, S., Lecollinet, S., Gutierrez, S., Van de Perre, P., Baldet, T., Foulongne, V., & Simonin, Y. (2019). Usutu virus: A new threat? *Epidemiology and Infection, 147*, e232. https://doi.org/10.1017/s0950268819001213

Constant, O., Bollore, K., Clé, M., Barthelemy, J., Foulongne, V., Chenet, B., Gomis, D., Virolle, L., Gutierrez, S., Desmetz, C., Moares, R. A., Beck, C., Lecollinet, S., Salinas, S., & Simonin, Y. (2020). Evidence of exposure to USUV and WNV in zoo animals in France. *Pathogens, 9*(12), 1005. https://doi.org/10.3390/pathogens9121005

Cox-Witton, K., Reiss, A., Woods, R., Grillo, V., Baker, R. T., Blyde, D. J., Boardman, W., Cutter, S., Lacasse, C., McCracken, H., Pyne, M., Smith, I., Vitali, S., Vogelnest, L., Wedd, D., Phillips, M., Bunn, C., & Post, L. (2014). Emerging infectious diseases in free-ranging wildlife-Australian zoo based wildlife hospitals contribute to national surveillance. *PLoS One, 9*(5), e95127. https://doi.org/10.1371/journal.pone.0095127

Darriba, D., Taboada, G. L., Doallo, R., & Posada, D. (2012). jModelTest 2: More models, new heuristics and parallel computing. *Nature Methods, 9*(8), 772. https://doi.org/10.1038/nmeth.2109

Durand, B., Balança, G., Baldet, T., & Chevalier, V. (2010). A metapopulation model to simulate West Nile virus circulation in Western Africa, Southern Europe and the Mediterranean basin. *Veterinary Research, 41*(3), 32. https://doi.org/10.1051/vetres/2010004

Edgar, R. C. (2004). MUSCLE: Multiple sequence alignment with high accuracy and high throughput. *Nucleic Acids Research, 32*(5), 1792–1797. https://doi.org/10.1093/nar/gkh340

Eiden, M., Gil, P., Ziegler, U., Rakotoarivony, I., Marie, A., Frances, B., L'Ambert, G., Simonin, Y., Foulongne, V., Groschup, M. H., Gutierrez, S., & Eloit, M. (2018). Emergence of two Usutu virus lineages in *Culex pipiens* mosquitoes in the Camargue, France, 2015. *Infection Genetics and Evolution, 61*, 151–154. https://doi.org/10.1016/j.meegid.2018.03.020

Eiden, M., Vina-Rodriguez, A., Hoffmann, B., Ziegler, U., & Groschup, M. H. (2010). Two new real-time quantitative reverse transcription polymerase chain reaction assays with unique target sites for the specific and sensitive detection of lineages 1 and 2 West Nile virus strains. *Journal of Veterinary Diagnostic Investigation, 22*(5), 748–753. https://doi.org/10.1177/104063871002200515

European Centre for Disease Prevention and Control (ECDC) (2018). *Epidemiological update: West Nile virus transmission season in Europe, 2018*. Retrieved from https://www.ecdc.europa.eu/en/news-events/epidemiological-update-west-nile-virus-transmission-season-europe-2018

Folly, A. J., Lawson, B., Lean, F. Z., McCracken, F., Spiro, S., John, S. K., Heaver, J. P., Seilern-Moy, K., Masters, N., Hernández-Triana, L. M., Phipps, L. P., Nuñez, A., Fooks, A. R., Cunningham, A. A., Johnson, N., & McElhinney, L. M. (2020). Detection of Usutu virus infection in wild birds in the United Kingdom, 2020. *Euro Surveillance, 25*(41), 2001732. https://doi.org/10.2807/1560-7917.ES.2020.25.41.2001732

Friedrich-Loeffler-Institut (FLI). (2020). *Aktuelle situation West-Nil-Virus*. Retrieved from https://www.fli.de/de/aktuelles/kurznachrichten/neues-einzelansicht/aktuelle-situation-west-nil-virus/

Gamino, V., & Höfle, U. (2013). Pathology and tissue tropism of natural West Nile virus infection in birds: A review. *Veterinary Research, 44*(1), 39. https://doi.org/10.1186/1297-9716-44-39

Goenaga, S., Goenaga, J., Boaglio, E. R., Enria, D. A., & Levis, S. D. C. (2020). Superinfection exclusion studies using West Nile virus and *Culex* flavivirus strains from Argentina. *Memorias do Instituto Oswaldo Cruz, 115*, e200012. https://doi.org/10.1590/0074-02760200012

Hoang, D. T., Chernomor, O., von Haeseler, A., Minh, B. Q., & Vinh, L. S. (2018). UFBoot2: Improving the ultrafast bootstrap approximation. *Molecular Biology and Evolution, 35*(2), 518–522. https://doi.org/10.1093/molbev/msx281

Hönig, V., Palus, M., Kaspar, T., Zemanova, M., Majerova, K., Hofmannova, L., Papezik, P., Sikutova, S., Rettich, F., Hubalek, Z., Rudolf, I., Votypka, J., Modry, D., & Ruzek, D. (2019). Multiple lineages of Usutu Virus (flaviviridae, flavivirus) in blackbirds (*Turdus merula*) and mosquitoes (*Culex pipiens, Cx. modestus*) in the Czech Republic (2016-2019). *Microorganisms, 7*(11), 568. https://doi.org/10.3390/microorganisms7110568

Hubálek, Z., Rudolf, I., & Nowotny, N. (2014). Arboviruses pathogenic for domestic and wild animals. *Advances in Virus Research, 89*, 201–275. https://doi.org/10.1016/B978-0-12-800172-1.00005-7

Jöst, H., Bialonski, A., Maus, D., Sambri, V., Eiden, M., Groschup, M. H., Günther, S., Becker, N., & Schmidt-Chanasit, J. (2011). Isolation of Usutu virus in Germany. *American Journal of Tropical Medicine and Hygiene, 85*(3), 551–553. https://doi.org/10.4269/ajtmh.2011.11-0248

Kanthong, N., Khemnu, N., Pattanakitsakul, S. N., Malasit, P., & Flegel, T. W. (2010). Persistent, triple-virus co-infections in mosquito cells. *BMC Microbiology, 10*, 14. https://doi.org/10.1186/1471-2180-10-14

Kenney, J. L., Solberg, O. D., Langevin, S. A., & Brault, A. C. (2014). Characterization of a novel insect-specific flavivirus from Brazil: Potential for inhibition of infection of arthropod cells with medically important flaviviruses. *Journal of General Virology, 95*(Pt 12), 2796–2808. https://doi.org/10.1099/vir.0.068031-0

Komar, N. (2003). West Nile virus: Epidemiology and ecology in North America. *Advances in Virus Research, 61*, 185–234. https://doi.org/10.1016/s0065-3527(03)61005-5

Lee, Y. M., Tscherne, D. M., Yun, S. I., Frolov, I., & Rice, C. M. (2005). Dual mechanisms of pestiviral superinfection exclusion at entry and RNA replication. *Journal of Virology, 79*(6), 3231–3242. https://doi.org/10.1128/JVI.79.6.3231-3242.2005

Lim, S. M., Geervliet, M., Verhagen, J. H., Müskens, G. J. D. M., Majoor, F. A., Osterhaus, A. D. M. E., & Martina, B. E. E. (2018). Serologic evidence of West Nile virus and Usutu virus infections in Eurasian coots in the Netherlands. *Zoonoses Public Health, 65*(1), 96–102. https://doi.org/10.1111/zph.12375

Ludwig, G. V., Calle, P. P., Mangiafico, J. A., Raphael, B. L., Danner, D. K., Hile, J. A., Clippinger, T. L., Smith, J. F., Cook, R. A., & McNamara, T. (2002). An outbreak of West Nile virus in a New York City captive wildlife population. *American Journal of Tropical Medicine and Hygiene, 67*(1), 67–75. https://doi.org/10.4269/ajtmh.2002.67.67

Lühken, R., Jöst, H., Cadar, D., Thomas, S. M., Bosch, S., Tannich, E., Becker, N., Ziegler, U., Lachmann, L., & Schmidt-Chanasit, J. (2017). Distribution of Usutu virus in Germany and its effect on breeding bird populations. *Emerging Infectious Diseases, 23*(12), 1994–2001. https://doi.org/10.3201/eid2312.171257

Mayr, A., Bachmann, P. A., Bibrack, B., & Wittmann, G. (1977). Neutralisationstest. In A. Mayr, P. A. Bachmann, B. Bibrack, & G. Wittmann (Eds.), *Virologische Arbeitsmethoden, Band II (Serologie)* (pp. 457–534). Gustav Fischer Verlag.

Michel, F., Fischer, D., Eiden, M., Fast, C., Reuschel, M., Müller, K., Rinder, M., Urbaniak, S., Brandes, F., Schwehn, R., Lühken, R., Groschup, M., & Ziegler, U. (2018). West Nile Virus and Usutu Virus monitoring of wild birds in Germany. *International Journal of Environmental Research and Public Health, 15*(1), 171. https://doi.org/10.3390/ijerph15010171

Michel, F., Sieg, M., Fischer, D., Keller, M., Eiden, M., Reuschel, M., Reuschel, M., Schmidt, V., Schwehn, R., Rinder, M., Urbaniak, S., Müller, K., Schmoock, M., Lühken, R., Wysocki, P., Fast, C., Lierz, M., Korbel, R., Vahlenkamp, T. W., … Ziegler, U. (2019). Evidence for West Nile Virus and Usutu Virus Infections in Wild and Resident Birds in Germany, 2017 and 2018. *Viruses, 11*(7), 674. https://doi.org/10.3390/v11070674

Minh, B. Q., Nguyen, M. A. T., von Haeseler, A. (2013). Ultrafast approximation for phylogenetic bootstrap. *Molecular Biology and Evolution, 30*(5), 1188–1195. https://doi.org/10.1093/molbev/mst024

Naturschutzbund Deutschland e.V. (NABU). (2018). *Usutu-Virus tötet mehr Vögel als je zuvor*. Retrieved from https://www.nabu.de/news/2018/09/usutu-news.html?werbecode=august

Nguyen L.-T., Schmidt H. A., von Haeseler A., Minh B. Q. (2015). IQ-TREE: A Fast and Effective Stochastic Algorithm for Estimating Maximum-Likelihood Phylogenies. *Molecular Biology and Evolution, 32*, (1), 268–274. http://dx.doi.org/10.1093/molbev/msu300.

Nikolay, B. (2015). A review of West Nile and Usutu virus co-circulation in Europe: How much do transmission cycles overlap? *Transactions of the Royal Society of Tropical Medicine and Hygiene, 109*(10), 609–618. https://doi.org/10.1093/trstmh/trv066

Oude Munnink, B. B., Kik, M., de Bruijn, N. D., Kohl, R., van der Linden, A., Reusken, C., & Koopmans, M. (2019). Towards high quality real-time whole genome sequencing during outbreaks using Usutu virus as example. *Infection, Genetics and Evolution, 73*, 49–54. https://doi.org/10.1016/j.meegid.2019.04.015

Oude Munnink, B. B., Münger, E., Nieuwenhuijse, D. F., Kohl, R., van der Linden, A., Schapendonk, C. M. E., van der Jeugd, H., Kik, M., Rijks, J. M., Reusken, C. B. E. M., & Koopmans, M. (2020). Genomic monitoring to understand the emergence and spread of Usutu virus in the Netherlands, 2016–2018. *Scientific Reports, 10*(1), 2798. https://doi.org/10.1038/s41598-020-59692-y

Pepin, K. M., Lambeth, K., & Hanley, K. A. (2008). Asymmetric competitive suppression between strains of dengue virus. *BMC Microbiology, 8*, 28. https://doi.org/10.1186/1471-2180-8-28

Percivalle, E., Cassaniti, I., Sarasini, A., Rovida, F., Adzasehoun, K. M. G., Colombini, I., Isernia, P., Cuppari, I., & Baldanti, F. (2020). West Nile or Usutu Virus? A three-year follow-up of humoral and cellular response in a group of asymptomatic blood donors. *Viruses, 12*(2), 157. https://doi.org/10.3390/v12020157

Pérez-Ramírez, E., Llorente, F., & Jiménez-Clavero, M. A. (2014). Experimental infections of wild birds with West Nile virus. *Viruses, 6*(2), 752–781. https://doi.org/10.3390/v6020752

Porterfield, J. S. (1986). Antibody-dependent enhancement of viral infectivity. *Advances in Virus Research, 31*, 335–355. https://doi.org/10.1016/S0065-3527(08)60268-7.

Quick, J., Grubaugh, N. D., Pullan, S. T., Claro, I. M., Smith, A. D., Gangavarapu, K., Oliveira, G., Robles-Sikisaka, R., Rogers, T. F., Beutler, N. A., Burton, D. R., Lewis-Ximenez, L. L., de Jesus, J. G., Giovanetti, M., Hill, S. C., Black, A., Bedford, T., Carroll, M. W., Nunes, M., … Loman, N. J. (2017). Multiplex PCR method for MinION and Illumina sequencing of Zika and other virus genomes directly from clinical samples. *Nature Protocols, 12*(6), 1261–1276. https://doi.org/10.1038/nprot.2017.066

Rijks, J. M., Kik, M. L., Slaterus, R., Foppen, R., Stroo, A., IJzer, J., Stahl, J., Gröne, A., Koopmans, M., van der Jeugd, H. P., & Reusken, C. (2016). Widespread Usutu virus outbreak in birds in the Netherlands, 2016. *Euro Surveillance, 21*(45), 30391. https://doi.org/10.2807/1560-7917.ES.2016.21.45.30391

Rubel, F., Brugger, K., Hantel, M., Chvala-Mannsberger, S., Bakonyi, T., Weissenböck, H., & Nowotny, N. (2008). Explaining Usutu virus dynamics in Austria: Model development and calibration. *Preventive Veterinary Medicine, 85*(3–4), 166–186. https://doi.org/10.1016/j.prevetmed.2008.01.006

Rudolf, I., Bakonyi, T., Šebesta, O., Mendel, J., Peško, J., Betášová, L., Blažejová, H., Venclíková, K., Straková, P., Nowotny, N., & Hubálek, Z. (2014). West Nile virus lineage 2 isolated from *Culex modestus* mosquitoes in the Czech Republic, 2013: Expansion of the European WNV endemic area to the North? *Eurosurveillance Weekly, 19*(31), 20867. https://doi.org/10.2807/1560-7917.Es2014.19.31.20867

Salaman, R. N. (1933). Protective Inoculation against a Plant Virus. *Nature, 131*(3309), 468. https://doi.org/10.1038/131468a0

Seidowski, D., Ziegler, U., von Rönn, J. A. C., Müller, K., Hüppop, K., Müller, T., Freuling, C., Mühle, R.-U., Nowotny, N., Ulrich, R. G., Niedrig, M., & Groschup, M. H. (2010). West Nile virus monitoring of migratory and resident birds in Germany. *Vector Borne and Zoonotic Diseases, 10*(7), 639–647. https://doi.org/10.1089/vbz.2009.0236

Sieg, M., Schmidt, V., Ziegler, U., Keller, M., Höper, D., Heenemann, K., Rückner, A., Nieper, H., Muluneh, A., Groschup, M. H., & Vahlenkamp, T. W. (2017). Outbreak and cocirculation of three different Usutu virus strains in Eastern Germany. *Vector Borne and Zoonotic Diseases, 17*(9), 662–664. https://doi.org/10.1089/vbz.2016.2096

Sikkema, R. S., Schrama, M., van den Berg, T., Morren, J., Munger, E., Krol, L., van der Beek, J. G., Blom, R., Chestakova, I., van der Linden, A., Boter, M., van Mastrigt, T., Molenkamp, R., Koenraadt, C. J., van den Brand, J. M., Oude Munnink, B. B., Koopmans, M. P., & van der Jeugd, H. (2020). Detection of West Nile virus in a common whitethroat (*Curruca communis*) and *Culex* mosquitoes in the Netherlands, 2020. *Euro Surveillance, 25*(40), 2001704. https://doi.org/10.2807/1560-7917.ES.2020.25.40.2001704

Sinigaglia, A., Pacenti, M., Martello, T., Pagni, S., Franchin, E., & Barzon, L. (2019). West Nile virus infection in individuals with pre-existing Usutu virus immunity, northern Italy, 2018. *Euro Surveillance, 24*(21), 1900261. https://doi.org/10.2807/1560-7917.ES.2019.24.21.1900261

Tamba, M., Bonilauri, P., Bellini, R., Calzolari, M., Albieri, A., Sambri, V., Dottori, M., & Angelini, P. (2011). Detection of Usutu virus within a West Nile virus surveillance program in Northern Italy. *Vector Borne and Zoonotic Diseases, 11*(5), 551–557. https://doi.org/10.1089/vbz.2010.0055

Troupin, A., & Colpitts, T. M. (2016). Overview of West Nile Virus transmission and epidemiology. *Methods in Molecular Biology, 1435*, 15–18. https://doi.org/10.1007/978-1-4939-3670-0_2

Tscherne, D. M., Evans, M. J., von Hahn, T., Jones, C. T., Stamataki, Z., McKeating, J. A., Lindenbach, B. D., & Rice, C. M. (2007). Superinfection exclusion in cells infected with hepatitis C virus. *Journal of Virology, 81*(8), 3693–3703. https://doi.org/10.1128/JVI.01748-06

Vilibic-Cavlek, T., Savic, V., Sabadi, D., Peric, L., Barbic, L., Klobucar, A., Miklausic, B., Tabain, I., Santini, M., Vucelja, M., Dvorski, E., Butigan, T., Kolaric-Sviben, G., Potocnik-Hunjadi, T., Balenovic, M., Bogdanic, M., Andric, Z., Stevanovic, V., Capak, K., … Savini, G. (2019). Prevalence and molecular epidemiology of West Nile and Usutu virus infections in Croatia in the 'One health' context, 2018. *Transbound and Emerging Diseases, 66*(5), 1946–1957. https://doi.org/10.1111/tbed.13225

Wang, H., Abbo, S. R., Visser, T. M., Westenberg, M., Geertsema, C., Fros, J. J., Koenraadt, C. J. M., & Pijlman, G. P. (2020). Competition between Usutu virus and West Nile virus during simultaneous and sequential infection of *Culex pipiens* mosquitoes. *Emerging Microbes & Infections, 9*(1), 2642–2652. https://doi.org/10.1080/22221751.2020.1854623

Weidinger, P., Kolodziejek, J., Bakonyi, T., Brunthaler, R., Erdélyi, K., Weissenböck, H., & Nowotny, N. (2020). Different dynamics of Usutu virus infections in Austria and Hungary, 2017–2018. *Transbound and Emerging Diseases, 67*(1), 298–307. https://doi.org/10.1111/tbed.13351

Wylezich C., Calvelage S., Schlottau K., Ziegler U., Pohlmann A., Höper D., Beer M. (2021). Next-generation diagnostics: virus capture facilitates a sensitive viral diagnosis for epizootic and zoonotic pathogens including SARS-CoV-2. *Microbiome, 9*, (1). https://doi.org/10.1186/s40168-020-00973-z.

Wylezich, C., Papa, A., Beer, M., & Höper, D. (2018). A versatile sample processing workflow for metagenomic pathogen detection. *Scientific Reports, 8*(1), 13108. https://doi.org/10.1038/s41598-018-31496-1

Zannoli, S., & Sambri, V. (2019). West Nile Virus and Usutu Virus co-circulation in Europe: Epidemiology and implications. *Microorganisms, 7*(7), 184. https://doi.org/10.3390/microorganisms7070184

Transboundary and Emerging Diseases —WILEY—| 17

Zeller, H. G., & Schuffenecker, I. (2004). West Nile virus: An overview of its spread in Europe and the Mediterranean basin in contrast to its spread in the Americas. *European Journal of Clinical Microbiology and Infectious Diseases*, *23*(3), 147–156. https://doi.org/10.1007/s1009 6-003-1085-1

Ziegler, U., Fast, C., Eiden, M., Bock, S., Schulze, C., Hoeper, D., Ochs, A., Schlieben, P., Keller, M., Zielke, D. E., Luehken, R., Cadar, D., Walther, D., Schmidt-Chanasit, J., & Groschup, M. H. (2016). Evidence for an independent third Usutu virus introduction into Germany. *Veterinary Microbiology*, *192*, 60–66. https://doi.org/10.1016/j.vetmic.2016.06.007

Ziegler, U., Jöst, H., Müller, K., Fischer, D., Rinder, M., Tietze, D. T., Danner, K.-J., Becker, N., Skuballa, J., Hamann, H.-P., Bosch, S., Fast, C., Eiden, M., Schmidt-Chanasit, J., & Groschup, M. H. (2015). Epidemic spread of Usutu virus in southwest Germany in 2011 to 2013 and monitoring of wild birds for Usutu and West Nile viruses. *Vector Borne and Zoonotic Diseases*, *15*(8), 481–488. https://doi.org/10.1089/vbz.2014.1746

Ziegler, U., Lühken, R., Keller, M., Cadar, D., van der Grinten, E., Michel, F., Albrecht, K., Eiden, M., Rinder, M., Lachmann, L., Höper, D., Vina-Rodriguez, A., Gaede, W., Pohl, A., Schmidt-Chanasit, J., & Groschup, M. H. (2019). West Nile virus epizootic in Germany, 2018. *Antiviral Research*, *162*, 39–43. https://doi.org/10.1016/j.antiv iral.2018.12.005

Ziegler, U., Santos, P. D., Groschup, M. H., Hattendorf, C., Eiden, M., Höper, D., Eisermann, P., Keller, M., Michel, F., Klopfleisch, R., Müller, K., Werner, D., Kampen, H., Beer, M., Frank, C., Lachmann, R., Tews, B. A., Wylezich, C., Rinder, M., Lühken, R. (2020). West Nile Virus epidemic in Germany triggered by epizootic emergence, 2019. *Viruses*, *12*(4), 448. https://doi.org/10.3390/v12040448

Zou, G., Zhang, B., Lim, P.-Y., Yuan, Z., Bernard, K. A., & Shi, P.-Y. (2009). Exclusion of West Nile virus superinfection through RNA replication. *Journal of Virology*, *83*(22), 11765–11776. https://doi.org/10.1128/jvi.01205-09

SUPPORTING INFORMATION

Additional supporting information may be found online in the Supporting Information section.

How to cite this article: Santos PD, Michel F, Wylezich C, et al. Co-infections: Simultaneous detections of West Nile virus and Usutu virus in birds from Germany. *Transbound Emerg Dis*. 2021;00:1–17. https://doi.org/10.1111/tbed.14050
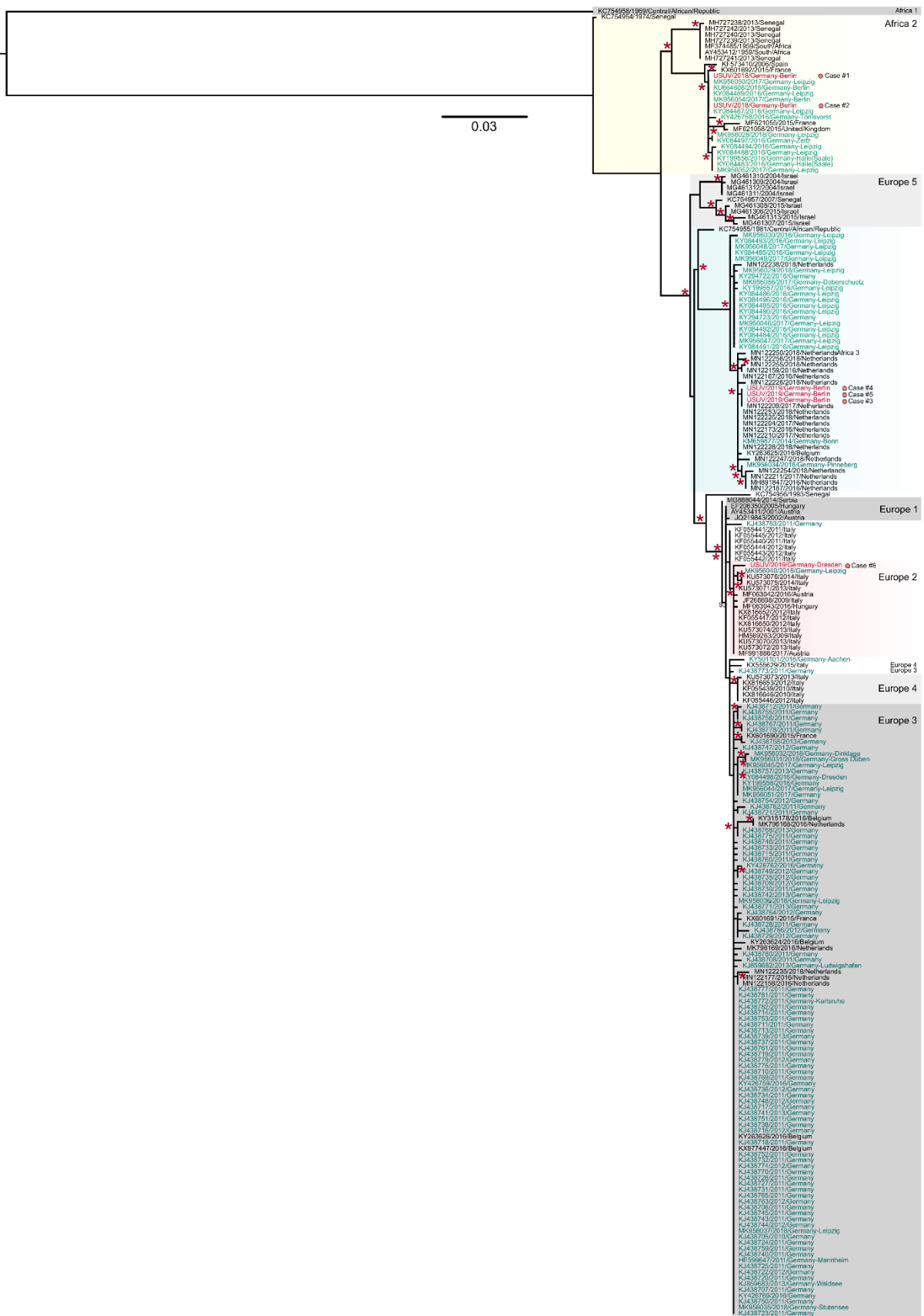
Figure S1. Phylogenetic analysis of Usutu virus partial envelope sequence (726 nucleotides). USUV sequences related to WNV-USUV co-infected birds are highlighted in red and with red dots, while other USUV sequences from Germany are highlighted in green. Taxon information includes the nucleotide accession number, collection year, and country of origin of the viruses. City of origin was also included for samples collected in Germany. Scale bar indicates the number of nucleotide substitutions per site. Red asterisks before the nodes denote bootstrap values ≥80%. The maximum likelihood tree was constructed using the best-selected nucleotide substitution model (GTR+I).
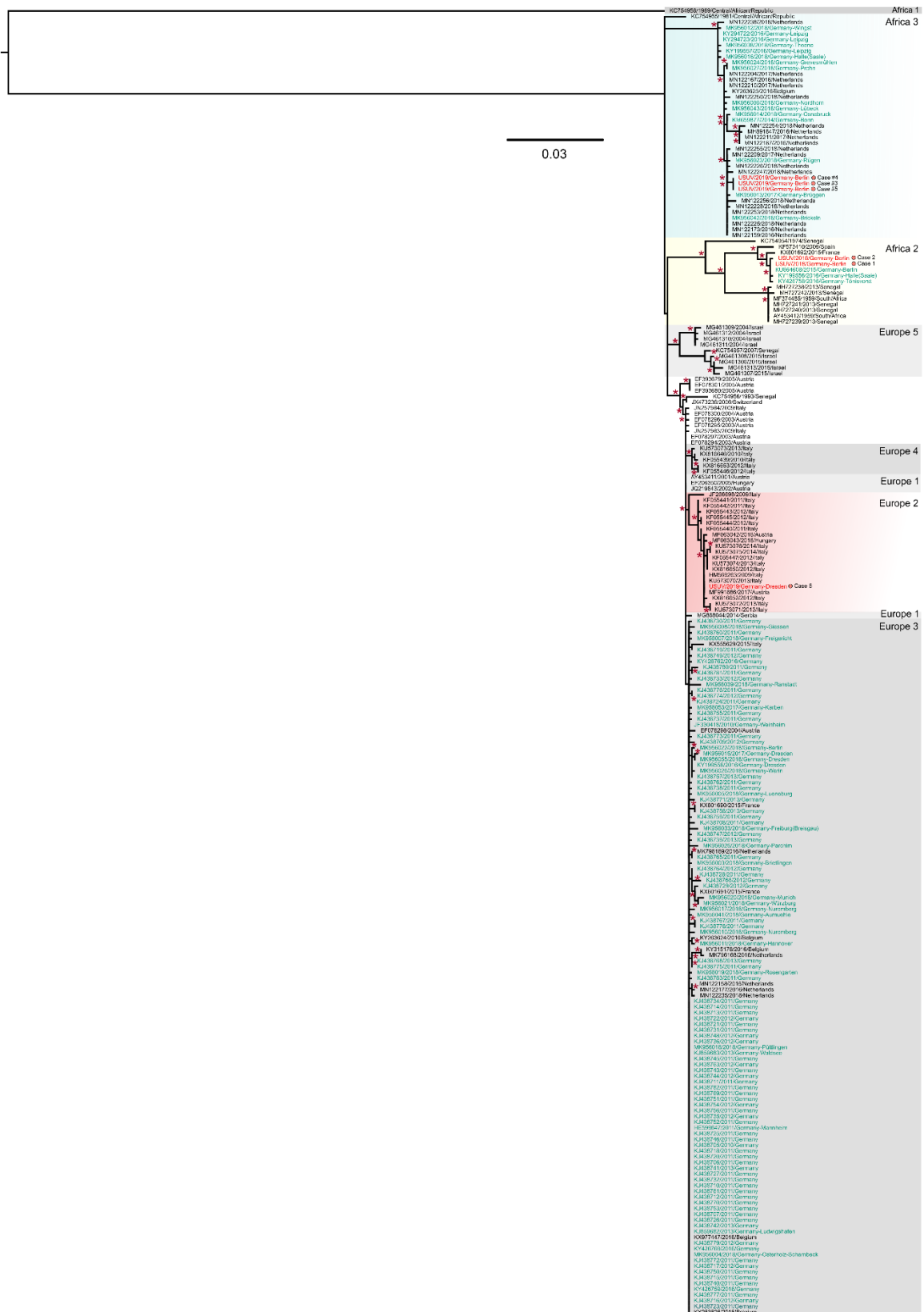
Figure S2. Phylogenetic analysis of Usutu virus partial envelope sequence (1066 nucleotides). USUV sequences related to WNV-USUV co-infected birds are highlighted in red and with red dots. while other USUV sequences from Germany are highlighted in green. Taxon information includes the nucleotide accession number, collection year, and country of origin of the viruses. City of origin are included for samples collected in Germany. Scale bar indicates the number of nucleotide substitutions per site. Red asterisks before the nodes denote bootstrap values ≥80%. The maximum likelihood tree was constructed using the best-selected nucleotide substitution model (GTR+I).

Table S1. Specific protocols for Usutu virus full genome sequencing. We indicated the library numbers in different library preparation steps (#1 and #2) for high-throughput sequencing per sample, and the primer pairs needed for supplementary single-plex PCR and Sanger sequencing steps.

Case number	Identifier code and Host name	Organ sample	Library number for HTS preparation #1	Library number for HTS preparation #2[†]	Single-plex PCR and Sanger sequencing[‡]	USUV Accession No.
1	ED-I-79/18 Snowy owl	Brain	lib04071	lib04107	primer pairs 31	LR989886
2	ED-I-107/18 Snowy owl	Brain	lib04073	lib04109	primer pairs 2, 19, and 31	LR989887
3	ED-I-115/19 Chinese Merganser	Liver	lib04074	lib04110	Not needed	LR989889
4	ED-I-116/19 Black-tailed Gull	Liver	lib04075	lib04111	primer pair 5[§]	LR989892
5	ED-I-119/19 Black-tailed Gull	Heart	lib04076	lib04112	Not needed	LR989894
6	ED-I-139/19 Great Tit	Liver+ Heart	lib04072	lib04108	Not needed	LR989890

Abbreviations: † - For library preparation #2, we selected necessary Oude Munnink et al. (2019) primer pairs for Mix 1 (primer pairs 5, 17, 19, 21, 23, and 31) and Mix 2 (primer pairs 2, 18, 20, 22, 24, 26, 30, and 32) to increase coverage in respective regions in USUV genome sequences. ‡ - Selected Oude Munnink et al. (2019) primer pairs for single-plex PCR and Sanger sequencing. § - Amplification and Sanger sequencing steps were not successful.

Table S2. List of European WNV lineage 2 full genome sequences retrieved from Genbank in 01 September 2020. The sequences were used from alignment and phylogenetic analysis as shown in Figure 2.

Sequence ID	Accession number	Sequence Length	Collection Year	Country	Host
KP780837/2008/Austria	KP780837	10963	2008	Austria	*Nestor notabilis* (kea)
MF984351/2016/Austria	MF984351	10980	2016	Austria	*Culex pipiens*
MF984340/2015/Austria	MF984340	10831	2015	Austria	*Homo sapiens*
MF984348/2016/Austria	MF984348	10832	2016	Austria	*Homo sapiens*
KM659876/2014/Austria	KM659876	11028	2014	Austria	*Homo sapiens*
MF984344/2015/Austria	MF984344	11024	2015	Austria	*goshawk*
MF984337/2015/Austria	MF984337	10990	2015	Austria	*Homo sapiens*
MF984341/2015/Austria	MF984341	10658	2015	Austria	*Homo sapiens*
KP109692/2014/Austria	KP109692	10988	2014	Austria	*Culex pipiens*
MF984352/2016/Austria	MF984352	10800	2016	Austria	*Culex pipiens*
KF179640/2008/Austria	KF179640	10998	2008	Austria	goshawk
MF984349/2016/Austria	MF984349	10720	2016	Austria	horse
KP780840/2014/Austria	KP780840	10963	2014	Austria	*Nestor notabilis* (kea)
MF984345/2015/Austria	MF984345	11013	2015	Austria	falcon
MF984338/2015/Austria	MF984338	10836	2015	Austria	*Homo sapiens*
MF984342/2015/Austria	MF984342	10831	2015	Austria	*Homo sapiens*
MF984350/2016/Austria	MF984350	10979	2016	Austria	horse
KP780839/2011/Austria	KP780839	10963	2011	Austria	*Nestor notabilis* (kea)
MF984346/2016/Austria	MF984346	10829	2016	Austria	*Homo sapiens*
MF984339/2015/Austria	MF984339	10831	2015	Austria	*Homo sapiens*
MF984343/2015/Austria	MF984343	11013	2015	Austria	*Homo sapiens*
KP109691/2014/Austria	KP109691	10988	2014	Austria	*Homo sapiens*
MF984347/2016/Austria	MF984347	10991	2016	Austria	*Homo sapiens*
KP780838/2009/Austria	KP780838	10963	2009	Austria	*Nestor notabilis* (kea)
MH021189/2017/Belgium	MH021189	11060	2017	Belgium	*Homo sapiens*
KU206781/2015/Bulgaria	KU206781	10983	2015	Bulgaria	*Homo sapiens*
MT341472/2018/Bulgaria	MT341472	10787	2018	Bulgaria	*Culex sp.*
KM203860/2013/Czech Republic	KM203860	11018	2013	Czech Republic	*Culex modestus*
KM203863/2013/Czech Republic	KM203863	11018	2013	Czech Republic	*Culex modestus*
KM203862/2013/Czech Republic	KM203862	11018	2013	Czech Republic	*Culex modestus*
KM203861/2013/Czech Republic	KM203861	11018	2013	Czech Republic	*Culex modestus*
LR743446/2019/Germany	LR743446	11018	2019	Germany	
MH986055/2018/Germany	MH986055	11029	2018	Germany	*Turdus merula*
LR743449/2019/Germany	LR743449	11018	2019	Germany	
LR743442/2019/Germany	LR743442	11073	2019	Germany	
LR743421/2019/Germany	LR743421	11029	2019	Germany	
LR743432/2019/Germany	LR743432	11022	2019	Germany	
LR743453/2019/Germany	LR743453	11019	2019	Germany	
LR743424/2019/Germany	LR743424	11079	2019	Germany	
LR743428/2019/Germany	LR743428	11067	2019	Germany	
LR743448/2019/Germany	LR743448	11022	2019	Germany	
LR743457/2019/Germany	LR743457	11022	2019	Germany	
LR743435/2019/Germany	LR743435	11019	2019	Germany	
MH986056/2018/Germany	MH986056	11018	2018	Germany	*Turdus merula*
MN794935/2019/Germany	MN794935	11043	2019	Germany	*Homo sapiens*
LR743422/2019/Germany	LR743422	11010	2019	Germany	
LR743443/2018/Germany	LR743443	11068	2018	Germany	
LR743452/2019/Germany	LR743452	11026	2019	Germany	
MN794939/2019/Germany	MN794939	11056	2019	Germany	*Prunella modularis*
LR743429/2018/Germany	LR743429	10930	2018	Germany	
LR743456/2019/Germany	LR743456	11019	2019	Germany	
LR743436/2018/Germany	LR743436	11069	2018	Germany	
LR743425/2019/Germany	LR743425	11060	2019	Germany	
LR743451/2019/Germany	LR743451	11024	2019	Germany	
LR743430/2019/Germany	LR743430	11025	2019	Germany	
LR743444/2019/Germany	LR743444	11076	2019	Germany	
LR743433/2018/Germany	LR743433	11072	2018	Germany	
LR743426/2019/Germany	LR743426	11022	2019	Germany	
MN794938/2019/Germany	MN794938	11056	2019	Germany	*Passer domesticus*
LR743437/2018/Germany	LR743437	11013	2018	Germany	
LR743455/2019/Germany	LR743455	10995	2019	Germany	
MH910045/2018/Germany	MH910045	10328	2018	Germany	*Homo sapiens*
MH924836/2018/Germany	MH924836	11080	2018	Germany	*Strix nebulosa*
LR743431/2019/Germany	LR743431	11019	2019	Germany	
LR743450/2019/Germany	LR743450	11019	2019	Germany	

LR743445/2019/Germany	LR743445	11029	2019	Germany	
LR743454/2019/Germany	LR743454	11023	2019	Germany	
LR743427/2019/Germany	LR743427	11019	2019	Germany	
MN794937/2019/Germany	MN794937	11056	2019	Germany	*Turdus merula*
LR743423/2019/Germany	LR743423	11027	2019	Germany	
LR743447/2019/Germany	LR743447	10995	2019	Germany	
LR743434/2018/Germany	LR743434	11079	2018	Germany	
LR743458/2019/Germany	LR743458	11022	2019	Germany	
KJ883345/2013/Greece	KJ883345	11008	2013	Greece	*Homo sapiens*
MT341471/2019/Greece	MT341471	10787	2019	Greece	*Culex sp.*
MN480793/2018/Greece	MN480793	10926	2018	Greece	*Homo sapiens*
HQ537483/2010/Greece	HQ537483	11028	2010	Greece	*Culex pipiens* mosquito pool
MN481589/2018/Greece	MN481589	10926	2018	Greece	chicken
MN481595/2010/Greece	MN481595	10926	2010	Greece	pigeon
MN652880/2018/Greece	MN652880	10926	2018	Greece	*Culex sp.*
KJ883349/2013/Greece	KJ883349	10967	2013	Greece	*Homo sapiens*
KJ883348/2013/Greece	KJ883348	11002	2013	Greece	*Homo sapiens*
KJ883344/2013/Greece	KJ883344	11003	2013	Greece	*Homo sapiens*
KF179639/2012/Greece	KF179639	11000	2012	Greece	*Homo sapiens*
MN481596/2011/Greece	MN481596	10926	2011	Greece	chicken
MN652879/2018/Greece	MN652879	10926	2018	Greece	*Culex sp.*
KJ883341/2013/Greece	KJ883341	11013	2013	Greece	*Homo sapiens*
MN480792/2018/Greece	MN480792	10926	2018	Greece	*Homo sapiens*
MN481592/2012/Greece	MN481592	10926	2012	Greece	mosquito
KJ883347/2013/Greece	KJ883347	11013	2013	Greece	*Homo sapiens*
MK473443/2017/Greece	MK473443	10946	2017	Greece	Eurasian magpie (*Pica pica*)
KJ883343/2013/Greece	KJ883343	11002	2013	Greece	*Homo sapiens*
MN481597/2012/Greece	MN481597	10926	2012	Greece	Chicken
MN480795/2018/Greece	MN480795	10926	2018	Greece	*Homo sapiens*
MN652878/2018/Greece	MN652878	10926	2018	Greece	Culex sp.
KJ577739/2013/Greece	KJ577739	11003	2013	Greece	*Homo sapiens*
MN481593/2012/Greece	MN481593	10926	2012	Greece	Mosquito
MN481591/2018/Greece	MN481591	10926	2018	Greece	Dog
KY594040/2010/Greece	KY594040	11050	2010	Greece	*Homo sapiens*
MH549209/2017/Greece	MH549209	10946	2017	Greece	*Pica pica* (Eurasian magpie)
KJ883346/2013/Greece	KJ883346	11000	2013	Greece	*Homo sapiens*
KJ883342/2013/Greece	KJ883342	11011	2013	Greece	*Homo sapiens*
MN480794/2018/Greece	MN480794	10926	2018	Greece	*Culex sp.*
MN481590/2018/Greece	MN481590	10926	2018	Greece	Horse
KJ577738/2013/Greece	KJ577738	10998	2013	Greece	Homo sapiens
MN481594/2012/Greece	MN481594	10926	2012	Greece	mosquito
MT341470/2019/Greece	MT341470	10787	2019	Greece	*Culex sp.*
KJ883350/2013/Greece	KJ883350	11013	2013	Greece	*Homo sapiens*
DQ116961/2004/Hungary	DQ116961	11028	2004	Hungary	Goshawk
KT359349/2014/Hungary	KT359349	10966	2014	Hungary	*Homo sapiens*
KC496015/2010/Hungary	KC496015	11028	2010	Hungary	Horse
KF823806/2013/Italy	KF823806	10975	2013	Italy	*Homo sapiens*
KP789957/2014/Italy	KP789957	10999	2014	Italy	*Homo sapiens* male born in 1963
KU573081/2013/Italy	KU573081	10778	2013	Italy	*Pica pica* (magpie)
KP789960/2013/Italy	KP789960	10949	2013	Italy	*Homo sapiens* male born in 1952
KF588365/2013/Italy	KF588365	10998	2013	Italy	*Homo sapiens*
KP789953/2014/Italy	KP789953	10994	2014	Italy	*Homo sapiens* male born in 1939
KU573082/2013/Italy	KU573082	10905	2013	Italy	Crow
JN858070/2011/Italy	JN858070	10520	2011	Italy	*Homo sapiens*; age: 56; sex: male
KP789956/2014/Italy	KP789956	10938	2014	Italy	*Homo sapiens* male born in 1938
KF647252/2013/Italy	KF647252	10974	2013	Italy	*Homo sapiens*
KF647248/2013/Italy	KF647248	11013	2013	Italy	*Homo sapiens*
KF647251/2013/Italy	KF647251	10994	2013	Italy	*Homo sapiens*
KU573083/2013/Italy	KU573083	10788	2013	Italy	*Culex pipiens*
KP789959/2014/Italy	KP789959	10947	2014	Italy	*Homo sapiens* female born in 1934
KF647249/2013/Italy	KF647249	10986	2013	Italy	*Homo sapiens*
KP789955/2014/Italy	KP789955	10995	2014	Italy	*Homo sapiens* female born in 1967
KT207792/2014/Italy	KT207792	10995	2014	Italy	Mosquito
KU573080/2013/Italy	KU573080	10984	2013	Italy	*Culex pipiens*
KP789958/2014/Italy	KP789958	11000	2014	Italy	*Homo sapiens* male born in 1945
KF647250/2013/Italy	KF647250	11013	2013	Italy	*Homo sapiens*
KF823805/2013/Italy	KF823805	11011	2013	Italy	*Homo sapiens*
KP789954/2014/Italy	KP789954	11000	2014	Italy	*Homo sapiens* male born in 1959
KC496016/2010/Serbia	KC496016	11028	2010	Serbia	*Culex pipiens*
KT757321/2013/Serbia	KT757321	10948	2013	Serbia	*Culex pipiens*
KX375812/2013/Serbia	KX375812	10359	2013	Serbia	*Homo sapiens*

KC407673/2012/Serbia	KC407673	11028	2012	Serbia	northern goshawk
KT757320/2013/Serbia	KT757320	10948	2013	Serbia	*Culex pipiens*
KT757323/2013/Serbia	KT757323	10948	2013	Serbia	*Culex pipiens*
KT757319/2013/Serbia	KT757319	10948	2013	Serbia	*Culex pipiens*
KT757322/2013/Serbia	KT757322	10948	2013	Serbia	*Culex pipiens*
KT757318/2013/Serbia	KT757318	10948	2013	Serbia	*Culex pipiens*
MH244511/2013/Slovakia	MH244511	11026	2013	Slovakia	northern goshawk
MH244513/2013/Slovakia	MH244513	11012	2013	Slovakia	Eurasian sparrow hawk
MH244512/2013/Slovakia	MH244512	11013	2013	Slovakia	northern goshawk
MH244510/2014/Slovakia	MH244510	11025	2014	Slovakia	northern goshawk

Table S3: List of European and African USUV full genome sequences retrieved from Genbank in 01 September 2020. The sequences were used from alignment and phylogenetic analysis as shown in Figure 3.

Sequence ID	Accession number	Sequence Length	Collection Year	Country	Host
AY453411/2011/Austria	AY453411	11066	2011	Austria	
MF063042/2016/Austria	MF063042	11062	2016	Austria	*Turdus merula* (blackbird)
JQ219843/2002/Austria	JQ219843	11047	2002	Austria	*Parus caeruleus* (blue tit)
MF991886/2017/Austria	MF991886	10792	2017	Austria	*Homo sapiens*
KY315178/2016/Belgium	KY315178	10959	2016	Belgium	*Gracula religiosa*
MK230892/2017/Belgium	MK230892	11065	2017	Belgium	*Turdus merula*
MK230893/2017/Belgium	MK230893	11065	2017	Belgium	*Turdus merula*
MK230891/2017/Belgium	MK230891	11065	2017	Belgium	*Turdus merula*
MK230890/2017/Belgium	MK230890	11065	2017	Belgium	*Turdus merula*
MK419834/2018/Belgium	MK419834	11066	2018	Belgium	*Melanitta nigra* (common scoter)
KX977447/2016/Belgium	KX977447	10325	2016	Belgium	*Turdus merula*
KY263624/2016/Belgium	KY263624	11065	2016	Belgium	*Turdus merula*
KY263625/2016/Belgium	KY263625	11066	2016	Belgium	*Turdus merula*
KY263626/2016/Belgium	KY263626	11066	2016	Belgium	*Turdus merula*
KC754955/1981/ CentralAfricanRepublic	KC754955	10800	1981	CentralAfricanRepublic	*Homo sapiens*
KC754958/1969/ Central1AfricanRepublic	KC754958	10745	1969	CentralAfricanRepublic	*Culex perfuscus*
KX601692/2015/France	KX601692	10995	2015	France	*Turdus merula* (common blackbird)
KX601690/2015/France	KX601690	11024	2015	France	*Turdus merula* (common blackbird)
KY128481/2016/France	KY128481	10475	2016	France	*Strix nebulosa*
KX601691/2015/France	KX601691	11065	2015	France	*Turdus merula* (common blackbird)
KY426752/2015/Germany	KY426752	10948	2015	Germany	*Turdus merula*
KJ438767/2011/Germany	KJ438767	11065	2011	Germany	*Culex cf. pipiens/torrentium*
KJ438718/2011/Germany	KJ438718	11065	2011	Germany	*Culex cf. pipiens/torrentium*
KJ438727/2011/Germany	KJ438727	11065	2011	Germany	*Turdus merula*
KJ438756/2011/Germany	KJ438756	11065	2011	Germany	*Turdus merula*
KY426754/2015/Germany	KY426754	10689	2015	Germany	*Turdus merula*
KY294722/2016/Germany	KY294722	10973	2016	Germany	*Turdus merula*
KY426769/2016/Germany	KY426769	11027	2016	Germany	*Turdus merula*
KJ438777/2011/Germany	KJ438777	11065	2011	Germany	*Turdus merula*
KY426755/2016/Germany	KY426755	11009	2016	Germany	*Turdus merula*
KJ438746/2011/Germany	KJ438746	11065	2011	Germany	*Turdus merula*
KJ438726/2011/Germany	KJ438726	11065	2011	Germany	*Turdus merula*
KJ438708/2011/Germany	KJ438708	11065	2011	Germany	*Culex pipiens*
KJ438749/2012/Germany	KJ438749	11065	2012	Germany	*Turdus merula*
KY426768/2016/Germany	KY426768	11042	2016	Germany	*Turdus merula*
KJ438717/2012/Germany	KJ438717	11065	2012	Germany	*Turdus merula*
KJ438738/2011/Germany	KJ438738	11065	2011	Germany	*Turdus merula*
KY426759/2016/Germany	KY426759	11016	2016	Germany	*Turdus merula*
KY426760/2016/Germany	KY426760	11019	2016	Germany	*Turdus merula*
KJ438779/2012/Germany	KJ438779	11060	2012	Germany	*Turdus merula*
KJ438766/2012/Germany	KJ438766	11066	2012	Germany	*Turdus merula*
KJ438737/2011/Germany	KJ438737	11065	2011	Germany	*Culex torrentium*
KJ438778/2011/Germany	KJ438778	11065	2011	Germany	*Turdus merula*
KJ438748/2012/Germany	KJ438748	11065	2012	Germany	*Turdus merula*
KJ438719/2011/Germany	KJ438719	11065	2011	Germany	*Turdus merula*
KY426761/2016/Germany	KY426761	10945	2016	Germany	*Turdus merula*
KJ438732/2011/Germany	KJ438732	11065	2011	Germany	*Turdus merula*
KJ438773/2011/Germany	KJ438773	11065	2011	Germany	*Turdus merula*
KJ438769/2011/Germany	KJ438769	11065	2011	Germany	*Turdus merula*
KJ438731/2011/Germany	KJ438731	11065	2011	Germany	*Turdus merula*
KJ438713/2011/Germany	KJ438713	11065	2011	Germany	*Turdus merula*
KJ438776/2011/Germany	KJ438776	11065	2011	Germany	*Turdus merula*
HE599647/2011/Germany	HE599647	11003	2011	Germany	*Turdus merula*
KJ438757/2013/Germany	KJ438757	11065	2013	Germany	*Turdus merula*
KY426767/2016/Germany	KY426767	11042	2016	Germany	*Turdus merula*
KJ438734/2011/Germany	KJ438734	11065	2011	Germany	*Sturnus vulgaris*
KJ438712/2011/Germany	KJ438712	11065	2011	Germany	*Turdus merula*
KY426753/2015/Germany	KY426753	10951	2015	Germany	*Turdus merula*
KJ438728/2011/Germany	KJ438728	11065	2011	Germany	*Turdus merula*
KY426770/2016/Germany	KY426770	10960	2016	Germany	*Turdus merula*
KY426763/2016/Germany	KY426763	10976	2016	Germany	*Turdus merula*
KJ438758/2013/Germany	KJ438758	11065	2013	Germany	*Turdus merula*
KY426751/2015/Germany	KY426751	10954	2015	Germany	*Turdus pilaris*

MN122194/2017/Netherlands	MN122194	10932	2017	Netherlands	*Turdus merula*
MN122155/2016/Netherlands	MN122155	10932	2016	Netherlands	*Turdus merula*
MN122195/2017/Netherlands	MN122195	10932	2017	Netherlands	*Turdus merula*
MH727239/2013/Senegal	MH727239	10841	2013	Senegal	*Mastomys natalensis* (multimammate rat)
KC754954/1974/Senegal	KC754954	10837	1974	Senegal	*Culex perfuscus*
MN813488/2003/Senegal	MN813488	10305	2003	Senegal	*Culex neavei*
MH727242/2013/Senegal	MH727242	10495	2013	Senegal	*Rattus rattus* (black rat)
KC754957/2007/Senegal	KC754957	10825	2007	Senegal	*Culex neavei*
KC754956/1993/Senegal	KC754956	10837	1993	Senegal	*Culex univittatus*
MH727238/2013/Senegal	MH727238	10853	2013	Senegal	*Mastomys natalensis* (multimammate rat)
MH727240/2013/Senegal	MH727240	10841	2013	Senegal	*Crocidura* sp. (shrew)
MH727241/2013/Senegal	MH727241	10843	2013	Senegal	*Mastomys natalensis* (multimammate rat)
MG888044/2014/Serbia	MG888044	10361	2014	Serbia	*Culex pipiens*
MN813492/1959/South_Africa	MN813492	10305	1959	South_Africa	*Culex neavei*
AY453412/1959/South_Africa	AY453412	11064	1959	South_Africa	
MF374485/1959/South_Africa	MF374485	11015	1959	South_Africa	*Homo sapiens*
KF573410/2006/Spain	KF573410	11064	2006	Spain	*Culex pipiens*
MN813489/2009/Spain	MN813489	10305	2009	Spain	*Culex perexiguus*
KU760915/2010/Spain	KU760915	11064	2010	Spain	
MN813491/2010/Uganda	MN813491	10305	2010	Uganda	*Culex sp.*

Table S4. Results of cell culture propagation of samples from case #1 and #2. Spleen from case #1 and brain from case #2 were inoculated to Vero B4 cells. Cell culture supernatant tested using WNV and USUV specific RT-qPCR. Cell culture supernatant originally intended for full-genome sequencing.

Case number	Scientific name (Common name)	Housing/ Area	Virus identifier	Organ Sample	Cq Values Original material		Cq Values Vero B4 cells 5 dpi	
					WNV	USUV	WNV	USUV
1	*Bubo scandiacus* (Snowy Owl)	captive Area A	ED-I-79/18	Brain	neg	28.76	not tested	not tested
				Spleen	34.81	37.63	32.04	Neg.
2	*Bubo scandiacus* (Snowy Owl)	captive Area A	ED-I-107/18	Brain	18.21	32.28	14.04	Neg.
				Kidney	29.50	36.12	not tested	not tested
				Liver	29.74	neg.	not tested	not tested
				Heart	31.33	neg.	not tested	not tested
				Lungs	30.60	neg.	not tested	not tested
				Spleen	30.55	neg.	not tested	not tested

Neg. – negative; dpi – day post infection: Area A – Tierpark Berlin. Cq – quantification cycles from RT-qPCR assays

(IV) In Action – An Early Warning System for the Detection of Unexpected or Novel Pathogens

Pauline Dianne Santos, Ute Ziegler, Kevin Szillat, Claudia A. Szentiks, Birte Strobel, Jasmin Skuballa, Sabine Merbach, Pierre Grothmann, Birke Andrea Tews, Martin Beer, and Dirk Höper

In action—an early warning system for the detection of unexpected or novel pathogens

Pauline Dianne Santos,[1,†] Ute Ziegler,[2,3] Kevin P. Szillat,[1,‡] Claudia A. Szentiks,[4] Birte Strobel,[5] Jasmin Skuballa,[5] Sabine Merbach,[6] Pierre Grothmann,[7] Birke Andrea Tews,[8,‖] Martin Beer,[1] and Dirk Höper[1,*,§]

[1]Friedrich-Loeffler-Institut, Federal Research Institute for Animal Health, Institute of Diagnostic Virology, Südufer 10, Greifswald, Insel Riems 17493, Germany, [2]Friedrich-Loeffler-Institut, Federal Research Institute for Animal Health, Institute of Novel and Emerging Infectious Diseases, Südufer 10, Greifswald, Insel Riems 17493, Germany, [3]German Centre for Infection Research, Partner Site Hamburg-Lübeck-Borstel-Riems, Südufer 10, Greifswald, Insel Riems 17493, Germany, [4]Department of Wildlife Diseases, Leibniz-Institute for Zoo- and Wildlife Research (IZW), Alfred-Kowalke-Straße 17, Berlin 10315, Germany, [5]Chemical and Veterinary Investigations Office Karlsruhe (CVUA Karlsruhe), Weissenburgerstrasse 3, Karlsruhe 76187, Germany, [6]State Institute for Chemical and Veterinary Analysis (CVUA) Westfalen, Zur Taubeneiche 10-12, Arnsberg 59821, Germany, [7]Practice for Zoo, Game and Wild Animals, Lintiger Str. 74, Geestland 27624, Germany and [8]Friedrich-Loeffler-Institut, Federal Research Institute for Animal Health, Institute of Infectology, Südufer 10, Greifswald, Insel Riems 17493, Germany

[†]https://orcid.org/0000-0003-4324-5967
[‡]https://orcid.org/0000-0003-1135-0244
[§]https://orcid.org/0000-0001-8408-2274
[‖]https://orcid.org/0000-0002-8647-0497
*Corresponding author: E-mail: dirk.hoeper@fli.de

Abstract

Proactive approaches in preventing future epidemics include pathogen discovery prior to their emergence in human and/or animal populations. Playing an important role in pathogen discovery, high-throughput sequencing (HTS) enables the characterization of microbial and viral genetic diversity within a given sample. In particular, metagenomic HTS allows the unbiased taxonomic profiling of sequences; hence, it can identify novel and highly divergent pathogens such as viruses. Newly discovered viral sequences must be further investigated using genomic characterization, molecular and serological screening, and/or *in vitro* and *in vivo* characterization. Several outbreak and surveillance studies apply unbiased generic HTS to characterize the whole genome sequences of suspected pathogens. In contrast, this study aimed to screen for novel and unexpected pathogens in previously generated HTS datasets and use this information as a starting point for the establishment of an early warning system (EWS). As a proof of concept, the EWS was applied to HTS datasets and archived samples from the 2018–9 West Nile virus (WNV) epidemic in Germany. A metagenomics read classifier detected sequences related to genome sequences of various members of *Riboviria*. We focused the further EWS investigation on viruses belonging to the families *Peribunyaviridae* and *Reoviridae*, under suspicion of causing co-infections in WNV-infected birds. Phylogenetic analyses revealed that the reovirus genome sequences clustered with sequences assigned to the species *Umatilla virus* (UMAV), whereas a new peribunyavirid, tentatively named 'Hedwig virus' (HEDV), belonged to a putative novel genus of the family *Peribunyaviridae*. In follow-up studies, newly developed molecular diagnostic assays detected fourteen UMAV-positive wild birds from different German cities and eight HEDV-positive captive birds from two zoological gardens. UMAV was successfully cultivated in mosquito C6/36 cells inoculated with a blackbird liver. In conclusion, this study demonstrates the power of the applied EWS for the discovery and characterization of unexpected viruses in repurposed sequence datasets, followed by virus screening and cultivation using archived sample material. The EWS enhances the strategies for pathogen recognition before causing sporadic cases and massive outbreaks and proves to be a reliable tool for modern outbreak preparedness.

Key words: high-throughput sequencing (HTS); early warning system; metagenomics; Germany; *Peribunyaviridae*; *Reoviridae*; outbreak; bird; mosquitos; Umatilla virus; Hedwig virus

1. Introduction

Based on our response to the 2009 H1N1 pandemic, the World Health Organization and other authorities warned that 'the world is ill-prepared to respond to a severe influenza pandemic or to any similarly global, sustained and threatening public-health emergency' (World Health Organization Director-General 2011; Fineberg 2014). This conclusion still stands for the 2013–6 Western African Ebola virus disease epidemic (Ross, Crowe, and Tyndall 2015) and the ongoing coronavirus disease 2019 pandemic, causing more than 4 million deaths to date (World Health Organization 2021). Emerging infectious disease preparedness involves activities that enhance the prevention and control of (re)-emerging pathogens to protect public and animal health (Brookes et al., 2015). Scientific and public health communities often focus on reactive approaches in handling emerging global epidemics (Bloom, Black, and Rappuoli 2017; Greenberger 2018;

Kelly et al., 2020), such as Disease X. However, the over-reliance on reactive responses can have a devastating impact on human lives and the global economy.

Investigating viral diversity in wildlife reservoirs is a building block for preparedness for future epidemics. The discovery of novel viruses in animal reservoirs can improve the rapid identification of emerging pathogens and their ecological niche, allowing risk reduction strategies for spillover events and diminishing the severity of emerging outbreaks (Epstein and Anthony 2017). However, as the vast majority of the wildlife virome is still unknown, hunting novel viruses remains an interminable task (Carroll et al., 2018; Carlson 2020). Traditionally, cell culture techniques were applied for virus discovery (Hsiung 1984; Leland and Ginocchio 2007). However, the vast number of viruses are nonculturable; thus, exploration of viral diversity necessitates culture-independent techniques, such as genomic sequencing (Gao and Moore 1996; Mokili, Rohwer, and Dutilh 2012; Mettenleiter 2017). Carroll et al. (2018) estimated that several billion dollars would be needed to unravel all unknown viral species in mammalian and avian hosts by using genomic sequencing.

Genomic sequencing techniques—such as the combined consensus polymerase chain reaction (cPCR) and deep sequencing, and metagenomic high-throughput sequencing (mHTS)—enable high-throughput discovery and taxonomic identification of novel viruses in a sample. The combined cPCR and deep sequencing approach utilizes degenerate primers to amplify conserved regions shared among the members of a viral group flanking their variable regions. This approach is cheaper and more sensitive than mHTS, but it can fail to recognize highly divergent sequences of novel viruses (Chiu 2013). However, mHTS enables hypothesis-free sequencing of all nucleic acids in a given sample, including genomes from completely unknown and highly divergent pathogens (Gu, Miller, and Chiu 2019). mHTS is widely used as a tool for virus discovery in humans (Wylie et al. 2012), wildlife reservoirs (Epstein et al., 2010; Quan et al., 2013b; Sachsenröder et al., 2014; Vibin et al., 2020), domestic animals (Blomström et al., 2009; Bennett et al., 2020; Cibulski et al., 2020), blood-sucking vectors (Brinkmann, Nitsche, and Kohl 2016), and other arthropods (Cox-Foster et al., 2007; Käfer et al., 2019), as well in determining etiological agents in clinical cases and outbreaks (Briese et al., 2009; Hoffmann et al., 2012; Pfaff et al., 2017; Schlottau et al., 2018; Chiu and Miller 2019; Forth et al., 2019; Chen et al., 2020). Several studies also discovered new viruses via data mining of publicly available transcriptome data (Schomacker, Collins, and Schmidt 2004; Basler, García-Sastre, and Palese 2005). However, Canuti and van der Hoek (2014) emphasized the importance of virus characterization after sequence-based discovery to understand their relevance in public and veterinary health. These follow-up investigations include epidemiological analyses using molecular and serological diagnostic tools alongside *in vitro* and *in vivo* characterization of newly discovered viruses.

Here, we introduce an early warning system (EWS) for the detection of novel or unexpected pathogens and applied it in a pilot study. This EWS takes advantage of HTS datasets from previous studies generated from libraries constructed using only untargeted shotgun sequencing procedures, i.e. datasets derived from generic sequencing approaches. These datasets are analyzed using a metagenomics read classifier to detect sequences that point toward the presence of potential pathogens in the samples from which these reanalyzed datasets are derived. After the initial detection of a potential pathogen, diverse analyses can be initiated, from in-depth genomic characterization of the detected potential pathogen through the design of reverse transcription

quantitative PCR (RT-qPCR) assays and subsequent screening of additional samples in the attempt of pathogen isolation. In a pilot study, we successfully applied this EWS to datasets that were generated for the analysis of West Nile viruses (WNV) from the 2018–9 epidemic in Germany (Ziegler et al., 2019, 2020), in which we detected at least two novel or unexpected viruses.

2. Materials and methods
2.1 Overview of the EWS workflow

Figure 1 outlines the process of the EWS. At the heart of the EWS is the detection of unexpected or novel pathogens by metagenomics analysis of datasets that were, for instance, generated during a routine outbreak investigation (depicted in gray). The datasets used for this purpose must have been generated with a generic workflow (Wylezich et al., 2018), i.e. a workflow that does not include any steps for targeting the sequencing like PCR (Quick et al., 2016; Oude Munnink et al., 2020) or target enrichment by capture approaches (Depledge et al., 2011; Wylezich et al., 2021). In more detail, the EWS starts with the taxonomic classification of all reads of the datasets using a metagenomics read classifier; here, the Reliable Information Extraction from Metagenomic Sequence datasets (RIEMS) software (Scheuch, Höper, and Beer 2015) was used. Depending on the initial taxonomic binning results ('known' but unexpected or 'unknown' pathogens identified), different confirmatory data analyses are applied. For known unexpected pathogens, additional analyses start by mapping along available reference sequences. For unknown pathogens, i.e. for which no suitable reference sequences are available, this starts with genome sequence assembly and BLAST (Basic Local Alignment Search Tool; Altschul et al., 1990). Regardless of the initial way, the generated sequences (labeled 'contigs' in Fig. 1) are used for targeted investigations toward the detected potential pathogen. Most importantly, in every case the actual presence of the detected potential pathogen needs to be confirmed. Hence, these targeted follow-up investigations can include, but are not limited to, (i) the selection of published or the design of new specific RT-qPCR assays for the confirmation of the presence of the pathogen and screening in samples from ongoing surveillance and in archived samples; (ii) qPCR-based selection of additional samples for the generation of additional (whole-genome) sequence information of the detected pathogen; (iii) bioinformatics analyses for genomic characterization including phylogenetic analyses; and (iv) pathogen isolation attempts. Isolated pathogens provide further possibilities for follow-up studies and could again be used for completing the genome sequence, functional analyses, or serologic screening and neutralization studies.

2.2 Data and *in silico* procedures
2.2.1 *Data*

For the performed pilot study, datasets generated for outbreak investigations of the 2018–9 WNV epidemic in Germany were utilized (Ziegler et al., 2019, 2020), each comprising between $2E+05$ and $1.2E+07$ reads. This represents the 'routine outbreak investigation' in Fig. 1. Information on the used datasets and the samples from which these datasets originated is summarized in Supplementary Table S1.

2.2.2 *Data analyses*

As outlined above, the available HTS datasets were analyzed using the metagenomics read classifier RIEMS (Scheuch, Höper, and Beer 2015) for the initial taxonomic classification of the
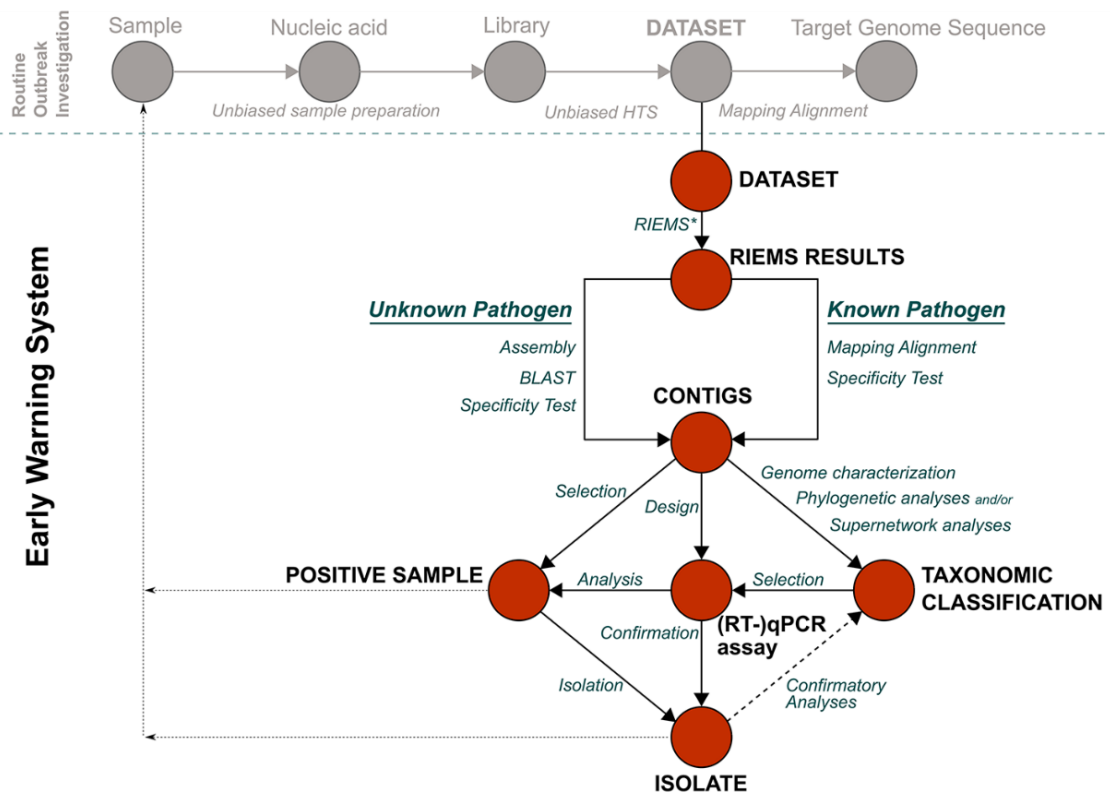
Figure 1. EWS for the detection and characterization of novel and co-infecting pathogens using archived unbiased HTS. Arrowheads indicated the flow of the pipeline. The gray circles and arrows indicate a routine outbreak investigation workflow to acquire the genome sequences of pathogens of interest. The EWS starts at the dataset. Blue text indicates the applied methods, and red dots indicate the results of the methods. For further details, please refer to the text. *RIEMS—the metagenomics read classifier used in this study.

sequence reads. For the confirmation of the initial taxonomic classification, either all reads were mapped along a suitable available sequence from the INSDC databases or reads classified to the superkingdom 'Virus' were assembled together with reads that remained unclassified. The resulting contigs as well as remaining singleton reads were analyzed using BLAST. In addition, to rule out cross-contaminations, all positive results were cross-checked with the virus content of samples processed in parallel. For all mappings and assemblies, the Newbler software (v 3.0, Roche/454 Life Sciences) was used. Sequence similarity searches were performed using BLAST ((Altschul et al., 1990); https://blast.ncbi.nlm.nih.gov/Blast.cgi last accessed: 21 September 2021) and the respective databases. The open reading frames (ORFs) of contigs were predicted and translated using Geneious Prime® 2019.2.3 (Biomatters, Auckland, New Zealand). Online bioinformatics tools were used to characterize assembled sequences. Conserved protein motifs were identified using MOTIF Search ((Ogiwara et al., 1996); https://www.genome.jp/tools/motif/ last accessed: 21 September 2021) based on the Pfam (Finn et al., 2014), NCBI-CDD (Marchler-Bauer et al., 2013), and PROSITE Pattern (Sigrist et al., 2013) databases. Signal peptide sequences, glycosylation sites, and putative transmembrane domains were predicted using SignalP-5.0 Server ((Almagro Armenteros et al., 2019); http://www.cbs.dtu.dk/services/SignalP/ last accessed: 21 September 2021), NetNGlyC 1.0 server ((Gupta and Brunak 2002); http://www.cbs.dtu.dk/services/NetNGlyc/ last accessed:

21 September 2021), and TMHMM Server v. 2.0 ((Krogh et al., 2001); http://www.cbs.dtu.dk/services/TMHMM/ last accessed: 21 September 2021), respectively.

Primers and probes for RT-qPCR assays (Table 1) were designed with Primer3 version 2.3.7 (Untergasser et al., 2012) implemented in Geneious. Amino acid sequences were aligned using MAFFT v.7.450 (Katoh and Standley 2013) and BLOSUM62 (Henikoff and Henikoff 1992) as the similarity matrix, and these alignments were visually inspected in Geneious. Maximum likelihood phylogenetic trees with 100,000 ultrafast bootstraps (Minh, Nguyen, and von Haeseler 2013) were calculated in IQ-TREE 1.6.8 (Nguyen et al., 2014) with the best-fit model defined using ModelFinder (Kalyaanamoorthy et al., 2017). Trees were visualized in FigTree v1.4.4 (http://tree.bio.ed.ac.uk/software/figtree/ last accessed: 21 September 2021). Consensus and supernetwork trees were calculated using SplitsTree v.4 (Huson and Bryant 2006). The results were visualized with R (v4.0; (R Core Team 2020)) in conjunction with Rstudio (v1.2.5033; (RStudio Team 2019)) and packages ggplot2 (Wickham 2016) and pheatmap (Kolde 2019). Prior to visualizations, datasets were normalized to read per million (RPM) and logarithmically scaled using the following formulae:

$$RPM = \frac{read\ count\ per\ family}{total\ number\ of\ sequence\ reads} \times 10^6$$

$$log_{10}RPM = log_{10}(RPM + 0.7)$$

Table 1. Primers and probes for UMAV- and HEDV-specific real-time quantitative polymerase chain reaction screening. Primers and probes targeting HEDV L segment were designed based on HEDV partial genome sequences (old), while new primers and probes were designed using the HEDV complete coding sequences.

Primer name	Primer sequences (5'– 3')	T_m (°C)	Target
118-F_L Hedwig	ATGAAGGCTTGACTGCTGCT	58	HEDV L
294-R_L Hedwig	ACCACTTGTGCTCACTTCGT	58	Segment (old)
161-P_L-6-Fam Hedwig	6-Fam-TGTGCCTCAGACACGATGCTTTTGGC-BHQ-1	69	
136-F_S Hedwig	TGGCTCGGGGAAATCAACTG	60	HEDV S
235-R_S Hedwig	TGTAGGGATGAAAGCGGACTG	61	Segment (new)
177-P_S-Hex Hedwig	HEX-TGCTTTTGGCGTGGTTGTGTGCGA-BHQ-1	73	
124-F_L Hedwig	GATGAAGGCTTGACTGCTGC	59	HEDV L
292-R_L Hedwig	GGATACCACTTGTGCTCACTTC	62	Segment (new)
180-P_L-6-Fam Hedwig	6-FAM-TGCTTTTGGCGTGGTTGTGTGCGA- BHQ-1	67	
Umatilla_Seg1_2196F	TCCATGACTCTTGAGCCTGT	58	UMAV
Umatilla_Seg1_2260P	HEX-TGTCCGGATTCGTTGGCCCTCCA-BHQ-2	68	Segment 1
Umatilla_Seg1_2345R	TGTTTCAATCCTTGCACCGC	58	
Umatilla_Seg5_769F	CGCAACATCGACCAACACAG	60	UMAV
Umatilla_Seg5_814P	6-FAM-TGCTGTCTGCTGGTGAGAGAACACGT-BHQ-1	69	Segment 5
Umatilla_Seg5_862R	TCCATCTCCAAAGTTCGTAGCA	60	

Abbreviations: T_m—melting temperature; F—forward; R—reverse; L—L segment; S—S segment; Seg—segment.

2.3 Laboratory procedures
2.3.1 *Samples, cell cultures and virus isolation*

RNA samples used for the small-scale screening and virus isolation attempts are summarized in Table 2. These samples were from the WNV study by Ziegler et al. (2019, 2020) (Panel 1) and WNV and USUV surveillance from 2018–20 (Panel 2). For virus isolation attempts, virus-positive bird samples were selected based on quantification cycle (C_q) values. Approx. 30 mg of tissue material were homogenized for 2 min at 30 Hz with 5 mm steel beads in 1 ml maintenance medium using a TissueLyser II instrument (QIAGEN, Hilden, Germany). All handling of tissue samples and virus isolation attempts in cell cultures were done under the respective necessary biosafety level.

All cell lines used in this study were obtained from the Collection of Cell Lines in Veterinary Medicine (CCLV) at the FLI Isle of Riems. Baby hamster kidney cells (BHK-21, RIE0164) and *Cercopithecus aethiops* kidney cells (Vero B4, CCLV1146; Vero E6 cells, CCLV0929) were cultured in minimal essential medium, supplemented with 10 per cent fetal calf serum (FCS), at 37°C and 5 per cent CO_2. Mosquito cells from *Aedes albopictus* (C6/36, RIE1299) and midge cells from *Culicoides sonorensis* (KC cells, CCLV1062) were cultured in Eagle's minimal essential medium, supplemented with 10 per cent FCS at 28°C and 2.5 per cent CO_2. Cells were seeded 1 day prior to infection. On the day of infection, the cells were washed once with a maintenance medium (supplemented with penicillin, streptomycin, and gentamicin) before they were infected with 100 µl of sample homogenate. After inoculation, the cells were cultured for 3 days (BHK-21) at 37°C, 5 per cent CO_2, for 4–7 days (Vero E6, Vero B4) at 37°C and 5 per cent CO_2, or for 7 days (C6/36 or KC cells) at 28°C, 2.5 per cent CO_2, before they were frozen at −20°C. Crude cell culture extracts from BHK-21 and C6/36 cells were thawed and passaged three times to the same cell line. Further details of cell-culture conditions are summarized in Supplementary Table S9. Where appropriate, host switching between BHK-21 and KC cells and vice-versa was also performed to mimic the natural transmission of arboviruses. All cell cultures were investigated for virus replication by RT-qPCR and cytopathic effects (CPE) in all setups.

Table 2. Summary of samples utilized for virus screening and virus isolation attempts. Panel 1 includes samples processed using the generic HTS approach in Ziegler et al. (2019, 2020) and panel 2 includes additional archived RNA samples collected in different regions of Germany from 2018 to 2020, which include samples that tested positive and negative for WNV and USUV.

Host	Year	Region	Panel	Number of samples
Bird	2018	Bavaria	1	2
		Berlin	1	2
		Berlin	2	9
		Saxony	1	1
		Saxony-Anhalt	1	2
	2019	Baden-Württemberg	2	3
		Berlin	1	7
		Berlin	2	40
		Brandenburg	1	3
		Mecklenburg-Western Pomerania	2	1
		North Rhine-Westphalia	2	5
		Saxony	1	9
		Saxony-Anhalt	1	8
	2020	Baden-Württemberg	2	3
		Lower Saxony	2	13
		Mecklenburg-Western Pomerania	2	1
		North Rhine-Westphalia	2	6
		Rhineland-Palatinate	2	10
Mammal	2018	Brandenburg	1	1
	2019	Berlin	2	13
		Saxony	1	1

2.3.2 *Nucleic acid extraction and RT-qPCR*

For the preparation of RNA for RT-qPCR, RNA extraction from cell cultures was performed using either Agencourt® RNAdvance™ Tissue kit (Beckman Coulter, Indianapolis, USA) or Qiagen RNeasy® Mini kit (Qiagen, Hilden, Germany) according to manufacturer's instructions. RT-qPCR assays were performed using the SensiFAST™ Probe® No-ROX One-Step Kit (Bioline Meridian Bioscience, USA) in 20 µl reaction volume. The reaction mixes consisted of 2× SensiFAST™ Probe® No-ROX One-Step Mix, 0.2 µl

Table 3. Additional samples for generic high-throughput sequencing. This includes the sample processing workflow, the library number, and the sequencing platform.

Sample type	Sample description	Sample processing	Library number	Sequencing platform
Tissue	ED-I-79/18 snowy owl 1 spleen tissue	Wylezich et al., 2018 RNAdvance	lib03211	Illumina
Cell culture supernatant	Second passage of ED-I-93/19 blackbird liver tissue in mosquito C6/36 cells (7 days post-infection)	Wylezich et al., 2018 LBE Buffer + RNAdvance	lib04217	Ion Torrent

reverse transcriptase, RNase free water, 0.4 μM each of forward and reverse primers, 0.1 μM probe (Table 1), and 2.5 μl total RNA. Amplification was performed in a CFX96™ Touch Real-Time PCR Detection System (Bio-Rad, Feldkirchen, Germany) using the following program: 10 min at 45°C for reverse transcription, 5 min at 95°C for polymerase activation; 45 cycles of 5 s at 95°C, 20 s at 60°C (with fluorescence detection during this step).

2.3.3 *Sequencing*

For additional sequencing, libraries were prepared from samples processed from sample disintegration until library preparation as described in Wylezich et al. (2018). Table 3 summarizes the samples and conditions that were used for sequencing. For library preparation, the appropriate platform-specific barcoded adapters were used as indicated in Table 3. Sequencing was done either using an Illumina MiSeq in 300 bp PE mode with MiSeq v3 600 cycle reagent kits (all Illumina Inc., San Diego, CA, USA) or an Ion Torrent S5 XL instrument with Ion 550 chips and chemistry in 200 bp runs (Thermo Fisher Scientific, Waltham, MA, USA).

3. Results and discussion

In the present proof-of-concept study, the EWS outlined above was used to analyze datasets previously generated for outbreak investigations. The initial rationale was to gain additional information from a few samples that were only weakly positive for WNV, the presumptive cause of death of the host animal. In these additional analyses of the generically generated HTS datasets, we detected sequences pointing toward the presence of new potential pathogens. The detection of reads pointing at viruses, bacteria, protozoa, and other parasites shows that datasets derived from generically prepared libraries are suitable for the detection of all classes of pathogens, as previously shown for the applied laboratory workflow (Wylezich et al., 2018, 2019, 2020; Bennett et al., 2020; Ziegler et al., 2020). Amongst others, sequence reads potentially belonging to bacteria (families *Pasteurellaceae*, *Clostridiaceae*, *Vibrionaceae*, *Shewanellaceae*, *Enterococcaceae*, *Campylobacteraceae*, *Helicobacteraceae*, and *Hafniaceae*), protozoa (families *Plasmodiidae*, *Eimeriidae*, *Babesiidae*, *Sarcocystidae*, and *Trypanosomatidae*), and other parasites (*Taeniidae*, *Ascarididae*, *Strongyloididae*, and *Schistosomatidae*) that probably infected these vertebrate hosts were detected (Supplementary Table S2). The sequence reads of bacterial and parasitic origin can be analyzed in the EWS downstream analysis. However, here we focused on viral sequence reads and attempted in-depth analyses of datasets for virus detection and characterization.

Since potentially new viruses were detected in the initially analyzed datasets, the same EWS strategy was applied to all remaining datasets of the WNV outbreak investigation. Besides several weak hits, we were able to assemble and characterize complete coding sequences of three unexpected viruses:

Alphamesonivirus 1, Umatilla virus (UMAV), and an unclassified member of the family *Peribunyaviridae*. We developed molecular diagnostic assays for two putative viral vertebrate pathogens and screened for these viruses in archived samples providing preliminary information on their hosts and potential tissue tropism. Moreover, we were able to isolate one of the viruses *in vitro*.

3.1 Overview of the initial screening results

Overall, following the EWS strategy, we detected non-WNV viral sequence reads in 15 out of 40 analyzed HTS datasets. Table 4 and Fig. 2 summarize the findings of these initial metagenomics analyses. As shown in Fig. 2A, expectedly (since tissue samples were analyzed and neither host depletion nor any enrichment was performed during sample preparation) the vast majority of the reads were classified as being of eukaryotic origin. Despite the low abundance of viral and unclassified sequence reads in most datasets (Fig. 2A), paired with a dominance of WNV among viral reads (Fig. 2B), a number of reads potentially belonging to other viruses than WNV were identified. While in datasets from cell cultures inoculated with *Culex pipiens* pools, only reads representing viruses that are commonly reported in invertebrate hosts (families *Chrysoviridae*, *Mesoniviridae*, *Nodaviridae*, *Tombusviridae*, *Tymoviridae*, and order *Tymovirales*) were detected, we found reads putatively representing the viral families *Peribunyaviridae*, *Reoviridae*, *Astroviridae*, *Totiviridae*, *Dicistroviridae*, and *Flaviviridae* (other than WNV) in datasets derived from bird samples. In addition, in both bird and mosquito datasets reads pointing toward the presence of viruses belonging to the family *Iflaviridae* or other members of *Riboviria* were present. Noteworthily, the results from samples inoculated in cell cultures, such as those obtained from the *C. pipiens* pools (datasets lib03481, lib03482, and lib03504), should be interpreted carefully due to the possibility of false-positive and false-negative results. These might result from, e.g. enrichment of adventitious or commensal viruses or inability to cultivate non-culturable viruses in a sample. Employing a broader diversity of cell lines and minimizing the storage period of samples prior to isolation might help increase the success rate of virus isolation.

Most of the previously mentioned viral taxonomic groups were only represented by few sequence reads with low sequence identities when compared to sequences from the databases (Table 4, Supplementary Table S3). Especially unclassified members of *Riboviria* were frequently found in bird datasets (Table 4, Supplementary Table S3). These viruses were previously detected in virome analyses of various invertebrate sample pools collected in China (Shi et al., 2016), and the birds probably obtained these viral sequences from their insect or arthropod diet without being infected by these viruses. In dataset lib03433, a contig was classified to the family *Totiviridae*, having the highest sequence identities with sequences of different species of viruses from apicomplexan hosts (Table 4 and Supplementary Table S3). However, corresponding sequences related to protozoan parasites

Table 4. The unexpected viral sequence reads detected in several generic HTS datasets sequenced from the 2018 to 2019 WNV epidemic in Germany and their closest relatives. Detailed information regarding the number of sequence reads and length of assembled contigs per closest blastx hits are described in Supplementary Table S3.

Dataset	Host	Taxonomic classification	Closest relative	Number of reads
lib02916	Tawny Owl	*Flaviviridae*	Rodent pestivirus	1
lib03038;	Snowy Owl #1	*Flaviviridae*	USUV	50
lib03039		*Peribunyaviridae*	ASUMV; low aa sequence identities with Thimiri virus; Guama virus	728
lib03041; lib03042	Snowy Owl #2	*Peribunyaviridae*	ASUMV; low aa sequence identities with Belmont virus; Mapputta virus	32
lib03381	Blue Tit #1	*Reoviridae*	UMAV (7 segments, 1 segment with low aa sequence identities); KHV (2 segments); stretch lagoon orbivirus (1 segment)	1654
		Totiviridae	Trichoderma koningiopsis totivirus 1	6
		Riboviria	Hubei toti-like virus 6; Wuhan insect virus 27	17
lib03417	Goshawk #3	*Riboviria*	Hubei toti-like virus 6	560
lib03419	Goshawk #5	*Riboviria*	Hubei toti-like virus 6	1
lib03422	Great Tit #1	*Flaviviridae*	USUV	2
		Reoviridae	Stretch lagoon orbivirus	1
lib03424	Goshawk #7	*Riboviria*	Hubei toti-like virus 6; Lake Sinai virus 5	2
lib03428	House Sparrow	*Dicistroviridae*	Barns Ness breadcrumb sponge dicistro-like virus 2	1
		Iflaviridae	King virus	1
		Picornavirales	Antarctic picorna-like virus 1	3
		Reoviridae	Avian orthoreovirus	2
		Riboviria	Jingmen tombus-like virus 1, Nadgee virus, Pink bollworm virus 4, Sanxia picorna-like virus 11, Sanxia picorna-like virus 9	8
lib03431	Great Grey Owl #5	*Picornaviridae*	Norway rat kobuvirus 2	3
		Astroviridae	Murine astrovirus	2
lib03433	Great Tit #2	*Flaviviridae*	Duck hepacivirus; Theiler's disease-associated virus; Jogalong virus	3
		Picornaviridae	Washington bat picornavirus	17
		Reoviridae	UMAV (7 segments, 1 segment with low aa identities); KHV (2 segments); stretch lagoon orbivirus (1 segment)	1062
		Totiviridae	*Eimeria stiedae* RNA virus 1; *Eimeria tenella* RNA virus 1; *E. brunetti* RNA virus 1; *Linepithema humile* toti-like virus 1; *Trichomonas vaginalis* virus 2	86
		Riboviria	*Hubei partiti-like* virus 48, Baker virus, Volivirus, *Hubei orthoptera* virus 4, Cordoba virus, *Hubei picorna-like* virus 71	132
lib03450	Goshawk #8	*Riboviria*	Wilkie narna-like virus 1	1
lib03481	Mosquito Pool #1	*Chrysoviridae*	Eskilstorp virus; Shuangao chryso-like virus 1	4
		Riboviria	Hubei chryso-like virus 1	3
lib03482	Mosquito Pool #2	*Mesoniviridae*	Alphamesonivirus 1	242,607
		Tymoviridae	Bombyx mori latent virus	1
		Tymovirales	Guadeloupe Culex tymo-like virus	1
lib03504	Mosquito Pool #3	*Nodaviridae*	Culex mosquito virus 1	29
		Picornavirales	Culex picorna-like virus 1	13
		Tombusviridae	Culex-associated Tombus-like virus	12
		Iflaviridae	Culex-Iflavi-like virus 4	5
		Riboviria	Hubei chryso-like virus 1	1

were not found in dataset lib03433, although, for instance, the protozoan *Eimeria brunetti* is known to cause coccidiosis in birds (Kawahara et al., 2014). In this group of viruses, represented by only a few reads, we also discovered viruses that potentially infect vertebrate hosts (Table 4 and Supplementary Table S3). This group comprises six viruses, namely an avian orthoreovirus (lib03428), an unclassified kobuvirus and an astrovirus (lib03431), an unclassified hepacivirus and a pegivirus (lib03433), and an unclassified pestivirus (lib02916). Although contigs could be assembled in

some instances, the information was insufficient for subsequent EWS steps.

Amongst the viruses represented by a low number of reads, we also detected Usutu virus (USUV) in datasets lib03038/lib03039 and lib03422 (Table 4). These findings confirmed the previously reported WNV/USUV co-infections in the animals from which these datasets were derived (Santos et al., 2021). However, we could not detect USUV reads in dataset lib03041/lib03042, which was also derived from a bird that tested positive for both WNV
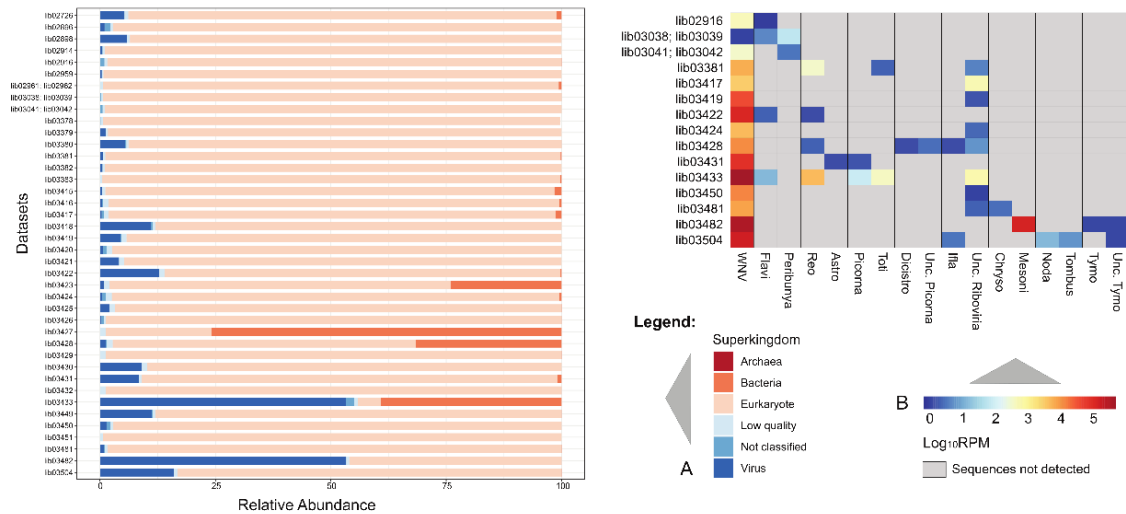
Figure 2. Distributions of sequence reads within generic HTS datasets derived from the 2018 to 2019 WNV epidemic in Germany according to taxonomic classification. (A) Relative abundance of each superkingdom per dataset. (B) Relative abundance of each virus taxon in selected generic HTS datasets. Frequencies of each virus taxon were normalized using the formulae in Section 2.2.2. Light gray boxes indicate that a specific virus sequence was not detected in the dataset. Abbreviations: WNV—West Nile virus; Flavi—*Flaviviridae* (except WNV); Peribunya—*Peribunyaviridae*; Reo—*Reoviridae*; Astro—*Astroviridae*; Picorna—*Picornaviridae*; Toti—*Totiviridae*; Dicistro—*Dicistroviridae*; Unc. Picorna—Unclassified *Picornavirales*; Ifla—Iflaviridae; Unc. Riboviria—Unclassified *Riboviria*; Chryso—*Chrysoviridae*; Mesoni—*Mesoniviridae*; Noda—*Nodaviridae*; Tombus—*Tombusviridae*; Tymo—*Tymoviridae*; Unc. Tymo—Unclassified *Tymovirales*.

and USUV. In our previous study, viral sequence enrichment and virus-specific multiplex PCR had to be employed to acquire the full genomes of both flaviviruses (Santos et al., 2021). Owing to the previously performed complete analysis, here we did not pursue USUV for EWS downstream analysis. Nevertheless, the low abundance of USUV in these samples caused two true-positive and one false-negative results regarding the presence of USUV. This highlights one potential drawback of this EWS, namely the eventually limited sensitivity. This can on the one hand be caused by the size of the available dataset, as shown in very much detail by Ebinger, Fischer, and Höper (2021). On the other hand, failure to detect can likewise be due to sequencing of less suitable sample matrices for the respective virus, depending on the virus's tissue tropism.

It is also noteworthy that three different viruses with high abundances were found in different samples. These were subsequently taken to the next level of analysis according to the EWS concept (Fig. 1). First, reads representing the family *Mesoniviridae* with highest identity with Alphamesonivirus 1 sequences were detected in one of the datasets (lib03482) generated from mosquito pools. Second, an unexpected orbivirus that had not been detected in Germany before was found in datasets lib03381 (>1600 reads) and lib03433 (>1000 reads). Third, more than 700 reads pointing toward the presence of an unexpected peribunyavirid were detected in dataset lib03038/lib03039. A few reads representing the same peribunyavirid were also detected in dataset lib03041/lib03042. The subsequent analyses and the obtained results are summarized in the following sections.

3.2 EWS follow-up analyses—genomic characterization
3.2.1 *Mosquito virus Alphamesonivirus 1*
The 20,125-nucleotide long contig from dataset lib03482 (mosquito pool #2 inoculated in C6/36 cells) had 99.5 per cent

nucleotide identity with an Alphamesonivirus 1 found in *C. pipiens* in Italy (Accession MF281710). Its RNA-dependent RNA polymerase (RdRp) amino acid sequence clustered with other strains of the species Alphamesonivirus 1 (Supplementary Fig. S1). Alphamesonivirus 1 species members are reported in a broad range of mosquito species collected in different parts of the world (Vasilakis et al., 2014) and as a co-infecting agent with Zika virus in the C6/36 cell culture (Sardi et al., 2020). Since this virus has not been associated with disease in vertebrates so far, we stopped the EWS investigation at this point.

3.2.2 *Unexpected orbivirus in two wild birds*
Nearly complete coding sequences of decapartite reovirus genomes were assembled from datasets lib03381 (blue tit) and lib03433 (great tit). In phylogenetic analyses (Fig. 3, Supplementary Fig. S2; Table S4), these genome sequences from Germany clustered with members of the species UMAV, with UMAV strains from the USA forming a separate subcluster. Except for the outer capsid protein (OCP) 1, high amino acid sequence identities among UMAV species were observed for all proteins (Supplementary Table S5). Sequence variations in OCP1 were expected since it is the major virus antigen of the genus *Orbivirus*, inducing specific neutralizing antibodies that distinguish distinct serotypes of each species (Mertens et al., 1989). Interestingly, further variations between the UMAV sequences were detected in their 3′ untranslated regions (3′ UTR). All UMAV except two strains from the USA have deletions in the 3′ UTR of the segments encoding the nonstructural protein 1 and OCP1 (Supplementary Fig. S3). Similar deletions were described before in Koyama Hill virus (KHV) segments in comparison with UMAV strain USA 1969 (Ejiri et al., 2014). These deletions within the 3′ UTR may cause lower levels of viral mRNA expression, as was previously shown for the Bluetongue virus, another member of the genus *Orbivirus* (Boyce, Celma, and Roy 2012). Hence, deletions at the 3′ UTR of NS1 and
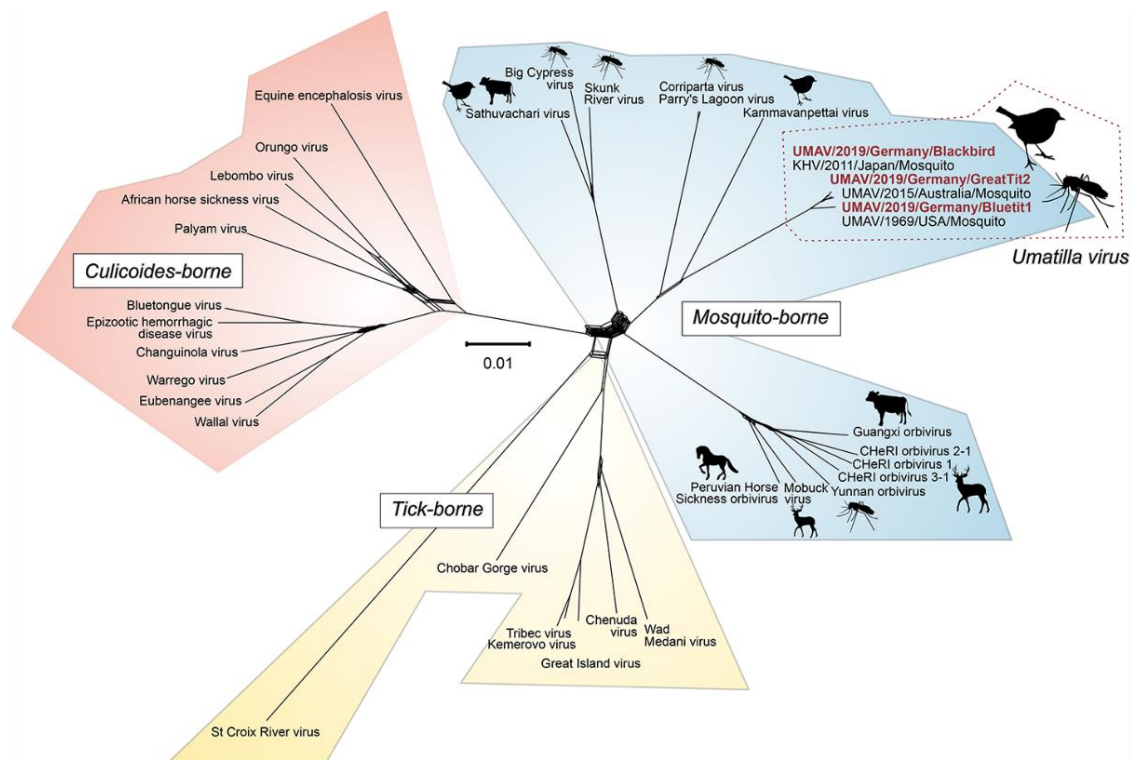
Figure 3. The genus *Orbivirus* supernetwork. This supernetwork analysis is based on ten maximum likelihood trees from representative *Orbivirus* species with complete segments (*n* = 10 segments). Red text indicates UMAV variants detected in this study. Accession numbers of available amino acid sequences from representative members of the genus *Orbivirus* are indicated in Supplementary Table S4. Images were acquired from Pixabay under Pixabay license (https://pixabay.com/service/license/ last accessed: 21 September 2021).

OCP1 coding segments in these viruses may affect their growth kinetics and pathogenicity.

Phylogenetic analyses (Fig. 3 and Supplementary Fig. S2) and comparison of the amino acid sequences derived from the RdRp and T2 encoding sequences (Supplementary Table S5) imply that according to the demarcation criteria specified for orbiviruses (Attoui et al., 2012), the detected reovirus belongs to the genus *Orbivirus*, species UMAV. In detail, the deduced RdRp sequences of UMAV strains from Germany have ≥37.8 per cent identity with RdRp of other orbiviruses (genus demarcation ≥30 per cent identity), while their deduced T2 sequences exhibit 94 per cent identity with T2 of other members of the UMAV species (species demarcation ≥91 per cent identity).

The species UMAV consists of the four recognized serotypes Umatilla and Llano Seco virus from the USA, Minnal virus from India, and Netivot virus from Israel (Mertens et al., 2005; Belaganahalli et al., 2011). Knowledge regarding the biological characteristics, host range, epidemiology, pathogenicity, and geographical distribution of UMAV species is limited. The aforementioned were mainly isolated from different *Culex* species (Dandawate and Shope 1975; Gubler and Rosen 1976; Karabatsos 1985; Tesh et al., 1986; Tangudu et al., 2019); other members of the species UMAV were detected in and isolated from *Culex* and *Aedes* mosquitoes from Australia (UMAV and stretch lagoon orbivirus, SLOV) and ornithophilic *Culex* mosquitoes in Japan (KHV). The only report of UMAV isolation from vertebrates was in house sparrows (*Passer domesticus*) collected in the USA in 1967 (Karabatsos 1985; Belaganahalli et al., 2011). Serological data suggest that

horses, donkeys, and goats are potential vertebrate hosts of SLOV, while neutralizing antibodies against Minnal virus were detected in sera from three human cases in India (Belaganahalli et al., 2011; Centers for Disease Control and Prevention; Cowled et al., 2009; Ejiri et al., 2014; Tangudu et al., 2019).

3.2.3 *Novel peribunyavirid in captive snowy owls*

To assemble the complete genome for the novel peribunyavirid, tentatively named HEDV as it was detected in datasets derived from captive snowy owls, additional sequence data had to be generated (lib03211). The new dataset was assembled with the preexisting datasets lib03038/lib03039 from the WNV study yielding three segment sequences of lengths 6,965 bases (L segment), 4,606 bases (M segment), and 1,079 bases (S segment).

As for the detected reovirus, we started with phylogenetic analysis for classification of the virus. In this analysis, representatives of the four established genera in the family *Peribunyaviridae* were considered, namely *Orthobunyavirus*, *Herbevirus*, *Pacuvirus*, and *Shangavirus* (Hughes et al., 2020). In addition, other related unclassified members of the family *Peribunyaviridae* that are listed by the International Committee on Taxonomy of Viruses (Hughes et al., 2020), encompassing Akhtuba virus (Quan et al., 2013a), Fulton virus (Williams et al., 2019), Khurdun virus (Al'kovskhovsk et al., 2013), Lakamha virus (Kopp et al., 2019), and largemouth bass bunyavirus (Waltzek et al., 2019) were included (Supplementary Table S6; results of pairwise sequence comparisons of representative viruses see Supplementary Table S7). Some of these viruses
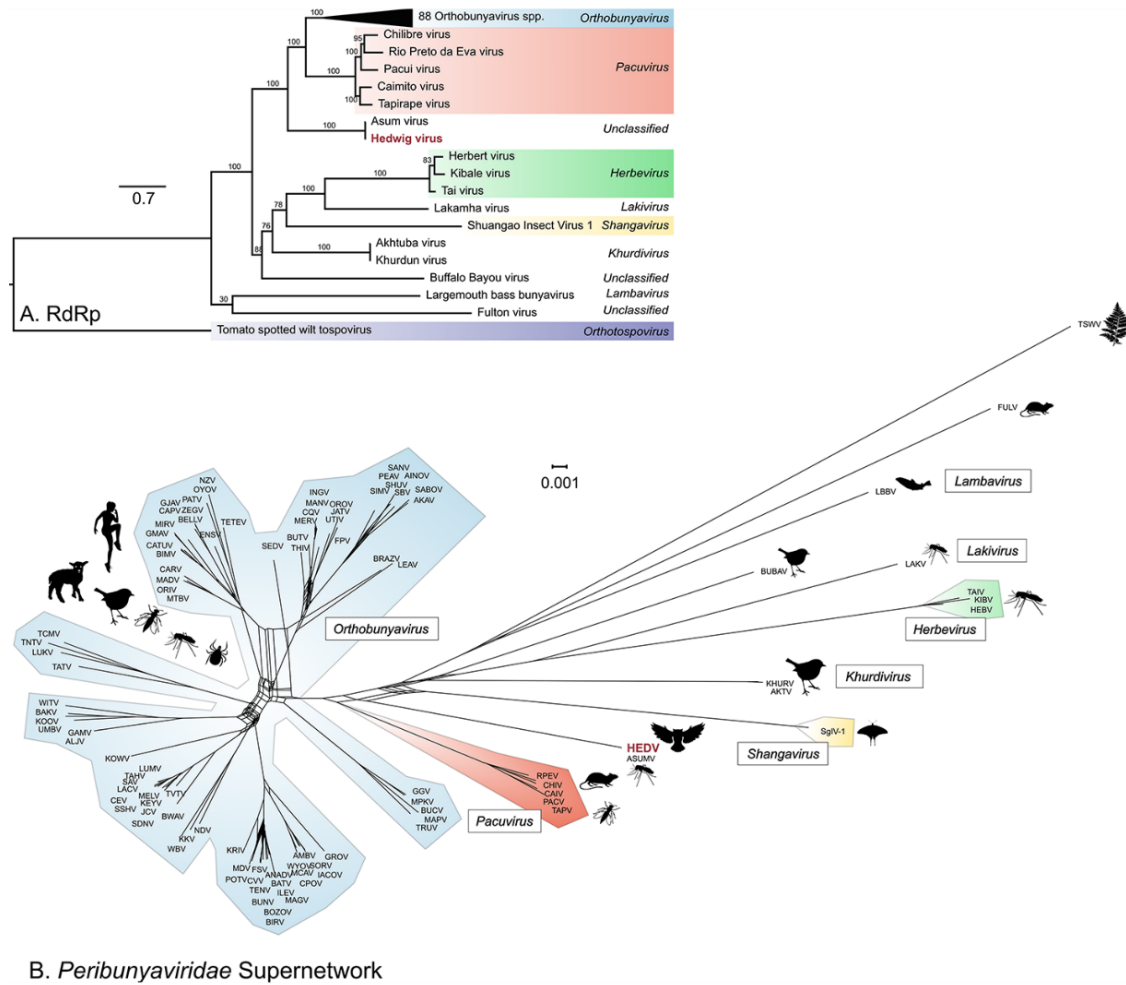
Figure 4. Phylogenetic analyses and supernetwork of representative peribunyavirid, ASUMV and HEDV (printed red). Blue, orange, yellow, green, and uncolored represent the genera *Orthobunyavirus*, *Pacuvirus*, *Shangavirus*, *Herbevirus*, and the recently proposed genera *Lakivirus*, *Lambavirus*, and *Khurdivirus* or the remaining unclassified members of the family *Peribunyaviridae*. (A) Maximum likelihood tree of the RdRp amino acid sequences. Ultrafast bootstrap analyses with 100,000 replicates supported the tree topology. Representative *Orthobunyavirus* species (*n* = 88) were collapsed into a triangle. Tomato spotted wilt tospovirus was used as an outgroup (violet). (B) Supernetwork of the 3 ML trees calculated for the RdRp, the glycoprotein precursor, and the nucleocapsid protein (for the latter two see Supplementary Fig. 4). Accession numbers of available amino acid sequences from representative members of the family *Peribunyaviridae* and the outlier strain are indicated in Supplementary Table S6. Images were acquired from Pixabay under Pixabay license (https://pixabay.com/service/license/ last accessed: 21 September 2021).

were assigned to the recently proposed new genera *Lakivirus, Lambavirus*, and *Khurdivirus* (Fig. 4 and Supplementary Table S6) (Jens Kuhn, personal communication). Moreover, Asum virus (ASUMV), which was recently reported with only its L segment sequence and not yet designated a member species of the family *Peribunyaviridae* (Pettersson et al., 2019; Hughes et al., 2020), was likewise taken into account, because with 97.2 per cent identity the ASUMV L segment is the closest relative of the HEDV L segment. To include the ASUMV complete genome in phylogenetic analyses, we retrieved the raw sequence dataset harboring its L segment (BioProject PRJNA516782) and mapped ASUMV sequences using HEDV sequences as references. This resulted in three contigs with lengths of 7,161 nucleotides (mean coverage 150), 4,606 nucleotides (mean coverage 298), and 1,235 nucleotides (mean coverage 345), which were included in the phylogenetic reconstruction. As Fig. 4A shows, phylogenetic analysis

of the RdRp sequences suggests that HEDV and ASUMV belong to a novel genus of the family since they do not cluster with other established or unclassified peribunyavirid genera (Hughes et al., 2020). In the supernetwork (Fig. 4B), HEDV together with ASUMV branches as a deep rooting lineage within the family *Peribunyaviridae*.

Further in-depth analyses of the tripartite HEDV genome showed an organization very similar to the genera *Orthobunyavirus* and *Pacuvirus*. The HEDV RdRp has the typical motifs within the N-terminal endonuclease domain and conserved sequences for pre-motif A and motifs A–E (Fig. 5A) (Amroun et al., 2017; Kopp et al., 2019). The predicted HEDV nucleocapsid ORF (Fig. 5C) shows two putative in-frame start codons, $_{80}$CUG and $_{101}$AUG. The non-AUG initiation is a natural but rather inefficient start codon. The large proportion of ribosomes will scan past the non-AUG site and initiate at the downstream AUG instead. It was assumed that this
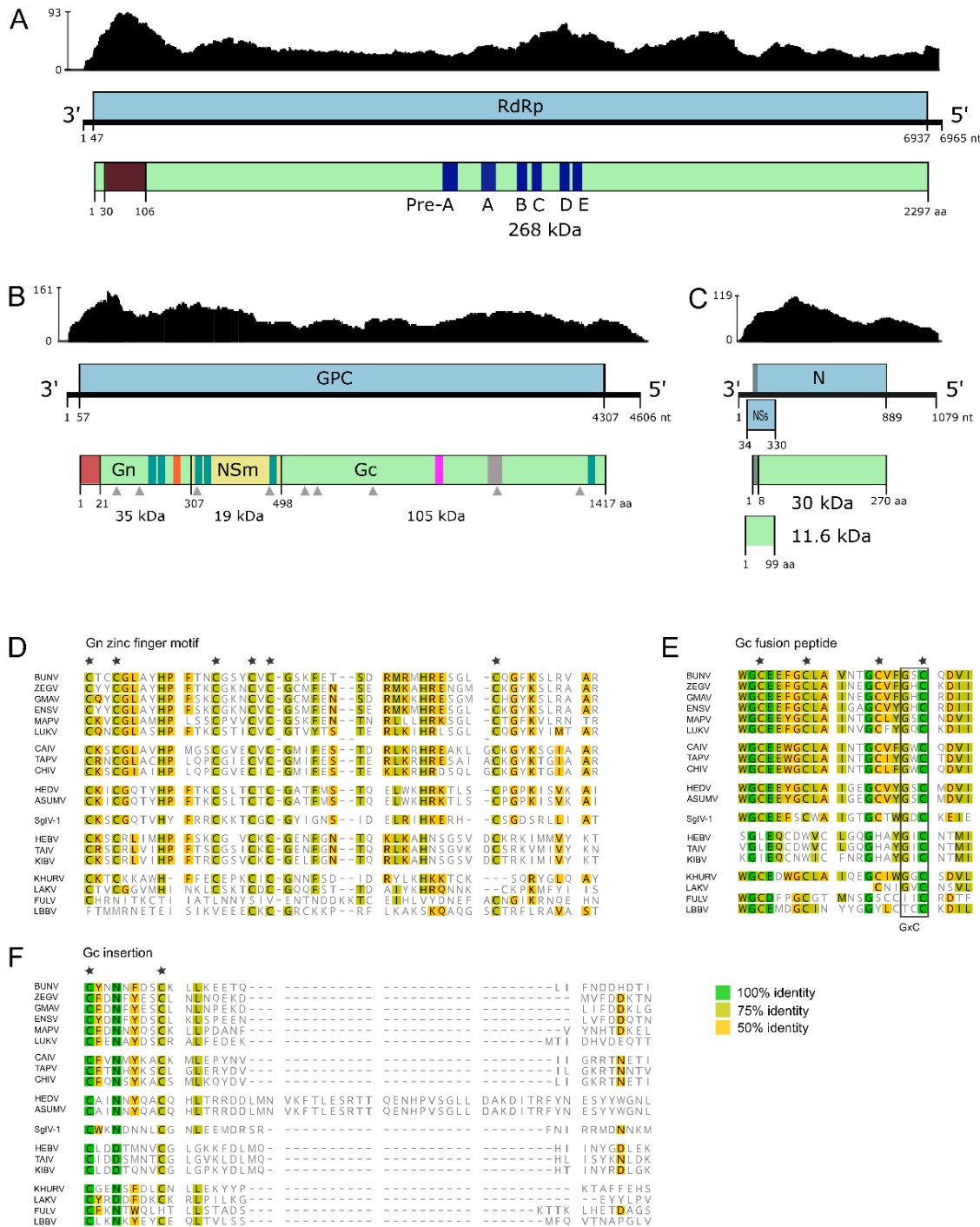
Figure 5. HEDV genome characterization. Schematic organization of HEDV genome segments coding for (A) RdRp, (B) glycoprotein precursor (GPC), and (C) nucleocapsid protein (N). ORFs are shown as light blue boxes, and light green boxes indicate predicted proteins. Genome positions and predicted protein masses are included. The graphs above the genomes show the sequence depths. (A) The brown box indicates the endonuclease domain and dark blue boxes represent pre-motif A and motifs A–E. (B) The red box indicates a putative signal peptide; gray triangles represent predicted N-linked glycosylation sites; teal boxes indicate putative transmembrane domains; the gray box indicates a predicted insertion in the GPC; Gn zinc finger and Gc fusion peptide motif are illustrated with orange and pink boxes, respectively. Alignments of amino acid sequences of conserved regions of (D) the Gn zinc finger motif, (E) the Gc fusion peptide, and (F) the insertion within in GPC. Green, yellow-green, and yellow indicate 100 per cent, 75 per cent, or 50 per cent identity, respectively. Conserved cysteines are indicated by stars above the aligned sequences. Accession numbers of available amino acid sequences from representative members of the family *Peribunyaviridae* are indicated in Supplementary Table S6.

leaky scanning mechanism leads to the generation of multiple protein variants with N-terminal extensions or from alternative reading frames (Firth and Brierley 2012). Analysis of the HEDV glycoprotein precursor implies that it is cleaved into Gn, NSm, and Gc proteins (Fig. 5B). However, the HEDV Gn C terminus (VKAI$_{306}$) does not comprise the highly conserved arginine found among the members of the genera *Orthobunyavirus* and *Pacuvirus*. It also differs from the termini of *Herbevirus*, *Shangavirus*, and unclassified viruses of the *Peribunyaviridae* (Fig. 5D). The HEDV glycoprotein precursor comprises a Gn zinc finger motif with conserved cysteine residues found in most peribunyaviridae (Fig. 5D) and a Gc fusion peptide with four conserved cysteine residues found only in *Orthobunyavirus*, *Pacuvirus*, *Shangavirus*, and Khurdun virus (Fig. 5E). The *Peribunyaviridae* glycoprotein precursor sequence alignment revealed a 26–35 amino acid insertion within the C terminal half of the HEDV Gc protein core region (Fig. 5F), i.e. in the region which mediates cell fusion (Shi et al., 2009).

Altogether, our results show that HEDV is a novel peribunyavirid and a representative species of a presumed novel genus within the family *Peribunyaviridae*. The second member of this putative new genus is its closest relative ASUMV, whose genome was previously only partially assembled from data generated from *C. pipiens* mosquito pools collected in Kristianstad, Sweden, in 2006–7 (Pettersson et al., 2019). Here, we were able to complete the genome of ASUMV, and pairwise alignments of the HEDV and ASUMV genomes demonstrated high nucleotide sequence identities between their L (97.21 per cent), M (96.23 per cent), and S (97.77 per cent) segments. While ASUMV was found in *C. pipiens*, we detected HEDV in two captive snowy owls. Hence, this study adds substantial knowledge regarding the vertebrate host of this potential arbovirus.

3.3 RT-qPCR screening—additional positive animals

Using the assembled UMAV and HEDV sequences, we designed virus specific RT-qPCR assays. With these assays, we screened for UMAV and HEDV in two sample panels collected from 2018 to 2020 composed of RNA extracted from 125 birds and 15 mammals (Table 2 and Supplementary Table S8) with known USUV and WNV status (included in Fig. 6) and some also pretested for other viruses. Unfortunately, RNA from some samples was limited; therefore, we could not test all samples for both HEDV and UMAV. Figure 6 summarizes the results of this small-scale screening. We detected UMAV RNA in fourteen wild birds (n = 112), hence, together with the UMAV-positive sample (dataset lib03433),
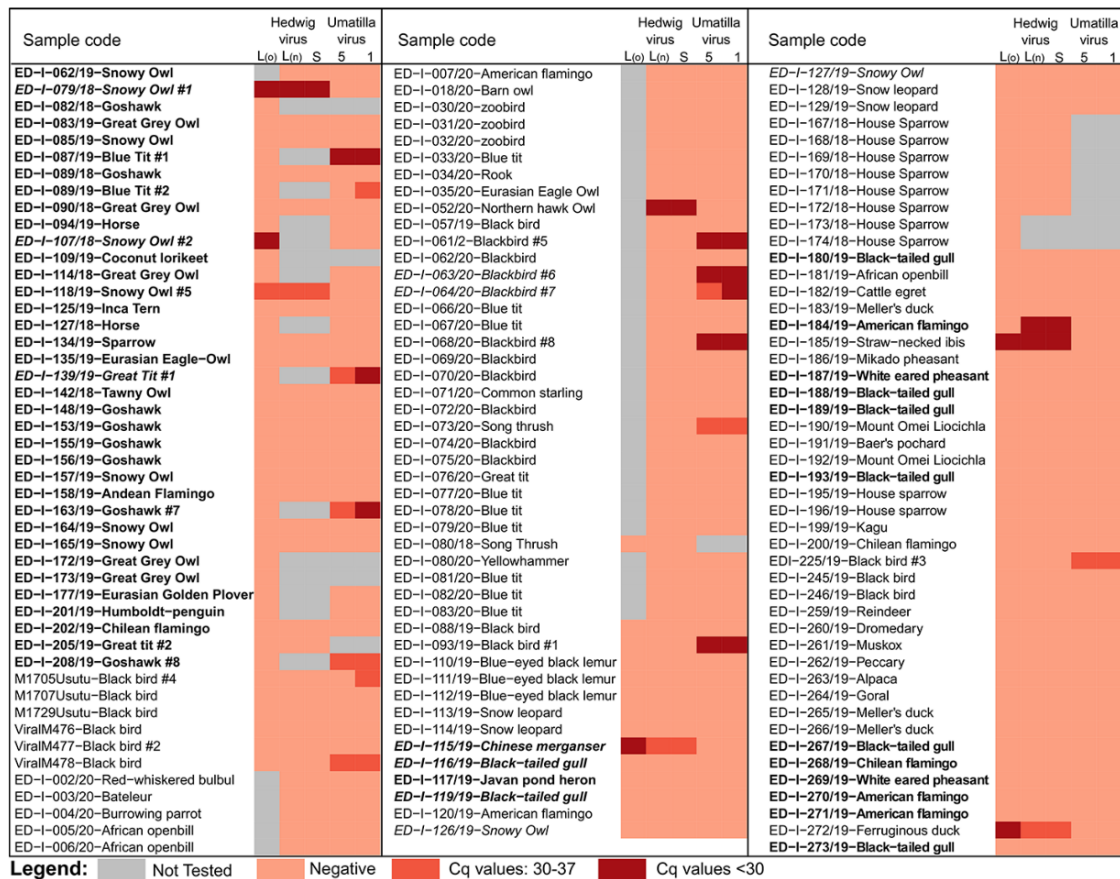
Figure 6. Samples tested using HEDV-specific and UMAV-specific real-time quantitative polymerase chain reaction assays. We designed two primer and probe sets (labeled o = old and n = new) specific to the HEDV L segment. Gray indicates not tested samples. The lightest shade of red indicates negative results, while darker shades of red indicate HEDV- or UMAV-positive samples. Bold indicates WNV-positive samples, italics indicate USUV-positive samples.

we found UMAV in fifteen birds but not in any mammals ($n = 13$). Eight out of 125 tested bird samples were found positive for HEDV, again, none of the tested mammals ($n = 15$) were positive. Out of the twenty-three UMAV- or HEDV-positive birds, twelve were co-infected with WNV and/or USUV. We found one UMAV-positive and three HEDV-positive birds with confirmed WNV and USUV co-infections (Fig. 6). Where available, we tested different organ samples of the birds (brain, liver, spleen, kidneys, heart, and lungs; Supplementary Table S8). Except for the relatively lower HEDV C_q value in the snowy owl #1 spleen, no marked tissue tropism was observed for both viruses.

The available necropsy reports of the dead birds were assessed to identify potential symptoms caused by HEDV or UMAV infection. Seven out of the fifteen UMAV-positive wild birds were negative for WNV, USUV, and Hepatitis E virus in RT-qPCR. Necropsy reports of these seven birds described splenomegaly, suggesting an acute infection. Three out of the eight HEDV-positive birds were negative for both WNV and USUV; however, only for two of these a necropsy report was available. According to these reports, the straw-necked ibis had necrotizing dermatitis and weakly pronounced interstitial pneumonia while the ferruginous duck had a swollen spleen and liver, but the suspected cause of death was septicemia due to sand penetration into the subcutaneous tissue of its head.

3.4 Virus isolation—UMAV isolated in cell culture

From all available samples, we selected those to attempt virus isolation based on the sequencing results and based on RT-qPCR results for unsequenced samples. While we failed to cultivate HEDV from the selected available organ samples in mammalian and insect cell lines, we successfully isolated UMAV from blackbird #1 liver in C6/36 mosquito cell lines (Supplementary Table S9). Failure to isolate HEDV *in vitro* could be caused by the cell lines used, which may not be suitable for HEDV cultivation, or by the long-term storage of organ samples that might have had a negative effect on the viability of HEDV (Leland and Ginocchio 2007; Ørpetveit et al., 2010).

This UMAV strain replicated in C6/36 cells with CPE but did not replicate in BHK-21 cells. Similar observations were reported for KHV, UMAV-IA08, and SLOV-IA08, which replicated and produced CPE in C6/36 cells but not in hamster cell lines (Ejiri et al., 2014; Tangudu et al., 2019). However, other studies reported that two UMAV isolates replicated and produced strong CPE in hamster cell lines (BHK-21 cells and BSR cells, respectively) (Cowled et al., 2009; Belaganahalli et al., 2011). For confirmation of the successful isolation, we generated an Ion Torrent compatible library (lib04217; see Table 3) with RNA isolated from UMAV infected C6/36 cells. We were able to assemble the complete UMAV genome from the generated dataset, which was included in the phylogenetic analyses. Except for the OCP1 encoding segment, this UMAV genome is identical with UMAV genomes from datasets great tit #2 and blue tit #1 (Supplementary Table S5).

4. Conclusion

The introduced EWS applies well-established protocols for pathogen discovery and characterization to enable a quasi-hypothesis-free screening for co-infecting and unexpected pathogens in outbreak and surveillance samples without *a priori* knowledge of their presence or even existence. The only hypothesis we employ is that we assume that something might circulate unnoticed and that it can be detected based on its nucleic acids. This only

excludes prions. The sensitivity of the EWS for the detection of nucleic acid containing pathogens depends on the pathogen content and dataset size, as shown by the USUV example.

The EWS builds on available datasets generated in the framework of routine outbreak investigations. These datasets must have been generated applying generic and unbiased procedures. Since no extra sample processing is necessary, the required time and resources for protocol development and optimization, but especially for sample collection, preparation, and sequencing can be reduced. This facilitates timely processing, enables integration into routine workflows, and hence helps identify (known) pathogens prior to their emergence.

The three presented examples from the pilot study are a proof of concept for the outlined EWS to detect unexpected or unknown pathogens, showing all possible stages included in the EWS concept. HEDV, detected in snowy owls and other captive birds, together with ASUMV forms a putative novel genus of the family *Peribunyaviridae*. Moreover, we here report the first detection of UMAV within central Europe and its re-detection in birds after more than 50 years. Based on information gained from in-depth genomic characterization, we were able to design RT-qPCR assays and finally isolate UMAV from a blackbird sample. This enables additional follow-up investigations for further virus characterization. The presented screening implies that the detected viruses most likely have circulated unnoticed in Germany. Hence, the EWS can provide necessary information and facilitate the development of diagnostic tools to respond rapidly to emerging infectious diseases before they turn into massive epidemics.

Data availability

The nucleotide sequences from this study are available from the INSDC databases under study accession PRJEB45282.

Supplementary data

Supplementary data is available at *Virus Evolution* online.

References

Al'kovskhovsk, S. V. et al. (2013) 'The Khurdun Virus (KHURV): A New Representative of the Orthobunyavirus (Bunyaviridae)', *Voprosy Virusologii*, 58: 10–3.

Almagro Armenteros, J. J. et al. (2019) 'SignalP 5.0 Improves Signal Peptide Predictions Using Deep Neural Networks', *Nature Biotechnology*, 37: 420–3.

Altschul, S. F. et al. (1990) 'Basic Local Alignment Search Tool', *Journal of Molecular Biology*, 215: 403–10.

Amroun, A. et al. (2017) 'Bunyaviridae RdRps: Structure, Motifs, and RNA Synthesis Machinery', *Critical Reviews in Microbiology*, 43: 753–78.

Attoui, H. et al. (2012) 'Part II: The Viruses – the Double Stranded RNA Viruses - Family Reoviridae'. In: A. M. Q. King (ed.) *Virus Taxonomy: Classification and Nomenclature of Viruses Ninth Report of the International Committee on Taxonomy of Viruses*, pp. 541–637. San Diego: Elsevier Academic Press.

Basler, C. F., García-Sastre, A., and Palese, P. (2005) 'A Novel Paramyxovirus?' *Emerging Infectious Diseases*, 11: 108–12.

Belaganahalli, M. N. et al. (2011) 'Umatilla Virus Genome Sequencing and Phylogenetic Analysis: Identification of Stretch Lagoon Orbivirus as a New Member of the Umatilla Virus Species', *PLoS One*, 6: e23605.

Bennett, A. J. et al. (2020) 'Relatives of Rubella Virus in Diverse Mammals', *Nature*, 586: 424–8.

Blomström, A.-L. et al. (2009) 'Detection of a Novel Porcine Boca-like Virus in the Background of Porcine Circovirus Type 2 Induced Postweaning Multisystemic Wasting Syndrome', *Virus Research*, 146: 125–9.

Bloom, D. E., Black, S., and Rappuoli, R. (2017) 'Emerging Infectious Diseases: A Proactive Approach', *Proceedings of the National Academy of Sciences of the United States of America*, 114: 4055–9.

Boyce, M., Celma, C. P., and Roy, P. (2012) 'Bluetongue Virus Nonstructural Protein 1 is a Positive Regulator of Viral Protein Synthesis', *Virology Journal*, 9: 178.

Briese, T. et al. (2009) 'Genetic Detection and Characterization of Lujo Virus, a New Hemorrhagic Fever-associated Arenavirus from Southern Africa', *PLoS Pathogens*, 5: e1000455.

Brinkmann, A., Nitsche, A., and Kohl, C. (2016) 'Viral Metagenomics on Blood-Feeding Arthropods as a Tool for Human Disease Surveillance', *International Journal of Molecular Sciences*, 17: 1743.

Brookes, V. J. et al. (2015) 'Preparedness for Emerging Infectious Diseases: Pathways from Anticipation to Action', *Epidemiology and Infection*, 143: 2043–58.

Canuti, M., and van der Hoek, L. (2014) 'Virus Discovery: Are We Scientists or Genome Collectors?' *Trends in Microbiology*, 22: 229–31.

Carlson, C. J. (2020) 'From PREDICT to Prevention, One Pandemic Later', *The Lancet Microbe*, 1: e6–e7.

Carroll, D. et al. (2018) 'The Global Virome Project', *Science (New York, N.Y.)*, 359: 872–4.

Centers for Disease Control and Prevention *Arbovirus Catalog* <https://wwwn.cdc.gov/Arbocat/VirusBrowser.aspx> accessed 16 May 2021.

Chen, L. et al. (2020) 'RNA Based mNGS Approach Identifies a Novel Human Coronavirus from Two Individual Pneumonia Cases in 2019 Wuhan Outbreak', *Emerging Microbes & Infections*, 9: 313–9.

Chiu, C. Y. (2013) 'Viral Pathogen Discovery', *Current Opinion in Microbiology*, 16: 468–78.

Chiu, C. Y., and Miller, S. A. (2019) 'Clinical Metagenomics', *Nature Reviews. Genetics*, 20: 341–55.

Cibulski, S. et al. (2020) 'Viral Metagenomics in Brazilian Pekin Ducks Identifies Two Gyrovirus, Including a New Species, and the Potentially Pathogenic Duck Circovirus', *Virology*, 548: 101–8.

R Core Team (2020), *R: A Language and Environment for Statistical Computing* (Vienna, Austria) <https://www.R-project.org/> accessed 21 Sep 2021.

Cowled, C. et al. (2009) 'Genetic and Epidemiological Characterization of Stretch Lagoon Orbivirus, a Novel Orbivirus Isolated from Culex and Aedes Mosquitoes in Northern Australia', *The Journal of General Virology*, 90: 1433–9.

Cox-Foster, D. L. et al. (2007) 'A Metagenomic Survey of Microbes in Honey Bee Colony Collapse Disorder', *Science (New York, N.Y.)*, 318: 283–7.

Dandawate, C. N., and Shope, R. E. (1975) 'Studies on Physicochemical and Biological Properties of Two Ungrouped Arboviruses: Minnal and Arkonam.', *Indian Journal of Medical Research*, 63: 1180–7.

Depledge, D. P. et al. (2011) 'Specific Capture and Whole-genome Sequencing of Viruses from Clinical Samples', *PLoS One*, 6: e27805.

Ebinger, A., Fischer, S., and Höper, D. (2021) 'A Theoretical and Generalized Approach for the Assessment of the Sample-specific Limit of Detection for Clinical Metagenomics', *Computational and Structural Biotechnology Journal*, 19: 732–42.

Ejiri, H. et al. (2014) 'First Isolation and Characterization of a Mosquito-borne Orbivirus Belonging to the Species Umatilla Virus in East Asia', *Archives of Virology*, 159: 2675–85.

Epstein, J. H., and Anthony, S. J. (2017) 'Viral Discovery as a Tool for Pandemic Preparedness', *Revue scientifique et technique (International Office of Epizootics)*, 36: 499–512.

Epstein, J. H. et al. (2010) 'Identification of GBV-D, a Novel GB-like Flavivirus from Old World Frugivorous Bats (*Pteropus giganteus*) in Bangladesh', *PLoS Pathogens*, 6: e1000972.

Fineberg, H. V. (2014) 'Pandemic Preparedness and Response—lessons from the H1N1 Influenza of 2009', *The New England Journal of Medicine*, 370: 1335–42.

Finn, R. D. et al. (2014) 'Pfam: The Protein Families Database', *Nucleic Acids Research*, 42: D222–30.

Firth, A. E., and Brierley, I. (2012) 'Non-canonical Translation in RNA Viruses', *The Journal of General Virology*, 93: 1385–409.

Forth, L. F. et al. (2019) 'Novel Picornavirus in Lambs with Severe Encephalomyelitis', *Emerging Infectious Diseases*, 25: 963–7.

Gao, S. J., and Moore, P. S. (1996) 'Molecular Approaches to the Identification of Unculturable Infectious Agents', *Emerging Infectious Diseases*, 2: 159–67.

Greenberger, M. (2018) 'Better Prepare than React: Reordering Public Health Priorities 100 Years after the Spanish Flu Epidemic', *American Journal of Public Health*, 108: 1465–8.

Gu, W., Miller, S., and Chiu, C. Y. (2019) 'Clinical Metagenomic Next-Generation Sequencing for Pathogen Detection', *Annual Review of Pathology*, 14: 319–38.

Gubler, D. J., and Rosen, L. (1976) 'A Simple Technique for Demonstrating Transmission of Dengue Virus by Mosquitoes without the Use of Vertebrate Hosts', *The American Journal of Tropical Medicine and Hygiene*, 25: 146–50.

Gupta, R., and Brunak, S. (2002) 'Prediction of Glycosylation across the Human Proteome and the Correlation to Protein Function', *Pacific Symposium on Biocomputing*, pp. 310–22. Lihue.

Henikoff, S., and Henikoff, J. G. (1992) 'Amino Acid Substitution Matrices from Protein Blocks', *Proceedings of the National Academy of Sciences*, 89: 10915.

Hoffmann, B. et al. (2012) 'Novel Orthobunyavirus in Cattle, Europe, 2011', *Emerging Infectious Diseases*, 18: 469–72.

Hsiung, G. D. (1984) 'Diagnostic Virology: From Animals to Automation', *The Yale Journal of Biology and Medicine*, 57: 727–33.

Hughes, H. R. et al. (2020) 'ICTV Virus Taxonomy Profile: Peribunyaviridae', *The Journal of General Virology*, 101: 1–2.

Huson, D. H., and Bryant, D. (2006) 'Application of Phylogenetic Networks in Evolutionary Studies', *Molecular Biology and Evolution*, 23: 254–67.

Käfer, S. et al. (2019) 'Re-assessing the Diversity of Negative Strand RNA Viruses in Insects', *PLoS Pathogens*, 15: e1008224.

Kalyaanamoorthy, S. et al. (2017) 'ModelFinder: Fast Model Selection for Accurate Phylogenetic Estimates', *Nature Methods*, 14: 587–9.

Karabatsos, N. (ed.) (1985) *International Catalogue of Arboviruses Including Certain Other Viruses of Vertebrates*. San Antonio, TX. https://www.ncbi.nlm.nih.gov/nlmcatalog/8906098.

Katoh, K., and Standley, D. M. (2013) 'MAFFT Multiple Sequence Alignment Software Version 7: Improvements in Performance and Usability', *Molecular Biology and Evolution*, 30: 772–80.

Kawahara, F. et al. (2014) 'Characterization of *Eimeria brunetti* Isolated from a Poultry Farm in Japan', *The Journal of Veterinary Medical Science*, 76: 25–9.

Kelly, T. R. et al. (2020) 'Implementing One Health Approaches to Confront Emerging and Re-emerging Zoonotic Disease Threats: Lessons from PREDICT', *One Health Outlook*, 2: 1.

Kolde, R. (2019), *Pretty Heatmaps (RRID:SCR_016418)* <https://CRAN.R-project.org/package=pheatmap> accessed 3 Feb 2021.

Kopp, A. et al. (2019) 'Detection of Two Highly Diverse Peribunyaviruses in Mosquitoes from Palenque, Mexico', *Viruses*, 11: 832.

Krogh, A. et al. (2001) 'Predicting Transmembrane Protein Topology with a Hidden Markov Model: Application to Complete Genomes', *Journal of Molecular Biology*, 305: 567–80.

Leland, D. S., and Ginocchio, C. C. (2007) 'Role of Cell Culture for Virus Detection in the Age of Technology', *Clinical Microbiology Reviews*, 20: 49–78.

Marchler-Bauer, A. et al. (2013) 'CDD: Conserved Domains and Protein Three-dimensional Structure', *Nucleic Acids Research*, 41: D348–52.

Mertens, P. et al. (1989) 'Analysis of the Roles of Bluetongue Virus Outer Capsid Proteins VP2 and VP5 in Determination of Virus Serotype', *Virology*, 170: 561–5.

Mertens, P. P. et al. (2005) 'Orbiviruses, Reoviridae'. In: C. M. Fauquet et al. (eds) *Virus Taxonomy Eighth Report of the International Committee on Taxonomy of Viruses*:, pp. 466–83. London: Elsevier/Academic Press.

Mettenleiter, T. C. (2017) 'Chapter One—The First "Virus Hunters"'. In: M. Beer, and D. Höper (eds) *In Loeffler's Footsteps – Viral Genomics in the Era of High-Throughput Sequencing*, pp. 1–16. Amsterdam: Academic Press.

Minh, B. Q., Nguyen, M. A. T., and von Haeseler, A. (2013) 'Ultrafast Approximation for Phylogenetic Bootstrap', *Molecular Biology and Evolution*, 30: 1188–95.

Mokili, J. L., Rohwer, F., and Dutilh, B. E. (2012) 'Metagenomics and Future Perspectives in Virus Discovery', *Current Opinion in Virology*, 2: 63–77.

Nguyen, L.-T. et al. (2014) 'IQ-TREE: A Fast and Effective Stochastic Algorithm for Estimating Maximum-Likelihood Phylogenies', *Molecular Biology and Evolution*, 32: 268–74.

Ogiwara, A. et al. (1996) 'Construction and Analysis of a Profile Library Characterizing Groups of Structurally Known Proteins', *Protein Science: A Publication of the Protein Society*, 5: 1991–9.

Ørpetveit, I. et al. (2010) 'Detection of Infectious Pancreatic Necrosis Virus in Subclinically Infected Atlantic Salmon by Virus Isolation in Cell Culture or Real-Time Reverse Transcription Polymerase Chain Reaction: Influence of Sample Preservation and Storage', *Journal of Veterinary Diagnostic Investigation*, 22: 886–95.

Oude Munnink, B. B. et al. (2020) 'Rapid SARS-CoV-2 Whole-genome Sequencing and Analysis for Informed Public Health Decision-making in the Netherlands', *Nature Medicine*, 26: 1405–10.

Pettersson, J. H.-O. et al. (2019) 'Meta-Transcriptomic Comparison of the RNA Viromes of the Mosquito Vectors *Culex pipiens* and *Culex torrentium* in Northern Europe', *Viruses*, 11: 1033.

Pfaff, F. et al. (2017) 'A Novel Astrovirus Associated with Encephalitis and Ganglionitis in Domestic Sheep', *Transboundary and Emerging Diseases*, 64: 677–82.

Quan, P.-L. et al. (2013a), *Akhtuba Virus, a New Member of the Bunyaviridae Family Isolated from Pintail Birds (Anas Acuta) in Russia* (30 Aug 2013) <https://www.ncbi.nlm.nih.gov/nuccore/KF601560.1> accessed 22 Oct 2020.

—— et al. (2013b) 'Bats are a Major Natural Reservoir for Hepaciviruses and Pegiviruses', *Proceedings of the National Academy of Sciences of the United States of America*, 110: 8194–9.

Quick, J. et al. (2016) 'Real-time, Portable Genome Sequencing for Ebola Surveillance', *Nature*, 530: 228–32.

Ross, A. G. P., Crowe, S. M., and Tyndall, M. W. (2015) 'Planning for the Next Global Pandemic', *International Journal of Infectious Diseases: IJID: Official Publication of the International Society for Infectious Diseases*, 38: 89–94.

RStudio Team (2019), *RStudio: Integrated Development Environment for R* (Boston, MA) <http://www.rstudio.com/> accessed 21 Sep 2021.

Sachsenröder, J. et al. (2014) 'Metagenomic Identification of Novel Enteric Viruses in Urban Wild Rats and Genome Characterization of A Group A Rotavirus', *The Journal of General Virology*, 95: 2734–47.

Santos, P. D. et al. (2021) 'Co-infections: Simultaneous Detections of West Nile Virus and Usutu Virus in Birds from Germany', *Transboundary and Emerging Diseases*, 7: 1–17.

Sardi, S. et al. (2020) 'High-Quality Resolution of the Outbreak-Related Zika Virus Genome and Discovery of New Viruses Using Ion Torrent-Based Metatranscriptomics', *Viruses*, 12: 782.

Scheuch, M., Höper, D., and Beer, M. (2015) 'RIEMS: A Software Pipeline for Sensitive and Comprehensive Taxonomic Classification of Reads from Metagenomics Datasets', *BMC Bioinformatics*, 16: 69.

Schlottau, K. et al. (2018) 'Fatal Encephalitic Borna Disease Virus 1 in Solid-Organ Transplant Recipients', *The New England Journal of Medicine*, 379: 1377–9.

Schomacker, H., Collins, P. L., and Schmidt, A. C. (2004) 'In Silico Identification of a Putative New Paramyxovirus Related to the Henipavirus Genus', *Virology*, 330: 178–85.

Shi, M. et al. (2016) 'Redefining the Invertebrate RNA Virosphere', *Nature*, 540: 539–43.

Shi, X. et al. (2009) 'Functional Analysis of the Bunyamwera Orthobunyavirus Gc Glycoprotein', *The Journal of General Virology*, 90: 2483–92.

Sigrist, C. J. A. et al. (2013) 'New and Continuing Developments at PROSITE', *Nucleic Acids Research*, 41: D344–7.

Tangudu, C. S. et al. (2019) 'Skunk River Virus, a Novel Orbivirus Isolated from Aedes Trivittatus in the United States', *The Journal of General Virology*, 100: 295–300.

Tesh, R. B. et al. (1986) 'Biological and Antigenic Characterization of Netivot Virus, an Unusual New Orbivirus Recovered from Mosquitoes in Israel', *The American Journal of Tropical Medicine and Hygiene*, 35: 418–28.

Untergasser, A. et al. (2012) 'Primer3—new Capabilities and Interfaces', *Nucleic Acids Research*, 40: e115.

Vasilakis, N. et al. (2014) 'Mesoniviruses are Mosquito-specific Viruses with Extensive Geographic Distribution and Host Range', *Virology Journal*, 11: 97.

Vibin, J. et al. (2020) 'Metagenomic Characterisation of Avian Parvoviruses and Picornaviruses from Australian Wild Ducks', *Scientific Reports*, 10: 12800.

Waltzek, T. B. et al. (2019) 'Characterization of a Peribunyavirus Isolated from Largemouth Bass (*Micropterus salmoides*)', *Virus Research*, 273: 197761.

Wickham, H. (2016), *Ggplot2: Elegant Graphics for Data Analysis* <https://ggplot2.tidyverse.org> accessed 21 Sep 2021.

Williams, S. H. et al. (2019) 'Discovery of Two Highly Divergent Negative-sense RNA Viruses Associated with the Parasitic Nematode, Capillaria Hepatica, in Wild *Mus musculus* from New York City', *The Journal of General Virology*, 100: 1350–62.

World Health Organization (2021), *WHO Coronavirus Disease (COVID-19) Dashboard* (20 Sep 2021) <https://covid19.who.int/> accessed 20 Sep 2021.

World Health Organization Director-General (2011), *Implementation of the International Health Regulations (2005): Report of the Review Committee on the Functioning of the International Health Regula-* *tions (2005) in Relation to Pandemic (H1N1) 2009* <https://apps.who.int/gb/ebwha/pdf_files/WHA64/A64_10-en.pdf> accessed 19 Jan 2021.

Wylezich, C. et al. (2019) 'Metagenomics for Broad and Improved Parasite Detection: A Proof-of-concept Study Using Swine Faecal Samples', *International Journal for Parasitology*, 49: 769–77.

——— et al. (2020) 'Untargeted Metagenomics Shows a Reliable Performance for Synchronous Detection of Parasites', *Parasitology Research*, 119: 2623–9.

——— et al. (2021) 'Next-generation Diagnostics: Virus Capture Facilitates a Sensitive Viral Diagnosis for Epizootic and Zoonotic Pathogens Including SARS-CoV-2', *Microbiome*, 9: 51.

——— et al. (2018) 'A Versatile Sample Processing Workflow for Metagenomic Pathogen Detection', *Scientific Reports*, 8: 13108.

Wylie, K. M. et al. (2012) 'Sequence Analysis of the Human Virome in Febrile and Afebrile Children', *PloS One*, 7: e27735.

Ziegler, U. et al. (2019) 'West Nile Virus Epizootic in Germany, 2018', *Antiviral Research*, 162: 39–43.

——— et al. (2020) 'West Nile Virus Epidemic in Germany Triggered by Epizootic Emergence, 2019', *Viruses*, 12: 448.

Supplementary Files:
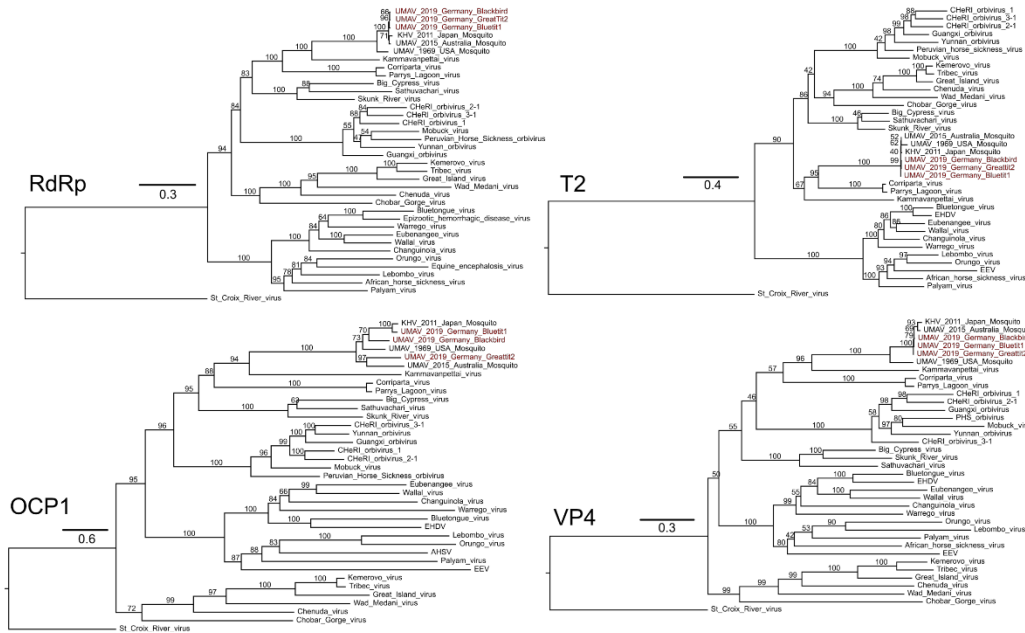
Figure S2 (1/3)
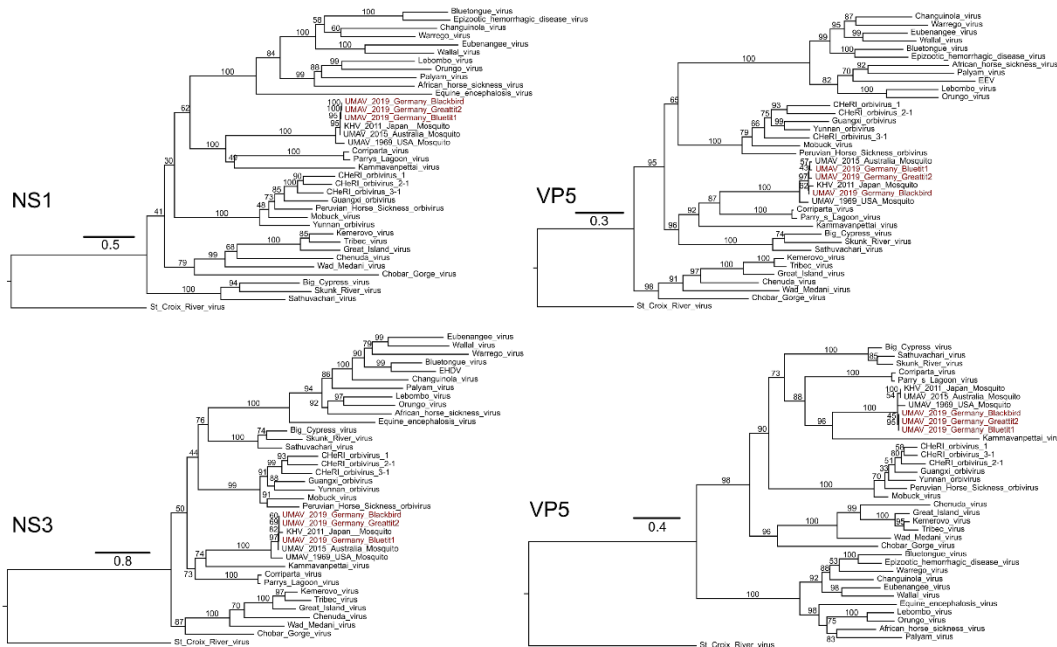
Figure S2 (2/3)
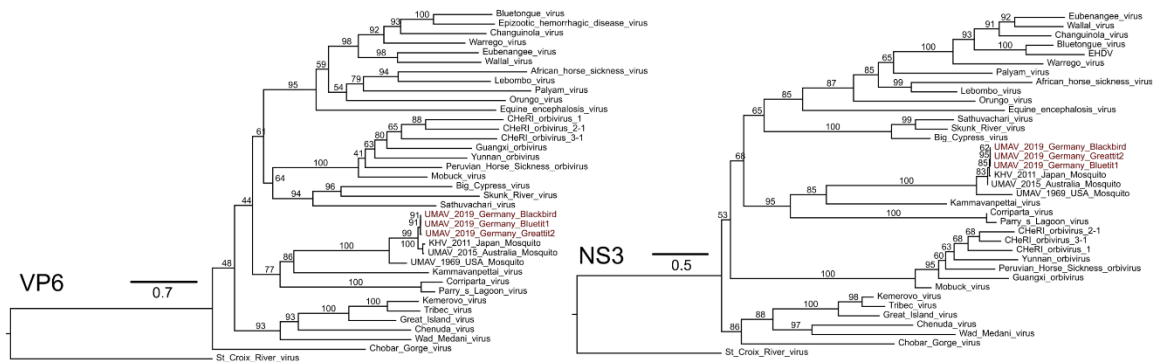
Figure S2 (3/3). Maximum likelihood phylogenetic trees of members of the genus *Orbivirus* using protein sequences from ten segments. Red text indicates genomes acquired in this study. Abbreviations: EEV – Equine encephalosis virus; EHDV – Epizootic hemorrhagic disease virus; AHSV – African Horse sickeness virus; PHS orbivirus – Peruvian Horse Sickness orbivirus
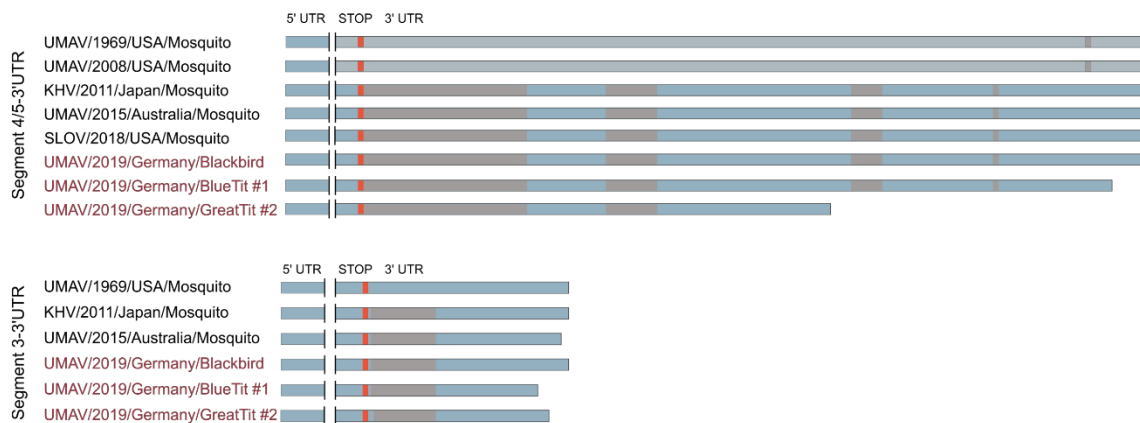
Figure S3. Schematic diagram of alignments of the 3' untranscribed regions (UTR) of UMAV segments that encode the NS1 gene (Above) and OCP1 gene (Below). Red texts indicate UMAV variants detected in this study. Blue, red, and grey boxes indicate aligned sequence, stop codon position (STOP), and gaps. The nucleotide sequences of the UMAV/2008/USA /Mosquito and SLOV/2018/USA/Mosquito segment 3 were not available in the database. The number below the gray boxes indicated the number of deleted nucleotides.

A. Glycoprotein
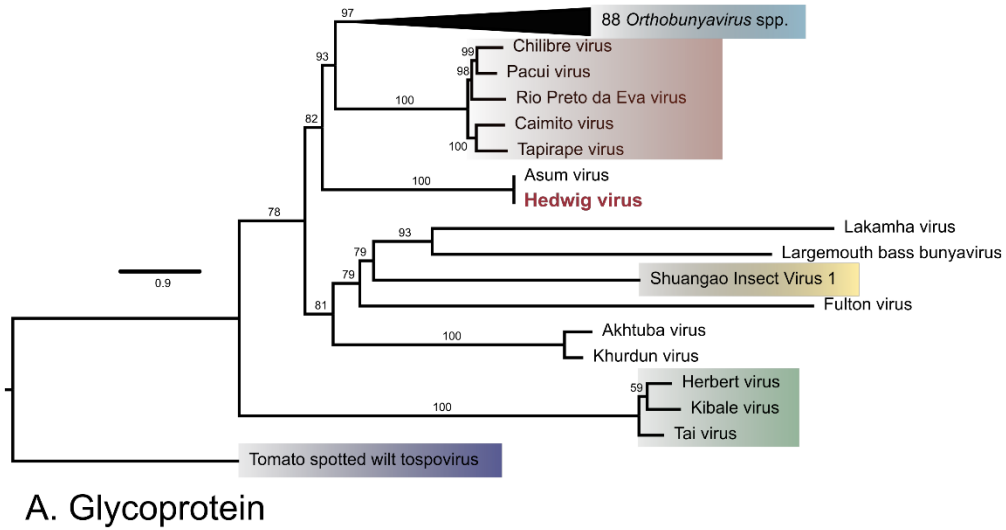
Figure S4 (1/2).
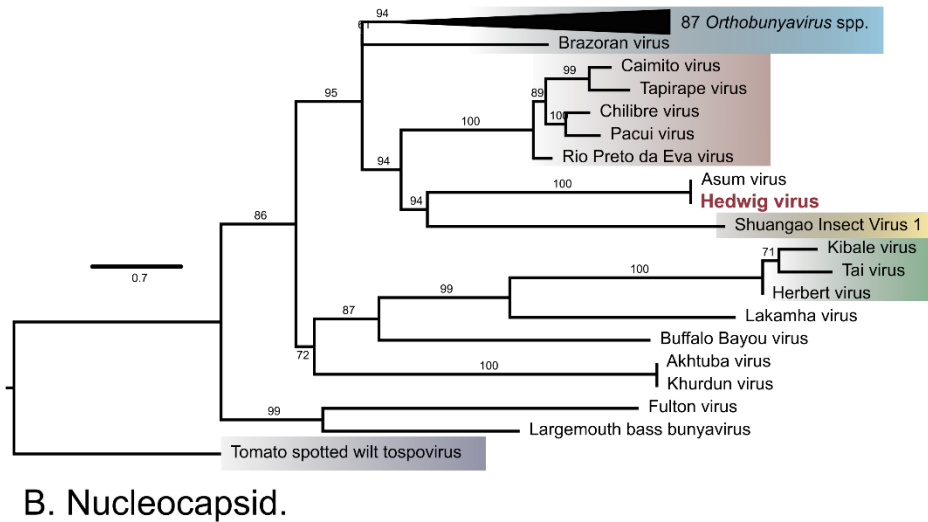
B. Nucleocapsid.

Figure S4 (2/2). Maximum likelihood trees of the the glycoprotein precursors (A) and nucleocapsid (B) of representative peribunyaviruses, Asum virus and Hedwig virus (printed red). Blue, orange, yellow, green, and uncolored represent the corresponding genera: *Orthobunyavirus, Pacuvirus, Shangavirus, Herbevirus,* and unclassified *Peribunyaviridae.* (A) Maximum likelihood tree of the RdRp amino acid sequences. Ultrafast bootstrap analyses with 100,000 replicates supported the tree topology. Representative *Orthobunyavirus species* were collapsed into a triangle. Tomato spotted wilt tospovirus was used as an outgroup (violet). Accession numbers of available amino acid sequences from representative members of the family *Peribunyaviridae* and the outlier strain are indicated in Table S6.

Table S1. The generic high throughput sequence (HTS) datasets from the 2018-29 West Nile Virus epidemics in Germany. Information includes sample identification number (FLI code), dataset name (library number), common names (host name) and species names of hosts, organ samples prepared for unbiased HTS, and total number of sequences reads per library.

FLI code	Library numb	Host/Code	Species name	Organ	City	Total Number of Reads
EDI-33/18	lib02726	Great Grey Owl #6	*Strix nebulosa*	Spleen tissue	Halle (Saale), Saxony-Anhalt	6,998,553
EDI-90/18	lib02896	Great Grey Owl #1	*Strix nebulosa*	brain tissue	Poing, Bavaria	9,151,821
EDI-114/18	lib02898	Great Grey Owl #2	*Strix nebulosa*	organ mix	Poing, Bavaria	6,815,738
EDI-82/18	lib02914	Goshawk #1	*Accipiter gentilis*	brain tissue	Klein Weissandt, Saxony-Anhalt	11,502,960
EDI-142/18	lib02916	Tawny Owl	*Strix aluco*	brain tissue	Bad Lauchstaedt, Saxony-Anhalt	3,367,811
EDI-89/18	lib02959	Goshawk #2	*Accipiter gentilis*	brain tissue	Bad Dueben, Saxony	10,508,755
EDI-127/18	lib02961	Horse #1	*Equus ferus caballus*	Brain tissue	Plessa OT Kahla, Brandenburg	5,712,820
EDI-127/18	lib02962	Horse #1	*Equus ferus caballus*	Spinal cord tissue	Plessa OT Kahla, Brandenburg	5,017,979
EDI-79/18	lib03038	Snowy Owl #1	*Bubo scandiacus*	Brain tissue	Berlin, Berlin	4,347,713
EDI-79/18	lib03039	Snowy Owl #1	*Bubo scandiacus*	Spleen tissue	Berlin, Berlin	6,960,872
EDI-107-18	lib03041	Snowy Owl #2	*Bubo scandiacus*	brain tissue	Berlin Friedrichsfelde, Berlin	5,876,065
EDI-107-18	lib03042	Snowy Owl #2	*Bubo scandiacus*	kidney tissue	Berlin Friedrichsfelde, Berlin	6,470,149
EDI-62/19	lib03378	Snowy Owl #3	*Bubo scandiacus*	heart tissue	Lutherstadt Wittenberg, Saxony Anhalt	2,709,343
EDI-83/19	lib03379	Great Grey Owl #3	*Strix nebulosa*	liver tissue	Lutherstadt Wittenberg, Saxony Anhalt	3,000,996
EDI-85/19	lib03380	Snowy Owl #4	*Bubo scandiacus*	liver tissue	Berlin Friedrichsfelde, Berlin	3,871,943
EDI-87/19	lib03381	Blue Tit #1	*Cyanistes caeruleus*	brain tissue	Halle, Saxony-Anhalt	4,378,747
EDI-118/19	lib03382	Snowy Owl #5	*Bubo scandiacus*	liver tissue	Berlin Friedrichsfelde, Berlin	3,548,613
EDI-125/19	lib03383	Inka Tern	*Larosterna inca*	liver tissue	Berlin, Berlin	2,937,284
EDI-157/19	lib03415	Snowy Owl #6	*Bubo scandiacus*	heart tissue	Berlin, Berlin	2,467,447
EDI-158/19	lib03416	Andean flamingo	*Phoenicoparrus andinus*	heart tissue	Berlin, Berlin	836,509
EDI-148/19	lib03417	Goshawk #3	*Accipiter gentilis*	heart tissue	Berlin, Berlin	1,049,529
EDI-156/19	lib03418	Goshawk #4	*Accipiter gentilis*	great brain tissue	Berlin Friedrichsfelde, Berlin	2,722,301
EDI-153/19	lib03419	Goshawk #5	*Accipiter gentilis*	great brain tissue	Brieselang, Brandenburg	925,060
EDI-155/19	lib03420	Goshawk #6	*Accipiter gentilis*	great brain tissue	Neuruppin, LK Ostprignitz-Ruppin, Brandenburg	797,977
EDI-89/19	lib03421	Blue tit #2	*Parus caeruleus*	Organ	Radebeul, Saxony	1,414,011
EDI-139/19	lib03422	Great tit #1	*Parus major*	liver/heart tissue	Dresden, Saxony	1,226,796
EDI-177/19	lib03423	Eurasian golden plover	*Pluvialis apricaria*	liver/spleen tissue	Kamenz/Biehla, LK Bautzen, Saxony	1,575,924
EDI-163/19	lib03424	Goshawk #7	*Accipiter gentilis*	brain tissue	Sandersdorf, LK Anhalt-Bitterfeld	1,023,309
EDI-164/19	lib03425	Snowy Owl #7	*Bubo scandiacus*	liver tissue	Magdeburg, Saxony-Anhalt	1,570,120
EDI-165/19	lib03426	Snowy Owl #8	*Bubo scandiacus*	liver tissue	Magdeburg, Saxony-Anhalt	3,767,075
EDI-109/19	lib03427	Coconut Lorikeet	*Trichoglossus haematodus*	organhomogenate-supernatant	Halle (Saale), Saxony-Anhalt	1,425,591
EDI-134/19	lib03428	House Sparrow	*Passer domesticus*	organhomogenate-supernatant	Rackwitz, LK Nordsachsen, Saxony	1,345,730
EDI-135/19	lib03429	Eurasian Eagle Owl	*Bubo bubo*	organhomogenate-supernatant	Bennewitz, LK Leipzig, Saxony	942,052
EDI-172/19	lib03430	Great Grey owl #4	*Strix nebulosa*	organhomogenate-supernatant	Chemnitz, Saxony	998,495
EDI-173/19	lib03431	Great Grey owl #5	*Strix nebulosa*	organhomogenate-supernatant	Chemnitz, Saxony	2,715,156
EDI-202/19	lib03432	Chilean flamingo	*Phoenicopterus chilensis*	organhomogenate-supernatant	Leipzig, Saxony	968,220
EDI-205/19	lib03433	Great tit #2	*Parus major*	organhomogenate-supernatant	Bad Dueben, LK Nordsachsen, Saxony	208,336
EDI-201/19	lib03449	Humboldt-penguin	*Spheniscus humboldti*	heart tissue	Cottbus, Brandenburg	2,723,390
EDI-208/19	lib03450	Goshawk #8	*Accipiter gentilis*	brain tissue	Stadt Merseburg, Saxony-Anhalt	2,322,112
EDI-94/19	lib03451	Horse #2	*Equus ferus caballus*	spinal cord (cervix part)	Krostitz, Sachsen	2,958,966
C6_T167_20	lib03481	Mosquito pool #1	*Culex pipiens*	Supernatant of a mosquito pool homogenate (10 individuals) inoculated in C6/36 mosquito cell lines (5 days post infection)	Berlin Friedrichsfelde, Berlin	1,896,219
C6_T167_57	lib03482	Mosquito pool #2	*Culex pipiens*	Supernatant of a mosquito pool homogenate (10 individuals) inoculated in C6/36 mosquito cell lines (5 days post infection)	Berlin Friedrichsfelde, Berlin	1,669,310
V_T166_60	Lib03504	Mosquito pool #3	*Culex pipiens*	Supernatant of a mosquito pool homogenate (10 individuals) inoculated in Vero cells (5 days post infection)	Berlin Friedrichsfelde, Berlin	1,906,013

Table S2. Number of sequence reads annotated as non-viral pathogens per dataset.

Table S2. Number of sequence reads annotated as non-viral pathogens per dataset.

Library number	Taxonomic Family	counts	Library number	Taxonomic Family	counts	Library number	Taxonomic Family	counts
lib02726	Sarcocystidae	11	lib03381	Plasmodiidae	64836	lib03427	Shewanellaceae	18
	Eimeriidae	1		Sarcocystidae	40		Vibrionaceae	1055197
lib02896	Plasmodiidae	165		Eimeriidae	29		Plasmodiidae	2
	Eimeriidae	31		Trypanosomatidae	1	lib03428	Hafniaceae	1
	Sarcocystidae	11	lib03382	Plasmodiidae	6525		Enterococcaceae	43974
lib02898	Plasmodiidae	25		Sarcocystidae	173		Campylobacteraceae	75760
	Taeniidae	34		Eimeriidae	41		Helicobacteraceae	85050
	Sarcocystidae	1	lib03383	Plasmodiidae	144181		Lactobacillaceae	1101
	Eimeriidae	1	lib03415	Plasmodiidae	346		Enterobacteriaceae	217895
	Trypanosomatidae	2		Eimeriidae	2		Sarcocystidae	3
lib02914	Plasmodiidae	440		Ascarididae	1		Eimeriidae	2724
	Eimeriidae	7		Sarcocystidae	3	lib03429	Clostridiaceae	4
	Sarcocystidae	2	lib03416	Clostridiaceae	65		Plasmodiidae	150
	Taeniidae	10		Vibrionaceae	24		Taeniidae	1
lib02916	Pasteurellaceae	793		Plasmodiidae	3		Sarcocystidae	7
	Plasmodiidae	310	lib03417	Plasmodiidae	21698		Trypanosomatidae	7
	Eimeriidae	2		Sarcocystidae	8	lib03430	Plasmodiidae	134
	Trypanosomatidae	6		Eimeriidae	39		Sarcocystidae	23
	Taeniidae	3	lib03418	Plasmodiidae	1415		Eimeriidae	6
lib02959	Plasmodiidae	3		Sarcocystidae	23		Trypanosomatidae	10
lib02961	Clostridiaceae	228		Eimeriidae	6	lib03431	Hafniaceae	1
	Plasmodiidae	1	lib03419	Plasmodiidae	313		Campylobacteraceae	99
lib02962	Clostridiaceae	33529		Sarcocystidae	4		Helicobacteraceae	13
	Plasmodiidae	6		Eimeriidae	2		Clostridiaceae	2
lib03038	Plasmodiidae	5	lib03420	Plasmodiidae	10		Plasmodiidae	204
	Eimeriidae	2		Taeniidae	25		Sarcocystidae	4
	Sarcocystidae	3		Eimeriidae	7		Eimeriidae	113
lib03039	Plasmodiidae	9	lib03421	Plasmodiidae	7879	lib03433	Hafniaceae	75303
	Eimeriidae	2		Sarcocystidae	18	lib03449	Clostridiaceae	50
lib03041	Plasmodiidae	48282	lib03422	Plasmodiidae	95		Plasmodiidae	12
	Eimeriidae	6	lib03423	Eimeriidae	32		Sarcocystidae	1
	Sarcocystidae	1393	lib03424	Plasmodiidae	22	lib03450	Plasmodiidae	2007
	Trypanosomatidae	5		Taeniidae	1	lib03451	Hafniaceae	1
lib03042	Plasmodiidae	15101		Eimeriidae	2		Plasmodiidae	1
	Eimeriidae	109	lib03425	Plasmodiidae	13		Schistosomatidae	7
	Sarcocystidae	92		Sarcocystidae	1	lib03481	Clostridiaceae	3
	Taeniidae	14		Eimeriidae	1		Plasmodiidae	9
lib03378	Plasmodiidae	15	lib03504	Sarcocystidae	15			
	Eimeriidae	4	lib03426	Plasmodiidae	190993			
lib03379	Plasmodiidae	19		Babesiidae	961			
	Eimeriidae	4		Sarcocystidae	1834			
lib03380	Plasmodiidae	64080		Eimeriidae	4225			
	Eimeriidae	434		Trypanosomatidae	3			

Table S3. More detailed taxonomic classification of viral sequence reads detected in generic high throughput sequence datasets derived from 2018-19 WNV Epidemic in Germany. Number of detected reads, length based on sequencing and assembly, and their closest hits (accession numbers, description, and blastx identities) from the database were included. Total number of sequence reads per library and sample information were indicated in Table S1.

Host	Library number	Taxonomic classification	Number of reads	Length (nt)	Accession number	Description	blastx identity (%)
Tawny Owl	lib02916	*Flaviviridae*	1	129	ATP66856.1	polyprotein [Rodent pestivirus]	41.38
Snowy Owl #1	lib03038	*Flaviviridae*	30	219-2342	API68248.1	polyprotein precursor [Usutu virus]	78.81-100
			4	183-548	AWI66603.1; QDQ46558.1	polyprotein [Usutu virus]	80.81-100
			9	399	YP_164808.1	core protein C [Usutu virus]	100
			7	257-372	AZP89717.1 QBA41160.1	NS5 protein [Usutu virus]	53.03-100.00
	lib03038	*Peribunyaviridae*	320 (1413)	6965	QGA70944.1	RNA-dependent RNA polymerase [Asum virus]	99.56
			298 (1113)	4606	AXP32071.1	glycoprotein precursor [Thimiri virus]	35.23
			110 (396)	1079	YP_009507880.1	nucleocapsid protein [Guama virus]	30.45
Snowy Owl #2	lib03041	*Peribunyaviridae*	21	158-720	QGA70944.1	RNA-dependent RNA polymerase [Asum virus]	47.54-100
			6	881	AMR73385.1	polyprotein [Belmont virus]	37.35
			5	758	AKO90202.1	nucleocapsid protein [Mapputta virus]	31.45
Blue Tit #1	lib03381	*Reoviridae*	240	3906	QCW07531.1	RNA-dependent RNA polymerase [Umatilla virus]	98
			162	2760	QCW07532.1	T2 [Umatilla virus]	99.34
			172	2355	YP_009047260.1	VP3 [Umatilla virus]	48.58
			185	1990	QCW07534.1	capsid protein [Umatilla virus]	95.99
			157	1923	QCW07535.1	tubule protein [Umatilla virus]	98.79
			169	1655	BAP18636.1	VP5 [Koyama Hill virus]	95.83
			180	1356	QCW07537.1	viral inclusion body protein [Umatilla virus]	98.52
			113	1139	AZJ37613.1	VP7 [Stretch Lagoon orbivirus]	100
			168	1073	QCW07539.1	helicase [Umatilla virus]	91.02
			108	859	BAP18640.1	NS3 [Koyama Hill virus]	97.68
		Totiviridae	6	774	QGA70770.1	capsid protein [Trichoderma koningiopsis totivirus 1]	29.29
		Riboviria	2	402	APG75978.1	hypothetical protein 2 [Hubei toti-like virus 6]	65.6-61.65
			15	1244	YP_009342434.1	hypothetical protein 2 [Wuhan insect virus 27]	42.42
Goshawk #3	lib03417	*Riboviria*	560	863-6986	APG75978.1	hypothetical protein 2 [Hubei toti-like virus 6]	37.61-57.34
Goshawk #5	lib03419	*Riboviria*	1	183	APG75978.1	hypothetical protein 2 [Hubei toti-like virus 6]	66.67
Great Tit #1	lib03422	*Flaviviridae*	1	342	YP_164817.1	NS4b [Usutu virus]	99.11
			1	462	QBA41160.1	nonstructural protein NS5 [Usutu virus]	100
		Reoviridae	1	366	YP_002925133.1	VP2 [stretch lagoon orbivirus]	56.88
Goshawk #7	lib03424	*Riboviria*	1	210	APG75978.1	hypothetical protein 2 [Hubei toti-like virus 6]	61.11
			1	243	AGU62876.1	RdRp [Lake Sinai virus 5 JR-2013]	38.71
House Sparrow	lib03428	*Dicistroviridae*	1	180	ASM94063.1	putative ORF1, partial [Barns Ness breadcrumb sponge dicistro-like virus 2]	36.67
		Iflaviridae	1	273	QCL1100.1	polyprotein [King virus]	35.21
		Picornavirales	2	219-237	YP_009255227.1	nonstructural proteins [Antarctic picorna-like virus 1]	38.39-48.72
			1	198	YP_009423855.1	hypothetical protein 2 [Tioga picorna-like virus 1]	53.33
		Reoviridae	1	180	BAQ19497	mu B [avian orthoreovirus]	98.33
			1	365	AED99913.1	muC [avian orthoreovirus]	89.29
		Riboviria	2	243-321	YP_009345892.1	hypothetical protein [Jingmen tombus-like virus 1]	50.82-60.19
			2	180-228	AYP67569.1	RdRp [Nadgee virus]	34.48-38.24
			1	222	QID77679.1	polyprotein [Pink bollworm virus 4]	60
			1	180	YP_009333140.1	RdRp [Behai narna-like virus 21]	64.29
			1	222	YP_009337713.1	hypothetical protein 1 [Sanxia picorna-like virus 11]	60.19
			1	264	YP_009337755.1	hypothetical protein 1 [Sanxia picorna-like virus 9]	47.73
Great Grey Owl #5	lib03431	*Picornaviridae*	3	243-453	AIU36252.1	polyprotein [Norway rat kobuvirus 2]	50.75-63.76
		Astroviridae	2	245-246	AFB18035.1	RNA-dependent RNA polymerase [Murine astrovirus]	98.57
Great Tit #2	lib03433	*Flaviviridae*	1	399	QDF44088.1	polyprotein [Duck hepacivirus]	37.31
			1	387	YP_009509001.1	putative NS3 [Theiler's disease associated virus]	56.07
			1	183	QHD25538.1	polyprotein [Jogalong virus]	55.36
		Picornaviridae	17	150-915	YP_009272812.1	polyprotein [Washington bat picornavirus]	43.08-71.43
		Reoviridae	211	3905	QCW07531.1	RNA-dependent RNA polymerase [Umatilla virus]	98
			161	2736	QCW07532.1	T2 [Umatilla virus]	99.34
			122	2363	YP_009047260.1	VP3 [Umatilla virus]	48.58
			126	1987	QCW07534.1	capsid protein [Umatilla virus]	95.99
			118	1857	QCW07535.1	tubule protein [Umatilla virus]	98.79
			112	1647	BAP18636.1	VP5 [Koyama Hill virus]	95.83
			72	1385	QCW07537.1	viral inclusion body protein [Umatilla virus]	98.52
			65	1140	AZJ37613.1	VP7 [Stretch Lagoon orbivirus]	100
			52	1077	QCW07539.1	helicase [Umatilla virus]	91.02
			23	832	BAP18640.1	NS3 [Koyama Hill virus]	97.68
		Totiviridae	3	168-393	YP_009551683.1	coat protein [Eimeria stiedai RNA virus 1]	46.90-70
			16	925	YP_009551684.1	RNA-dependent RNA polymerase [Eimeria stiedai RNA virus 1]	61.39
			3	114-243	YP_009115499.1	coat protein [Eimeria tenella RNA virus 1]	45.71-52.08
			8	273-915	YP_009115500.1	RNA-dependent RNA polymerase [Eimeria tenella RNA virus 1]	42.35-54.77
			32	1484	YP_009551684.1	RNA-dependent RNA polymerase [Eimeria brunetti RNA virus 1]	47.08
			14	1456	NP_108650.1	coat protein [Eimeria brunetti RNA virus 1]	39.61
			3	174-177	AXA52555.1	putative polycapsid [Linepithema humile toti-like virus 1]	58.62
			7	182	AAF29445.1	RNA-dependent RNA polymerase [Trichomonas vaginalis virus 2]	43.86
		Riboviria	120	1438	APG78218	RdRp [Hubei partiti-like virus 48]	57.3
			8	721	AOC55077.1	polyprotein [Baker virus]	41.53
			1	249	APO40851.1	structural protein [Volivirus sp]	40.74
			1	309	YP_009337883.1	RdRp [Hubei orthoptera virus 4]	35.90-37.86
			1	201	AQM55304.1	hypothetical protein 1 [Cordoba virus]	68.97
			1	243	YP_009337174.1	hypothetical protein [Hubei picorna-like virus 71]	36.36
Goshawk #8	lib03450	*Riboviria*	1	177	ASA47364.1	RdRp [Wilkie narna-like virus 1]	53.45
Mosquito Pool #1	lib03481	*Chrysoviridae*	3	138-288	QGA70949.1	RdRp [Eskilstorp virus]	100
			1	159	ASA47448.1	hypothetical protein [Shuangao chryso-like virus 1]	67.31
		Riboviria	3	111-231	ASA47351.1	hypothetical protein [Hubei chryso-like virus 1]	71.43-84.42
Mosquito Pool #2	lib03482	*Mesoniviridae*	242607	20125	ALP32023.1	pp1ab polyprotein [Alphamesonivirus 1]	99.69
		Tymoviridae	1	198	YP_009505642.1	RdRp [Bombyx mori latent virus]	51.52
		Tymovirales	1	243	QEM39124.1	RdRp [Guadeloupe Culex tymo-like virus]	48.75
Mosquito Pool #3	lib03504	*Nodaviridae*	29	1766	AXQ04817.1	hypothetical protein [Culex mosquito virus 1]	97.04
		Picornavirales	13	99-444	AWC26954.1	polyprotein [Culex picorna-like virus 1]	75.36-100
		Tombusviridae	12	111-898	YP_009552018.1	hypothetical protein [Culex-associated Tombus-like virus]	88.89-100
		Iflaviridae	5	111-231	YP_009553231.1	polyprotein [Culex-Iflavi-like virus 4]	57.78-100
		Riboviria	1	309	AWR88280.1	hypothetical protein [Hubei chryso-like virus 1]	93.2

Table S4. Accession numbers for different protein sequences of representative Orbivirus species. These protein sequences included tubule forming proteins or nonstructural protein 1 (NS1), viral inclusion bodies or nonstructural protein 2 (NS2), nonstructural protein 3 (NS3), RNA dependent RNA polymerase (RdRp), inner shell protein (T2), outer core or viral protein 7 (T13), outer capsid protein 1 (OCP1), capping enzyme or viral protein 4 (VP4), outer capsid or viral protein 5 (VP5), and helicase or viral protein 6 (VP6).

Orbivirus species	NS1	NS2	NS3	RdRp	T2	T13	OCP1	VP4	VP5	VP6
African horse sickness virus	YP_052965.1	YP_052961.1	YP_052954.1	YP_052966.1	CAP04842.1	YP_052956.1	YP_052941.1	YP_052957.1	YP_052963.1	YP_052964.1
Big Cypress virus	AZK31319.1	AZK31320.1	AZK31321.1	AZK31312.1	AZK31314.1	AZK31318.1	AZK31313.1	AZK31315.1	AZK31316.1	AZK31317.1
Bluetongue virus	AJG44860	YP_052952.1	YP_052960.1	ADI49561.1	AJG44858.1	YP_052967.1	YP_052958.1	YP_052969.2	YP_052955.1	YP_052953.2
Changuinola virus	YP_008719922.1	YP_008719924.1	YP_008719925.1	YP_008719926.1	YP_008719921.1	YP_008719923.1	YP_008719920.1	YP_008719927.1	YP_008719928.1	YP_008719929.1
CheRI orbivirus 1	QCQ85343.1	QCQ85344.1	QCQ85345.1	QCQ85336.1	QCQ85338.1	QCQ85342.1	QCQ85337.1	QCQ85339.1	QCQ85340.1	QCQ85341.1
CheRI orbivirus 2	QCQ85353.1	QCQ85354.1	QCQ85355.1	QCQ85346.1	QCQ85348.1	QCQ85352.1	QCQ85347.1	QCQ85349.1	QCQ85350.1	QCQ85351.1
CheRI orbivirus 3	QCQ85373.1	QCQ85374.1	QCQ85375.1	QCQ85366.1	QCQ85368.1	QCQ85372.1	QCQ85367.1	QCQ85369.1	QCQ85370.1	QCQ85371.1
Chenuda virus	YP_009158882.1	YP_009158895.1	YP_009158899.1	YP_009158878.1	YP_009158879.1	YP_009158896.1	YP_009158881.1	YP_009158880.1	YP_009158894.1	YP_009158897.1
Chobar Gorge virus	YP_009158905.1	YP_009158908.1	YP_009158911.1	YP_009158901.1	YP_009158902.1	YP_009158907.1	YP_009158904.1	YP_009158903.1	YP_009158906.1	YP_009158909.1
Corriparta virus	YP_009507677.1	YP_009507685.1	YP_009507681.1	YP_009507680.1	YP_009507675.1	YP_009507686.1	YP_009507683.1	YP_009507676.1	YP_009507684.1	YP_009507678.1
Epizootic hemorrhagic disease virus	YP_003240112.1	YP_003240115.1	YP_003240117.1	YP_003240108.1	YP_003240110.1	YP_003240114.1	YP_003240109.1	YP_003240111.1	YP_003240113.1	YP_003240116.1
Equine encephalosis virus	YP_009507689.1	YP_009507696.1	YP_009507693.1	YP_009507687.1	YP_009507688.1	YP_009507691.1	YP_009507695.1	YP_009507694.1	YP_009507690.1	YP_009507692.1
Eubenangee virus	YP_009507698.1	YP_009507700.1	YP_009507706.1	YP_009507705.1	YP_009507697.1	YP_009507702.1	YP_009507701.1	YP_009507704.1	YP_009507699.1	YP_009507703.1
Great Island virus	YP_003896061.1	YP_003896065.1	YP_003896068.1	YP_003896059.1	YP_003896059.1	YP_003896064.1	YP_003896062.1	YP_003896060.1	YP_003896063.1	YP_003896066.1
Guangxi orbivirus	YP_009551625.1	YP_009551618.1	YP_009551619.1	YP_009551622.1	YP_009551623.1	YP_009551621.1	YP_009551620.1	YP_009553738.1	YP_009551624.1	YP_009551626.1
Kammavanpettai virus	AXF35754.1	AXF35755.1	AXF35756.1	AXF35757.1	AXF35759.1	AXF35764.1	AXF35758.1	AXF35760.1	AXF35761.1	AXF35763.1
Kemerovo virus	ADZ96233.1	ADZ96235.1	ADZ96238.1	ADZ96229.1	ADZ96230.1	ADZ96236.1	ADZ96232.1	ADZ96231.1	ADZ96234.1	ADZ96237.1
Koyama Hill virus	BAP18634.1	BAP18637.1	BAP18640.1	BAP18631.1	BAP18632.1	BAP18638.1	BAP18633.1	BAP18635.1	BAP18636.1	BAP18639.1
Lebombo virus	YP_009507714.1	YP_009507711.1	YP_009507715.1	YP_009507707.1	YP_009507713.1	YP_009507712.1	YP_009507708.1	YP_009507709.1	YP_009507710.1	YP_009507716.1
Mobuck virus	AYA60495.1	AYA60496.1	AYA60497.1	AYA60488.1	AYA60490.1	AYA60494.1	AYA60489.1	AYA60491.1	AYA60492.1	AYA60493.1
Orungo virus	YP_009507725.1	YP_009507722.1	YP_009507728.1	YP_009507718.1	YP_009507724.1	YP_009507721.1	YP_009507719.1	YP_009507720.1	YP_009507723.1	YP_009507726.1
Palyam virus	YP_052938.1	YP_052939.1	YP_052940.1	YP_052935.1	YP_052934.1	YP_052933.1	YP_052931.1	YP_052936.1	YP_052932.1	YP_052937.1
Parry's Lagoon virus	ANH10673.1	ANH10676.1	ANH10679.1	ANH10670.1	ANH10671.1	ANH10677.1	ANH10672.1	ANH10675.1	ANH10674.1	ANH10678.1
Peruvian horse sickness virus	YP_460045.1	YP_460046.1	YP_460047.1	YP_460038.1	ABB72771.1	YP_460044.1	YP_460040.1	YP_460041.1	YP_460042.1	YP_460043.1
Sathuvachari virus	AGE32267.1	YP_052948.1	AGE32269.1	AGE32260.1	AGE32262.1	AGE32266.1	AGE32261.1	AGE32263.1	AGE32264.1	AGE32265.1
Skunk River virus	AZJ37601.1	AZJ37603.1	AZJ37606.1	AZJ37597.1	AZJ37598.1	AZJ37604.1	AZJ37599.1	AZJ37600.1	AZJ37602.1	AZJ37605.1
St Croix River virus	YP_052947.1	YP_052948.1	YP_052951.1	YP_052942.1	YP_052943.1	YP_052949.1	YP_052944.1	YP_052945.1	YP_052946.1	YP_052950.1
SLOV/2002/Australia/Mosquito				YP_002925132.1	YP_002925133.1					
Tribec virus	ADZ96222.1	ADZ96225.1	ADZ96228.1	ADZ96219.1	ADZ96220.1	ADZ96226.1	ADZ96223.1	ADZ96221.1	ADZ96224.1	ADZ96227.1
UMAV/1969/USA/Mosquito	AEE98371.1	AEE98374.1	AEE98374.1	AEE98368.1	AEE98369.1	AEE98375.1	AEE98370.1	AEE98372.1	AEE98373.1	
UMAV/2015/Australia/Mosquito	QCW07535.1	QCW07537.1	QCW07537.1	QCW07531.1	QCW07532.1	QCW07538.1	QCW07533.1	QCW07534.1	QCW07536.1	
Wad Medani virus	YP_009158886.1	YP_009158888.1	YP_009158892.1	YP_009158877.1	YP_009158883.1	YP_009158889.1	YP_009158885.1	YP_009158884.1	YP_009158887.1	YP_009158890.1
Wallal virus	YP_008658419.1	YP_008658425.1	YP_008658422.1	YP_008658416.1	YP_008658418.1	YP_008658420.1	YP_008658417.1	YP_008658423.1	YP_008658424.1	YP_008658421.1
Warrego virus	YP_009507733.1	YP_009507738.1	YP_009507732.1	YP_009507729.1	YP_009507730.1	YP_009507737.1	YP_009507735.1	YP_009507731.1	YP_009507736.1	YP_009507734.1
Yunnan orbivirus	YP_443929.1	YP_443931.1	YP_443934.1	YP_443925.1	YP_443926.1	YP_443932.1	YP_443927.1	YP_443928.1	YP_443930.1	YP_443933.1
SLOV/2018/USA/Mosquito	AZJ37612.1	AZJ37620.1		AZJ37607.1	AZJ37608.1	MK100585.1		AZJ37610.1	AZJ37612.1	AZJ37614.1
UMAV/2008/USA/Mosquito	AZJ37619.1			MK100587.1	AZJ37616.1			AZJ37618.1	AZJ37619.1	AZJ37621.1

Table S5. Pairwise identity percentages of amino acid sequences of Orbivirus RdRp and Orbivirus T2 (upper box: lower left and upper right, respectively) and Orbivirus T13 and Orbivirus OCP1 proteins (lower box: lower left and upper right, respectively).

Table S5. Pairwise identity percentages of amino acid sequences of Orbivirus RdRp and Orbivirus T2 (upper box: lower left and upper right, respectively) and Orbivirus OCP1 proteins (lower box: lower left and upper right, respectively).

RdRp (lower left) / T2 (upper right)

	UMAV/2019/Germany/Blackbird	UMAV/2019/Germany/Bluetit	UMAV/2019/Germany/GreatTit	SLOV/2018/USA/Mosquito	UMAV/2015/Australia/Mosquito	KHV/2011/Japan/Mosquito	SLOV/2002/Australia/Mosquito	UMAV/2008/USA/Mosquito	UMAV/1969/USA/Mosquito	Kammavanpettai virus	Corriparta virus	Peruvian_Horse_Sickness_virus	Big Cypress virus	Bluetongue virus	African horse sickness virus	Great Island virus	St Croix River virus
UMAV/2019/Germany/Blackbird		99.23	99.56	98.78	99.12	98.45	98.79	94.59	94.81	43.8	47.74	42.97	44.66	34.66	35.02	44.38	21.83
UMAV/2019/Germany/Bluetit	99.15		99.45	99.23	99.56	98.9	99.23	95.03	95.25	44	47.95	42.86	44.66	34.66	35.13	44.38	21.83
UMAV/2019/Germany/GreatTit	99.15	99.07		99	99.34	98.67	99.01	94.8	95.02	43.84	47.79	42.8	44.39	34.59	35.17	44.32	21.75
SLOV/2018/USA/Mosquito	99.35	99.35	99.17		99.67	99.23	100	95.14	95.36	43.8	48.06	42.8	44.76	34.88	35.35	44.54	21.83
UMAV/2015/Australia/Mosquito	98.14	98.15	98	98.15		99.12	99.67	95.47	95.69	43.8	47.95	42.8	44.66	34.88	35.35	44.54	21.83
KHV/2011/Japan/Mosquito	97.37	97.3	97.07	97.22	97.61		99.23	95.14	95.36	43.8	48.06	42.9	44.55	35.21	35.57	44.65	21.83
SLOV/2002/Australia/Mosquito	96.75	96.68	96.69	96.48	97.38	96		95.14	95.36	43.8	48.06	42.75	44.76	34.88	35.35	44.49	21.83
UMAV/2008/USA/Mosquito	89.54	89.44	89.52	89.27	89.53	88.91	87.99		99.56	44.42	47.95	43.12	43.92	35.43	35.68	43.88	22.16
UMAV/1969/USA/Mosquito	89.62	89.51	89.6	89.36	89.61	88.99	88.07	99.77		44.42	47.85	42.8	43.6	35.32	35.68	43.77	22.16
Kammavanpettai virus	63.83	63.77	63.57	63.56	63.36	63.36	62.06	63.75	63.9		46.11	42.02	45.67	33.68	34.83	42.65	22.62
Corriparta virus	58.08	57.97	57.92	58.73	58.03	58.11	57.19	58.65	58.8	57.96		44.6	47.53	34.94	35.36	43.34	21.93
Peruvian Horse Sickness virus	51.45	51.52	51.41	51.96	51.45	51.75	50.76	52.44	52.28	50.95	51.18		48.36	35.54	35.1	44.91	22.53
Big Cypress virus	54.74	54.72	54.75	55.23	55.01	54.71	53.96	54.86	54.86	55.35	54.15	50.68		33.55	35.24	46.03	22.64
Bluetongue virus	47.09	46.65	46.62	46.9	46.96	46.35	45.82	47.49	47.57	45.21	45.73	44.55	46.12		57.9	35.72	21.33
African horse sickness virus	48.09	47.87	47.84	48.36	47.95	47.65	47.12	47.65	47.57	47.92	46.68	46.82	47.82	55.16		35.31	21.57
Great Island virus	49.34	49.19	49.38	50.69	49.42	49.42	48.42	49.58	49.65	48.62	48.92	46.57	49.55	44.4	45.4		23.69
St Croix River virus	37.6	37.24	37.44	38.21	37.48	37.63	37.04	37.26	37.19	37.66	36.25	34.48	36.72	33.99	35.92	53.09	

T13 (lower left) / OCP1 (upper right)

	UMAV/2019/Germany/Blackbird	UMAV/2019/Germany/Bluetit	UMAV/2019/Germany/GreatTit	SLOV/2018/USA/Mosquito	UMAV/2015/Australia/Mosquito	KHV/2011/Japan/Mosquito	SLOV/2002/Australia/Mosquito	UMAV/2008/USA/Mosquito	UMAV/1969/USA/Mosquito	Kammavanpettai virus	Corriparta virus	Peruvian_Horse_Sickness_virus	Big Cypress virus	Bluetongue virus	African horse sickness virus	Great Island virus	St Croix River virus
UMAV/2019/Germany/Blackbird		57.77	48.58		47.88	58.11			60.44	11.19	13.71	11.29	11.96	8.34	7.15	6.92	8.01
UMAV/2019/Germany/Bluetit	100		47.04		47.4	86.83			55.94	12.24	13.49	11.35	12.11	7.92	6.77	7.76	7.95
UMAV/2019/Germany/GreatTit	100	100			47.81	47.11			48.39	10.76	13.27	11.33	11.3	6.16	6.85	6.64	7.59
SLOV/2018/USA/Mosquito	100	100	100														
UMAV/2015/Australia/Mosquito	96.85	96.86	96.87	96.87		45.28			48.34	11.9	13.04	11.35	11.74	7.74	6.58	6.76	8.34
KHV/2011/Japan/Mosquito	96.56	96.57	96.58	96.58	99.72				56.47	11.51	13.5	11.57	11.54	7.73	6.52	7.28	8.08
SLOV/2002/Australia/Mosquito																	
UMAV/2008/USA/Mosquito																	
UMAV/1969/USA/Mosquito	93.41	93.43	93.45	93.45	91.74	91.45				33.62	40.68	30.59	35.98	24.29	22.6	26.33	15.53
Kammavanpettai virus	33.52	33.43	33.62	33.62	33.33	33.05			33.62		30.4	26.5	27.64	19.37	18.87	20.45	12.96
Corriparta virus	41.76	41.64	41.81	41.81	40.96	40.96			40.68	30.4		33.33	35.31	23.58	22.75	30.45	19.16
Peruvian Horse Sickness virus	29.91	29.83	30.03	30.03	30.59	30.59			30.59	26.5	33.33		31.44	21.65	19.44	28.85	15.79
Big Cypress virus	37.04	36.93	37.11	37.11	37.11	37.11			35.98	27.64	35.31	31.44		24.22	23.38	29.97	18.16
Bluetongue virus	24.14	24.07	24.29	24.29	24	24			24.29	19.37	23.58	21.65	24.22		42.94	20.56	16.67
African horse sickness virus	21.88	21.81	22.03	22.03	21.47	21.47			22.6	18.87	22.75	19.44	23.38	42.94		22.28	17.37
Great Island virus	27.53	27.45	27.65	27.65	27.17	27.17			26.33	20.45	30.45	28.85	29.97	20.56	22.28		15.67
St Croix River virus	15.34	15.3	15.53	15.53	16.05	16.05			15.53	12.96	19.16	15.79	18.16	16.67	17.37	15.67	

Table S6. Accession numbers for different protein sequences (RNA dependent RNA polymerase/RdRp, glycoprotein precursor/GPC and nucleocapsid) of representative *Peribunyaviridae* virus strains and the outgroup Tomato spotted wilt virus. Virus acronym for each virus were also indicated.

Virus Family	Genera	Abbreviations	Virus Name	RdRp	GPC	Nucleocapsid
Peribunyaviridae	*Herbevirus*	HEBV	Herbert_virus	YP_009507855.1	YP_009507854.1	YP_009507853.1
		KIBV	Kibale_virus	YP_009362027.1	YP_009362035.1	YP_009362025.1
		TAIV	Tai_virus	YP_009362026.1	YP_009362028.1	YP_009362024.1
	Orthobunyavirus	AINOV	Aino_virus	YP_006590079.1	YP_006590070.1	YP_006590071.1
		AKTV	Akhtuba virus	AIL53813.1	AIL53814.1	AIL53815.1
		ALAJV	Alajuela_virus	YP_009507859.1	YP_009507856.1	YP_009507857.1
		AMBV	Anhembi_virus	YP_009666889.1	YP_009666890.1	YP_009666891.1
		ANADV	Anadyr_virus	ANB45710.1	ANB45709.1	ANB45707.1
		BAKV	Baakal_virus	QEO75948.1	QEO75949.1	QEO75950.1
		BATV	Batai_virus	AFY52608.1	AFY52604.1	AFY52615.1
		BELLV	Bellavista_virus	YP_009666954.1	YP_009666957.1	YP_009666955.1
		BIMV	Bimiti_virus	YP_009507866.1	YP_009507865.1	YP_009507867.1
		BIRV	Birao_virus	YP_009666996.1	YP_009666997.1	YP_009666994.1
		BOZOV	Bozo_virus	YP_009667001.1	YP_009666998.1	YP_009666999.1
		BRAZV	Brazoran_virus	AGS94386.1	AGS94385.1	AGS94383.1
		BUCRV	Buffalo_Creek_virus	AJD77610.1	AJD77609.1	AJD77608.1
		BUNV	Bunyamwera_virus	NP_047211.1	NP_047212.1	NP_047213.1
		BUTV	Buttonwillow_virus	YP_009666926.1	YP_009666928.1	YP_009666927.1
		BWAV	Bwamba_orthobunyavirus	YP_009362049.1	YP_009362064.1	YP_009362050.1
		CAIV	*Caimito_pacuvirus*	QCI62735	QCI62736.1	QCI62737.1
		CAPV	*Capim_orthobunyavirus*	ALP92388.1	ALP92389.1	ALP92390.1
		CATUV	Catu_virus	YP_009507870.1	YP_009507869.1	YP_009507868.1
		CEV	*California_encephalitis_orthobunyavirus*	APA29013	APA29014	APA29015.1
		CHIV	*Chilibre_pacuvirus*	QCI62738.1	QCI62739.1	QCI62740.1
		CPV	*Cachoeira_Porteira_orthobunyavirus*	AEZ35283	AEZ35284	AEZ35285.1
		CTQV	Cat_Que_virus	AXQ05038.1	AXQ05039.1	AXQ05040.1
		ENSV	Enseada_virus	YP_009666945.1	YP_009666942.1	YP_009666944.1
		FACV	Facey's_Paddock_virus	AHY22330.1	AHY22339.1	AHY22348.1
		FSV	Fort_Sherman_virus	YP_009666949.1	YP_009666946.1	YP_009666947.1
		GAMV	Gamboa_virus	YP_009507871.1	YP_009507872.1	YP_009507873.1
		GGV	Gan_Gan_virus	ALQ43836.1	ALQ43837.1	ALQ43838.1
		GJAV	Guajara_orthobunyavirus	YP_009507877.1	YP_009507876.1	YP_009507875.1
		GMAV	Guama_virus	YP_009507879.1	YP_009507878.1	YP_009507880.1
		GROV	Guaroa_virus	YP_009362061.1	YP_009362080.1	YP_009362058.1
		IACOV	Iaco_virus	YP_009666893.1	YP_009666892.1	YP_009666894.1
		ILEV	Ilesha_virus	YP_009666916.1	YP_009666915.1	YP_009666913.1
		INGV	Ingwavuma_virus	YP_009666917.1	YP_009666918.1	YP_009666919.1
		JATV	Jatobal_virus	YP_009666904.1	YP_009666903.1	YP_009666901.1
		JCV	Jamestown_Canyon_virus	YP_009666884.1	YP_009666885.1	YP_009666882.1
		KEYV	Keystone_virus	YP_009666964.1	YP_009666961.1	YP_009666962.1
		KHURV	Khurdun_virus	AHL27166.1	AHL27167.1	AHL27168.1
		KOOV	Koongol_virus	YP_009507885.1	YP_009507886.1	YP_009507887.1
		KOWV	Kowanyama_virus	AMR73391.1	AMR73392.1	AMR73393.1
		KRIV	Kairi_virus	YP_009507881.1	YP_009507882.1	YP_009507883.1
		LAKV	Lakamha_virus	QEO75951.1	QEO75952.1	QEO75953.1
		LMBV	Largemouth_bass_bunyavirus	QDJ95875.1	QDJ95876.1	QDJ95877.1
		LUKV	Lukuni_virus	YP_009507862.1	YP_009507860.1	YP_009507861.1
		LUMBV	Lumbo_virus	YP_009666968.1	YP_009666965.1	YP_009666966.1
		MADV	Madrid_virus	YP_009362071.1	YP_009362079.1	YP_009362072.1
		MAGV	Maguari_virus	ATJ04177.1	ATJ04178.1	ATJ04179.1
		MANV	Manzanilla_virus	AHY22334.1	AHY22343.1	AHY22352.1

Table S6. Accession numbers for different protein sequences (RNA dependent RNA polymerase/RdRp, glycoprotein precursor/GPC and nucleocapsid) of representative *Peribunyaviridae* virus strains and the outgroup Tomato spotted wilt virus. Virus acronym for each virus were also indicated.

Virus Family	Genera	Abbreviation	Virus Name	RdRp	GPC	Nucleocapsid
		MAPV	Mapputta_virus	AJD77604	AJD77603	AJD77602
		MCAV	Macaua_virus	AEZ35261.1	AEZ35262.1	AEZ35263.1
		MDV	Main_Drain_virus	AXP32030.1	AXP32031.1	AXP32032.1
		MELV	Melao_virus	YP_009666970.1	YP_009666969.1	YP_009666971.1
		MERV	*Mermet_orthobunyavirus*	AHY22335.1	AHY22344.1	AHY22353.1
		MIRV	Mirim_virus	APM83098.1	APM83099.1	APM83100.1
		MPKV	Maprik_virus	AJD77607	AJD77606	AJD77605
		MTBV	Marituba_virus	YP_009362068.1	YP_009362078.1	YP_009362069.1
		NDOV	Nyando_virus	YP_009362066.1	YP_009362065.1	YP_009362052.1
		NZV	Ness_Ziona_virus	QBH98892.1	QBH98893.1	QBH98894.1
		ORIV	Oriboca_virus	YP_009362043.1	YP_009362062.1	YP_009362044.1
		OROV	Oropouche_virus	NP_982304.1	NP_982303.1	NP_982305.1
		OYOV	Oyo_virus	AEE01391.1	AEE01390.1	AEE01389.1
		PATV	Patois_virus	AXP33560.1	AXP33566.1	AXP33555.1
		PEAV	Peaton_virus	YP_009666872.1	YP_009666873.1	YP_009666870.1
		POTV	Potosi_virus	YP_009666985.1	YP_009666984.1	YP_009666986.1
		SABOV	Sabo_virus	YP_009666875.1	YP_009666874.1	YP_009666876.1
		SANV	Sango_virus	YP_009666879.1	YP_009666878.1	YP_009666880.1
		SAV	San_Angelo_virus	YP_009666975.1	YP_009666976.1	YP_009666973.1
		SBV	Schmallenberg_virus	YP_009666911.1	YP_009666912.1	YP_009666909.1
		SDNV	Serra_do_Navio_virus	YP_009666980.1	YP_009666977.1	YP_009666978.1
		SEDV	Sedlec_virus	AXP32058.1	AXP32059.1	AXP32060.1
		SHUV	Shuni_orthobunyavirus	YP_009667053.1	YP_009667050.1	YP_009667051.1
		SIMV	Simbu_orthobunyavirus	YP_006590082.1	YP_006590085.1	YP_006590083.1
		SORV	Sororoca_virus	YP_009666895.1	YP_009666896.1	YP_009666897.1
		SSHV	Snowshoe_hare_virus	ABW87611.2	ABX47014.1	ABX89407.1
		TAHV	Tahyna_virus	ACF72885.1	ACF32415.1	ACF32417.1
		TATV	Tataguine_virus	YP_009666936.1	YP_009666937.1	YP_009666935.1
		TENV	Tensaw_virus	YP_009666865.1	YP_009666869.1	YP_009666866.1
		TETEV	Tete_orthobunyavirus	YP_009512923.1	YP_009512922.1	YP_009512924.1
		THIV	Thimiri_orthobunyavirus	AXP32070.1	AXP32071.1	AXP32072.1
		TNTV	Triniti_virus	AZM68667.1	AZM68673.1	AZM68670.1
		TPPV	Tapirape_virus	AIN55747.1	AIN55748.1	AIN55749.1
		TRUV	Trubanaman_virus	ALQ43839.1	ALQ43840.1	ALQ43841.1
		TVTV	Trivittatus_virus	ALI93835.1	ALI93834.1	ALI93832.1
		UMBV	Umbre_virus	YP_009664559.1	YP_009664558.1	YP_009664556.1
		UTIV	Utinga_virus	YP_009666923.1	YP_009666924.1	YP_009666925.1
		WBV	Wolkberg_virus	YP_009362987.1	YP_009362985.1	YP_009362986.1
		WITV	Witwatersrand_virus	YP_009667021.1	YP_009667022.1	YP_009667019.1
		WYOV	Wyeomyia_orthobunyavirus	YP_009512925.1	YP_009512926.1	YP_009512927.1
		ZEGV	Zegla_virus	YP_009667038.1	YP_009667039.1	YP_009667037.1
	Pacuvirus	CARV	*Caraparu_orthobunyavirus*	AGW82134.1	AGW82135.1	AGW82136.1
		CVV	Cache_Valley_virus	YP_009666950.1	YP_009666951.1	YP_009666952.1
		PACV	Pacui_virus	YP_009666929.1	YP_009666931.1	YP_009666930.1
		RPEV	Rio_Preto_da_Eva_virus	YP_009666934.1	YP_009666932.1	YP_009666933.1
		TCMV	Tacaiuma_orthobunyavirus	YP_009667044.1	YP_009667046.1	YP_009667045.1
	Shangavirus	SHUIV1	Shuangao_Insect_Virus_1	1_YP_009300681.1	1_YP_009300682.1	1_YP_009300683.1
	Unclassified	AKAV	Akabane_virus	YP_001497159.1	YP_001497160.1	YP_001497161.1
		ASUMV	Asum_virus	QGA70944	This study	This study
		BUBAV	Buffalo_bayou_virus	QFQ60707	NA	QFQ60708
		FULV	Fulton_virus	QEQ50490.1	QEQ50491.1	QEQ50492.1
		HEDV	Hedwig_virus	This study	This study	This study
		KKV	Kaeng_Khoi_virus	YP_009362074.1	YP_009362075.1	YP_009362076.1
		LCV	La_Crosse_virus	ABQ12631.1	ABQ12630.1	ABQ12628.1
		LEAV	Leanyer_virus	YP_009666888.1	YP_009666886.1	YP_009666887.1
Tospoviridae	*Orthotospovirus*	TSWV	Tomato_spotted_wilt_virus	NP_049362.1	NP_049359.1	NP_049361.1

Table S7. Pairwise identity percentages of amino acid sequences of nucleocapsid (top), glycoprotein precursor (middle) and RNA dependent RNA polymerase (bottom) proteins of representative Peribunyaviridae and and the outgroup Tomato spotted wilt virus. The corresponding acronyms and accession numbers of representative peribunyaviruses were shown in Table S2.

	BUNV	MAPV	BRAZV	CAIV	TAPV	CHIV	HEDV	ASUMV	SgIV-1	HEBV	TAIV	KIBV	KHURV	LAKV	FULV	LBBV	BUBAV	TSWV
BUNV																		
MAPV	36.86																	
BRAZV	30.25	26.02																
CAIV	25.53	25.63	21.43															
TAPV	30.64	28.15	25.94	67.62														
CHIV	30.51	25.52	23.13	58.2	57.38													
HEDV	22.27	20.68	19.86	22.54	24.59	23.27												
ASUMV	22.27	20.68	19.86	22.54	24.59	23.27	99.24											
SgIV-1	16.73	21.25	14.95	15.41	18.05	17.98	17.99	17.99										
HEBV	20.5	18.11	14.46	12.45	15.35	16.12	11.52	11.52	12.92									
TAIV	19.75	18.6	14.92	12.5	15.83	17.84	11.94	11.94	12.59	66.22								
KIBV	17.57	17.28	16.87	12.86	14.94	15.29	13.38	13.38	13.65	72.57	60.89							
KHURV	19.49	19.25	17.72	18.91	15.97	18.07	16.81	16.81	12.31	16.95	15.74	17.8						
LAKV	16.25	19.42	7.42	15.87	16.67	17.32	17	17	12.45	24.67	24.34	23.79	16.03					
FULV	13.67	13.8	15.51	13.18	15.05	16.43	14.5	14.5	10.9	13.91	11.97	13.51	13.19	8.63				
LBBV	16.8	12.85	13.21	13.13	14.67	15	12.81	12.46	11.74	15.42	14.23	13.33	17.57	14.06	19.49			
BUBAV	17.87	18.14	15.09	16.8	15.57	16.73	13.69	13.69	16.79	17.24	16.88	17.67	15.65	16.87	12.52	15.64		
TSWV	14.74	13.65	13.51	14.62	17.69	16.09	12.86	12.86	11.99	11.81	8.52	12.55	13.6	11.58	9.49	12.81	8.98	

Nucleocapsid

	BUNV	MAPV	BRAZV	CAIV	TAPV	CHIV	HEDV	ASUMV	SgIV-1	HEBV	TAIV	KIBV	KHURV	LAKV	FULV	LBBV	BUBAV	TSWV
BUNV																		
MAPV	30.44																	
BRAZV	31.85	28.63																
CAIV	27.28	26.68	27.01															
TAPV	27.59	25.42	25.56	60.92														
CHIV	27.47	25.97	26.81	59.02	58.5													
HEDV	24.14	22.06	23.64	22.16	22.04	20.9												
ASUMV	24.01	22.13	23.64	22.16	22.04	21.04	98.87											
SgIV-1	17.4	16.17	15.96	16.18	15.76	15.97	14.68	14.92										
HEBV	10.27	11.26	10.32	10.51	10.78	10.61	11.42	11.49	10.07									
TAIV	10.94	11.82	11.45	10.64	11.04	10.54	11.48	11.48	9.75	70.59								
KIBV	10.96	11.56	11.2	10.05	10.59	9.63	11.5	11.5	9.89	69.47	67.47							
KHURV	16.69	17.23	16.71	16.03	16.34	16.43	16.69	16.62	12.98	14.71	14.69	14.92						
LAKV	10.8	9.6	9.7	9.57	9.24	9.6	10.48	10.48	8.45	14.99	16.44	14.92	12.56					
FULV	11.06	11.7	10.59	10.24	10.09	10.46	10.46	10.25	9.38	7.56	7.89	7.96	10.24	7.92				
LBBV	11.42	10.23	11.21	9.92	9.41	10.44	10.47	10.47	8.54	10.67	11.01	10.76	12.44	11.14	11.39			
BUBAV																		
TSWV	11.74	11.34	11.08	11.34	11.21	10.42	10.74	10.68	9.42	9.74	9.56	10.6	12.5	9.4	9.7	10.25		

GPC

	BUNV	MAPV	BRAZV	CAIV	TAPV	CHIV	HEDV	ASUMV	SgIV-1	HEBV	TAIV	KIBV	KHURV	LAKV	FULV	LBBV	BUBAV	TSWV
BUNV																		
MAPV	48.74																	
BRAZV	48.74	46.4																
CAIV	43.63	41.34	43.35															
TAPV	43.53	41.39	43.28	76.52														
CHIV	42.29	40.54	43.2	71.11	70.13													
HEDV	36.06	37	37.33	36.1	35.83	36.94												
ASUMV	36.02	36.95	37.38	36.14	35.79	36.81	99.56											
SgIV-1	20.5	21.24	20.87	19.92	20.26	20.15	19.71	19.63										
HEBV	24.83	24.14	24.36	24.44	24.43	23.81	23.34	23.42	19.89									
TAIV	24.9	24.66	24.75	24.2	24.59	24.09	22.71	22.71	19.81	79.31								
KIBV	24.4	24.19	24.49	24.17	24.68	23.98	22.88	22.92	19.65	79.98	78.61							
KHURV	31.03	30.77	30.84	31.85	31.04	30.93	29.68	29.63	20.97	27.35	27.92	27.48						
LAKV	25.74	25.92	26.16	25.75	25.04	25.55	24.49	24.49	19.9	30.66	30.91	30.54	28.38					
FULV	19.16	18.24	18.79	18.4	18.09	17.83	19.19	19.19	15.09	17.81	17.84	17.88	18.52	16.68				
LBBV	21.36	20.16	20.73	20.98	20.79	20.99	20.61	20.7	15.89	20.14	19.94	19.87	23.29	19.37	17.22			
BUBAV	26.81	26.02	25.89	25.92	26.11	26.99	24.7	24.7	19.33	23.71	23.36	23.56	26.62	23.53	17.7	19.57		
TSWV	13.73	14.38	14.11	14.27	13.99	14.22	13.44	13.47	11.5	13.2	13.53	13.07	12.84	13.81	12.86	12.46	13.41	

RdRp

Table S8. Samples tested in RT-qPCR screening for Umatilla virus and Hedwig virus. RNA samples grouped to panel 1 belong to animal samples with representative organ/s processed using high throughput sequencing, while the remaining animal samples (without representative sample for sequencing) were categorized in panel 2. NT, not tested

Table S8. Samples tested in RT-qPCR screening for Umatilla virus and Hedwig virus. RNA samples grouped to panel 1 belong to animal samples with representative organ/s processed using high throughput sequencing, while the remaining animal samples (without representative sample for sequencing) were categorized in panel 2. NT, not tested

Sample code	Year	Panel number	Host (Common English name)	Organ	Hedwig virus (Old primers and probes) L-Seg	Hedwig virus (New primers and probes) L-Seg	S-Seg	Umatilla Virus Seg-5	Seg-1	Sample location; Federal States	Sample location; Specific details
ED-I-062/19	2019	1	Snowy Owl	heart	NT	neg	neg	neg	neg	Saxony-Anhalt	Tierpark Wittenberg
ED-I-079/18	2018	1	Snowy Owl	Brain	26.84	NT	NT	NT	NT	Berlin	Tierpark
ED-I-079/18	2018	1	Snowy Owl	Spleen	21.77	NT	NT	NT	NT		
ED-I-079/18	2018	1	Snowy Owl	Liver	22.6	NT	NT	NT	NT		
ED-I-079/18	2018	1	Snowy Owl	Heart	22.73	NT	NT	NT	NT		
ED-I-079/18	2018	1	Snowy Owl	Kidney	22.76	NT	NT	NT	NT		
ED-I-079/18	2018	1	Snowy Owl	Brain	25.18	NT	NT	neg	neg		
ED-I-079/18	2018	1	Snowy Owl	Spleen	18.06	19.06	19.69	neg	neg		
ED-I-082/18	2018	1	Goshawk	Brain	Neg	NT	NT	NT	NT	Saxony-Anhalt	Klein-Weißandt
ED-I-089/18	2018	1	Goshawk	Brain	neg	neg	neg	neg	neg	Saxony	Bad Düben
ED-I-083/19	2019	1	Great Grey Owl	liver	Neg	neg	neg	neg	neg	Saxony-Anhalt	
ED-I-085/19	2019	1	Snowy Owl	Brain	Neg	neg	neg	neg	neg	Berlin	Tierpark Berlin
ED-I-085/19	2019	1	Snowy Owl	Spleen	Neg	neg	neg	neg	neg		
ED-I-085/19	2019	1	Snowy Owl	Liver	Neg	neg	neg	neg	neg		
ED-I-085/19	2019	1	Snowy Owl	Kidney	neg	neg	neg	neg	neg		
ED-I-085/19	2019	1	Snowy Owl	Brain	neg	NT	NT	NT	NT		
ED-I-085/19	2019	1	Snowy Owl	Spleen	neg	NT	NT	NT	NT		
ED-I-085/19	2019	1	Snowy Owl	Liver	neg	NT	NT	NT	NT		
ED-I-085/19	2019	1	Snowy Owl	Kidney	neg	NT	NT	NT	NT		
ED-I-085/19	2019	1	Snowy Owl	liver	neg	NT	NT	neg	neg		
ED-I-087/19	2019	1	Blue Tit	brain	neg	NT	NT	27.43	29.13	Saxony-Anhalt	Halle (Saale)
ED-I-089/19	2019	1	Blue Tit	organ	neg	NT	NT	neg	37.03	Saxony	Radebeul
ED-I-090/18	2018	1	Great Grey Owl	Brain	neg	neg	neg	neg	neg	Bavaria	Wildpark Poing
ED-I-094/19	2019	1	Horse Spinal	Spinal cord	neg	NT	NT	neg	neg	Saxony	Landkreis Nordsachsen
ED-I-107/18	2018	1	Snowy Owl	Brain	25.24	NT	NT	NT	NT	Berlin	Tierpark
ED-I-107/18	2018	1	Snowy Owl	Liver	22.61	NT	NT	NT	NT		
ED-I-107/18	2018	1	Snowy Owl	Spleen	27.77	NT	NT	NT	NT		
ED-I-107/18	2018	1	Snowy Owl	Kidney	25.8	NT	NT	NT	NT		
ED-I-107/18	2018	1	Snowy Owl	Heart	28.51	NT	NT	NT	NT		
ED-I-107/18	2018	1	Snowy Owl	Lungs	25.99	NT	NT	NT	NT		
ED-I-107-18	2018	1	Snowy Owl	Brain	23.7	NT	NT	neg	neg		
ED-I-107-18	2018	1	Snowy Owl	Kidney	23.8	NT	NT	neg	neg		
ED-I-109/19	2019	1	Coconut lorikeet	Organ homogenate supernatant	neg	NT	NT	NT	NT	Saxony-Anhalt	Zoo Halle
ED-I-114/18	2018	1	Great Grey Owl	Organmix probe	neg	NT	NT	neg	neg	Bavaria	Wildpark Poing
ED-I-118/19	2019	1	Snowy Owl	Brain	42.42	NT	NT	neg	neg	Berlin	Tierpark
ED-I-118/19	2019	1	Snowy Owl	Spleen	36.08	NT	NT	neg	neg		
ED-I-118/19	2019	1	Snowy Owl	Liver	32.56	NT	NT	neg	neg		
ED-I-118/19	2019	1	Snowy Owl	Kidney	33.1	NT	NT	neg	neg		
ED-I-118/19	2019	1	Snowy Owl	Brain	34.48	NT	NT	NT	NT		
ED-I-118/19	2019	1	Snowy Owl	Spleen	31.92	33.54	31.41	NT	NT		
ED-I-118/19	2019	1	Snowy Owl	Liver	30.64	30.49	30.49	NT	NT		
ED-I-118/19	2019	1	Snowy Owl	Lung	32.46	32.97	32.22	NT	NT		
ED-I-118/19	2019	1	Snowy Owl	liver	29.04	NT	NT	neg	neg		
ED-I-125/19	2019	1	Inca Tern	liver	neg	NT	NT	NT	NT	Berlin	Zoo Berlin
ED-I-125/19	2019	1	Inca Tern	Brain	neg	neg	neg	neg	neg		
ED-I-125/19	2019	1	Inca Tern	Liver	neg	neg	neg	neg	neg		
ED-I-127/18	2018	1	Horse	Brain	neg	NT	NT	neg	neg	Brandenburg	Elbe-Elster-Kreis
ED-I-127/18	2018	1	Horse	Spinal cord	neg	NT	NT	neg	neg		
ED-I-127/18	2018	1	Horse	Spinal cord	neg	NT	NT	neg	neg		
ED-I-134/19	2019	1	Sparrow	Organ homogenate supernatant	neg	neg	neg	neg	neg	Saxony	Landkreis Nordsachsen
ED-I-135/19	2019	1	Eurasian Eagle-Owl	Organ homogenate supernatant	neg	neg	neg	neg	neg	Saxony	
ED-I-139/19	2019	1	Great Tit	heart/liver	neg	NT	NT	32.03	29.21	Saxony	04828 Bennewitz, Dresden,
ED-I-142/18	2018	1	Tawny Owl	Brain	neg	neg	neg	neg	neg	Saxony-Anhalt	06246 Bad Lauchstädt
ED-I-148/19	2019	1	Goshawk	heart	neg	neg	neg	neg	neg	Berlin	
ED-I-153/19	2019	1	Goshawk	brain	neg	neg	neg	neg	neg	Brandenburg	Brieselang
ED-I-155/19	2019	1	Goshawk	brain	neg	neg	neg	neg	neg	Brandenburg	Neuruppin
ED-I-156/19	2019	1	Goshawk	brain	neg	neg	neg	neg	neg	Berlin	
ED-I-157/19	2019	1	Snowy Owl	heart	neg	neg	neg	neg	neg	Berlin	Zoo Berlin
ED-I-158/19	2019	1	Andean Flamingo	heart	neg	neg	neg	neg	neg	Berlin	Zoo Berlin
ED-I-163/19	2019	1	Goshawk	brain	neg	NT	NT	31.53	28.11	Saxony-Anhalt	Sandersdorf,
ED-I-164/19	2019	1	Snowy Owl	liver	neg	neg	neg	neg	neg	Saxony-Anhalt	Zoo Magdeburg
ED-I-165/19	2019	1	Snowy Owl	liver	neg	neg	neg	neg	neg	Saxony-Anhalt	Zoo Magdeburg
ED-I-172/19	2019	1	Great Grey Owl	Organ homogenate supernatant	neg	NT	NT	NT	NT	Saxony	Tierpark Chemnitz
ED-I-173/19	2019	1	Great Grey Owl	Organ homogenate supernatant	neg	NT	NT	NT	NT	Saxony	Tierpark Chemnitz
ED-I-177/19	2019	1	Eurasian Golden Plover	Spleen/liver	neg	NT	NT	neg	neg	Saxony	Kamenz / Biehla
ED-I-201/19	2019	1	Humboldt-penguin	Heart	neg	NT	NT	neg	neg	Brandenburg	Tierpark Cottbus
ED-I-202/19	2019	1	Chilean flamingo	Organ homogenate supernatant	neg	neg	neg	neg	neg	Saxony	Zoo Leipzig
ED-I-205/19	2019	1	Great tit	Organ homogenate supernatant	neg	neg	neg	NT	NT	Saxony	Bad Düben,
ED-I-208/19	2019	1	Goshawk	brain	neg	NT	NT	36.44	34.02	Saxony-Anhalt	Stadt Merseburg,
M1705Usutu	2019	2	Black bird	Spleen	neg	neg	neg	neg	37.96	Baden Württemburg	Baden, Baden,
M1707Usutu	2019	2	Black bird	Spleen	neg	neg	neg	neg	neg	Baden Württemburg	

Sample code	Year	Panel number	Host (Common English name)	Organ	Hedwig virus (Old primers and probes)	Hedwig virus (New primers and probes)		Umatilla Virus		Sample location; Federal States	Sample location; Specific details
					L-Seg	L-Seg	5-Seg	Seg-5	Seg-1		
M1729Usutu	2019	2	Thrush	Spleen	neg	neg	neg	neg	neg	Baden Württemburg	
ViralM476	2020	2	Black bird	Spleen	neg	neg	neg	neg	neg	Baden Württemburg	Karlsruhe
ViralM477	2020	2	Black bird	Spleen	neg	neg	neg	neg	neg	Baden Württemburg	Heidelberg
ViralM478	2020	2	Black bird	Spleen	neg	neg	neg	31.54	38.63	Baden Württemburg	Heidelberg
ED-I-002/20	2019	2	Red-whiskered bulbul	Brain	NT	neg	neg	neg	neg	Berlin	Tierpark Berlin
ED-I-002/20	2019	2	Red-whiskered bulbul	Spleen	NT	neg	neg	neg	neg		
ED-I-003/20	2019	2	Bateleur	Brain	NT	neg	neg	neg	neg	Berlin	Tierpark Berlin
ED-I-003/20	2019	2	Bateleur	Spleen	NT	neg	neg	neg	neg		
ED-I-004/20	2019	2	Burrowing parrot	Brain	NT	neg	neg	neg	neg	Berlin	Tierpark Berlin
ED-I-004/20	2019	2	Burrowing parrot	Spleen	NT	neg	neg	neg	neg		
ED-I-005/20	2019	2	African openbill	Brain	NT	neg	neg	neg	neg	Berlin	Tierpark Berlin
ED-I-005/20	2019	2	African openbill	Spleen/Liver	NT	neg	neg	neg	neg		
ED-I-005/20	2019	2	African openbill	Kidney	NT	neg	neg	neg	neg		
ED-I-006/20	2019	2	African openbill	Brain	NT	neg	neg	neg	neg	Berlin	Tierpark Berlin
ED-I-006/20	2019	2	African openbill	Spleen	NT	neg	neg	neg	neg		
ED-I-007/20	2019	2	American flamingo	Brain	NT	neg	neg	neg	neg	Berlin	Tierpark Berlin
ED-I-007/20	2019	2	American flamingo	Spleen	NT	neg	neg	neg	neg		
ED-I-018/20	2020	2	Barn owl	Brain	NT	neg	neg	neg	neg	North Rhine Westphalia	59597 Erwitte-Weckinghausen
ED-I-018/20	2020	2	Barn owl	Liver	NT	neg	neg	neg	neg		
ED-I-030/20	2020	2	zoobird	Brain	NT	neg	neg	neg	neg	Lower Saxony	21224 Rosengarten
ED-I-030/20	2020	2	zoobird	Liver	NT	neg	neg	neg	neg		
ED-I-031/20	2020	2	zoobird	Brain	NT	neg	neg	neg	neg	Lower Saxony	21224 Rosengarten
ED-I-031/20	2020	2	zoobird	Liver	NT	neg	neg	neg	neg		
ED-I-032/20	2020	2	zoobird	Brain	NT	neg	neg	neg	neg	Lower Saxony	21224 Rosengarten
ED-I-032/20	2020	2	zoobird	Liver	NT	neg	neg	neg	neg		
ED-I-033/20	2020	2	Blue tit	Brain	NT	neg	neg	neg	neg	Mecklenburg West Pomerania	17493 Greifswald-Insel Riems
ED-I-033/20	2020	2	Blue tit	Liver/Kidney	NT	neg	neg	neg	neg		
ED-I-034/20	2020	2	Rook	Brain	NT	neg	neg	neg	neg	North Rhine Westphalia	59494 Soest
ED-I-034/20	2020	2	Rook	Liver	NT	neg	neg	neg	neg		
ED-I-035/20	2020	2	Eurasian Eagle Owl	Brain	NT	neg	neg	neg	neg	North Rhine Westphalia	58095 Hagen
ED-I-035/20	2020	2	Eurasian Eagle Owl	Liver	NT	neg	neg	neg	neg		
ED-I-052/20	2020	2	Northern hawk-owl	Brain	NT	25.66	25.05	neg	neg	Lower Saxony	Wingst,
ED-I-052/20	2020	2	Northern hawk-owl	Liver	NT	24.68	24.77	neg	neg		
ED-I-057/19	2019	2	Carrion crow	Liver	NT	neg	neg	neg	neg	North Rhine Westphalia	58313 Herdecke
ED-I-061/20	2020	2	Blackbird	Brain	NT	neg	neg	27.61	24.01	North Rhine Westphalia	Minden
ED-I-061/20	2020	2	Blackbird	Liver/Spleen	NT	neg	neg	28.44	25.12		
ED-I-062/20	2020	2	Blackbird	Brain	NT	neg	neg	neg	neg	Lower Saxony	31552 Rodenberg
ED-I-062/20	2020	2	Blackbird	Liver/Spleen	NT	neg	neg	neg	neg		
ED-I-063/20	2020	2	Blackbird	Brain	NT	neg	neg	neg	neg	North Rhine Westphalia	Bad Oeynhausen,
ED-I-063/20	2020	2	Blackbird	Liver/Spleen	NT	neg	neg	32455,00	28.67		
ED-I-064/20	2020	2	Blackbird	Brain	NT	neg	neg	neg	neg	Lower Saxony	Bad Nenndorf
ED-I-064/20	2020	2	Blackbird	Liver/Spleen	NT	neg	neg	34.69	29.97		
ED-I-066/20	2020	2	Blue tit	Brain	NT	neg	neg	neg	neg	Rhineland-Palatinate	54338 Schweich
ED-I-066/20	2020	2	Blue tit	Liver/Heart	NT	neg	neg	neg	neg		
ED-I-067/20	2020	2	Blue tit	Brain	NT	neg	neg	neg	neg	Rhineland-Palatinate	56754 Dünfus
ED-I-067/20	2020	2	Blue tit	Liver/Heart	NT	neg	neg	neg	neg		
ED-I-068/20	2020	2	Blackbird	Brain	NT	neg	neg	30.2	26.49	Lower Saxony	Stadthagen
ED-I-068/20	2020	2	Blackbird	Liver/Spleen	NT	neg	neg	29.7	27.07		
ED-I-069/20	2020	2	Blackbird	Brain	NT	neg	neg	neg	neg	Lower Saxony	31867 Lauenau
ED-I-069/20	2020	2	Blackbird	Liver/Spleen	NT	neg	neg	neg	neg		
ED-I-070/20	2020	2	Blackbird	Brain	NT	neg	neg	neg	neg	Lower Saxony	31629 Leeseringen
ED-I-070/20	2020	2	Blackbird	Liver/Spleen	NT	neg	neg	neg	neg		
ED-I-071/20	2020	2	Common starling	Brain	NT	neg	neg	neg	neg	Lower Saxony	31547 Münchenhagen
ED-I-071/20	2020	2	Common starling	Liver/Spleen	NT	neg	neg	neg	neg		
ED-I-072/20	2020	2	Blackbird	Brain	NT	neg	neg	neg	neg	Lower Saxony	31789 Hameln
ED-I-072/20	2020	2	Blackbird	Liver/Spleen	NT	neg	neg	neg	neg		
ED-I-073/20	2020	2	Song thrush	Brain	NT	neg	neg	neg	34.16	Lower Saxony	Sachsenhagen,
ED-I-073/20	2020	2	Song thrush	Liver/Spleen	NT	neg	neg	34.45	34.98		
ED-I-074/20	2020	2	Blackbird	Brain	NT	neg	neg	neg	neg	North Rhine Westphalia	32584 Löhne
ED-I-074/20	2020	2	Blackbird	Liver/Spleen	NT	neg	neg	neg	neg		
ED-I-075/20	2020	2	Blackbird	Brain	NT	neg	neg	neg	neg	Lower Saxony	49419 Wagenfeld
ED-I-075/20	2020	2	Blackbird	Liver/Spleen	NT	neg	neg	neg	neg		
ED-I-076/20	2020	2	Great tit	Brain	NT	neg	neg	neg	neg	Rhineland-Palatinate	55606 Meckenbach
ED-I-076/20	2020	2	Great tit	Liver/Heart	NT	neg	neg	neg	neg		
ED-I-077/20	2020	2	Blue tit	Brain	NT	neg	neg	neg	neg	Rhineland-Palatinate	55767 Brücken
ED-I-077/20	2020	2	Blue tit	Liver/Heart	NT	neg	neg	neg	neg		
ED-I-078/20	2020	2	Blue tit	Brain	NT	neg	neg	neg	neg	Rhineland-Palatinate	66871 Pfeffelbach
ED-I-078/20	2020	2	Blue tit	Liver/Heart	NT	neg	neg	neg	neg		
ED-I-079/20	2020	2	Blue tit	Brain	NT	neg	neg	neg	neg	Rhineland-Palatinate	55767 Wilzenberg
ED-I-079/20	2020	2	Blue tit	Liver/Heart	NT	neg	neg	neg	neg		

Sample code	Year	Panel number	Host (Common English name)	Organ	Hedwig virus (Old primers and probes)	Hedwig virus (New primers and probes)		Umatilla Virus		Sample location; Federal States	Sample location; Specific details
					L-Seg	L-Seg	S-Seg	Seg-5	Seg-1		
ED-I-080/18	2018	2	Song Thrush	Brain	neg	neg	neg	NT	NT	Berlin	Tierpark Berlin
ED-I-080/18	2018	2	Song Thrush	Spleen	neg	neg	neg	NT	NT		
ED-I-080/18	2018	2	Song Thrush	Kidney	neg	neg	neg	NT	NT		
ED-I-080/18	2018	2	Song Thrush	Spleen	neg	neg	neg	NT	NT		
ED-I-080/20	2020	2	Yellowhammer	Brain	NT	neg	neg	neg	neg	Rhineland-Palatinate	57610 Ingelbach
ED-I-080/20	2020	2	Yellowhammer	Liver/Heart	NT	neg	neg	neg	neg		
ED-I-081/20	2020	2	Blue tit	Brain	NT	neg	neg	neg	neg	Rhineland-Palatinate	57632 Rott
ED-I-081/20	2020	2	Blue tit	Liver/Heart	NT	neg	neg	neg	neg		
ED-I-082/20	2020	2	Blue tit	Brain	NT	neg	neg	neg	neg	Rhineland-Palatinate	57629 Streithausen
ED-I-082/20	2020	2	Blue tit	Liver/Heart	NT	neg	neg	neg	neg		
ED-I-083/20	2020	2	Blue tit	Brain	NT	neg	neg	neg	neg	Rhineland-Palatinate	57610 Altenkirchen
ED-I-083/20	2020	2	Blue tit	Liver/Heart	NT	neg	neg	neg	neg		
ED-I-088/19	2019	2	Black bird	Liver	neg	neg	neg	neg	neg	North Rhine Westphalia	58313 Herdecke
ED-I-088/19	2019	2	Black bird	Spleen	neg	neg	neg	neg	neg		
ED-I-088/19	2019	2	Black bird	Spleen	neg	neg	neg	neg	neg		
ED-I-093/19	2019	2	Black bird	Spleen	neg	neg	neg	28.04	24.87	Mecklenburg, West Pomerania	Roggentin,
ED-I-093/19	2019	2	Black bird	Liver	neg	neg	neg	29.02	24.51		
ED-I-093/19	2019	2	Black bird	Brain	neg	neg	neg	27.27	24.07		
ED-I-093/19	2019	2	Black bird	Lungs	neg	neg	neg	26.48	22.95		
ED-I-093/19	2019	2	Black bird	Kidney	neg	neg	neg	27.67	23.55		
ED-I-093/19	2019	2	Black bird	Heart	neg	neg	neg	27.14	23.68		
ED-I-093/19	2019	2	Black bird	Liver	neg	neg	neg	29.02	24.51		
ED-I-093/19	2019	2	Black bird	Liver	neg	neg	neg	29.08	23.87		
ED-I-093/19	2019	2	Black bird	Spleen	neg	neg	neg	28.04	24.87		
ED-I-110/19	2019	2	Blue-eyed black lemur	Brain	neg	neg	neg	neg	neg	Berlin	Tierpark Berlin
ED-I-110/19	2019	2	Blue-eyed black lemur	Spleen	neg	neg	neg	neg	neg		
ED-I-111/19	2019	2	Blue-eyed black lemur	Brain	neg	neg	neg	neg	neg	Berlin	Tierpark Berlin
ED-I-111/19	2019	2	Blue-eyed black lemur	Spleen	neg	neg	neg	neg	neg		
ED-I-112/19	2019	2	Blue-eyed black lemur	Liver	neg	neg	neg	neg	neg	Berlin	Tierpark Berlin
ED-I-112/19	2019	2	Blue-eyed black lemur	Spleen	neg	neg	neg	neg	neg		
ED-I-113/19	2019	2	Snow leopard	Spleen	neg	neg	neg	neg	neg	Berlin	Tierpark Berlin
ED-I-113/19	2019	2	Snow leopard	Liver	neg	neg	neg	neg	neg		
ED-I-114/19	2019	2	Snow leopard	Brain	neg	neg	neg	neg	neg	Berlin	Tierpark Berlin
ED-I-114/19	2019	2	Snow leopard	Spleen	neg	neg	neg	neg	neg		
ED-I-115/19	2019	2	Chinese merganser	Brain	32.91	22.96	23.3	neg	neg	Berlin	Tierpark Berlin
ED-I-115/19	2019	2	Chinese merganser	Spleen	34.32	23.13	23.69	neg	neg		
ED-I-115/19	2019	2	Chinese merganser	Liver	32.27	20.57	20.87	neg	neg		
ED-I-115/19	2019	2	Chinese merganser	Kidney	neg	24.29	24.85	neg	neg		
ED-I-116/19	2019	2	Black-tailed gull	Brain	neg	neg	neg	neg	neg	Berlin	Tierpark Berlin
ED-I-116/19	2019	2	Black-tailed gull	Spleen	neg	NT	NT	NT	NT		
ED-I-116/19	2019	2	Black-tailed gull	Liver	neg	neg	neg	neg	neg		
ED-I-117/19	2019	2	Javan pond heron	Brain	neg	neg	neg	neg	neg	Berlin	Tierpark Berlin
ED-I-117/19	2019	2	Javan pond heron	Liver	neg	neg	neg	neg	neg		
ED-I-119/19	2019	2	Black-tailed gull	Brain	neg	neg	neg	neg	neg	Berlin	Tierpark Berlin
ED-I-119/19	2019	2	Black-tailed gull	Liver	neg	neg	neg	neg	neg		
ED-I-119/19	2019	2	Black-tailed gull	Kidney	neg	neg	neg	neg	neg		
ED-I-119/19	2019	2	Black-tailed gull	Heart	neg	neg	neg	neg	neg		
ED-I-120/19	2019	2	American flamingo	Brain	neg	neg	neg	neg	neg	Berlin	Tierpark Berlin
ED-I-120/19	2019	2	American flamingo	Liver	neg	neg	neg	neg	neg		
ED-I-120/19	2019	2	American flamingo	Kidney	neg	neg	neg	neg	neg		
ED-I-120/19	2019	2	American flamingo	Heart	neg	neg	neg	neg	neg		
ED-I-126/19	2019	2	Snowy Owl	EDTA-Full blood	neg	neg	neg	neg	neg	Berlin	Tierpark Berlin
ED-I-127/19	2019	2	Snowy Owl	EDTA-Full blood	neg	neg	neg	neg	neg	Berlin	Tierpark Berlin
ED-I-128/19	2019	2	Snow leopard	EDTA-Full blood	neg	neg	neg	neg	neg	Berlin	Tierpark Berlin
ED-I-129/19	2019	2	Snow leopard	EDTA-Full blood	neg	neg	neg	neg	neg	Berlin	Tierpark Berlin
ED-I-167/18	2018	2	House Sparrow	Spleen	neg	neg	neg	NT	NT	Berlin	Berlin-Johannisthal
ED-I-168/18	2018	2	House Sparrow	Spleen	neg	neg	neg	NT	NT	Berlin	Berlin-Johannisthal
ED-I-169/18	2018	2	House Sparrow	Spleen	neg	neg	neg	NT	NT	Berlin	Berlin-Johannisthal
ED-I-170/18	2018	2	House Sparrow	Spleen	neg	neg	neg	NT	NT	Berlin	Berlin-Johannisthal
ED-I-171/18	2018	2	House Sparrow	Spleen	neg	neg	neg	NT	NT	Berlin	Berlin-Johannisthal
ED-I-172/18	2018	2	House Sparrow	Spleen	neg	neg	neg	NT	NT	Berlin	Berlin-Johannisthal
ED-I-173/18	2018	2	House Sparrow	Spleen	neg	NT	NT	NT	NT	Berlin	Berlin-Johannisthal
ED-I-174/18	2018	2	House Sparrow	Spleen	neg	NT	NT	NT	NT	Berlin	Berlin-Johannisthal
ED-I-180/19	2019	2	Black-tailed gull	Liver	neg	neg	neg	neg	neg	Berlin	Tierpark Berlin
ED-I-180/19	2019	2	Black-tailed gull	Kidney	neg	neg	neg	neg	neg		
ED-I-181/19	2019	2	African openbill	Liver	neg	neg	neg	neg	neg	Berlin	Tierpark Berlin
ED-I-181/19	2019	2	African openbill	Kidney	neg	neg	neg	neg	neg		
ED-I-182/19	2019	2	Cattle egret	Liver	neg	neg	neg	neg	neg	Berlin	Tierpark Berlin
ED-I-182/19	2019	2	Cattle egret	Kidney	neg	neg	neg	neg	neg		
ED-I-183/19	2019	2	Meller's duck	Liver	neg	neg	neg	neg	neg	Berlin	Tierpark Berlin
ED-I-183/19	2019	2	Meller's duck	Kidney	neg	neg	neg	neg	neg		

Table S8. Samples tested in RT-qPCR screening for Umatilla virus and Hedwig virus. RNA samples grouped to panel 1 belong to animal samples with representative organ/s processed using high throughput sequencing, while the remaining animal samples (without representative sample for sequencing) were categorized in panel 2. NT, not tested

Sample code	Year	Panel number	Host (Common English name)	Organ	Hedwig virus (Old primers and probes) L-Seg	Hedwig virus (New primers and probes) L-Seg	S-Seg	Umatilla Virus Seg-5	Seg-1	Sample location; Federal States	Sample location; Specific details
ED-I-184/19	2019	2	American flamingo	Liver	neg	20.93	24.14	neg	neg	Berlin	Tierpark Berlin
ED-I-184/19	2019	2	American flamingo	Kidney	neg	20.31	23.42	neg	neg		
ED-I-185/19	2019	2	Straw-necked ibis	Spleen	26.45	28.2	25	neg	neg	Berlin	Tierpark Berlin
ED-I-185/19	2019	2	Straw-necked ibis	Liver	28.62	30.5	29	NT	NT		
ED-I-186/19	2019	2	Mikado pheasant	Brain	neg	neg	neg	neg	neg	Berlin	Tierpark Berlin
ED-I-186/19	2019	2	Mikado pheasant	Spleen	neg	neg	neg	neg	neg		
ED-I-187/19	2019	2	White eared pheasant	Brain	neg	neg	neg	neg	neg	Berlin	Tierpark Berlin
ED-I-187/19	2019	2	White eared pheasant	Spleen	neg	neg	neg	neg	neg		
ED-I-187/19	2019	2	White eared pheasant	Liver	neg	neg	neg	neg	neg		
ED-I-187/19	2019	2	White eared pheasant	Kidney	neg	neg	neg	neg	neg		
ED-I-187/19	2019	2	White eared pheasant	Heart	neg	neg	neg	neg	neg		
ED-I-188/19	2019	2	Black-tailed gull	Brain	neg	neg	neg	neg	neg	Berlin	Tierpark Berlin
ED-I-188/19	2019	2	Black-tailed gull	Liver	neg	neg	neg	neg	neg		
ED-I-189/19	2019	2	Black-tailed gull	Brain	neg	neg	neg	neg	neg	Berlin	
ED-I-189/19	2019	2	Black-tailed gull	Liver	neg	neg	neg	neg	neg		
ED-I-190/19	2019	2	Mount Omei Liocichla	Brain	neg	neg	neg	neg	neg	Berlin	Tierpark Berlin
ED-I-190/19	2019	2	Mount Omei Liocichla	Liver	neg	neg	neg	neg	neg		
ED-I-191/19	2019	2	Baer's pochard	Brain	neg	neg	neg	neg	neg	Berlin	Tierpark Berlin
ED-I-191/19	2019	2	Baer's pochard	Liver	neg	neg	neg	neg	neg		
ED-I-192/19	2019	2	Mount Omei Liocichla	Brain	neg	neg	neg	neg	neg	Berlin	Tierpark Berlin
ED-I-192/19	2019	2	Mount Omei Liocichla	Liver	neg	neg	neg	neg	neg		
ED-I-193/19	2019	2	Black-tailed gull	Brain	neg	neg	neg	neg	neg	Berlin	Tierpark Berlin
ED-I-193/19	2019	2	Black-tailed gull	Liver	neg	neg	neg	neg	neg		
ED-I-195/19	2019	2	House sparrow	Spleen	neg	neg	neg	neg	neg	Berlin	Tierpark Berlin
ED-I-195/19	2019	2	House sparrow	Liver	neg	neg	neg	neg	neg		
ED-I-196/19	2019	2	House sparrow	Liver	neg	neg	neg	neg	neg	Berlin	Tierpark Berlin
ED-I-196/19	2019	2	House sparrow	Kidney	neg	neg	neg	neg	neg		
ED-I-199/19	2019	2	Kagu	Brain	neg	neg	neg	neg	neg	Berlin	Zoo Berlin
ED-I-199/19	2019	2	Kagu	Spleen	neg	neg	neg	neg	neg		
ED-I-199/19	2019	2	Kagu	Liver	neg	neg	neg	neg	neg		
ED-I-200/19	2019	2	Chilean flamingo	Brain	neg	neg	neg	neg	neg	Berlin	Zoo Berlin
ED-I-200/19	2019	2	Chilean flamingo	Liver	neg	neg	neg	neg	neg		
EDI-225/19	2019	2	Black bird	Liver	neg	neg	neg	neg	36.68	North Rhine Westphalia	58730 Fröndenberg in NRW, Westfalen,
EDI-225/19	2019	2	Black bird	Spleen	neg	neg	neg	35.74	33.99		
ED-I-225/19	2019	2	Black bird	Spleen	neg	neg	neg	35.74	33.99		
ED-I-225/19	2019	2	Black bird	Liver	neg	neg	neg	neg	36.68		
ED-I-225/19	2019	2	Black bird	Brain	neg	neg	neg	neg	36.68		
ED-I-225/19	2019	2	Black bird	Spleen	neg	neg	neg	32.17	29.49		
ED-I-245/19	2019	2	Black bird	Liver	neg	neg	neg	neg	neg	North Rhine Westpł	both juvenile black birds from 57074 Siegen (Kreis S
ED-I-246/19	2019	2	Black bird	Liver	neg	neg	neg	neg	neg	North Rhine Westphalia	
ED-I-259/19	2019	2	Reindeer	Spleen	neg	neg	neg	neg	neg	Berlin	Tierpark Berlin
ED-I-259/19	2019	2	Reindeer	Liver	neg	neg	neg	neg	neg		
ED-I-260/19	2019	2	Dromedary	Brain	neg	neg	neg	neg	neg	Berlin	Tierpark Berlin
ED-I-260/19	2019	2	Dromedary	Spleen	neg	neg	neg	neg	neg		
ED-I-261/19	2019	2	Muskox	Brain	neg	neg	neg	neg	neg	Berlin	Tierpark Berlin
ED-I-261/19	2019	2	Muskox	Spleen	neg	neg	neg	neg	neg		
ED-I-262/19	2019	2	Peccary	Brain	neg	neg	neg	neg	neg	Berlin	Tierpark Berlin
ED-I-262/19	2019	2	Peccary	Spleen	neg	neg	neg	neg	neg		
ED-I-263/19	2019	2	Alpaca	Brain	neg	neg	neg	neg	neg	Berlin	Tierpark Berlin
ED-I-263/19	2019	2	Alpaca	Spleen	neg	neg	neg	neg	neg		
ED-I-264/19	2019	2	Goral	Brain	neg	neg	neg	neg	neg	Berlin	Tierpark Berlin
ED-I-264/19	2019	2	Goral	Spleen	neg	neg	neg	neg	neg		
ED-I-265/19	2019	2	Meller's duck	Brain	neg	neg	neg	neg	neg	Berlin	Tierpark Berlin
ED-I-265/19	2019	2	Meller's duck	Heart	neg	neg	neg	neg	neg		
ED-I-266/19	2019	2	Meller's duck	Brain	neg	neg	neg	neg	neg	Berlin	Tierpark Berlin
ED-I-266/19	2019	2	Meller's duck	Spleen+Heart	neg	neg	neg	neg	neg		
ED-I-267/19	2019	2	Black-tailed gull	Spleen+Kidney	neg	neg	neg	neg	neg	Berlin	Tierpark Berlin
ED-I-267/19	2019	2	Black-tailed gull	Liver+Lung	neg	neg	neg	neg	neg		
ED-I-268/19	2019	2	Chilean flamingo	Brain	neg	neg	neg	neg	neg	Berlin	Tierpark Berlin
ED-I-268/19	2019	2	Chilean flamingo	Spleen	neg	neg	neg	neg	neg		
ED-I-269/19	2019	2	White eared pheasant	Brain	neg	neg	neg	neg	neg	Berlin	Tierpark Berlin
ED-I-269/19	2019	2	White eared pheasant	Spleen	neg	neg	neg	neg	neg		
ED-I-270/19	2019	2	American flamingo	Brain	neg	neg	neg	neg	neg	Berlin	Tierpark Berlin
ED-I-270/19	2019	2	American flamingo	Spleen	neg	neg	neg	neg	neg		
ED-I-271/19	2019	2	American flamingo	Brain	neg	neg	neg	neg	neg	Berlin	Tierpark Berlin
ED-I-271/19	2019	2	American flamingo	Spleen	neg	neg	neg	neg	neg		
ED-I-272/19	2019	2	Ferruginous duck	Brain	29.38	34.2	32.5	NT	NT	Berlin	Tierpark Berlin
ED-I-272/19	2019	2	Ferruginous duck	Spleen	30.49	29.4	32.5	neg	neg		
ED-I-273/19	2019	2	Black-tailed gull	Brain	neg	neg	neg	neg	neg	Berlin	Tierpark Berlin
ED-I-273/19	2019	2	Black-tailed gull	Spleen	neg	neg	neg	neg	neg		

Table S9. Results of reverse transcription quantitative polymerase chain reaction (RT-qPCR) Results for (A) Umatilla virus or (B) Hedwig virus specific screening in different cell cultures passages.

Inoculum	Cells	Passage number	days post infection	Cytopathic effect	CT values		HTS
A. Umatilla virus					Seg 1	Seg 5	
ED-I-93/19 Blackbird Liver	BHK-21 cells: 24 well plate	1	3	None	33.1	34.14	
Crude cell extracts from P1	BHK-21 cells: 24 well plate	2	3	None	NA	39.12	
Crude cell extracts from P2	BHK-21 cells: 24 well plate	3	3	None	NA	NA	
ED-I-93/19 Blackbird Spleen	BHK-21 cells: 24 well plate	1	3	None	34.61	34.82	
Crude cell extracts from P1	BHK-21 cells: 24 well plate	2	3	None	NA	38.47	
Crude cell extracts from P2	BHK-21 cells: 24 well plate	3	3	None	NA	NA	
ED-I-93/19 Blackbird Liver	Mosquito C6/36 cells: 24 well plate	1	7	Present	17.46	16.67	
Crude cell extracts from P1	Mosquito C6/36 cells: 24 well plate	2	7	Present	17.22	15.74	
Crude cell extracts from P2	Mosquito C6/36 cells: 24 well plate	3	7	Present	17.66	15.66	lib04217
ED-I-93/19 Blackbird Spleen	Mosquito C6/36 cells: 24 well plate	1	7	Present	34.29	34.52	
Crude cell extracts from P1	Mosquito C6/36 cells: 24 well plate	2	7	Present	37.81	36.05	
Crude cell extracts from P2	Mosquito C6/36 cells: 24 well plate	3	7	Present	35.65	35.29	
B. Hedwig virus					L-Segment	S segment	
ED-I 185/19 Straw necked-ibis Liver	Vero Cells B4 T12.5 Flask	1	5	Atypical		Neg	
ED-I 185/19 Straw necked-ibis Liver	C6/36 cells T12.5 Flask	1	5	None	37.46	Neg	
	C6/36 cells T12.5 Flask	1	6	None	Neg	Neg	
ED-I 185/19 Straw necked-ibis Liver	Vero Cells E6 T12.5 Flask	1	4	None	neg	Neg	
	Vero Cells E6 T12.5 Flask	1	6	None	neg	neg	
ED-I 185/19 Straw necked-ibis Liver	C6/36 cells T12.5 Flask	1	4	Atypical	neg	neg	
	C6/36 cells T12.5 Flask	1	6	Atypical	neg	neg	
ED-I 185/19 Straw necked-ibis Liver	BHK-21 T12.5 Flask	1	4	None	neg	neg	
	BHK-21 T12.5 Flask	1	6	None	neg	neg	
ED-I 185/19 Straw necked-ibis Kidney	Vero Cells B4 T12.5 Flask	1	4	Atypical	neg	neg	
ED-I 185/19 Straw necked-ibis Kidney	C6/36 cells T12.5 Flask	1	4	None	35.71	neg	
ED-I 185/19 Straw necked-ibis Kidney	Vero Cells E6 T12.5 Flask	1	4	None	neg	neg	
ED-I-272/19 Ferruginous duck spleen	Vero Cells E6 T12.5 Flask	1	4	None	neg	neg	
	Vero Cells E6 T12.5 Flask	1	6	None	neg	neg	
ED-I-272/19 Ferruginous duck spleen	C6/36 cells T12.5 Flask	1	4	Atypical	neg	neg	
	BHK-21 T12.5 Flask	1	4	None	neg	neg	
ED-I-272/19 Ferruginous duck spleen	C6/36 cells T12.5 Flask	1	6	Atypical	neg	neg	
	BHK-21 T12.5 Flask	1	6	None	neg	neg	
ED-I-115/19 Chinese merganser Liver	C6/36 cells T12.5 Flask	1	4	Atypical	32.23	33.56	
	C6/36 cells T12.5 Flask	1	6	Atypical	29.72	31.83	
ED-I-115/19 Chinese merganser Liver	BHK-21 T12.5 Flask	1	4	None	34.4	33.19	
	BHK-21 T12.5 Flask	1	6	None	36.79	37.36	
Supernatant from P1 ED-I-115/19	C6/36 cells T12.5 Flask	2	4	None	neg	Neg	
Chinese merganser Liver in C6/36 cells T12.5 Flask 6 dpi	C6/36 cells T12.5 Flask	2	5	None	neg	Neg	
	C6/36 cells T12.5 Flask	2	6	None	32.46	35.26	
	C6/36 cells T12.5 Flask	2	7	None	33.92	36.18	
Supernatant from P1 ED-I-115/19	BHK-21 T12.5 Flask	2	4	erminated earlier			
Chinese merganser Liver in C6/36 cells T12.5 Flask 6 dpi	BHK-21 T12.5 Flask	2	5	erminated earlier			
	BHK-21 T12.5 Flask	2	6	erminated earlier			
	BHK-21 T12.5 Flask	2	7	erminated earlier			
Supernatant from P2 ED-I-115/19	C6/36 cells T12.5 Flask	3	4	None	Neg	neg	
Chinese merganser Liver in C6/36 cells T12.5 Flask 6 dpi	C6/36 cells T12.5 Flask	3	5	None	39.55	neg	
	C6/36 cells T12.5 Flask	3	6	None	Neg	neg	
	C6/36 cells T12.5 Flask	3	7	None	39.83	neg	
Supernatant from P2 ED-I-115/19	Vero Cells E6 T12.5 Flask	3	4	None	Neg	neg	
Chinese merganser Liver in C6/36 cells T12.5 Flask 6 dpi	Vero Cells E6 T12.5 Flask	3	5	None	Neg	neg	
	Vero Cells E6 T12.5 Flask	3	6	None	Neg	neg	
	Vero Cells E6 T12.5 Flask	3	7	None	39.21	neg	
ED-I-52/20 Northern hawk-owl Brain	BHK-21 24 well plates	1	3	None			
Supernatant from P1 ED-I-52/20 Northern hawk-owl Brain BHK-21	BHK-21 24 well plates	2	3	None	Neg	neg	
Supernatant from P2 ED-I-52/20 Northern hawk-owl Brain BHK-21	BHK-21 24 well plates	3	3	None	Neg	neg	
ED-I-52/20 Northern hawk-owl Liver	BHK-21 24 well plates	1	3	None			
Supernatant from P1 ED-I-52/20 Northern hawk-owl Liver BHK-21	BHK-21 24 well plates	2	3	None	Neg	neg	
Supernatant from P2 ED-I-52/20 Northern hawk-owl Liver BHK-21	BHK-21 24 well plates	3	3	None	Neg	neg	
ED-I-52/20 Brain	BHK-21 24 well plates	1	3	None			
Supernatant from P1 ED-I-52/20 Northern hawk-owl Brain BHK-21	KC cells 24 well plates	2	7	None			
Supernatant from P2 ED-I-52/20 Northern hawk-owl Brain KC Cells	BHK-21 24 well plates	3	3	None	Neg	neg	
Supernatant from P3 ED-I-52/20 Northern hawk-owl Brain BHK-21	KC cells 24 well plates	4	7	None	Neg	neg	
ED-I-52/20 Brain	KC cells 24 well plates	1	7	None			
Supernatant from P1 ED-I-52/20 Northern hawk-owl Brain KC Cells	BHK-21 24 well plates	2	3	None	Neg	neg	
Supernatant from P2 ED-I-52/20 Northern hawk-owl Brain BHK-21	KC cells 24 well plates	3	7	None	Neg	neg	
ED-I-52/20 Liver	BHK-21 24 well plates	1	3	None			
Supernatant from P1 ED-I-52/20 Northern hawk-owl Liver BHK-21	KC cells 24 well plates	2	7	None			
Supernatant from P2 ED-I-52/20 Northern hawk-owl Liver KC Cells	BHK-21 24 well plates	3	3	None	Neg	neg	
Supernatant from P3 ED-I-52/20 Northern hawk-owl Liver BHK-21	KC cells 24 well plates	4	7	None	Neg	neg	
ED-I-52/20 Liver	KC cells 24 well plates	1	7	None			
Supernatant from P1 ED-I-52/20 Northern hawk-owl Liver KC Cells	BHK-21 24 well plates	2	3	None	Neg	neg	
Supernatant from P2 ED-I-52/20 Northern hawk-owl Liver BHK-21	KC cells 24 well plates	3	7	None	Neg	neg	

4. Own Contributions

(I) Kinsella C, <u>Santos PD</u>❦, Postigo-Hidalgo I❦, Folgueiras-González A❦, Passchier TC, Szillat KP❦, Akello JO❦, Álvarez-Rodríguez B❦, Martí-Carreras J❦. Preparedness needs research: how fundamental science and international collaboration accelerated the response to COVID-19. *PLOS Pathogens*. 2020 Oct 09; 16(10), e1008902. doi: 10.1371/journal.ppat.1008902.

❦ These authors contributed equally.

Cormac M. Kinsella:	Conceptualization and study design, review of related literatures, data analyses, manuscript writing, consolidation and organization of the review paper
<u>Pauline Dianne Santos:</u>	Conceptualization and study design, review of related literatures, data analyses, manuscript writing
Ignacio Postigo-Hidalgo:	Conceptualization and study design, review of related literatures, data analyses, manuscript writing
Alba Folgueiras-Gonzalez:	Conceptualization and study design, review of related literatures, data analyses, manuscript writing
Tim Casper Passchier:	Conceptualization and study design, review of related literatures, data analyses, manuscript writing
Kevin P. Szillat:	Conceptualization and study design, review of related literatures, data analyses, manuscript writing
Joyce Odeke Akello:	Conceptualization and study design, review of related literatures, data analyses, manuscript writing
Beatriz Alvarez Rodrıguez:	Conceptualization and study design, review of related literatures, data analyses, manuscript writing
Joan Martı-Carreras:	Conceptualization and study design, review of related literatures, data analyses, manuscript writing

(II)   Ziegler U[ℰ], <u>Santos PD[ℰ]</u>, Groschup MH, Hattendorf C, Eiden M, Höper D, Eisermann P, Keller M, Michel F, Klopfleisch R, Müller K, Werner D, Kampen H, Beer M, Frank C, Lachmann R, Tews BA, Wylezich C, Rinder M, Lachmann L, Grünewald T, Szentiks CA, Sieg M, Schmidt-Chanasit J, Cadar D[ℰ], Lühken R[ℰ]. West Nile Virus Epidemic in Germany Triggered by Epizootic Emergence, 2019. *Viruses*. 2020 Apr 15; 12(4), 448. doi: 10.3390/v12040448.

[ℰ] These authors contributed equally.

Ute Ziegler:	Conceptualization and study design, case reports for WNV, processing of bird and horse samples for RT-qPCR and serological screening, RT-qPCR assays, serological screening, data interpretation, preparation of original manuscript draft, and study coordination
<u>Pauline Dianne Santos:</u>	Conceptualization and study design, preparation of samples and libraries for sequencing, WNV whole-genome sequencing using generic high-throughput sequencing approach, phylogenetic analyses via maximum likelihood and Bayesian MCC approaches, analyses of selection pressure, data interpretation, formatting of sequences for depositing in public repositories, and preparation of original manuscript draft
Martin H. Groschup:	Conceptualization and study design, formal analysis, investigation, writing—original draft preparation, and study coordination
Carolin Hattendorf:	Methodology, Investigation, Resources
Martin Eiden:	Methodology, Investigation, Resources
Dirk Höper:	Conceptualization and study design, formal analysis, investigation, writing—original draft preparation, and study coordination
Philip Eisermann:	Methodology, Investigation, Resources
Markus Keller:	Methodology, Investigation, Resources
Friederike Michel:	Case reports for WNV, processing of bird and horse samples for RT-qPCR and serological screening, RT-qPCR, serological screening, investigation
Robert Klopfleisch:	Methodology, Investigation, Resources
Kerstin Müller:	Methodology, Investigation, Resources
Doreen Werner:	Methodology, Investigation, Resources
Helge Kampen:	Mosquito samples collection, WNV RT-qPCR screening
Martin Beer:	Conceptualization and study design, writing—original draft preparation, and study coordination
Christina Frank:	Methodology, Investigation, Resources
Raskit Lachmann:	Methodology, Investigation, Resources
Birke Andrea Tews:	Investigation, virus propagation in cell culture, WNV RT-qPCR screening

Claudia Wylezich:	Probe-based target enrichment of samples with high Cq values for WNV, high-throughput sequencing, sequence data analyses, mapping analyses of WNV whole-genome sequences
Monika Rinder:	Provision of samples
Lars Lachmann:	Provision of samples
Thomas Grünewald:	Provision of samples
Claudia A. Szentiks:	Provision of samples
Michael Sieg:	Provision of samples
Jonas Schmidt-Chanasit:	Conceptualization and study design, data interpretation, preparation of original manuscript draft
Daniel Cadar:	Conceptualization and study design, Phylogenetic analyses, phylogeography, and spatiotemporal dynamics, population dynamics, protein changes, analyses of selection pressure, preparation of original manuscript draft
Renke Lühken:	Conceptualization and study design, Spatial risk analyses, Conceptualization and study design, data interpretation, preparation of original manuscript draft, consolidation of the manuscript

All authors took part in writing and editing of the manuscript.

(III)   <u>Santos PD</u>, Michel F, Wylezich C, Höper D, Keller M, Holicki CM, Szentiks CA, Eiden M, Muluneh A, Neubauer-Juric A, Thalheim S, Globig A, Beer M, Groschup MH, Ziegler U. Co-Infections: Simultaneous Detections of West Nile Virus and Usutu Virus in Birds from Germany. *Transboundary and Emerging Diseases.* 2021 Mar 02; Volume 00, Article 1-17, Online ahead of print. doi: 10.1111/tbed.14050.

<u>Pauline Dianne Santos:</u>	Conceptualization and study design, preparation of samples for sequencing, WNV and USUV RT-qPCR screening of samples for sequencing, USUV-specific multiplex PCR for targeted high-throughput sequencing, Sanger sequencing, sequence data analyses, mapping analyses of viral whole-genomes, reconstruction of maximum likelihood phylogenetic tree, data interpretation, formatting of sequences for depositing in public repositories, preparation of original manuscript draft and visualization
Friederike Michel:	Case reports for WNV and USUV, processing of bird samples for RT-qPCR and serological screening, RT-qPCR, serological screening, investigation
Claudia Wylezich:	Probe-based target enrichment of samples with high Cq values for WNV, high-throughput sequencing sequence data analyses, mapping analyses of full genomes
Dirk Höper:	Conceptualization and study design, formal analysis, investigation, manuscript preparation, study coordination, project administration
Markus Keller:	Methodology, Software, Investigation
Cora M. Holicki:	Investigation
Claudia A. Szentiks:	Investigation, Resources
Martin Eiden:	Methodology, Investigation
Aemero Muluneh:	Methodology, Investigation, Resources
Antonie Neubauer-Juric:	Methodology, Investigation, Resources
Sabine Thalheim:	Methodology, Investigation, Resources
Anja Globig:	Methodology, Investigation, Resources
Martin Beer:	Conceptualization and study design, study coordination, funding acquisition, data interpretation
Martin H. Groschup:	Conceptualization and study design, study coordination, funding acquisition
Ute Ziegler:	Conceptualization and study design, case reports for WNV and USUV co-infected birds, processing of bird samples for RT-qPCR and serological screening, environmental investigation, RT-qPCR assays, serological screening, data interpretation, original manuscript draft preparation, study coordination, and project administration

(IV)   <u>Santos PD</u>, Ziegler U, Szillat K, Szentiks CA, Birte Strobel, Skuballa J, Merbach S, Grothmann P, Tews BA, Beer M, Höper D. In Action – An Early Warning System for the Detection of Unexpected or Novel Pathogens. *Virus Evolution*. 2021 Sep 25; Volume 7, Issue 2. doi: 10.1093/ve/veab085.

<u>Pauline Dianne Santos:</u>	Conceptualization and study design, metagenomic analyses of generic HTS datasets derived from WNV outbreak samples, mapping and *de-novo* assembly of viral whole-genome sequences, primer and probe design, RT-qPCR screening in samples, phylogenetic analyses, data interpretation, HEDV isolation attempt, sample and library preparation for sequencing and re-sequencing, original manuscript draft preparation and visualization, and study coordination
Ute Ziegler:	Conceptualization and study design, case reports for WNV-infected birds and horses, processing of bird and horse samples, RT-qPCR assay, data interpretation, cell culture propagation of HEDV, and study coordination
Kevin Szillat:	Cell culture propagation of UMAV
Claudia A. Szentiks:	Provision of samples and necropsy reports, investigation
Birte Strobel	Provision of samples and necropsy reports, investigation
Jasmin Skuballa:	Provision of samples and necropsy reports, investigation
Sabine Merbach:	Provision of samples and necropsy reports, investigation
Pierre Grothmann:	Provision of samples, investigation
Birke Andrea Tews:	Investigation, virus propagation in cell culture, WNV RT-qPCR screening
Martin Beer:	Conceptualization and study design, data interpretation and discussion
Dirk Höper:	Conceptualization and study design, manuscript preparation, data interpretation and discussion, and study coordination

In agreement:

_____   _____   _____

Prof. Dr. Dr. h.c. Thomas C. Mettenleiter   Prof. Dr. Martin Beer   Pauline Dianne Santos

5. Results and Discussion

Early warning systems (EWS) and outbreak investigations are two effective approaches for mitigating and preventing future infectious disease outbreaks. In this thesis, a unified and generic pipeline was established for outbreak investigation and surveillance of novel and unexpected pathogens using high-throughput sequencing (HTS) approaches, bioinformatics, and virus characterization techniques (Figure 4). As a proof-of-concept, this unified pipeline evaluated generic HTS datasets derived from the 2018-19 West Nile virus (WNV) epidemic accompanied by the ongoing Usutu virus (USUV) epizooty in Germany [Publication II].
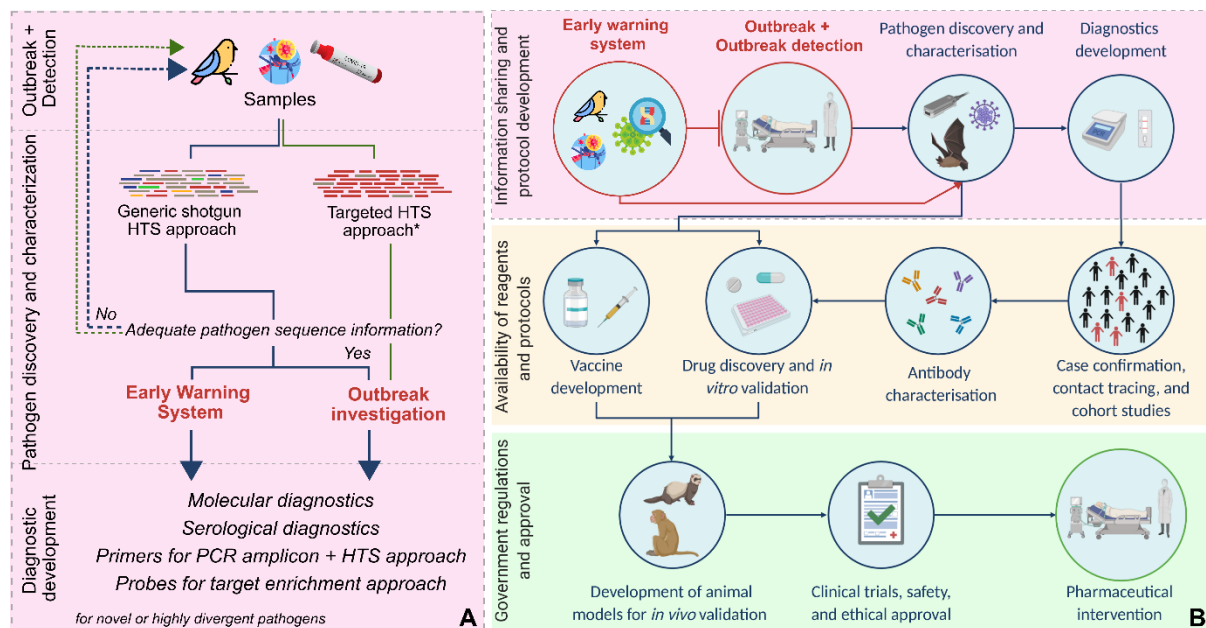
FIGURE 4. The proposed model for the enhanced outbreak investigation. A. The unified and generic pipeline for outbreak investigation and the early warning system (EWS). Violet lines indicate analyses that can be performed using generic HTS datasets, and green lines indicate possible analyses using targeted HTS datasets (*i.e.,* target enrichment HTS approach, PCR amplicon HTS approach). *Datasets generated using the target enrichment HTS approach can also be utilized for the EWS. B. The proposed addition of the unified pipeline for outbreak investigation and EWS in key response to viral outbreaks. Figure 4B was modified from Kinsella et al. [Publication I, Figure 1] under CC BY 4.0 (https://creativecommons.org/licenses/by/4.0/).

Outbreak samples (n=39) with sufficient WNV viral loads (quantitation cycle or C_q values ≤20) or with interesting conditions (*e.g.,* horse samples, samples with USUV co-infection) were selected for the generic HTS approach to yield WNV whole-genome sequences. Overall, WNV whole-genome sequences were obtained from 34 generic HTS datasets [Publication II], while five generic HTS datasets have 0-16 WNV sequence reads [Publication IV]. In this study, WNV whole-genome sequences were assembled from generic HTS datasets with >500 WNV sequence reads. Selected generic HTS datasets (*e.g.,* with few WNV sequences or samples with suspected USUV co-infection) were examined using a metagenomic analysis tool to check for other potential pathogens that may have caused infections in corresponding birds and horses (Figure 4, violet line). Interestingly, sequence reads from USUV and an unclassified

peribunyavirus were also detected in these tested HTS datasets. Hence, an EWS utilizing repurposed generic HTS datasets was established since these datasets can contain abundant sequence information from novel, unexpected, and silently circulating pathogens [Publication IV].

Generic HTS libraries that yield insufficient virus sequences can be subjected to re-sequencing to generate more sequence reads and complete viral genome sequences. However, re-sequencing the same HTS libraries can be costly, especially when these libraries were derived from samples with low virus-to-host nucleic acid (NA) ratios. For example, only five WNV sequence reads were detected in datasets derived from snowy owl #1 samples (lib03038:lib03039), consisting of 11,308,585 sequence reads [Publication IV]. Therefore, re-sequencing these libraries to acquire the WNV whole-genome sequence is impractical, and other HTS approaches should be considered.

The virus enrichment approach for HTS can also involve the propagation of virus-positive samples in cell culture. However, virus cultivation can be time-consuming, labor-intensive, and the virus may not successfully replicate in cell culture [119,123]. For example, USUV failed to replicate in the Vero B4 cell culture after attempting to co-propagate WNV and USUV [Publication III, Table S4]. As a result, only WNV sequence reads were detected in the HTS dataset derived from harvested cell culture supernatant inoculated with a WNV and USUV double-positive tissue sample (5 days post-infection).

This study employed two established targeted HTS approaches to generate viral whole-genome sequences of samples with low viral loads [reviewed in 50]. In particular, the probe-based target-enrichment HTS approach [64] was utilized to improve WNV sequence detection in six generic sequencing libraries [Publications II and III] and the USUV-specific multiplex PCR-HTS approach [68] was applied on samples with WNV and USUV co-infection. These respective targeted approaches yielded three WNV whole-genome sequences, three WNV partial genome sequences, five USUV whole-genome sequences, and one nearly complete USUV genome sequence [Publications II and III]. Hence, these targeted HTS approaches were incorporated in the unified pipeline as supplementary methods for acquiring viral genome sequences (Figure 4, green line).

Both targeted HTS approaches have higher sensitivity in sequencing target viruses than the generic HTS approach. The PCR amplicon-HTS approach is typically pathogen species-specific; however, few mismatches between target genomes and primers can prevent successful amplification. On the contrary, the probe-based target-enrichment HTS approach can simultaneously enrich several virus species [reviewed in 50]. For instance, Wylezich and colleagues [64] designed a probe panel targeting >30 viral pathogen sequences and reported the simultaneous enrichment of different virus species in a sequencing library. However, the latter

was not utilized for USUV genome sequencing since USUV-specific probes were not included in this specific panel [64]. In general, datasets produced using targeted HTS approaches are not optimal for the screening part of the proposed EWS due to their limited ability to sequence novel and highly divergent pathogens [reviewed in 50]. Nevertheless, datasets from the target enrichment HTS approach can still contain sequences from novel viruses with low sequence identities to the probe panel since this approach can tolerate a few mismatches between probes and target sequences [64]. Thus, these datasets should also be investigated using the EWS.

This unified pipeline delivered viral whole-genome sequences that facilitated the genomic-based investigation of the 2018-19 WNV epidemic in Germany using phylogenetic and phylogeographic analyses [Publication II] and presented substantial evidence for WNV and USUV co-infection in avian hosts [Publication III; see section 5.1]. In addition, the EWS detected sequences from USUV and other potential pathogens using the same generic HTS datasets derived from the WNV epidemic. Among these sequences, two new viruses were further characterized using genomic analyses, molecular-based screening, and virus cultivation [Publication IV, see section 5.2]. This thesis recommends incorporating the unified and generic workflow in the key response to viral outbreaks [Publication I] to enhance the outbreak preparedness and response strategy (Figure 4).

5.1 HTS-based outbreak investigation: a response to the West Nile virus epidemic accompanied by a Usutu virus epizooty in Germany 2018-19

In 2018, WNV-infection in birds and horses was reported for the first time in Germany, followed by the emergence of a WNV epidemic the following year. The WNV epidemic caused considerably higher numbers of infected birds and horses, and the first autochthonous human cases and WNV-positive mosquito samples were reported [Publication II]. The WNV epizooty and epidemic overlapped with the ongoing USUV epizooty in Germany. USUV has been circulating since 2010 [124–128]. Six suspected WNV and USUV co-infection cases in birds were reported during the first two years of WNV and USUV co-circulation in Germany. These samples have high USUV-specific C_q values (28.76-37.83), with two samples considered "possible" USUV-positive (C_q values > 37). Hence, WNV and USUV genome sequences were obtained to present the first reliable evidence for flavivirus co-infection in captive and wild birds [Publication III].

The wild and resident bird monitoring study from 2017-18 was the latest published information regarding the USUV epizooty in Germany [129]. Hence, phylogenetic analyses of USUV partial and whole-genome sequences provide preliminary insights regarding the 2019 USUV epizooty in Germany. These phylogenies exhibited the further dispersal of the USUV lineage Africa 3 and the probable overwintering of USUV lineage Europe 2 in Germany. However, phylogenetic inferences using USUV partial envelope gene sequences were

insufficient to trace the immediate origin of the USUV lineage Africa 3. Moreover, a comprehensive genomic epidemiology investigation for USUV epizooty was not performed in Publication III since only six samples were sequenced out of >1,200 USUV-positive cases in Germany from 2018-19. Additionally, only partial envelope sequences were available from the 2017-18 USUV epizooty in Germany [129].

In contrast, the phylogenetic and phylogeographic inferences allow comprehensive analyses of the 2018-19 WNV epidemic in Germany. West Nile virus variants involved in this epidemic belonged to the Central and Eastern European clade (CEC) and branched into six distinct subclades. The majority of the German WNV variants clustered into a well-defined monophyletic subclade named the "Eastern German Clade (EGC)," including viruses derived from humans, mosquitoes, birds with WNV and USUV co-infection, and a horse [Publications II and III].

It was hypothesized that the WNV EGC subclade was introduced to Germany as a single introduction event [Publication II]; therefore, branching within the WNV EGC subclade was further investigated using two phylogenetic inferences (Figure 5). Interestingly, the ML phylogenetic tree demonstrated six distinct branches with reliable bootstrap replicates (≥70%) within the WNV EGC subclade, and minimal substitutions per site were observed among WNV EGC variants (Figure 5C). In contrast, the Bayesian MCC inference exhibited four distinct branches with only one internal node having a significant posterior probability value (pp ≥0.9; Figure 5D). These two phylogenetic trees demonstrated almost similar topologies except for two differences. First, WNV variants that clustered in the WNV EGC branch 3 of the Bayesian MCC tree were found in three distinct branches (3.1 -3.3) of the ML phylogenetic tree. Second, the WNV LR743430 had inconsistent clustering between these phylogenetic trees (Figure 5; red dot). These inconsistencies probably arise due to the low frequency of nucleotide substitutions among WNV EGC variants. Furthermore, the factor of time and location were included in the reconstruction of the Bayesian MCC tree.

These phylogenetic inferences provide hints that the WNV EGC subclade was more likely introduced to Germany in multiple introduction events. For example, WNV EGC branch 1 variants are relatively divergent compared to other WNV EGC variants (Figure 5C). Moreover, the most recent common ancestor (MRCA) between branch 1 variants and branches 2-4 variants was estimated to exist around 2012 (Figure 5D). Thus, if the WNV EGC subclade was introduced to Germany in a single event, then the MRCA of WNV EGC variants should have circulated in Germany some years before the first report of WNV-infection in 2018. However, this assumption is highly unlikely since the nationwide surveillance network, which systematically monitors WNV in birds, horses and mosquitoes, reported all WNV-negative results until 2018 [124–132].
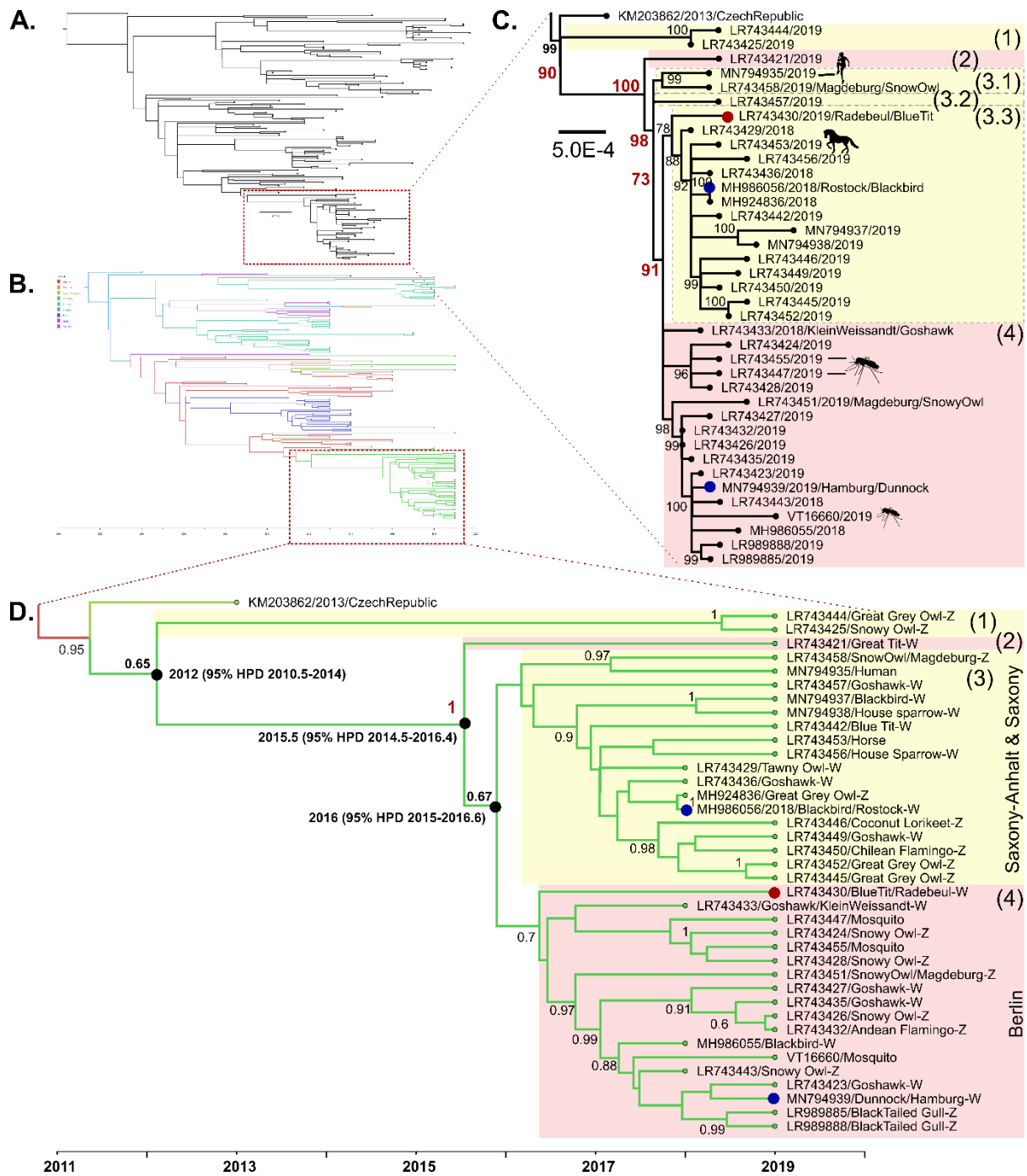
Figure 5. Phylogenetic inferences of European West Nile virus (WNV) lineage 2 complete coding sequences. Overview of maximum likelihood phylogenetic tree (A.) and Bayesian maximum credibility clade phylogenetic tree (B.) using European WNV lineage 2 sequences. (C.) Magnified view of maximum likelihood phylogenetic tree focusing WNV Eastern German clade variants. Scale bar indicates units of substitutions per site. Tip labels include the accession number and sample collection year. Sample locations were also included in variants collected >200 kilometers (blue dot) from the location of clusters and the variant with inconsistent clustering. Bootstrap values ≥70% were shown and significant values are highlighted in red. Figures showed the host species origin of the WNV sequences; otherwise, WNV sequences were acquired from avian hosts. (D.) Magnified view of Bayesian maximum credibility clade phylogenetic tree focusing WNV Eastern German clade variants. The scale at the bottom of the tree represents calendar years. Tip labels include accession number, host species and bird habitat: Z – zoo birds and W – wild bird. Sample locations were also included in variants collected >200 kilometers from the location (blue dot; labeled in the box) of clusters and the variant with inconsistent clustering. Posterior probabilities ≥60% were shown and significant values are highlighted in red. The estimated time to the most recent common ancestor (MRCA) of three nodes were shown with 95% posterior time intervals in parentheses (HPD -highest posterior density). Regarding the main differences of these trees: Distinct branches in this phylogenetic tree were indicated by numbers 1-4. Variants that clustered in the WNV EGC branch 3 in the Bayesian MCC tree were distributed in three distinct branches in ML phylogenetic tree WNV EGC branches 3.1-3.3. A red dot indicated the variant that inconsistently clustered in two phylogenies. Images of samples were acquired from Pixabay under the Pixabay license (https://pixabay.com/service/terms/#license).

Therefore, WNV EGC branch 1 variants are most likely transferred to Germany in a separate and recent introduction event.

Furthermore, the Bayesian MCC tree also suggested that WNV EGC branch 2-4 variants were introduced to Germany in multiple introduction events (Figure 5D). The MRCA of WNV EGC branch 2-4 variants was estimated to exist around May/June 2015, while WNV EGC branch 3-4 variants' MRCA probably existed around 2016. However, uncertainties of these calculated ages overlapped, as shown by 95% HPD values in nodes 2 and 3. Moreover, unknown factors may increase these uncertainties (Figure 5D). Given these data, probable locations and ages of these MRCA and the number of WNV EGC introduction events in Germany cannot be precisely estimated.

The majority of WNV EGC branch 3 (3.1-3.3) and branch 4 variants were detected in clusters of WNV cases (hotspot areas) in Saxony and Saxony Anhalt (branch 3), and Berlin (branch 4; Figure 5D). These geographical clustering can indicate that their progenitors successfully caused localized outbreaks. Moreover, very few variants from these branches were detected >200 km outside of these clusters, *i.e.,* MH986056 (Rostock) and MN794939 (Hamburg). WNV MH986056 and MN794939 were detected in a blackbird and a dunnock, categorized as both resident and partial migrant birds [130,133]. These birds potentially got infected within these WNV-infection hotspot areas and dispersed these WNV variants to Rostock and Hamburg during migration. Thus, bird migration and movement patterns should be monitored in more detail to understand the local WNV dispersal.

As of 2019, progenitors of WNV EGC branches 3 and 4 variants can be considered the most successful WNV German variants for causing local WNV outbreaks. However, which factors made them more successful than other WNV EGC variants? In genetic factors, WNV German variants have low and homogenous genetic variations across their genomes, although the WNV EGC subclade shared a distinct nonsynonymous mutation in their NS3 gene [Publication II; Figure 7]. However, it can only be hypothesized whether this unique mutation provided the WNV EGC variants with an extra advantage. So far, WNV MH986056, MN794939, and other WNV EGC variants (branches 1 and 2) have not yet been reported to cause a localized outbreak. Hence, ecological and environmental factors may have played a more important role in a variant's ability to cause outbreaks, as stated in the review of Rizzoli and colleagues [134].

Potential WNV mosquito vectors occur throughout Germany and are active within the vegetative seasons [135]. Moreover, most reported WNV cases were collected in areas with a low average extrinsic incubation period (EIP), a temperature-dependent variable that calculates mosquitoes' ability to transmit WNV [Publication II, Figure 1]. Briefly, WNV transmission risks increase (=decrease EIP) as average local temperatures increase. Hence, these newly introduced variants may have comparable opportunities for causing outbreaks. However, changes in

temperature and EIP in the following years after WNV introduction should also be accounted. For instance, the decreased average temperatures in Poing and Rostock in 2019 may have hindered the WNV re-emergence in these areas [Publication II].

In terms of vertebrate hosts, WNV is an ecological generalist [136] and feeding patterns of most WNV vectors have extreme host heterogeneity, enabling multi-host species WNV transmission [137–139]. The absence of clustering based on host species in the WNV EGC subclade supports these statements (Figure 5D). However, different avian species have varying susceptibility and reservoir competence to WNV. For instance, avian species under taxonomic orders Passeriformes, Charadriiformes, Falconiformes, and Strigiformes can be considered competent WNV reservoirs [140]. The ecology of WNV and its mosquito vectors demonstrate that areas with dense naïve and susceptible bird populations (*e.g.,* zoological gardens) are highly vulnerable to a WNV outbreak emergence, as shown in, *e.g.,* Berlin [Publication II]. This factor likely increased the success of WNV EGC branches 3 and 4's progenitors since several of their member variants were derived from competent bird species collected in zoos (Figure 5D).

However, WNV EGC branch 1 variants (Wittenberg), LR743448 (Cottbus), and LR743437 and LR743437 (Poing) were also derived from competent and susceptible birds collected in zoological gardens, but a local outbreak was not detected in these areas. The detection of WNV infection in captive birds is a good indicator that a local mosquito population infected with WNV is present in the area. Hence, varying densities of potential WNV vectors and competent bird populations may have caused different WNV transmission rates in these zoological gardens.

Moreover, an introduced WNV variant most likely needs sufficient time to adapt to a new area successfully. The review from Pesko and Ebel [136] highlighted the evidence of WNV geographic clustering being only observed a few years after a WNV variant was introduced into a new area. In this study, strong geographical clustering was only observed a year after the first report of WNV-infection within Saxony and Saxony-Anhalt (branch 3) and Berlin (branch 4). Hence, the outbreak potential of other WNV variants is unclear since most of them were collected in 2019 [Publication II, Figure 2]. Therefore, the situation of the 2020 WNV epidemic in Germany can provide better insights into whether other WNV variants have managed to cause outbreaks.

This thesis provided evidence that the presence of susceptible bird species and time have important roles in a WNV variant's outbreak potential. However, this study cannot elucidate whether a specific mutation provided advantages for the WNV EGC variants; hence, this hypothesis has to be studied in more detail in further analyses. In addition, including detailed information regarding the density of competent host and vector populations in WNV-infected areas, such as Kampen and colleagues' study [135], may elucidate their effects on the outbreak

potential of a WNV variant. Other factors were also not included in this analysis, including sampling bias, mosquito species distributions, human interventions, host immunity, and others. Hence, this study suggested to incorporate these factors in future WNV phylogenetic analyses to understand WNV lineage 2 dispersal, establishment, and viral population diversity.

Within the European context, geographical-based clustering in the WNV lineage 2 phylogenetic tree was observed in variants from Italy, Greece, and Germany (EGC subclade). In contrast, WNV variants from Austria, the Czech Republic, Slovakia, and Germany (non-EGC variants) are interspersed in the Bayesian MCC tree [Publication II, Figure 2]. These observations were supported by Zehender and colleagues' [141] phylogeographic analysis, which revealed that Greece and Italy are receiving areas (sinks) of the European WNV lineage 2 migration while Hungary and Austria serve as radiation centers (virus sources). Therefore, it is interesting to observe Germany's role in WNV lineage 2 migration and dispersal in Europe. Recently, Sikkema and colleagues [142] demonstrated that WNV CEC variants from Utrecht, the Netherlands (MW036633-MW036634: mosquito pools from 2020) clustered with WNV CEC variant from Cottbus, Germany (LR743448: captive bird from 2019). However, the most recent ancestors, origin and mode of dispersal of these variants have to be further investigated.

Although Publications II and III provided 42 WNV whole-genome sequences from the 2018-19 WNV epidemic in Germany, missing WNV whole-genome sequences from different European countries (from 2004 to present), especially from Eastern Europe, hinder the more precise reconstruction of the phylogenetic and phylogeographic inferences of the WNV lineage 2 circulation in Europe and Germany. Oude Munnink and colleagues [68] encountered similar problems in reconstructing the evolutionary history of Usutu virus in Europe even when their study included 112 USUV whole-genome sequences from the Netherlands (2016-18). Their study could not elucidate the emergence of USUV lineages Africa 3 and Europe 2 in the Netherlands since USUV whole-genome sequences from other European countries (*e.g.,* Germany, Belgium) are unavailable.

Since the countrywide WNV and USUV monitoring and sequencing are inadequate to elucidate the evolutionary histories of these viruses, this study strongly recommends systematic WNV and USUV whole-genome sequencing from representative virus-positive samples (*e.g.,* birds, mosquitoes, horses, humans) collected in different European countries at continuous sampling periods, including past and recent outbreaks. This study also highlights the necessity of a "One-health" approach in monitoring WNV and USUV infections in clinical, veterinary, and environmental settings. Moreover, long-term international collaboration among countries affected by WNV or USUV is highly recommended to enhance the exchange of information, protocols, and strategies for the surveillance and control of these pathogens. Different research institutions are also encouraged to employ an open data-sharing platform, such as the

Nextstrain [90], to provide real-time interactive analyses of WNV or USUV evolution and transmission in Europe.

5.2 Advanced outbreak preparedness through an early warning system: A pilot study using the 2018-19 WNV epidemic generic HTS datasets

An early warning system (EWS) enables the timely detection of emerging pathogens, which is helpful in preventing a "spillover event" or containing an outbreak. However, utilizing metagenomic HTS for EWS can be time-consuming, labor-intensive, and expensive. As a possible alternative, this study proposed to exploit the rich sequence information found in generic HTS datasets obtained from previous surveillance and outbreak studies to screen for sequences of novel pathogens.

The proposed EWS consists of pathogen screening using generic HTS datasets and pathogen characterization techniques to determine the relevance of detected pathogens in public and animal health. This EWS is a generic platform, which can be established when the following components are available: (1) generic HTS datasets, (2) bioinformatic tools for metagenomic analysis and phylogenetic analyses, (3) samples associated with HTS datasets, and (4) capacities for HTS, RT-qPCR, and cell and virus culture [Publication IV, Figure 1]. These components are also utilized in the routine HTS-based outbreak investigation. This EWS aimed to maximize the extracted information from outbreak and surveillance samples without spending additional resources for sample collection and sequencing. However, the added sequence information offered by the EWS depends on samples (*e.g.,* sample type and quality, pathogen concentration) processed by previous studies. Moreover, the sizes of available HTS datasets may also affect EWS's ability to detect other pathogens.

In this pilot study, the EWS investigated generic HTS datasets derived from the 2018-19 WNV epidemic in Germany, focusing on potential virus pathogens. The metagenomic analysis pipeline "RIEMS" [143] detected sequences of several putative pathogens, including bacteria, protozoa, WNV, and other viruses. However, characterizing all detected putative pathogen sequences can be a highly demanding task. Moreover, some sequences may have incorrect taxonomic classifications. Therefore, stepwise criteria were specified in selecting suspected pathogens for the EWS reporting (criteria I-II) and EWS downstream analyses (criteria I-IV). In detail, these criteria include: (I) virus sequence reads must have true-positive taxonomic classification at least in the realm level; (II) sequences are unlikely to originate from other samples; (III) suspected viruses should have adequate sequence information; and (IV) suspected viruses can be associated with vertebrate hosts.

Criterion I requires that pathogen sequences have accurate taxonomic classification. Taxonomic classifications are based on the contents of the selected reference database, such as

public databases (*e.g.,* Genbank nucleotide collection nr/nt database). Public databases can contain sequences with erroneous taxonomic assignments since these databases are not curated. For example, several sequence reads initially classified as *Guanarito mammarenavirus* were, in fact, identified as ribosomal RNA sequences from eukaryotic organisms after performing a confirmatory homology search (Table 2).

Table 2. Representative virus sequences (non-WNV) detected in generic HTS datasets obtained from the 2018-19 WNV epidemic. The red box and "X" indicate that the sequence did not attain the respective criterion, the orange box and "?" indicate difficulty in verification, and the green box denotes that the criterion was satisfied.

Virus Family	Species	Library number	Count	I	II	III	IV	Assessment
Arenaviridae	Guanarito mammarenavirus	lib02898, lib03038:lib03039 lib03041:lib03042 lib03383,lib03417 lib03431	1-61	X				**False hit.** Sequence from eukaryotic rRNA sequences.
Peribunyaviridae	*Bunyamwera Orthobunyavirus*	lib03426, lib03038: lib03039	1; 1	X				**False hit.** Sequence from eukaryotic rRNA sequences.
Rhabdoviridae	European bat 1 lyssavirus	lib02898	2		X			**False hit.** True hit but a cross-contaminant
Phenuiviridae	Rift Valley fever phlebovirus	lib03431; lib03432; lib03433	1; 1; 2		?			**Unclear hit.** Possible cross-contaminants but with unknown source.[1]
Reoviridae	Avian *orthoreovirus*	lib03428	2			X		**Reported in the EWS** Few sequence information.
Unclassifired Ribovaria	Wuhan insect virus 27	lib03381	15				X	**Reported in the EWS** Invertebrate associated virus
Myoviridae	Escherichia virus VR7	lib03423	1				X	**Reported in the EWS** Bacteriophage
Totiviridae	Eimeria stiedai RNA virus 1; Eimeria tenella RNA virus 1;	lib03433	76			X	X	**Reported in the EWS** Few sequence information; Protist associated virus
Chrysoviridae	Eskilstorp virus	lib03481	3			X	X	**Reported in the EWS** Few sequence information; Mosquito associated virus
Mesoniviridae	*Alphamesonivirus 1*	lib03482	24260 7				X	**Reported in the EWS** Mosquito-associated virus
Flaviviridae	Usutu virus	lib03038: lib03039, lib03422	50; 2			X		**Reported in the EWS** Too few sequence information[2]
Reoviridae	*Umatilla* virus species	lib03381, lib03422,lib03433	1588; 1; 960					**EWS reporting + downstream analysis**
Peribunyaviridae	*Peribunyaviridae* species	lib03038:lib03039 lib03041:lib03042	151; 9					**EWS reporting + downstream analysis**

1 – Colleagues are informed for follow-up investigations. 2 – Confirmed the suspicion for WNV and USUV co-infection

Criterion II checks that these sequences are unlikely to originate from other samples (cross-contaminants). It also excludes falsely labeled sequence reads due to index hopping and contaminants from run-to-run carryover, commonly reported in the Illumina sequencing platform [49,55]. For instance, two European Bat 1 lyssavirus (EBLV-1) sequences were detected in lib02898. These sequences were considered contaminants since lib02898 and EBLV-1-positive

HTS libraries were processed in parallel (Table 2). The alignment of EBLV-1 sequences from these sequencing libraries showed very high nucleotide sequence identities. Suspected virus sequences, which passed criteria I and II, were reported to respective colleagues from different institutions for follow-up investigations.

In some cases, tracing the origin of viral sequences can be challenging. For example, Rift Valley fever virus (RVFV) sequence reads were detected in three generic HTS datasets derived from bird samples (Table 2). RVFV sequences are suspected cross-contaminants since an RVFV-related outbreak has not been reported in Europe [144]. Moreover, RVFV-related diseases are commonly reported in humans, ruminants, and camels [144].

In this EWS, potential sources of RVFV sequences were traced to confirm whether they are contaminants or derived from a potential circulating RVFV strain in Germany. The EWS traced an RVFV-positive library that was processed before the preparation of lib03431, lib03432, and lib03433. Short RVFV sequences detected by the EWS were aligned with RVFV sequences obtained from the laboratory and public database. This alignment demonstrated high nucleotide identities (>99%), which led to an inconclusive assessment. Thus, the HTS library lib03433 was also subjected to probe-based target enrichment to enhance RVFV sequence detection; however, an RVFV sequence was not detected in the targeted HTS dataset. This result suggests that RVFV sequences were derived from a run-to-run carryover or the target-enrichment HTS approach is inefficient for RVFV sequence enrichment. However, Wylezich and colleagues [64] demonstrated that the same probe-based target-enrichment HTS approach effectively enriches RVFV sequence reads. Thus, in the selected example, RVFV sequences can be considered as contaminants. For further confirmation, this finding was also forwarded to colleagues from the reference laboratory for follow-up investigations.

Criteria III and IV are specified for selecting potential viruses for EWS downstream analyses. Criterion III requires that the sequence information should be adequate for further virus characterization. For instance, RIEMS detected two avian orthoreovirus sequences in the dataset lib03428, which are inadequate for RT-qPCR design and reconstruct a reliable phylogenetic tree. Thus, the EWS investigation for this putative virus was paused until new sequences will be found in other datasets. However, some relevant viruses (*e.g.,* disease-related viruses) may not always comply with criterion III due to sensitivity issues of the generic HTS approach, as described in the study of Schlaberg and colleagues [120]. When there is a hint that the virus sequence is related to a relevant infection, then an appropriate HTS approach should be performed to increase virus sequence reads. For example, ≤60 USUV sequence reads were detected in two generic HTS datasets (Table 2), providing stronger evidence for WNV and USUV co-infection in their respective samples. However, these USUV sequences were inadequate for USUV subspecies classification and reconstruction of a reliable USUV phylogenetic tree. Thus,

an USUV-specific multiplex PCR–HTS approach was employed to obtain adequate USUV genome sequences, which were finally analyzed in Publication III.

Criterion IV requires that the putative viruses can be associated with vertebrate hosts. The RIEMS pipeline classified several sequences as viruses associated with bacteria, protists, and invertebrates (Table 2). Moreover, the phylogenetic inference demonstrates that viral sequences from dataset lib03482 clustered with mosquito-associated viruses (*Mesoniviridae*) [Publication IV, Figure S1], suggesting that this virus has a low probability of infecting vertebrate hosts. Thus, the EWS investigation for these viruses was stopped at this point.

Virus sequences classified as mosquito-borne *Reoviridae* (Umatilla virus; UMAV) and unclassified *Peribunyaviridae* (Hedwig virus; HEDV) comply with all four criteria for the EWS downstream analysis. Nearly complete coding sequences of UMAV and partial genome sequences of HEDV were detected in a few generic HTS datasets (Table 2). Although their closest relatives were detected from mosquitoes [145–149], these virus sequences were discovered in HTS libraries derived from WNV-infected bird samples.

These two potential pathogens were characterized using genetic analyses, molecular screening, and attempts for virus cultivation. The UMAV coding sequences were completed by re-sequencing lib03381 and lib03433, while an initial RT-qPCR was developed based on HEDV partial genome sequences to select the best candidate sample for the generic HTS approach [Publication IV]. The HEDV complete coding sequences were assembled from dataset lib03038:lib03039 and dataset lib03211 derived from the tissue sample with the highest HEDV RNA concentration. Newly developed virus-specific RT-qPCR assays detected 8 (6.4% of 125 tested bird samples) HEDV-positive captive birds and 14 (12.5% of 112 tested bird samples) UMAV-positive wild birds in small sample sets. Another UMAV-positive sample, confirmed by the metagenomic analysis, was not tested using RT-qPCR assay since its RNA sample was already depleted. Splenomegaly was observed in seven UMAV only-positive wild birds, which suggests an acute infection. Meanwhile, HEDV only-positive birds demonstrated varying diagnoses in their necropsy reports. Furthermore, Umatilla virus was successfully propagated in a mosquito cell culture [Publication IV].

The developed EWS also aims to enhance outbreak responses by providing viral genome sequences essential for developing molecular and serological diagnostic assays and targeted-HTS approaches (Figure 4). Virus-specific RT-qPCR assays were already developed in Publication IV, while a new probe panel for the target enrichment HTS approach was designed using UMAV and HEDV genome sequences for future outbreak investigation. However, the EWS does not include virus characterization techniques that can prove the association of newly discovered viruses with the disease based on Henle-Loeffler-Koch's postulates [118] or the modified metagenomic Henle-Loeffler-Koch's postulates [27]. Nevertheless, the EWS provides

important contributions to test these postulates. Virus-specific RT-qPCR assays are essential tools to screen for viruses in healthy and diseased animals. Moreover, the propagated Umatilla virus in C6/36 mosquito cells can serve as starting material to produce pure virus stocks, which can be utilized in infection trials and pathogenicity studies or for the development of additional diagnostic assays (*e.g.,* virus neutralization test) [1].

5.3 Conclusions

The here reported study provided evidence that the unified and generic pipeline is an effective tool to jointly investigate outbreaks and discover potential pathogens using the same generic HTS datasets. As a proof-of-concept, this pipeline obtained 34 WNV whole-genome sequences and detected sequences of USUV and other unexpected viruses from generic HTS datasets derived from the 2018-19 WNV epidemic and USUV epizooty in Germany. In addition, two targeted HTS approaches were incorporated in this pipeline to resolve the limitation of the generic HTS approach in obtaining sufficient virus sequences in samples with low viral loads.

Viral genome sequences acquired by the unified pipeline were utilized in understanding the 2018-19 WNV epidemic in Germany using phylogenetic and phylogeographic analyses, providing substantial evidence for the first reported WNV and USUV co-infection cases in birds, and detecting and characterizing suspected virus pathogens using the EWS. In particular, this EWS led to the first detection of UMAV in Europe and the discovery of a novel peribunyavirus in birds. Therefore, incorporating this unified and generic pipeline in routine outbreak investigation workflows, especially with investigations adhering to the "One-Health" approach, can advance preparedness and response strategies by early detection of novel and unexpected pathogens before they spillover to humans or cause a larger epizooty in animal populations.

As an outlook, this unified pipeline can also utilize third-generation sequencing technologies (e.g., Oxford Nanopore Technologies), especially in combination with the PCR amplicon HTS approach. For instance, the multiplex PCR assays specific for USUV and Zika virus were designed and optimized for second-generation and third-generation HTS technologies [66,150]. However, further development and refinement are needed to incorporate third-generation sequencing technologies with the generic HTS approach and the target enrichment HTS approach since they have high reported error rates (10–30%) and relatively low-throughput (<100,000 reads per flow cell) [151,152].

6. Summary

Infectious diseases remain a significant threat to the wellbeing of humans and animals worldwide. Thus, infectious disease outbreaks should be investigated to understand the emergence of these pathogens, leading to prevention and mitigation strategies for future outbreaks. High-throughput sequencing (HTS) and bioinformatic analysis tools are reshaping the surveillance of viral infectious diseases through genome-based outbreak investigations. In particular, analyzing generic HTS datasets using a metagenomic analysis pipeline enable simultaneous identification, characterization, and discovery of pathogens.

In this thesis, generic HTS datasets derived from the 2018-19 WNV epidemic and USUV epizooty in Germany were evaluated using a unified pipeline for outbreak investigation and an early warning system (EWS). This pipeline obtained 34 West Nile virus (WNV) whole-genome sequences and detected several sequences of Usutu virus (USUV) and other potential pathogens. A few WNV and USUV genome sequences were completed using targeted HTS approaches. Phylogenetic and phylogeographic inferences, reconstructed using WNV whole-genome sequences, revealed that Germany experienced at least six WNV introduction events. The majority of WNV German variants clustered into the so-called "Eastern German clade (EGC)," consisting of variants derived from birds, mosquitoes, a horse, and human cases. The progenitors of the EGC subclade probably circulated within Eastern Europe around 2011. These flavivirus genome sequences also provided substantial evidence for the first reported cases of WNV and USUV co-infection in birds. Phylogenetic inferences of USUV genome sequences showed the further spread of the USUV lineage Africa 3 and might indicate the overwintering of the USUV lineage Europe 2 in Germany. Among viral sequences reported in the EWS, Hedwig virus (HEDV; a novel peribunyavirus) and Umatilla virus (UMAV; detected in Europe for the first time) were investigated using genome characterization, molecular-based screening, and virus cultivation since these viruses were suspected of causing co-infections in WNV-infected birds. The EWS detected overall 8 HEDV-positive and 15 UMAV-positive birds in small sets of samples, and UMAV could be propagated in a mosquito cell culture Future studies are necessary to investigate the pathogenicity of these viruses and their role in the health of wild and captive birds.

In conclusion, this study provided a proof-of-concept that the developed unified and generic pipeline is an effective tool for outbreak investigation and pathogen discovery using the same generic HTS datasets derived from outbreak and surveillance samples. Therefore, this thesis recommends incorporating the unified pipeline in the key response to viral outbreaks to enhance outbreak preparedness and response.

7. Zusammenfassung

Infektionskrankheiten stellen nach wie vor eine erhebliche Bedrohung für das Wohlergehen von Menschen und Tieren weltweit dar. Daher sollten Ausbrüche von Infektionskrankheiten untersucht werden, um die Entstehung dieser Erreger zu verstehen und Präventions- sowie Eindämmungsstrategien für künftige Ausbrüche entwickeln zu können. Die Hochdurchsatz-Sequenzierung (HTS) und bioinformatische Analysetools verändern die Überwachung viraler Infektionskrankheiten durch genombasierte Ausbruchsuntersuchungen. Insbesondere die Analyse von generischen HTS-Datensätzen mit Hilfe einer metagenomischen Analysepipeline ermöglicht die gleichzeitige Identifizierung, Charakterisierung und Entdeckung von Pathogenen.

In dieser Arbeit wurden generische HTS-Datensätze, die von der WNV-Epidemie 2018-19 und der USUV-Epizootie in Deutschland stammen, mit einer einheitlichen Pipeline für die Ausbruchsuntersuchung und einem Frühwarnsystem (EWS) ausgewertet. Diese Pipeline lieferte 34 Ganzgenomsequenzen des West-Nil-Virus (WNV) und wies mehrere Sequenzen des Usutu-Virus (USUV) und anderer potenzieller Erreger nach. Einige WNV- und USUV-Genomsequenzen wurden durch gezielte HTS-Ansätze vervollständigt. Phylogenetische und phylogeographische Schlussfolgerungen, die anhand von WNV-Ganzgenomsequenzen rekonstruiert wurden, ergaben, dass es in Deutschland mindestens sechs WNV-Einschleppungsereignisse gab. Die Mehrzahl der deutschen WNV-Varianten stammt von Fällen bei Vögeln, Stechmücken, einem Pferd und Menschen und wurde in der so genannten "Eastern German Clade" (EGC) zusammengefasst. Die Vorläufer der EGC-Subklade zirkulierten wahrscheinlich um 2011 in Osteuropa. Diese Flavivirus-Genomsequenzen lieferten auch wesentliche Beweise für die ersten gemeldeten Fälle von WNV- und USUV-Koinfektionen bei Vögeln. Phylogenetische Rückschlüsse aus den USUV-Genomsequenzen zeigten die weitere Verbreitung der USUV-Linie Afrika 3 und könnten auf die Überwinterung der USUV-Linie Europa 2 in Deutschland hinweisen. Von den im EWS gemeldeten Virensequenzen wurden das Hedwig-Virus (HEDV; ein neuentdecktes Peribunyavirus) und das Umatilla-Virus (UMAV; zum ersten Mal in Europa entdeckt) mittels Genomcharakterisierung, molekularbasiertem Screening und Viruskultivierung untersucht, da diese Viren im Verdacht standen, Co-Infektionen bei WNV-infizierten Vögeln zu verursachen. Das EWS wies insgesamt 8 HEDV-positive sowie 15 UMAV-positive Vögel in kleinen Probensätzen nach außerdem konnte UMAV in einer Stechmücken-Zellkultur vermehrt werden. Es sind zukünftig weitere Studien notwendig, um die Pathogenität dieser Viren und ihre Rolle für die Gesundheit von Wildvögeln und in Gefangenschaft gehaltenen Vögeln zu untersuchen.

Zusammenfassend lässt sich sagen, dass diese Studie den Nachweis erbracht hat, dass die entwickelte einheitliche und generische Pipeline ein wirksames Instrument für die Untersuchung von Ausbrüchen und die Entdeckung von Krankheitserregern ist, wobei dieselben generischen HTS-Datensätze verwendet werden, die aus Ausbruchs- und Überwachungsproben stammen. Daher wird in dieser Arbeit empfohlen, die einheitliche Pipeline in die zentrale Reaktion auf Virusausbrüche einzubeziehen, um die Bereitschaft und Reaktion auf Ausbrüche zu verbessern.

8. Literature

1. van der Hoek L, Verschoor E, Beer M, Höper D, Wernike K, van Ranst M, et al. Host switching pathogens, infectious outbreaks and zoonosis: A Marie Skłodowska-Curie innovative training network (HONOURs). Virus Res. 2018; 257:120–4. doi: 10.1016/j.virusres.2018.09.002 PMID: 30316331.

2. Bloom DE, Cadarette D. Infectious Disease Threats in the Twenty-First Century: Strengthening the Global Response. Front Immunol. 2019; 10:549. doi: 10.3389/fimmu.2019.00549 PMID: 30984169.

3. World Health Organization. WHO Coronavirus Disease (COVID-19) Dashboard. World Health Organization 2020 [updated 28 May 2021; cited 28 May 2021]. Available from: https://covid19.who.int/.

4. International Monetary Fund. World Economic Outlook Update, June 2020: A Crisis Like No Other, An Uncertain Recovery [updated June 2020; cited 22 Mar 2021]. Available from: https://www.imf.org/en/Publications/WEO/Issues/2020/06/24/WEOUpdateJune2020.

5. Murray K, Selleck P, Hooper P, Hyatt A, Gould A, Gleeson L, et al. A morbillivirus that caused fatal disease in horses and humans. Science. 1995; 268:94–7. doi: 10.1126/science.7701348 PMID: 7701348.

6. Chua KB, Bellini WJ, Rota PA, Harcourt BH, Tamin A, Lam SK, et al. Nipah virus: a recently emergent deadly paramyxovirus. Science. 2000; 288:1432–5. doi: 10.1126/science.288.5470.1432 PMID: 10827955.

7. Kuiken T, Fouchier R am, Schutten M, Rimmelzwaan GF, van Amerongen G, van Riel D, et al. Newly discovered coronavirus as the primary cause of severe acute respiratory syndrome. The Lancet. 2003; 362:263–70. doi: 10.1016/S0140-6736(03)13967-0.

8. Zaki AM, van Boheemen S, Bestebroer TM, Osterhaus ADME, Fouchier RAM. Isolation of a novel coronavirus from a man with pneumonia in Saudi Arabia. N Engl J Med. 2012; 367:1814–20. doi: 10.1056/NEJMoa1211721 PMID: 23075143.

9. Gire SK, Goba A, Andersen KG, Sealfon RSG, Park DJ, Kanneh L, et al. Genomic surveillance elucidates Ebola virus origin and transmission during the 2014 outbreak. Science. 2014; 345:1369–72. doi: 10.1126/science.1259657.

10. Buonsenso D, Barone G, Onesimo R, Calzedda R, Chiaretti A, Valentini P. The re-emergence of dengue virus in non-endemic countries: a case series. BMC Research Notes. 2014; 7:596. doi: 10.1186/1756-0500-7-596.

11. Powers AM, Brault AC, Tesh RB, Weaver SC. Re-emergence of Chikungunya and O'nyong-nyong viruses: evidence for distinct geographical lineages and distant evolutionary relationships. J Gen Virol. 2000; 81:471–9. doi: 10.1099/0022-1317-81-2-471 PMID: 10644846.

12. Lanciotti RS, Roehrig JT, Deubel V, Smith J, Parker M, Steele K, et al. Origin of the West Nile virus responsible for an outbreak of encephalitis in the northeastern United States. Science. 1999; 286:2333–7. doi: 10.1126/science.286.5448.2333 PMID: 10600742.

13. Bakonyi T, Ivanics E, Erdélyi K, Ursu K, Ferenczi E, Weissenböck H, et al. Lineage 1 and 2 strains of encephalitic West Nile virus, central Europe. Emerg Infect Dis. 2006; 12:618–23. doi: 10.3201/eid1204.051379 PMID: 16704810.

14. Faria NR, Azevedo, Raimunda do Socorro da Silva, Kraemer MUG, Souza R, Cunha MS, Hill SC, et al. Zika virus in the Americas: Early epidemiological and genetic findings. Science. 2016; 352:345–9. doi: 10.1126/science.aaf5036.

15. Oļševskis E, Guberti V, Seržants M, Westergaard J, Gallardo C, Rodze I, et al. African swine fever virus introduction into the EU in 2014: Experience of Latvia. Res Vet Sci. 2016; 105:28–30. Epub 2016/01/14. doi: 10.1016/j.rvsc.2016.01.006 PMID: 27033903.

16. Morse SS, Mazet JAK, Woolhouse M, Parrish CR, Carroll D, Karesh WB, et al. Prediction and prevention of the next pandemic zoonosis. The Lancet. 2012; 380:1956–65. doi: 10.1016/S0140-6736(12)61684-5.

17. Alexander KA, Carlson CJ, Lewis BL, Getz WM, Marathe MV, Eubank SG, et al. The Ecology of Pathogen Spillover and Disease Emergence at the Human-Wildlife-Environment Interface. In: Hurst CJ, editor. The connections between ecology and infectious disease. Cham: Springer; 2018. pp. 267–98.

18. Grubaugh ND, Ladner JT, Lemey P, Pybus OG, Rambaut A, Holmes EC, et al. Tracking virus outbreaks in the twenty-first century. Nat Microbiol. 2019; 4:10–9. doi: 10.1038/s41564-018-0296-2 PMID: 30546099.

19. World Health Organization. Annual Review of Diseases Prioritized Under the Research and Development Blueprint. Informal consultation. Geneva, Switzerland: 2018 [cited 11 Mar 2021]. Available from: https://www.who.int/emergencies/diseases/2018prioritization-report.pdf?ua=1.

20. Fineberg HV. Pandemic preparedness and response—lessons from the H1N1 influenza of 2009. N Engl J Med. 2014; 370:1335–42. doi: 10.1056/NEJMra1208802 PMID: 24693893.

21. World Health Organization Director-General. Implementation of the International Health Regulations (2005): Report of the Review Committee on the Functioning of the International Health Regulations (2005) in relation to Pandemic (H1N1) 2009. 5 May 2011:12. Available from: https://apps.who.int/gb/ebwha/pdf_files/WHA64/A64_10-en.pdf.

22. Ross AGP, Crowe SM, Tyndall MW. Planning for the Next Global Pandemic. Int J Infect Dis. 2015; 38:89–94. Epub 2015/04/08. doi: 10.1016/j.ijid.2015.07.016 PMID: 26253461.

23. Commission on a Global Health Risk Framework for the Future. The Neglected Dimension of Global Security: A Framework to Counter Infectious Disease Crises. Washington (DC); 2016.

24. Moon S, Sridhar D, Pate MA, Jha AK, Clinton C, Delaunay S, et al. Will Ebola change the game? Ten essential reforms before the next pandemic. The report of the Harvard-LSHTM Independent Panel on the Global Response to Ebola. The Lancet. 2015; 386:2204–21. doi: 10.1016/S0140-6736(15)00946-0.

25. Gostin LO. Our Shared Vulnerability to Dangerous Pathogens. Med Law Rev. 2017; 25:185–99. doi: 10.1093/medlaw/fwx016 PMID: 28419346.

26. Chiu CY. Viral pathogen discovery. Curr Opin Microbiol. 2013; 16:468–78. Epub 2013/05/29. doi: 10.1016/j.mib.2013.05.001 PMID: 23725672.

27. Mokili JL, Rohwer F, Dutilh BE. Metagenomics and future perspectives in virus discovery. Curr Opin Virol. 2012; 2:63–77. doi: 10.1016/j.coviro.2011.12.004 PMID: 22440968.

28. Ladner JT, Beitzel B, Chain PSG, Davenport MG, Donaldson EF, Frieman M, et al. Standards for sequencing viral genomes in the era of high-throughput sequencing. mBio. 2014; 5:e01360-14. doi: 10.1128/mBio.01360-14 PMID: 24939889.

29. Heather JM, Chain B. The sequence of sequencers: The history of sequencing DNA. Genomics. 2016; 107:1–8. doi: 10.1016/j.ygeno.2015.11.003 PMID: 26554401.

30. Bleidorn C. Third generation sequencing: technology and its potential impact on evolutionary biodiversity research. Systematics and Biodiversity. 2016; 14:1–8. doi: 10.1080/14772000.2015.1099575.

31. Hess JF, Kohl TA, Kotrová M, Rönsch K, Paprotka T, Mohr V, et al. Library preparation for next generation sequencing: A review of automation strategies. Biotechnol Adv. 2020; 41:107537. doi: 10.1016/j.biotechadv.2020.107537 PMID: 32199980.

32. Head SR, Komori HK, LaMere SA, Whisenant T, van Nieuwerburgh F, Salomon DR, et al. Library construction for next-generation sequencing: overviews and challenges. Biotechniques. 2014; 56:61-77. doi: 10.2144/000114133 PMID: 24502796.

33. Illumina. Illumina Sequencing Technology. Technology Spotlight: Illumina® Sequencing. 2010 [updated 2010; cited 26 Feb 2021]. Available from: https://www.illumina.com/documents/products/techspotlights/techspotlight_sequencing.pdf.

34. Rothberg JM, Hinz W, Rearick TM, Schultz J, Mileski W, Davey M, et al. An integrated semiconductor device enabling non-optical genome sequencing. Nature. 2011; 475:348–52. doi: 10.1038/nature10242 PMID: 21776081.

35. Thermo Fisher Scientific. Torrent Suite™ Software 5.12. USER GUIDE. 2019 [updated 5 Nov 2019; cited 11 Mar 2021]. Available from: https://assets.thermofisher.com/TFS-Assets/LSG/manuals/MAN0017972_031419_TorrentSuite_5_12_UG_.pdf.

36. Ewing B, Hillier L, Wendl MC, Green P. Base-calling of automated sequencer traces using phred. I. Accuracy assessment. Genome Res. 1998; 8:175–85. doi: 10.1101/gr.8.3.175 PMID: 9521921.

37. Pereira R, Oliveira J, Sousa M. Bioinformatics and Computational Tools for Next-Generation Sequencing Analysis in Clinical Genetics. J Clin Med. 2020; 9:132. doi: 10.3390/jcm9010132 PMID: 31947757.

38. Srivastav R, Suneja G. Recent Advances in Microbial Genome Sequencing. In: Tripathi V, Kumar P, Tripathi P, Kishore A, Kamle M, editors. Microbial Genomics in Sustainable Agroecosystems: Volume 2. Singapore: Springer Singapore; 2019. pp. 131–44.

39. atdbio Ltd. Next generation sequencing. Figure 5 | Ion Torrent semiconductor sequencing. United Kingdom: [updated 2021; cited 27 May 2021]. Available from: https://www.atdbio.com/content/58/Next-generation-sequencing.

40. Thermo Fisher Scientific. Ion Xpress™ Ion Xpress™ Plus gDNA Fragment Library Preparation. 2020 [cited 21 Mar 2021]. Available from: https://assets.thermofisher.com/TFS-Assets/LSG/manuals/MAN0009847_IonXpressPlus_gDNA_FragLibraryPrep_UG.pdf.

41. Nakano M, Komatsu J, Matsuura S, Takashima K, Katsura S, Mizuno A. Single-molecule PCR using water-in-oil emulsion. Journal of Biotechnology. 2003; 102:117–24. doi: 10.1016/S0168-1656(03)00023-3.

42. Dressman D, Yan H, Traverso G, Kinzler KW, Vogelstein B. Transforming single DNA molecules into fluorescent magnetic particles for detection and enumeration of genetic variations. Proceedings of the National Academy of Sciences. 2003; 100:8817–22. Epub 2003/07/11. doi: 10.1073/pnas.1133470100 PMID: 12857956.

43. Golan D, Medvedev P. Using state machines to model the Ion Torrent sequencing process and to improve read error rates. Bioinformatics. 2013; 29:i344-51. doi: 10.1093/bioinformatics/btt212 PMID: 23813003.

44. Niedringhaus TP, Milanova D, Kerby MB, Snyder MP, Barron AE. Landscape of next-generation sequencing technologies. Anal Chem. 2011; 83:4327–41. Epub 2011/05/25. doi: 10.1021/ac2010857 PMID: 21612267.

45. Bragg LM, Stone G, Butler MK, Hugenholtz P, Tyson GW. Shining a light on dark sequencing: characterising errors in Ion Torrent PGM data. PLoS Comput Biol. 2013; 9:e1003031. doi: 10.1371/journal.pcbi.1003031 PMID: 23592973.

46. Quail MA, Swerdlow H, Turner DJ. Improved protocols for the illumina genome analyzer sequencing system. Curr Protoc Hum Genet. 2009; 62:18.2.1-18.2.27. doi: 10.1002/0471142905.hg1802s62 PMID: 19582764.

47. Bentley DR, Balasubramanian S, Swerdlow HP, Smith GP, Milton J, Brown CG, et al. Accurate whole human genome sequencing using reversible terminator chemistry. Nature. 2008; 456:53–9. doi: 10.1038/nature07517 PMID: 18987734.

48. Laehnemann D, Borkhardt A, McHardy AC. Denoising DNA deep sequencing data-high-throughput sequencing errors and their correction. Brief Bioinform. 2016; 17:154–79. Epub 2015/05/29. doi: 10.1093/bib/bbv029 PMID: 26026159.

49. Mukherjee S, Huntemann M, Ivanova N, Kyrpides NC, Pati A. Large-scale contamination of microbial isolate genomes by Illumina PhiX control. Stand Genomic Sci. 2015; 10:18. Epub 2015/03/30. doi: 10.1186/1944-3277-10-18 PMID: 26203331.

50. Houldcroft CJ, Beale MA, Breuer J. Clinical and biological insights from viral genome sequencing. Nat Rev Microbiol. 2017; 15:183–92. doi: 10.1038/nrmicro.2016.182 PMID: 28090077.

51. Fischer N, Indenbirken D, Meyer T, Lütgehetmann M, Lellek H, Spohn M, et al. Evaluation of Unbiased Next-Generation Sequencing of RNA (RNA-seq) as a Diagnostic Method in Influenza Virus-Positive Respiratory Samples. J Clin Microbiol. 2015; 53:2238–50. Epub 2015/05/13. doi: 10.1128/JCM.02495-14 PMID: 25972420.

52. Aguiar-Pulido V, Huang W, Suarez-Ulloa V, Cickovski T, Mathee K, Narasimhan G. Metagenomics, Metatranscriptomics, and Metabolomics Approaches for Microbiome Analysis. Evol Bioinform Online. 2016; 12:5–16. Epub 2016/05/12. doi: 10.4137/EBO.S36436 PMID: 27199545.

53. Gu W, Miller S, Chiu CY. Clinical Metagenomic Next-Generation Sequencing for Pathogen Detection. Annu Rev Pathol. 2019; 14:319–38. doi: 10.1146/annurev-pathmechdis-012418-012751 PMID: 30355154.

54. Nooij S, Schmitz D, Vennema H, Kroneman A, Koopmans MPG. Overview of Virus Metagenomic Classification Methods and Their Biological Applications. Front Microbiol. 2018; 9:749. doi: 10.3389/fmicb.2018.00749 PMID: 29740407.

55. Forth LF, Höper D. Highly efficient library preparation for Ion Torrent sequencing using Y-adapters. Biotechniques. 2019; 67:229–37. doi: 10.2144/btn-2019-0035 PMID: 31621374.

56. Shendure J, Ji H. Next-generation DNA sequencing. Nature Biotechnology. 2008; 26:1135–45. doi: 10.1038/nbt1486 PMID: 18846087.

57. López-Labrador FX, Brown JR, Fischer N, Harvala H, van Boheemen S, Cinek O, et al. Recommendations for the introduction of metagenomic high-throughput sequencing in clinical virology, part I: wet lab procedure. Journal of Clinical Virology. 2020; 134:104691. doi: 10.1016/j.jcv.2020.104691.

58. Hoffmann B, Scheuch M, Höper D, Jungblut R, Holsteg M, Schirrmeier H, et al. Novel orthobunyavirus in Cattle, Europe, 2011. Emerg Infect Dis. 2012; 18:469–72. doi: 10.3201/eid1803.111905 PMID: 22376991.

59. Hause BM, Collin EA, Peddireddi L, Yuan F, Chen Z, Hesse RA, et al. Discovery of a novel putative atypical porcine pestivirus in pigs in the USA. J Gen Virol. 2015; 96:2994–8. doi: 10.1099/jgv.0.000251 PMID: 26219947.

60. Briese T, Paweska JT, McMullan LK, Hutchison SK, Street C, Palacios G, et al. Genetic detection and characterization of Lujo virus, a new hemorrhagic fever-associated arenavirus from southern Africa. PLoS Pathog. 2009; 5:e1000455. doi: 10.1371/journal.ppat.1000455 PMID: 19478873.

61. Zhu N, Zhang D, Wang W, Li X, Yang B, Song J, et al. A Novel Coronavirus from Patients with Pneumonia in China, 2019. N Engl J Med. 2020; 382:727–33. doi: 10.1056/NEJMoa2001017 PMID: 31978945.

62. Depledge DP, Palser AL, Watson SJ, Lai IY-C, Gray ER, Grant P, et al. Specific capture and whole-genome sequencing of viruses from clinical samples. PLoS One. 2011; 6:e27805. Epub 2011/11/18. doi: 10.1371/journal.pone.0027805 PMID: 22125625.

63. Thomson E, Ip CLC, Badhan A, Christiansen MT, Adamson W, Ansari MA, et al. Comparison of Next-Generation Sequencing Technologies for Comprehensive Assessment of Full-Length

Hepatitis C Viral Genomes. J Clin Microbiol. 2016; 54:2470–84. Epub 2016/07/06. doi: 10.1128/JCM.00330-16 PMID: 27385709.

64. Wylezich C, Calvelage S, Schlottau K, Ziegler U, Pohlmann A, Höper D, et al. Next-generation diagnostics: virus capture facilitates a sensitive viral diagnosis for epizootic and zoonotic pathogens including SARS-CoV-2. Microbiome. 2021; 9:51. Epub 2021/02/20. doi: 10.1186/s40168-020-00973-z PMID: 33610182.

65. Noyes NR, Weinroth ME, Parker JK, Dean CJ, Lakin SM, Raymond RA, et al. Enrichment allows identification of diverse, rare elements in metagenomic resistome-virulome sequencing. Microbiome. 2017; 5:142. Epub 2017/10/17. doi: 10.1186/s40168-017-0361-8 PMID: 29041965.

66. Quick J, Grubaugh ND, Pullan ST, Claro IM, Smith AD, Gangavarapu K, et al. Multiplex PCR method for MinION and Illumina sequencing of Zika and other virus genomes directly from clinical samples. Nat Protoc. 2017; 12:1261–76. doi: 10.1038/nprot.2017.066 PMID: 28538739.

67. Quick J, Loman NJ, Duraffour S, Simpson JT, Severi E, Cowley L, et al. Real-time, portable genome sequencing for Ebola surveillance. Nature. 2016; 530:228–32. doi: 10.1038/nature16996 PMID: 26840485.

68. Oude Munnink BB, Münger E, Nieuwenhuijse DF, Kohl R, van der Linden A, Schapendonk CME, et al. Genomic monitoring to understand the emergence and spread of Usutu virus in the Netherlands, 2016-2018. Sci Rep. 2020; 10:2798. doi: 10.1038/s41598-020-59692-y PMID: 32071379.

69. Oude Munnink BB, Sikkema RS, Nieuwenhuijse DF, Molenaar RJ, Munger E, Molenkamp R, et al. Transmission of SARS-CoV-2 on mink farms between humans and mink and back to humans. Science. 2020; 371:172–7. doi: 10.1126/science.abe5901 PMID: 33172935.

70. Armstrong GL, MacCannell DR, Taylor J, Carleton HA, Neuhaus EB, Bradbury RS, et al. Pathogen Genomics in Public Health. N Engl J Med. 2019; 381:2569–80. doi: 10.1056/NEJMsr1813907 PMID: 31881145.

71. Chaguza C, Nyaga MM, Mwenda JM, Esona MD, Jere KC. Using genomics to improve preparedness and response of future epidemics or pandemics in Africa. The Lancet Microbe. 2020; 1:e275-e276. doi: 10.1016/S2666-5247(20)30169-5.

72. Lipsitch M, Cohen T, Cooper B, Robins JM, Ma S, James L, et al. Transmission dynamics and control of severe acute respiratory syndrome. Science. 2003; 300:1966–70. Epub 2003/05/23. doi: 10.1126/science.1086616 PMID: 12766207.

73. Kiss IZ, Green DM, Kao RR. Disease contact tracing in random and clustered networks. Proc Biol Sci. 2005; 272:1407–14. doi: 10.1098/rspb.2005.3092 PMID: 16006334.

74. Ladner JT, Grubaugh ND, Pybus OG, Andersen KG. Precision epidemiology for infectious disease control. Nat Med. 2019; 25:206–11. Epub 2019/02/06. doi: 10.1038/s41591-019-0345-2 PMID: 30728537.

75. Wohl S, Schaffner SF, Sabeti PC. Genomic Analysis of Viral Outbreaks. Annu Rev Virol. 2016; 3:173–95. Epub 2016/08/03. doi: 10.1146/annurev-virology-110615-035747 PMID: 27501264.

76. Duffy S, Shackelton LA, Holmes EC. Rates of evolutionary change in viruses: patterns and determinants. Nat Rev Genet. 2008; 9:267–76. Epub 2008/03/04. doi: 10.1038/nrg2323 PMID: 18319742.

77. Holland J, Spindler K, Horodyski F, Grabau E, Nichol S, VandePol S. Rapid evolution of RNA genomes. Science. 1982; 215:1577–85. doi: 10.1126/science.7041255 PMID: 7041255.

78. Gorbalenya AE, Lauber C. Phylogeny of Viruses ☆. Reference Module in Biomedical Sciences. 2017:no page. doi: 10.1016/B978-0-12-801238-3.95723-4.

79. Theys K, Lemey P, Vandamme A-M, Baele G. Advances in Visualization Tools for Phylogenomic and Phylodynamic Studies of Viral Diseases. Frontiers in Public Health. 2019; 7:208. Epub 2019/08/02. doi: 10.3389/fpubh.2019.00208 PMID: 31428595.

80. Holder M, Lewis PO. Phylogeny estimation: traditional and Bayesian approaches. Nat Rev Genet. 2003; 4:275–84. doi: 10.1038/nrg1044 PMID: 12671658.

81. Felsenstein J. Evolutionary trees from DNA sequences: a maximum likelihood approach. J Mol Evol. 1981; 17:368–76. doi: 10.1007/bf01734359 PMID: 7288891.

82. Douady CJ, Delsuc F, Boucher Y, Doolittle WF, Douzery EJP. Comparison of Bayesian and maximum likelihood bootstrap measures of phylogenetic reliability. Mol Biol Evol. 2003; 20:248–54. doi: 10.1093/molbev/msg042 PMID: 12598692.

83. Huelsenbeck JP, Ronquist F, Nielsen R, Bollback JP. Bayesian inference of phylogeny and its impact on evolutionary biology. Science. 2001; 294:2310–4. doi: 10.1126/science.1065889 PMID: 11743192.

84. Baele G, Dellicour S, Suchard MA, Lemey P, Vrancken B. Recent advances in computational phylodynamics. Curr Opin Virol. 2018; 31:24–32. Epub 2018/09/22. doi: 10.1016/j.coviro.2018.08.009 PMID: 30248578.

85. Vaiente MA, Scotch M. Going back to the roots: Evaluating Bayesian phylogeographic models with discrete trait uncertainty. Infect Genet Evol. 2020; 85:104501. Epub 2020/08/13. doi: 10.1016/j.meegid.2020.104501 PMID: 32798768.

86. Lemey P, Rambaut A, Drummond AJ, Suchard MA. Bayesian phylogeography finds its roots. PLoS Comput Biol. 2009; 5:e1000520. Epub 2009/09/25. doi: 10.1371/journal.pcbi.1000520 PMID: 19779555.

87. Smith GJD, Vijaykrishna D, Bahl J, Lycett SJ, Worobey M, Pybus OG, et al. Origins and evolutionary genomics of the 2009 swine-origin H1N1 influenza A epidemic. Nature. 2009; 459:1122–5. doi: 10.1038/nature08182 PMID: 19516283.

88. Mena I, Nelson MI, Quezada-Monroy F, Dutta J, Cortes-Fernández R, Lara-Puente JH, et al. Origins of the 2009 H1N1 influenza pandemic in swine in Mexico. Elife. 2016; 5:e16777. Epub 2016/06/28. doi: 10.7554/eLife.16777 PMID: 27350259.

89. Briese T, Mishra N, Jain K, Zalmout IS, Jabado OJ, Karesh WB, et al. Middle East respiratory syndrome coronavirus quasispecies that include homologues of human isolates revealed through whole-genome analysis and virus cultured from dromedary camels in Saudi Arabia. mBio. 2014; 5:e01146-14. Epub 2014/04/29. doi: 10.1128/mBio.01146-14 PMID: 24781747.

90. Hadfield J, Brito AF, Swetnam DM, Vogels CBF, Tokarz RE, Andersen KG, et al. Twenty years of West Nile virus spread and evolution in the Americas visualized by Nextstrain. PLoS Pathog. 2019; 15:e1008042. Epub 2019/10/31. doi: 10.1371/journal.ppat.1008042 PMID: 31671157.

91. Steele L, Orefuwa E, Bino S, Singer SR, Lutwama J, Dickmann P. Earlier Outbreak Detection-A Generic Model and Novel Methodology to Guide Earlier Detection Supported by Data From Low- and Mid-Income Countries. Frontiers in Public Health. 2020; 8:452. Epub 2020/09/11. doi: 10.3389/fpubh.2020.00452 PMID: 33014967.

92. FAO-OIE-WHO. Global early warning and response system for major animal diseases, including zoonoses. [updated 10 May 2021; cited 10 May 2021]. Available from: https://www.who.int/zoonoses/outbreaks/glews/en/.

93. Carroll D, Morzaria S, Briand S, Johnson CK, Morens D, Sumption K, et al. Preventing the next pandemic: the power of a global viral surveillance network. BMJ. 2021; 372:n485. doi: 10.1136/bmj.n485.

94. Corman VM, Landt O, Kaiser M, Molenkamp R, Meijer A, Chu DK, et al. Detection of 2019 novel coronavirus (2019-nCoV) by real-time RT-PCR. Euro Surveill. 2020; 25:pii=2000045. doi: 10.2807/1560-7917.ES.2020.25.3.2000045 PMID: 31992387.

95. Li Z, Yi Y, Luo X, Xiong N, Liu Y, Li S, et al. Development and clinical application of a rapid IgM-IgG combined antibody test for SARS-CoV-2 infection diagnosis. J Med Virol. 2020; 92:1518–24. Epub 2020/04/13. doi: 10.1002/jmv.25727 PMID: 32104917.

96. Thi Nhu Thao T, Labroussaa F, Ebert N, V'kovski P, Stalder H, Portmann J, et al. Rapid reconstruction of SARS-CoV-2 using a synthetic genomics platform. Nature. 2020; 582:561–5. doi: 10.1038/s41586-020-2294-9.

97. Sahin U, Muik A, Derhovanessian E, Vogler I, Kranz LM, Vormehr M, et al. COVID-19 vaccine BNT162b1 elicits human antibody and TH1 T cell responses. Nature. 2020; 586:594–9. doi: 10.1038/s41586-020-2814-7.

98. World Health Organization. Severe acute respiratory syndrome (SARS). Report by the Secretariat EB113/33. 2003 [updated 23 Jan 2004; cited 19 May 2021]. Available from: https://apps.who.int/iris/bitstream/handle/10665/20038/eeb11333r1.pdf?sequence=1&isAllowed=y.

99. Rota PA, Oberste MS, Monroe SS, Nix WA, Campagnoli R, Icenogle JP, et al. Characterization of a novel coronavirus associated with severe acute respiratory syndrome. Science. 2003; 300:1394–9. Epub 2003/05/01. doi: 10.1126/science.1085952 PMID: 12730500.

100. Marra MA, Jones SJM, Astell CR, Holt RA, Brooks-Wilson A, Butterfield YSN, et al. The Genome sequence of the SARS-associated coronavirus. Science. 2003; 300:1399–404. Epub 2003/05/01. doi: 10.1126/science.1085953 PMID: 12730501.

101. Drosten C, Günther S, Preiser W, van der Werf S, Brodt H-R, Becker S, et al. Identification of a novel coronavirus in patients with severe acute respiratory syndrome. N Engl J Med. 2003; 348:1967–76. Epub 2003/04/10. doi: 10.1056/NEJMoa030747 PMID: 12690091.

102. Centers for Disease Control and Prevention (CDC). Update: novel influenza A (H1N1) virus infections - worldwide, May 6, 2009. MMWR Morb Mortal Wkly Rep. 2009; 58:453–8.

103. Center for Disease Control and Prevention, National Center for Immunization and Respiratory Diseases (NCIRD). 2009 H1N1 Pandemic Timeline. Center for Disease Control and Prevention 2009 [updated 8 May 2019; cited 27 May 2021]. Available from: https://www.cdc.gov/flu/pandemic-resources/2009-pandemic-timeline.html.

104. van Boheemen S, Graaf M de, Lauber C, Bestebroer TM, Raj VS, Zaki AM, et al. Genomic characterization of a newly discovered coronavirus associated with acute respiratory distress syndrome in humans. mBio. 2012; 3:e00473-12. Epub 2012/11/20. doi: 10.1128/mBio.00473-12 PMID: 23170002.

105. Blomström A-L, Belák S, Fossum C, McKillen J, Allan G, Wallgren P, et al. Detection of a novel porcine boca-like virus in the background of porcine circovirus type 2 induced postweaning multisystemic wasting syndrome. Virus Res. 2009; 146:125–9. doi: 10.1016/j.virusres.2009.09.006.

106. Cibulski S, Weber MN, Sales Lima FE de, Lima DA de, Fernandes dos Santos H, Teixeira TF, et al. Viral metagenomics in Brazilian Pekin ducks identifies two gyrovirus, including a new species, and the potentially pathogenic duck circovirus. Virology. 2020; 548:101–8. doi: 10.1016/j.virol.2020.05.013.

107. Epstein JH, Quan P-L, Briese T, Street C, Jabado O, Conlan S, et al. Identification of GBV-D, a novel GB-like flavivirus from old world frugivorous bats (Pteropus giganteus) in Bangladesh. PLoS Pathog. 2010; 6:e1000972. doi: 10.1371/journal.ppat.1000972 PMID: 20617167.

108. Quan P-L, Firth C, Conte JM, Williams SH, Zambrana-Torrelio CM, Anthony SJ, et al. Bats are a major natural reservoir for hepaciviruses and pegiviruses. Proc Natl Acad Sci U S A. 2013; 110:8194–9. doi: 10.1073/pnas.1303037110 PMID: 23610427.

109. Sachsenröder J, Braun A, Machnowska P, Ng TFF, Deng X, Guenther S, et al. Metagenomic identification of novel enteric viruses in urban wild rats and genome characterization of a group A rotavirus. J Gen Virol. 2014; 95:2734–47. doi: 10.1099/vir.0.070029-0 PMID: 25121550.

110. Vibin J, Chamings A, Klaassen M, Bhatta TR, Alexandersen S. Metagenomic characterisation of avian parvoviruses and picornaviruses from Australian wild ducks. Sci Rep. 2020; 10:12800. doi: 10.1038/s41598-020-69557-z PMID: 32733035.

111. Bennett AJ, Paskey AC, Ebinger A, Pfaff F, Priemer G, Höper D, et al. Relatives of rubella virus in diverse mammals. Nature. 2020; 586:424–8. doi: 10.1038/s41586-020-2812-9.

112. Brinkmann A, Nitsche A, Kohl C. Viral Metagenomics on Blood-Feeding Arthropods as a Tool for Human Disease Surveillance. Int J Mol Sci. 2016; 17:1743. doi: 10.3390/ijms17101743 PMID: 27775568.

113. Cox-Foster DL, Conlan S, Holmes EC, Palacios G, Evans JD, Moran NA, et al. A metagenomic survey of microbes in honey bee colony collapse disorder. Science. 2007; 318:283–7. doi: 10.1126/science.1146498 PMID: 17823314.

114. Käfer S, Paraskevopoulou S, Zirkel F, Wieseke N, Donath A, Petersen M, et al. Re-assessing the diversity of negative strand RNA viruses in insects. PLoS Pathog. 2019; 15:e1008224. doi: 10.1371/journal.ppat.1008224 PMID: 31830128.

115. Ge X, Li Y, Yang X, Zhang H, Zhou P, Zhang Y, et al. Metagenomic Analysis of Viruses from Bat Fecal Samples Reveals Many Novel Viruses in Insectivorous Bats in China. J Virol. 2012; 86:4620–30. doi: 10.1128/JVI.06671-11.

116. Hjelmsø MH, Mollerup S, Jensen RH, Pietroni C, Lukjancenko O, Schultz AC, et al. Metagenomic analysis of viruses in toilet waste from long distance flights—A new procedure for global infectious disease surveillance. PLoS One. 2019; 14:e0210368. doi: 10.1371/journal.pone.0210368.

117. Canuti M, van der Hoek L. Virus discovery: are we scientists or genome collectors. Trends Microbiol. 2014; 22:229–31. doi: 10.1016/j.tim.2014.02.004 PMID: 24786864.

118. Loeffler F. Untersuchungen über die Bedeutung der Mikroorganismen für die Entstehung der Diphtherie beim Menschen, bei der Taube und beim Kalbe. [Berlin]; 1884.

119. Fredricks DN, Relman DA. Sequence-based identification of microbial pathogens: a reconsideration of Koch's postulates. Clin Microbiol Rev. 1996; 9:18–33. doi: 10.1128/CMR.9.1.18-33.1996 PMID: 8665474.

120. Schlaberg R, Chiu CY, Miller S, Procop GW, Weinstock G, the Professional Practice Committee and Committee on Laboratory Practices of the American Society for Microbiology, et al. Validation of Metagenomic Next-Generation Sequencing Tests for Universal Pathogen Detection. Arch Pathol Lab Med. 2017; 141:776–86. doi: 10.5858/arpa.2016-0539-RA.

121. Gardy JL, Loman NJ. Towards a genomics-informed, real-time, global pathogen surveillance system. Nat Rev Genet. 2018; 19:9–20. doi: 10.1038/nrg.2017.88 PMID: 29129921.

122. Epstein JH, Anthony SJ. Viral discovery as a tool for pandemic preparedness. Rev Sci Tech. 2017; 36:499–512. doi: 10.20506/rst.36.2.2669 PMID: 30152468.

123. Breitbart M, Rohwer F. Method for discovering novel DNA viruses in blood using viral particle selection and shotgun sequencing. Biotechniques. 2005; 39:729–36. doi: 10.2144/000112019 PMID: 16312220.

124. Jöst H, Bialonski A, Maus D, Sambri V, Eiden M, Groschup MH, et al. Isolation of usutu virus in Germany. Am J Trop Med Hyg. 2011; 85:551–3. doi: 10.4269/ajtmh.2011.11-0248 PMID: 21896821.

125. Cadar D, Maier P, Müller S, Kress J, Chudy M, Bialonski A, et al. Blood donor screening for West Nile virus (WNV) revealed acute Usutu virus (USUV) infection, Germany, September 2016. Euro Surveill. 2017; 22:30501. doi: 10.2807/1560-7917.es.2017.22.14.30501 PMID: 28422005.

126. Cadar D, Becker N, Campos RdM, Börstler J, Jöst H, Schmidt-Chanasit J. Usutu virus in bats, Germany, 2013. Emerg Infect Dis. 2014; 20:1771–3. doi: 10.3201/eid2010.140909 PMID: 25271769.

127. Becker N, Jöst H, Ziegler U, Eiden M, Höper D, Emmerich P, et al. Epizootic emergence of Usutu virus in wild and captive birds in Germany. PLoS One. 2012; 7:e32604. Epub 2012/02/28. doi: 10.1371/journal.pone.0032604 PMID: 22389712.

128. Ziegler U, Jöst H, Müller K, Fischer D, Rinder M, Tietze DT, et al. Epidemic Spread of Usutu Virus in Southwest Germany in 2011 to 2013 and Monitoring of Wild Birds for Usutu and West Nile Viruses. Vector Borne Zoonotic Dis. 2015; 15:481–8. doi: 10.1089/vbz.2014.1746 PMID: 26273809.

129. Michel F, Sieg M, Fischer D, Keller M, Eiden M, Reuschel M, et al. Evidence for West Nile Virus and Usutu Virus Infections in Wild and Resident Birds in Germany, 2017 and 2018. Viruses. 2019; 11:674. doi: 10.3390/v11070674 PMID: 31340516.

130. Michel F, Fischer D, Eiden M, Fast C, Reuschel M, Müller K, et al. West Nile Virus and Usutu Virus Monitoring of Wild Birds in Germany. International Journal of Environmental Research and Public Health. 2018; 15:171. Epub 2018/01/22. doi: 10.3390/ijerph15010171 PMID: 29361762.

131. Cadar D, Lühken R, van der Jeugd H, Garigliany M, Ziegler U, Keller M, et al. Widespread activity of multiple lineages of Usutu virus, western Europe, 2016. Euro Surveill. 2017; 22:30452. doi: 10.2807/1560-7917.ES.2017.22.4.30452 PMID: 28181903.

132. Ziegler U, Fast C, Eiden M, Bock S, Schulze C, Hoeper D, et al. Evidence for an independent third Usutu virus introduction into Germany. Veterinary Microbiology. 2016; 192:60–6. Epub 2016/06/16. doi: 10.1016/j.vetmic.2016.06.007 PMID: 27527765.

133. Mullarney K, Svensson L, editors. Der Kosmos-Vogelführer. Alle Arten Europas, Nordafrikas und Vorderasiens. 2nd ed. Stuttgart: Kosmos; 2015.

134. Rizzoli A, Jimenez-Clavero MA, Barzon L, Cordioli P, Figuerola J, Koraka P, et al. The challenge of West Nile virus in Europe: knowledge gaps and research priorities. Euro Surveill. 2015; 20:21135. Epub 2015/05/21. doi: 10.2807/1560-7917.es2015.20.20.21135 PMID: 26027485.

135. Kampen H, Holicki CM, Ziegler U, Groschup MH, Tews BA, Werner D. West Nile Virus Mosquito Vectors (Diptera: Culicidae) in Germany. Viruses. 2020; 12:493. Epub 2020/04/28. doi: 10.3390/v12050493 PMID: 32354202.

136. Pesko KN, Ebel GD. West Nile virus population genetics and evolution. Infect Genet Evol. 2012; 12:181–90. Epub 2011/12/27. doi: 10.1016/j.meegid.2011.11.014 PMID: 22226703.

137. Kilpatrick AM, Daszak P, Jones MJ, Marra PP, Kramer LD. Host heterogeneity dominates West Nile virus transmission. Proc Biol Sci. 2006; 273:2327–33. doi: 10.1098/rspb.2006.3575 PMID: 16928635.

138. Börstler J, Jöst H, Garms R, Krüger A, Tannich E, Becker N, et al. Host-feeding patterns of mosquito species in Germany. Parasit Vectors. 2016; 9:318. doi: 10.1186/s13071-016-1597-z.

139. Muñoz J, Ruiz S, Soriguer R, Alcaide M, Viana DS, Roiz D, et al. Feeding Patterns of Potential West Nile Virus Vectors in South-West Spain. PLoS One. 2012; 7:e39549. doi: 10.1371/journal.pone.0039549.

140. Tolsá MJ, García-Peña GE, Rico-Chávez O, Roche B, Suzán G. Macroecology of birds potentially susceptible to West Nile virus. Proc Biol Sci. 2018; 285:20182178. doi: 10.1098/rspb.2018.2178 PMID: 30963915.

141. Zehender G, Veo C, Ebranati E, Carta V, Rovida F, Percivalle E, et al. Reconstructing the recent West Nile virus lineage 2 epidemic in Europe and Italy using discrete and continuous phylogeography. PLoS One. 2017; 12:e0179679. Epub 2017/07/05. doi: 10.1371/journal.pone.0179679 PMID: 28678837.

142. Sikkema RS, Schrama M, van den Berg T, Morren J, Munger E, Krol L, et al. Detection of West Nile virus in a common whitethroat (Curruca communis) and Culex mosquitoes in the Netherlands, 2020. Euro Surveill. 2020; 25:2001704. doi: 10.2807/1560-7917.ES.2020.25.40.2001704 PMID: 33034280.

143. Scheuch M, Höper D, Beer M. RIEMS: a software pipeline for sensitive and comprehensive taxonomic classification of reads from metagenomics datasets. BMC Bioinformatics. 2015; 16:69. doi: 10.1186/s12859-015-0503-6.

144. Nielsen SS, Alvarez J, Bicout DJ, Calistri P, Depner K, Drewe JA, et al. Rift Valley Fever - epidemiological update and risk of introduction into Europe. EFSA J. 2020; 18:e06041. Epub 2020/03/06. doi: 10.2903/j.efsa.2020.6041 PMID: 33020705.

145. Pettersson JH-O, Shi M, Eden J-S, Holmes EC, Hesson JC. Meta-Transcriptomic Comparison of the RNA Viromes of the Mosquito Vectors Culex pipiens and Culex torrentium in Northern Europe. Viruses. 2019; 11:1033. Epub 2019/11/06. doi: 10.3390/v11111033 PMID: 31698792.

146. Belaganahalli MN, Maan S, Maan NS, Tesh R, Attoui H, Mertens PPC. Umatilla virus genome sequencing and phylogenetic analysis: identification of stretch lagoon orbivirus as a new member of the Umatilla virus species. PLoS One. 2011; 6:e23605. Epub 2011/08/29. doi: 10.1371/journal.pone.0023605 PMID: 21897849.

147. Ejiri H, Kuwata R, Tsuda Y, Sasaki T, Kobayashi M, Sato Y, et al. First isolation and characterization of a mosquito-borne orbivirus belonging to the species Umatilla virus in East Asia. Arch Virol. 2014; 159:2675–85. Epub 2014/06/07. doi: 10.1007/s00705-014-2117-0 PMID: 24906523.

148. Cowled C, Palacios G, Melville L, Weir R, Walsh S, Davis S, et al. Genetic and epidemiological characterization of Stretch Lagoon orbivirus, a novel orbivirus isolated from Culex and Aedes mosquitoes in northern Australia. J Gen Virol. 2009; 90:1433–9. Epub 2009/03/12. doi: 10.1099/vir.0.010074-0 PMID: 19282430.

149. Tangudu CS, Charles J, Hurt SL, Dunphy BM, Smith RC, Bartholomay LC, et al. Skunk River virus, a novel orbivirus isolated from Aedes trivittatus in the United States. J Gen Virol. 2019; 100:295–300. Epub 2019/01/11. doi: 10.1099/jgv.0.001219 PMID: 30632960.

150. Oude Munnink BB, Kik M, Bruijn ND de, Kohl R, van der Linden A, Reusken CBEM, et al. Towards high quality real-time whole genome sequencing during outbreaks using Usutu virus as example. Infect Genet Evol. 2019; 73:49–54. Epub 2019/04/20. doi: 10.1016/j.meegid.2019.04.015 PMID: 31014969.

151. Greninger AL, Naccache SN, Federman S, Yu G, Mbala P, Bres V, et al. Rapid metagenomic identification of viral pathogens in clinical samples by real-time nanopore sequencing analysis. Genome Med. 2015; 7:99. Epub 2015/09/29. doi: 10.1186/s13073-015-0220-9 PMID: 26416663.

152. Forth JH, Forth LF, King J, Groza O, Hübner A, Olesen AS, et al. A Deep-Sequencing Workflow for the Fast and Efficient Generation of High-Quality African Swine Fever Virus Whole-Genome Sequences. Viruses. 2019; 11:846. Epub 2019/09/11. doi: 10.3390/v11090846 PMID: 31514438.

Eigenständigkeitserklärung

Hiermit erkläre ich, dass diese Arbeit bisher von mir weder an der Mathematisch Naturwissenschaftlichen Fakultät der Universität Greifswald noch einer anderen wissenschaftlichen Einrichtung zum Zwecke der Promotion eingereicht wurde.

Ferner erkläre ich, dass ich diese Arbeit selbstständig verfasst und keine anderen als die darin angegebenen Hilfsmittel und Hilfen benutzt und keine Textabschnitte eines Dritten ohne Kennzeichnung übernommen habe.

_____

Pauline Dianne Santos

Curriculum Vitae

Surname	Santos
First names	Pauline Dianne
Middle name	Madlangsakay
Place of birth	Guiguinto, Philippines
Date of birth	22.04.1988
Nationality	Filipino

Education

06/2013 – 06/2017	Master of Science (M.Sc.) in Microbiology, University of the Philippines (UP) Diliman
06/2005 – 04/2013	Bachelor of Science (B.Sc.) in Biology, University of the Philippines (UP) Diliman
06/2001 – 04/2005	High School Diploma Bulacan State University Laboratory High School

Professional Experience

12/2017 – 05/2021	PhD position at Friedrich-Loeffler-Institut (FLI), Institut für Virusdiagnostik, Greifswald-Insel Riems
01/2017 – 11/2017	Laboratory Instructor at UP Diliman Institute of Biology, College of Science
11/2015 – 11/2017	University Research Associate I at UP Diliman Natural Sciences Research Institute
01/2015 – 10/2015	University Research Associate II at UP Diliman Institute of Biology, College of Science
08/2013 – 02/2014	Research Associate I at UP Diliman Institute of Biology, College of Science

_____

Pauline Dianne Santos

Publications & Talks

(I) Scientific publications included in this thesis

Kinsella CM, <u>Santos PD</u>[e], Postigo-Hidalgo I[e], Folgueiras-Gonzalez A[e], Passchier TM[e], Szillat KP[e], Akello JO[e], Alvarez-Rodrıguez B[e], Martı-Carreras J[e]. Preparedness needs research: How fundamental science and international collaboration accelerated the response to COVID-19. 2020 Oct 9. *PLoS Pathogen*; 16(10): e1008902, doi: 10.1371/journal.ppat.1008902.

Ziegler U[e], <u>Santos PD</u>[e], Groschup MH, Hattendorf C, Eiden M, Höper D, Eisermann P, Keller M, Michel F, Klopfleisch R, Müller K, Werner D, Kampen H, Beer M, Frank C, Lachmann R, Tews BA, Wylezich C, Rinder M, Lachmann L, Grünewald T, Szentiks CA, Sieg M, Schmidt-Chanasit J, Cadar D[e], Lühken R[e]. West Nile Virus Epidemic in Germany Triggered by Epizootic Emergence, 2019. 2020 04 15. *Viruses*, 12(4): 448, doi: 10.3390/v12040448

<u>Santos PD</u>, Michel F, Wylezich C, Höper D, Keller M, Holicki CM, Szentiks CA, Eiden M, Muluneh A, Neubauer-Juric A, Thalheim S, Globig A, Beer M, Groschup MH, Ziegler U. Co-Infections: Simultaneous Detections of West Nile Virus and Usutu Virus in Birds from Germany. 2021 03 02. *Transboundary and Emerging Diseases*, 00: 1-17, doi: 10.1111/tbed.14050

<u>Santos PD</u>, Ziegler U, Szillat K, Szentiks CA, Skuball J, Merbach S, Grothmann P, Tews BA, Beer M, Höper D. In Action – An Early Warning System for the Detection of Unexpected or Novel Pathogens. *Virus Evolution*, 7(2): 1-15, doi: 10.1093/ve/veab085

[e] These authors contributed equally

(II) Additional scientific publications

<u>Santos PDM,</u> Widmer KW, Rivera WL. PCR-based detection and serovar identification of *Salmonella* in retail meat collected from wet markets in Metro Manila, Philippines. PLoS ONE. 2020 Sep 30; 15(9): e0239457, doi: 10.1371/journal.pone.0239457.

Justo CAC, Mapile MRF, <u>Santos PDM,</u> Rivera WL. Determination of the optimal pre-enrichment period for the detection of *Salmonella enterica* in artificially inoculated meat products using culture, PCR and LAMP assays. Philippine Science Letter. 2018 Jun 16. 11 (Supplement):043-050.

Calayag AMB, Paclibare PAP, <u>Santos PDM</u>, Bautista CAC, Rivera WL. Molecular characterization and antimicrobial resistance of *Salmonella enterica* from swine slaughtered in two different types of Philippine abattoir. Food Microbiology. 2017 Jan 31; 65:51-56, doi: 10.1016/j.fm.2017.01.016.

(III) Oral and poster presentations

International Virus Bioinformatics Meeting 2020. Bern, Switzerland (online). 8-9 October 2020. Oral presentation. 'Metagenomics analyses of West Nile Virus Outbreak samples from Germany'. <u>Santos PD</u>, Ziegler U, Beer M, Höper D.

6th World One Health Conference 2020. Virtual edition. 30 October – 3 November 2020. Poster Presentation. 'Novel Peribunyavirus Discovered in Samples from the West Nile Virus Outbreak in Germany'. <u>Santos PD</u>, Ziegler U, Beer M, Höper D.

Junior Scientist Symposium 2019, Jena, Germany. 25-27 September 2019. Poster presentation. "Unexpected Novel *Peribunyaviridae* Virus Found in Snowy Owls from Tierpark Berlin-Friedrichsfelde". <u>Santos PD</u>, Ziegler U, Keller M, Beer M, Höper D.

Junior Scientist Symposium 2018, Greifswald, Germany. 24-26 September 2018. Poster presentation. 'Optimization of a Universal and Unbiased Diagnostic Metagenomics Workflow'. <u>Santos PD</u>, Beer M, Höper D.

Acknowledgements